

https://dspace.org/

Development of lymphocyte specific internalising aptamers

Millroy, Laura Ann

2014-04-23
http://hdl.handle.net10539/14570

Downloaded from a DSpace repository. https://dspace.org/

DEVELOPMENT OF LYMPHOCYTE SPECIFIC INTERNALISING APTAMERS

LAURA MILLROY

A thesis submitted to the Faculty of Health Sciences, University of the Witwatersrand, Johannesburg, in fulfilment of the requirements for the degree of Doctor of Philosophy.

Johannesburg, October 2013

DECLARATION

I, Laura Millroy, declare that this thesis, which I hereby submit for the degree of Doctor of Philosophy at the University of the Witwatersrand, is my own work. It has not been previously submitted by me for a degree at this or any other tertiary institution.

Signature: _____

Date: _____

ACKNOWLEDGEMENTS

There are many people that helped and guided me along the way to completing this project and I would like to thank each of them in turn.

To Dr Marco Weinberg, thank you for your support and guidance along the way. You were always available with words of encouragement and insight. Your wealth of knowledge and passion for science is something I will always admire.

To Dr Makobetsa Khati (Shooz), thank you for providing me with the opportunity to do my PhD and for supporting me to take up the opportunities that came my way: FOGARTY fellowship to the USA and attending many meetings. Thank you for always pushing me to give of my best, I know that I am stronger for it.

To Dr John Rossi, thank you for hosting me at the Beckman Research Institute for three months in 2012. You and your team taught me a great deal and for that I am truly grateful.

To the Aptamer lab, past and present, you have made this a really memorable experience. Thank you for all the good times, the laughs, the cakes, the encouragement and the heartfelt conversations. A special thank you goes to Dr Nthato Chirwa (Prof) and Dr Hazel Mufhandu for proof reading my thesis drafts and for providing invaluable feedback.

To Luca, thank you for keeping me grounded, you are my rock. You have always been there to help me through the stressful times with laughter and a brilliant sound track.

To my family, thank you for being there for me when I needed help, support and a push in the right direction. A special thanks to mom and dad for proof reading my thesis even if it meant a google search per page!

Lastly I would like to thank the CSIR Biosciences for funding this project.

PREFACE

A provisional patent application (entitled A CD7 Receptor-internalizing RNA Aptamer, listed inventors are Laura Millroy, Makobetsa Khati and Marco Saul. Weinberg) is being filed through the Wits Enterprise office to protect the invention disclosed here. As such, the research details have not been published in a journal article.

CONFERENCE PRESENTATIONS

The following conference presentations arose from work presented in this thesis.

Laura Millroy, Marco Weinberg, Makobetsa Khati. Selection of internalising aptamers for the targeted delivery of siRNA as a prophylactic against HIV infection, (2012). SASBMB/FASBMB, Drakensburg, Kwazulu Natal, South Africa

Laura Millroy, Marco Weinberg, Makobetsa Khati. Selection of internalising aptamers for the targeted delivery of siRNA as a prophylactic against HIV infection, (2012). AIDS 2012, Washington DC, USA

Laura Millroy, Marco Weinberg, Makobetsa Khati. Selection of internalising aptamers for targeted delivery of anti-HIV siRNA, (2012). EMBO Global Exchange Lecture Course on Innate Immunity, Johannesburg, Gauteng, South Africa

Laura Millroy, Marco Weinberg, Makobetsa Khati. In vivo SELEX-derived anti-CD7 aptamer for the delivery of prophylactic anti-HIV siRNA, (2012). 8th annual meeting of the Oligonucleotide therapeutics society, Boston, MA, USA

The following publications and conference presentations arose from work not presented in this thesis.

Laura Millroy, Hazel Mufhandu, Walter Campos, Makobetsa Khati. Entry inhibition of adult and paediatric HIV-1 subtype C isolates using a shortened synthetic derivative of a gp120 binding aptamer, (2010). Oxford Virology Symposium, Christ Church, Oxford, England

Laura Millroy, Grace London, Robert Veale, Marco Weinberg, Makobetsa Khati. Characterisation and Kinetics of Aptamer Binding to HIV-1 Subtype C gp120, (2011). EMBO HIV Course, Stias, Stellenbosch, Western Cape, South Africa

Grace London, **Laura Millroy**, Maphuti Madiga, Elin Gray, Thandeka Khoza, Lynn Morris and Makobetsa Khati. Isolation, characterisation, and efficacy of novel aptamers against HIV-1 subtype C, (2011). Keystone: Protection from HIV: Targeted Intervention Strategies, Whistlers, British Columbia, Canada

Laura Millroy, Grace London, Robert Veale, Marco Weinberg, Makobetsa Khati. Characterisation and Kinetics of Aptamer Binding to HIV-1 Subtype C gp120, (2011). SA AIDS conference, ICC Durban, Kwazulu Natal, South Africa

OTHER PUBLICATIONS

Millroy, L., and Khati, M. Nucleic Acid Toolkit: Potential Diagnosis and Treatment of Major Infectious Diseases Endemic in Developing Countries (2011) Lambert Academic Press

Khati, M, and **Millroy L**. Chapter 5: Point mutations associated with HIV-1 drug resistance, Evasion of the Immune system response and AIDS pathogenesis. Point Mutations Edited by Colin Logie, (2012) InTech Publishers

ABSTRACT

Aptamers are synthetic nucleic acid molecules designed to bind with high specificity and affinity to a selected target. The aptamer selection method, called the systematic evolution of ligands by exponential enrichment (SELEX), was first described in 1990 and has been adapted for the selection of aptamers for a number of applications. One such application is the selective targeting of cells for therapeutic delivery. This thesis explores this application with the selection and characterisation of internalising aptamers specific to the T lymphocyte specific receptor, CD7. The CD7 receptor is expressed on thymus derived progenitor lymphocytes and remains after T cell activation and expression of the CD4 receptor. As such, the CD7 receptor is a noteworthy target for lymphocyte cancers, HIV-1 and other T lymphocyte tropic viruses.

A heterogeneous pool of internalising CD7-aptamers was enriched through six rounds of positive selection in a stably transduced CD7-HeLa cell line. Aptamers were selected using a modified whole cell SELEX method that selected specifically for internalising aptamers. Aptamer specificity for CD7-HeLa cells over HeLa cells was screened by flow cytometry. CD7 specific aptamers were screened for binding after blocking CD7-HeLa cells with an anti-CD7 antibody. Eight CD7 specific aptamer clones were selected from CD7-HeLa screening for evaluation in Jurkat cells (T lymphocyte cell line endogenously expressing the CD7 receptor). Three aptamer clones showed high level binding to Jurkat cells by flow cytometry (CSIR 3.14, CSIR 3.37 and CSIR 3.42). Kinetic analysis of aptamer internalisation was analysed using flow cytometry and determined to be within the femtomolar range. Aptamer CSIR 3.14 had a dissociation constant of 2.1 fM and an association rate of $4.7 \pm 2.4 \times 10^5$ $Molar^{-1}minute^{-1}$, aptamer CSIR 3.37 had a dissociation constant of 0.23 fM and an association rate of $4.3 \pm 3.3 \times 10^6$ $Molar^{-1}minute^{-1}$ and aptamer CSIR 3.42 had a dissociation constant of 1.1 fM with an association rate of $7.9 \pm 5.1 \times 10^5$ $Molar^{-1}minute^{-1}$. Aptamer CSIR 3.14 internalisation was tracked by confocal microscopy and the kinetics calculated with an association rate of 6.3×10^4 $Molar^{-1}minute^{-1}$ and K_d of 13 fM. Deletions within the CSIR 3.14 sequence that altered the predicted structures significantly reduced the aptamer binding. Combined, the data presented in this thesis identifies aptamer CSIR 3.14 as a lymphocyte specific internalising aptamer with potential for therapeutic delivery.

TABLE OF CONTENTS

Declaration ..... **i**
Acknowledgements ..... **ii**
Preface ..... **iii**
Conference presentations iii
Other publications iv
Abstract ..... **v**
List of figures ..... **x**
List of tables ..... **xii**
List of abbreviations ..... **xiii**

Chapter 1. Literature review **1**
1.1 Introduction **1**
1.2 Aptamer background and development **2**
1.2.1 The discovery of aptamers 2
1.2.2 Aptamers characteristics 4
1.2.3 Aptamer development 7
1.3 Systematic evolution of ligands by exponential enrichment **13**
1.3.1 Recombinant protein selection 13
1.3.2 In silico selection 15
1.3.3 Automation of selection 20
1.3.4 Whole cell selection 20
1.4 Applications of aptamers as tools **26**
1.4.1 Aptamers as therapeutics 26
1.4.2 Diagnostics and biomarker discovery 29
1.4.3 Logic gates and molecular signalling 30
1.5 Aptamers for target specific delivery **33**
1.6 Targeting T lymphocytes through the CD7 receptor **37**
1.7 Thesis scope and objectives **39**

Chapter 2. Development of internalising anti-CD7 aptamers **40**
2.1 Introduction **40**
2.2 Materials and methods **42**
2.2.1 Production of a CD7 receptor gene cloning vector 42
2.2.1.1 Cloning of CD7 receptor gene into chemically competent cells 43
2.2.1.2 Validation of CD7 receptor cloning reaction and plasmid production 43
2.2.2 Transfection to generate a stable cell line expressing surface CD7 receptor 44
2.2.3 Flow cytometry analysis to confirm surface expression of CD7 receptor on generated stable CD7-HeLa cell line 44

2.2.4 Fluorescent microscopy analysis to confirm surface expression of CD7 receptor in generated stable CD7-HeLa cell line ... 45
2.2.5 Selection of internalising anti-CD7 aptamers by whole cell SELEX ... 45
2.2.5.1 Random oligonucleotide library used for aptamer selection ... 45
2.2.5.2 Selection of anti-CD7 aptamers by whole cell SELEX ... 46
2.2.5.3 Cloning and sequencing of RNA anti-CD7 aptamers ... 49
2.2.6 Mammalian cell culture ... 50
2.2.6.1 CEM T lymphocytes ... 50
2.2.6.2 Jurkat T lymphocytes ... 50
2.2.6.3 Jeko-1 B lymphocytes ... 50
2.2.6.4 HeLa cells ... 50
2.2.6.5 CD7-HeLa cells ... 50
2.3 Results ... 51
2.3.1 Production of a stable CD7-HeLa cell line for selection of CD7 specific aptamers ... 51
2.3.2 Selection of internalising anti-CD7 aptamers by whole cell SELEX ... 53
2.4 Discussion ... 61

Chapter 3. Characterisation and optimisation of anti-CD7 aptamers binding exogenously expressed cell surface CD7 receptor ... 63
3.1 Introduction ... 63
3.2 Materials and methods ... 65
3.2.1 Anti-CD7 aptamer production by PCR and in vitro transcription ... 65
3.2.2 Fluorescent labelling of anti-CD7 aptamers ... 65
3.2.3 Flow cytometry analysis of cell surface binding of anti-CD7 aptamers ... 66
3.2.4 Confocal microscopy analysis of anti-CD7 aptamer internalisation ... 67
3.2.5 Confocal microscopy analysis of anti-CD7 aptamer internalisation after pre-blocking of the CD7 receptor ... 67
3.2.6 Computational prediction of the anti-CD7 aptamer secondary structure ... 68
3.2.7 Mammalian cell culture ... 68
3.3 Results ... 69
3.3.1 Anti-CD7 aptamer binding and internalisation specificity to recombinant cell line, CD7-HeLa ... 69
3.3.2 Structure comparison of CD7 specific aptamers ... 74
3.4 Discussion ... 79

Chapter 4. Anti-CD7 aptamers characterisation in T lymphocytes ... 81
4.1 Introduction ... 81
4.2 Materials and methods ... 83
4.2.1 Anti-CD7 aptamer production by PCR and in vitro transcription ... 83
4.2.2 Fluorescent labelling of anti-CD7 aptamers ... 83
4.2.3 Characterisation of endogenous surface expression of CD7 receptor on Jurkat cells ... 83
4.2.3.1 Microscopy analysis ... 83

4.2.3.2 Flow cytometry analysis 84
4.2.4 Anti-CD7 aptamer association to endogenously expressed surface CD7 receptor on T lymphocytes 84
4.2.5 Anti-CD7 aptamer association rates and binding characterisation 85
4.2.5.1 Kinetic analysis by time course assay 85
4.2.5.2 Limit of detection for aptamer association with Jurkat cells 86
4.2.6 Anti-CD7 aptamer internalisation characterisation and localisation 86
4.2.7 Anti-CD7 aptamer kinetics of internalisation 87
4.2.8 Aptamer CSIR 3.14 binding site mutation characterisation 87
4.2.9 Mammalian cell culture 88
4.3 Results 89
4.3.1 Anti-CD7 aptamer internalisation specificity and kinetics to T lymphocyte cell line, Jurkat cells 89
4.3.2 Anti-CD7 aptamer CSIR 3.14 internalisation localisation and kinetics 95
4.3.3 Anti-CD7 aptamer CSIR 3.14 binding site mutation characterisation 101
4.4 Discussion 103

Chapter 5. General discussion 105
5.1 Next generation sequencing and aptamer selection 105
5.2 Therapeutic application of a Lymphocyte specific aptamer 107
5.2.1 T lymphocyte tropic virus treatment: HIV-1 107
5.2.2 T lymphocyte disease targeting: rheumatoid arthritis and leukaemia 110
5.3 Aptamer-siRNA chimeras 112
5.4 Concluding remarks 114

Chapter 6. Appendix 115
6.1 General methods and optimisation results 115
6.1.1 Mini prep kit preparation 115
6.1.2 PCR clean up kit protocol 115
6.1.3 DNA / RNA quantification by spectrophotometry 116
6.1.4 Quantification of fluorescent labelling by spectrophotometry 116
6.1.5 RNA purification using the NucAway clean up kit 116
6.1.6 Phenol chloroform extraction of RNA 117
6.1.7 Polyacrylamide gel electrophoresis of RNA 117
6.1.8 Glycerol stock production 117
6.1.9 Kill curve analysis and optimisation 117
6.1.10 Ligation and transformation methods 119
6.1.11 PCR optimisation for CD7 gene vector production 119
6.1.12 PCR optimisation in SELEX 121
6.2 Confirmation of negative selection by flow cytometry 122
6.3 Statistical information for the phylogenetic tree of aptamer sequences 123

6.4 Characterisation of endogenous surface expression of CD7 receptor on T and B lymphocyte cell lines..... 127
6.4.1 Methods..... 127
6.4.1.1 Microscopy analysis..... 127
6.4.1.2 Flow cytometry analysis..... 127
6.4.2 Results and discussion..... 128
6.5 Surface plasmon resonance analysis of aptamer – CD7 protein interaction. 130
6.5.1 Methods..... 130
6.5.1.1 Recombinant CD7 protein preparation and quantification..... 130
6.5.1.2 Recombinant human CD7 protein immobilisation, pH scouting and regeneration optimisation 131
6.5.1.3 Aptamer binding analysis to recombinant human CD7 protein interaction..... 131
6.5.2 Results..... 132
6.5.2.1 Human recombinant CD7 protein preparation and quantification..... 132
6.5.2.2 Optimisation of protein immobilisation..... 134
6.5.2.3 Aptamer binding to recombinant human CD7 receptor..... 136
6.5.3 Discussion..... 138
6.6 Negative control for aptamer association at 24 hour incubation..... 139
6.7 Aptamer CSIR 3.14 time course imaging of internalisation..... 140

Chapter 7. References..... 141

LIST OF FIGURES

Figure 1-1: Central dogma of molecular biology as proposed by Francis Crick 2
Figure 1-2: Selection of aptamers by SELEX 10
Figure 1-3: Aptamer selection by *in silico* maturation 17
Figure 1-4: Aptamer controlled ribozyme (Aptazyme) 19
Figure 1-5: Whole cell SELEX method overview 23
Figure 1-6: Logic gates and their functions 32
Figure 1-7: Receptor expression during lymphocyte development 38

Figure 2-1: Flow cytometry confirmation of surface CD7 receptor expression 52
Figure 2-2: Microscopy confirmation of cell surface CD7 receptor expression 53
Figure 2-3: Procedure of whole cell SELEX to select internalising aptamers 54
Figure 2-4: Recovery from internalising whole cell SELEX 55
Figure 2-5: PCR amplification of the enriched pool of CD7 specific aptamers 56
Figure 2-6: Vector insert screening using M13 primers 56
Figure 2-7: Maximum likelihood phylogenetic tree of aptamer sequences 58

Figure 3-1: Aptamer specificity to CD7-HeLa cells over HeLa cells 70
Figure 3-2: Aptamer CSIR 3.23, CSIR 3.3 and CSIR 3.53 internalisation specificity 71
Figure 3-3: Aptamer binding competition with the anti-CD7 monoclonal antibody 72
Figure 3-4: Microscopy analysis of aptamer CSIR 3.42 binding to CD7 receptor on CD7-HeLa cells 73
Figure 3-5: Receptor mediated internalisation of aptamer CSIR 3.42 into CD7-HeLa cells 74
Figure 3-6: Computational secondary structure prediction for aptamer CSIR 3.39, CSIR 3.35 and CSIR 3.28 75
Figure 3-7: Computational secondary structure prediction for aptamer CSIR 3.42, CSIR 3.37 and CSIR 3.48 77
Figure 3-8: Computational secondary structure prediction for aptamer CSIR 3.14 and CSIR 3.31 78

Figure 4-1: Validation of surface CD7 receptor expression on Jurkat cells 90
Figure 4-2: Aptamer association with endogenously expressed CD7 receptor on Jurkat cells 91

Figure 4-3: Time course association of aptamer CSIR 3.14, CSIR 3.37 and CSIR 3.42 93
Figure 4-4: Concentration gradient binding analysis of aptamers CSIR 3.14 and CSIR 3.37 95
Figure 4-5: Diagrammatic representation of a Z stack through an image section 96
Figure 4-6: Image slices through an individual cell along the Z axis for localisation of aptamer CSIR 3.14 96
Figure 4-7: Time course of aptamer CSIR 3.14 internalisation 97
Figure 4-8: Orthogram illustrating CSIR3.14 cellular localisation 98
Figure 4-9: Kinetics of internalisation for CSIR 3.14 100
Figure 4-10: Association of aptamer CSIR 3.14 full length, mutants and CSIR 3.14 DNA to Jurkat cells 102

Figure 5-1: HIV-1 genome organisation 108
Figure 5-2: The HIV-1 lifecycle presented with antiretroviral interactions 109

Figure 6-1: Spectrophotometer quantification of labelled aptamer RNA 116
Figure 6-2: Antibiotic gradient for minimum concentration selection 118
Figure 6-3: PCR optimisation for CD7 receptor gene amplification 120
Figure 6-4: Alignment of CD7 receptor plasmid sequences to the GenBank consensus sequence for human CD7 receptor 120
Figure 6-5: Pilot PCR to optimise cycle number for SELEX DNA amplification 121
Figure 6-6: Confirmation of control HeLa selection using flow cytometry 122
Figure 6-7: Confirmation of cell surface expression of CD7 receptor on lymphocytes 129
Figure 6-8: Flow cytometry confirmation of surface CD7 receptor expression 129
Figure 6-9: Recombinant human CD7 protein size verification 133
Figure 6-10: Recombinant human CD7 protein quantification 133
Figure 6-11: Production of CD7 aptamers 134
Figure 6-12: Recombinant human CD7 protein immobilisation pH scouting 135
Figure 6-13: Anti-CD7 antibody binding Recombinant human CD7 protein 135
Figure 6-14: Recombinant human CD7 protein immobilisation stability test 136
Figure 6-15: Immobilisation of recombinant CD7 protein 137
Figure 6-16: Anti-CD7 aptamer binding recombinant protein 137
Figure 6-17: Aptamer binding response units to recombinant CD7 protein 138
Figure 6-18: Time course association of aptamer CSIR 3.31 139
Figure 6-19: Aptamer CSIR 3.14 time course internalisation 140

LIST OF TABLES

Table 1-1: The history of aptamer selection methods.....12
Table 2-1: CD7 specific internalising aptamer clone sequences 59

LIST OF ABBREVIATIONS

A	adenosine
AIDS	acquired immune deficiency syndrome
AICD	activation induced cell death
AMD	age-related macular degeneration
AptaBiD	aptamer-facilitated biomarker discovery
AptaPIC	aptamer-facilitated isolation of proteins from cells
ARV	antiretroviral
ASKAS	aptamer selection by K-mer analysis of sequences
ATP	adenosine triphosphate
AuNP	gold nanoparticle
BSA	bovine serum albumen
BCA	bicinchoninic acid
bp	base-pair
bPrP	bovine prion protein
C	cytosine
CCR5	chemokine (C – C motif) receptor 5
CXCR4	chemokine (C – X – C motif) receptor 4
CD4	cluster of differentiation 4
CD7	cluster of differentiation 7
cDNA	complementary DNA
CHO	chinese hamster ovary
Cy3	cyanine 3
CT	computed topography
DAPI	4',6-diamidino-2-phenylindole
DNA	deoxyribonucleic acid
DNase	deoxyribonuclease
dNTP	deoxynucleoside triphosphate
DMEM	Dulbecco's modified eagle's medium
DMSO	dimethyl sulfoxide
Dox	Doxorubicin
EDTA	Ethylenediaminetetraacetic acid
EI	entry inhibitor
EGFR	epidermal growth factor receptor
ELISA	enzyme linked immunosorbant assay
ELONA	enzyme linked oligonucleotide assay
Env	envelope glycoprotein

EpCAM	epithelial cell adhesion molecule
FAM	6-carboxy-fluorescein
FBS	foetal bovine serum
FITC	fluorescein isothiocyanate
FMN	flavin
G	guanine
gD	envelope glycoprotein
Gem	Gemcitabine
gp120	120 kDa glycoprotein
gp41	41 kDa glycoprotein
HAART	highly active antiretroviral therapy
HA	hemagglutinin
HeLa	Henrietta Lax
HEPES	4-(2-hydroxyethyl)-1-piperazineethanesulfonic acid
HIV	human immunodeficiency virus
HIV-1	human immunodeficiency virus type 1
HSV-2	herpes simples virus type 2
HTS	high throughput sequencing
IC_{50}	concentration for 50 % inhibition
II	integrase inhibitor
kd	ligand dissociation
ka	ligand association
K_d	dissociation constant
kDa	kilo dalton
LB	Luria Bertani
MAb	monoclonal antibody
MG	myasthenia gravis
mRNA	messenger RNA
mPrP	mouse prion protein
Mw	molecular weight
NAbs	neutralising antibodies
NRTI	nucleoside reverse transcriptase inhibitor
NNRTI	non-nucleoside reverse transcriptase inhibitor
PBS	phosphate buffered saline
PCR	polymerase chain reaction
PEG	polyethylene glycol
PI	protease inhibitor
PI 3K	phosphatidylinositol 3-kinase
PFA	paraformaldehyde
PSMA	prostate specific membrane antigen
RA	rheumatoid arthritis

RNA	ribonucleic acid
RNAi	RNA interference
RNase	ribonuclease
ROI	region of interest
rpm	revolutions per minute
RPMI	Roswell Parks Memorial Institute Media
RSV	Rous Sarcoma Virus
RU	response units
SDS	sodium dodecyl sulphate
SDS-PAGE	SDS – polyacrylamide gel electrophoresis
SELEX	systematic evolution of ligands exponential enrichment
siRNA	short interfering ribonucleic acid
SPR	surface plasmon resonance
ss	single-stranded
T	thymine
TECS-SELEX	Target expressed on cell surface – SELEX
Theo	theopholine
TTF1	thyroid transcription factor 1
tRNA	transfer ribonucleic acid
T20	enfurvirtide, fuzeon
U	uracil
UV	ultraviolet
VEGF	vascular endothelial growth factor
ΔG	Gibbs free energy

Chapter 1. LITERATURE REVIEW

1.1 INTRODUCTION

The discovery and application of aptamers has changed the nucleic acid research landscape in a dramatic way. Aptamers are nucleic acid sequences, usually RNA or DNA, that make use of the structural properties of nucleic acid polymers for target specific interactions. Before the discovery of aptamers, RNA has long been identified as having information storage, structural and catalytic properties. Advances in molecular biology methods has allowed for the routine conversion by reverse transcription of RNA to complementary DNA (cDNA), followed by DNA amplification with the polymerase chain reaction (PCR). These techniques paved the way for the development of a method to efficiently select and characterise aptamers. Aptamers have since been applied to a number of applications including therapeutics, biomarker discovery, diagnostics and targeted delivery.

The work contained in this thesis will focus on the development of new tools for targeting T lymphocytes for drug development and diagnostics. Specialised cell-internalising aptamers were identified as the tool of choice and the pan leucocytic CD7 receptor as the target. The rationale for selecting the CD7 receptor is covered in detail in section 1.5. Current T lymphocyte targeting strategies have previously made use of aptamers that target the CD4 receptor. This receptor is abundantly expressed on a number of different cell types but only after maturation which can limit gene therapy strategies where precursor cells would be preferable. New CD7 receptor targeting aptamers will aid in the development of novel targeted therapeutics as well as diagnostics. The literature review will survey the history of the aptamer field and the different selection methods for aptamer development. The various applications of aptamer technology will be described and how these have been applied in clinical development followed by an in depth discussion of aptamer mediated target specific delivery. The biophysical properties of the CD7 receptor will be discussed along with a rationale for targeting it.

1.2 APTAMER BACKGROUND AND DEVELOPMENT

1.2.1 THE DISCOVERY OF APTAMERS

RNA was initially thought to be the intermediate step in the Central Dogma of molecular biology which describes the flow of information in biological systems. The Central Dogma was first stated by Francis Crick in 1958 and later published in Nature in 1970 (Crick 1970). Crick described how the flow of information in a cell would travel from DNA to RNA to protein (Figure 1-1). The notion of information transfer from RNA to DNA and from RNA to RNA was conceived as possible under certain circumstances. While the transfer of information from protein to DNA or RNA was classed as an unknown transfer and believed not to occur.

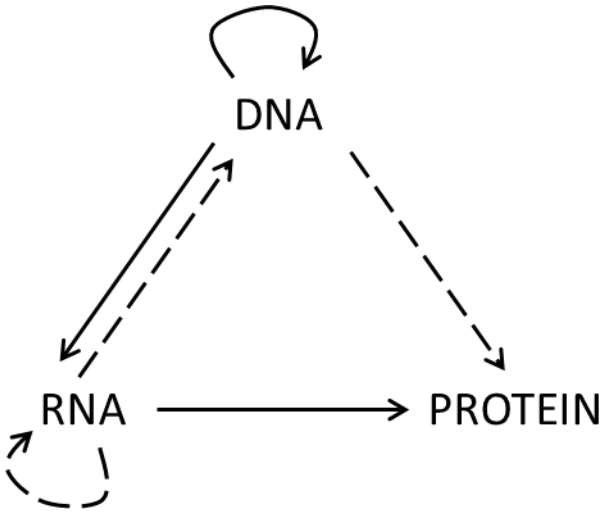

FIGURE 1-1: CENTRAL DOGMA OF MOLECULAR BIOLOGY AS PROPOSED BY FRANCIS CRICK
This illustration is redrawn from the original figure by Francis Crick in the 1970 Nature publication (Crick 1970). The flow of information is defined by three categories: 1. known transfers of information illustrated by a solid arrow, 2. possible transfers illustrated by a dotted arrow and 3. unknown transfers indicated by an absent arrow.

Although there was speculation that RNA may perform functions other than information storage (Crick 1968; Orgel 1968), there was no experimental validation of this for a number of years. Two ground breaking, independent studies showed RNA to have catalytic properties in the absence of protein. These discoveries lead to Thomas Cech and Sydney Altman being awarded the 1990 Nobel Prize in chemistry. Sydney Altman identified the importance of the RNA component of RNAse P in his work on tRNA in *E. coli* (Guerrier-Takada, Gardiner et al. 1983) and Thomas Cech discovered an RNA enzyme

capable of catalysing its own splicing (Kruger, Grabowski et al. 1982). This lead to the establishment of the RNA World Hypothesis in which Walter Gilbert proposed the existence of a world predating DNA and protein where life existed as RNA alone (Gilbert 1986). With an increase in nucleic acid research and the general acceptance that not all RNA is destined to be translated into proteins, the Central Dogma evolved.

RNA and DNA were identified as having the ability to modulate gene expression and have been applied in both functional genomics and therapeutics. This modulating function was derived principally from the ability of nucleic acids to hybridize through Watson-Crick complementarity. Initially, single stranded DNA (ssDNA) was shown to inhibit RNA transcription in a cell free system (Paterson, Roberts et al. 1977). Later, this was applied in cell culture where a synthetic ssDNA sequence was shown to inhibit viral production in chick embryo fibroblast tissue culture (Zamecnik and Stephenson 1978). Zamecnik et al. identified a repeated sequence in the genome of Rous sarcoma virus (RSV) and synthesised a 13 nucleotide complementary DNA strand. When the short nucleotide sequence was added to RSV infected fibroblast tissue culture, viral production was significantly reduced. This study has been credited as the first demonstration of antisense technology and introduced the term "hybridon" to describe the inhibitory oligonucleotides. Other groups, at the same time, were working in the same field of synthetic oligonucleotides and noted similar effects in cell culture (Tennant, Farrelly et al. 1973; Miller, Braiterman et al. 1977; Simons and Kleckner 1983). These studies identified that although oligonucleotides could function as gene modulators, their persistence *in vitro* and thus *in vivo* was problematic because of nuclease digestion. In order to avoid the effects of ubiquitous nuclease activity, chemical modifications to the oligonucleotides were introduced. These modifications needed to allow for nuclease resistance while not inhibiting oligonucleotide inhibitory activity. The modifications can be classed into three groups: the use of unnatural bases, modified phosphate backbone and modified 2′ group. Oligonucleotide modification will be discussed in greater detail in section 1.2.3 but it is important to note that methods of stabilising oligonucleotides *in vitro* were being developed before aptamer technology was established. The development of modified nucleotides allowed for the extension of the RNA half-life and, as such, its usability *in vitro*. This facilitated the development of the field of RNA research as a whole and together with advances in molecular biology techniques, was essential for the development of aptamers.

The *in vitro* evolution of nucleic acids was first reported in a cell free system in the 1960s (Mills, Peterson et al. 1967). The RNA genome of the Qβ bacteriophage evolved *in*

vitro to reduce complexity for increased efficiency of copy rate by the viral replicase. This method was later applied to select for sequences that conferred resistance to ethidium bromide (Saffhill, Schneider-Bernloehr et al. 1970). Although this discovery showcased the researcher's ability to direct the evolution of oligonucleotides towards a function, aptamer selection was not described for another 20 years. This is because, the improved molecular techniques allowing for the generation of cDNA, the amplification of DNA by PCR and the advances in synthesising oligonucleotides were fundamental in the development of the eventual aptamer selection method.

It was shown that molecules with high affinity and specificity could be generated from a starting pool of random oligonucleotides in which every sequence position on a strand can be occupied by any of the four bases; adenine, cytosine, guanine or uracil. An efficient method to select for molecules with affinity to a particular target requires the removal of the non-binding molecules from the binding molecules. Evolution of the high affinity and specificity molecules is achieved after rounds of amplification and selection against a target. This *in vitro* method for the selection of nucleic acids was used to develop molecules specific to organic dyes (Ellington and Szostak 1990) and T4 DNA polymerases (Teurk and Gold 1990) and was the first example of aptamer selection. The method for aptamer selection was termed the systematic evolution of ligands by exponential enrichment (SELEX). This synthetic process changed the scope of nucleic acid research by enabling the development of nucleic acid molecules specific to an abundance of biologically relevant targets previously unattainable. The selection relies on the evolution of a pool of random oligonucleotides towards specificity allowing for non-immunogenic and toxic molecules to be targeted.

1.2.2 APTAMERS CHARACTERISTICS

Aptamers have been colloquially termed "synthetic antibodies" due to their similar mode of action. Both antibodies and aptamers have been used as affinity ligands for purification and labelling as well as therapeutic molecules and in various diagnostic applications. Aptamers have been shown to be able to replace antibodies in various applications including affinity chromatography as affinity ligands (Hage 1999) and recently, the first aptamer to a plant virus was described that was shown to outcompete commercially available antibodies in a variety of tests (Balogh, Lautner et al. 2010). This study identified DNA aptamers specific to the viral coat proteins of two apple stem pitting virus isolates (MT32 and PSA-H) and tested them in a number of diagnostic tests usually performed with antibodies. The aptamers were

able to diagnose the viral infection from crude extracts in all tests emphasising the potential of aptamers as recognition molecules in diverse immunoassay methods. The advantages and limitations of antibodies for therapeutic and diagnostic use has been reviewed elsewhere (Leavy 2010). This section will focus on the characteristics of aptamers that make them molecules of choice for therapeutics, diagnostics and molecular tools.

For both diagnostics and therapeutics, aptamers that bind strongly with low dissociation constants are preferred. The dissociation constant of a molecule is calculated from the ratio of the molecule and its ligand in a bound state to the molecule and its ligand in the unbound state illustrated in the equation below. As such, the dissociation constant gives insight into the strength of the bond and the stability of the bound state. The lower the dissociation constant, the stronger the bond and the more the molecule tend toward the bound state with the ligand.

$$K_d = \frac{[A] + [B]}{[AB]}$$

K_d = Dissociation constant

[A] = Concentration of molecule A

[B] = Concentration of ligand B

[A+B] = Concentration of molecule A bound to ligand B

Aptamers bind with very tight association to their ligand and have dissociation constants ranging from low picomolar to low nanomolar (O'Sullivan 2002; Zhang, Blank et al. 2004). For both therapeutic and diagnostic applications, aptamers with such low dissociation constants will be able to bind to their targets for longer. This would allow for a sustained blocking of a target molecule such as the one involved in viral entry or strong labelling of a disease maker for identification and diagnosis. As much as target affinity and sustained binding are important factors for application of aptamers, so is target specificity. High specificity is important for all aspects of aptamer application. In diagnostics, high specificity helps avoid misdiagnosis. As molecular tools, high specificity would allow for accurate labelling of specific proteins for identification or purification. In therapeutics,

aptamers are used as targeting or effector molecules. Either of these requires high specificity to avoid off target side effects and toxicity. Aptamers have been shown to be able to discriminate between targets with subtle structural differences such as isoforms of a protein (Jenison 1994; Gopinath 2006) and are able to discriminate between targets based on subtle structural changes such as the presence or absence of a methyl or hydroxyl group (O'Sullivan 2002).

The size of aptamers is another important consideration for their downstream application. Aptamers are roughly 30 kDa and can be reduced in size by truncation, which makes them relatively small molecular tools when compared to antibodies. Their small size allows for their adoption into miniaturised diagnostic systems such as biosensors and nanoparticle diagnostics (Discussed further in section 1.4.2). For therapeutic application, aptamer small size allows for their transport into biological compartments which allows for a diverse range of molecules that can be targeted. This however, also results in rapid renal clearance and reduced circulating time which need to be overcome to increase their functional use as a therapeutic (Dassie, Liu et al. 2009). The circulating time of an aptamer can be increased by increasing the effective size of the molecule by conjugating it to another molecule with a larger molecular weight such as poly(lactic acid)-block-polyethylene glycol (PEG) (Leverett 1971) or liposomes (Levere and Pindyck 1971). A thoilated aptamer conjugated to liposomes had the same circulation time as the liposome alone but had increased specificity resulting in rapid accumulation at the tumour site in *in vivo* studies (Levere and Pindyck 1971). The addition of a 20 kDa PEG was shown to increase the *in vivo* circulating time of an RNA aptamer from under 35 minutes to over 30 hours (Dassie, Liu et al. 2009). These chemical modifications can be included at different stages of aptamer development and can significantly increase the cost of production. A lot of research has gone into the effects of nucleotide modifications and the possibility of inducing an immune response. To date, no aptamers have shown immunogenicity in the animal trials published so far which provides support for the use of modified nucleotides in therapeutics without adverse effects caused by the modifications. Aptamers used for targeted delivery of therapeutics can be modified at either end to ensure site specific interactions with the drug carrier molecule (Leverett 1971). In addition, the synthetic evolution of aptamers allows for their selection against a wide range of macromolecules including those that have low immunogenicity or are toxic (O'Sullivan 2002; Wei and Ling-Yun 2009). Finally, aptamers can be stored long term at ambient temperature (Wei and Ling-Yun 2009) which is important

for the commercialisation of aptamers as it allows for shipping and storage of aptamer based products at room temperature.

1.2.3 APTAMER DEVELOPMENT

Aptamer selection methods have evolved from the initial discovery in 1990 to include a number of different targeting strategies. However diverse the techniques used in the selection, the core experimental design of aptamer selection remains the same. This section will cover the central aspects of aptamer selection and design including library selection, chemical modification and the main techniques. An overview of the history of aptamer selection methods will be discussed as an introduction to the more in depth explanation of aptamer selection in section 1.3.

The first aspect of aptamer selection is the design of the starting library. The starting library contains random chemically synthesised DNA molecules. The oligonucleotides are generated with a length of random nucleotides flanked by fixed sequences. The fixed sequences provide the region for annealing of primers for amplification of the sequences by PCR. When selecting for RNA aptamers, the DNA library needs to be transcribed into RNA before the selection. As such, the fixed sequences for RNA aptamers will need to include an additional promoter sequence for the T7 polymerase typically used for *in vitro* transcription. The promoter region is usually included in the primer sequence to ensure that it is incorporated in the pool at each round. The length of the random region is directly linked to the complexity of the library (Zhang, Blank et al. 2004) as this allows for increased diversity in the aptamer structures. With a 40 nucleotide random region, the DNA / RNA library can theoretically be composed of 10^{24} distinct molecules. From this level of sequence complexity, the number of possible structures is far greater as a single oligonucleotide strand can fold to form a number of different structures. An increase in library complexity may be advantageous for the identification of the best candidate aptamers.

Native RNA molecules have a very short half-life in serum and are not suitable for downstream therapeutic application. As such, modifications by chemical synthesis are required for nucleic acid aptamers to be made resistant to nuclease induced degradation. For the selection of RNA aptamers, 2′ Fluoro modified pyrimidines are included during the transcription of the RNA library. Other modifications such as the 4′thioRNA are incorporated after aptamer selection as they are generated by chemical synthesis and cannot be

incorporated during *in vitro* transcription. Modifications to the library increase the overall cost of the selection and must not interfere with the functioning of the amplification and transcription enzymes used in the selection. This limits the nucleic acid modifications that can be included at this stage as it relies on the availability of mutant polymerases that can incorporate the modified bases. Modifications post selection could disrupt aptamer binding as the structure of the aptamer may change due to the modified base side chains. Regardless of the strategy used, modified nucleotides need to be included in the aptamer sequence to increase the stability not only for *in vitro* handling but also for *in vivo* applications.

Stabilising modifications include alternate development techniques such as the production of circular RNA aptamers (Umekage and Kikuchi 2009), using locked nucleic acid modifications (Darfeuille 2004) or chemical modifications such as 2′ Fluoro, 2′-*O*-MeRNA and 4′ thioRNA. The chemical modification of nucleic acids dates back to the development of therapeutic antisense RNAs in the 1960s. Eckstein et al. are credited with generating the first generation of nucleotide modification for antisense application (De Clercq, Eckstein et al. 1969). The study generated a phosphothioated oligonucleotide by replacing a non-bridging oxygen atom in the phosphate backbone with a sulphur atom. This substitution significantly increased the nucleotide resistance to pancreatic nuclease by up to 100 times. This modification was applied to a number of antisense molecules with continued efficacy and a greatly increased half-life *in vitro* and *in vivo* (Matsukura, Shinozuka et al. 1987; Agrawal, Temsamani et al. 1991). Since then, additional modifications have been introduced including alkyl modifications of the 2′ position of the ribose sugar such as 2′-*O*-Me and 2′ Fluoro modifications. The chemical modification of oligonucleotides has been widely adopted in all nucleic acid applications due to their inherent resistance to nuclease degradation and favourable synthesis and hybridisation properties (Chan, Mobley et al. 1997; Ma, Lie et al. 1997; Jhaveri 1998; Xu, Chenna et al. 2012). The 2′ FluoroRNA modified bases have been included in aptamer selection from the beginning as they can be incorporated by unmodified polymerases. A study of human polymerases α and γ found that the 2′ FluoroRNA modified bases could be incorporated into a growing strand while 2′ *O*-MeRNA modified bases could not. Although this is an advantage for selection using 2′ FluoroRNA modified bases, it may have negative implications as a therapeutic if the modified bases are recycled in the human body. However, at this stage no adverse effects have been reported due to this. The aptamer based therapy on the market, Macugen®, was selected with 2′ FluoroRNA modified bases and later chemically synthesized with 2′-*O*-MeRNA modified

bases for extra stability (Moore, Bunka et al. 2011). The efficiency of a polymerase using modified nucleotides as compared to wild type nucleotides is low. As such, Sousa and Padilla conducted a study where they mutated the active site of the T7 polymerase to identify a modified enzyme that could incorporate 2′-deoxy (DNA) nucleotides along with the 2′-hydroxy (RNA) nucleotides (Sousa and Padilla 1995). They discovered a T7 polymerase with a phenylalanine in place of a tyrosine at position 639 (Y693F variant) in the active site resulted in an enzyme that could incorporate 2′-deoxy (DNA) nucleotides without affecting promoter specificity or enzyme activity. This lead to the discovery that other 2′ modified nucleotides could be incorporated by the Y639F variant of T7 polymerase, including 2′ Fluoro modified nucleotides (Huang, Eckstein et al. 1997). This modified polymerase is now commercially available and is widely used to generate modified RNA by *in vitro* transcription. Further development of this polymerase lead to the identification of a double mutant Y639F/H784A T7 polymerase able to incorporate bulkier 2′-position modified pyrimidines such as 2′-azido and 2′-O-methyl modifications (Padilla and Sousa 1999). The most commonly used modified nucleotides in the selection of aptamers are 2′ Fluoro pyrimidines. Aptamers with 2′-*O*-MeRNA modified bases can be selected directly (Burmeister, Lewis et al. 2005) while other modifications such as 4′thioRNA modified bases or bases with multiple modifications such as 2′ Fluoro-4′thioRNA or 2′-*O*-Me-4′thioRNA can only be added after selection, as they need to be incorporated by chemical synthesis.

A comprehensive study was conducted on nuclease stability of different single stranded modifications, 2′ Fluoro-4′thioRNA, 2′-*O*-Me-4′thioRNA, 2′ FluoroRNA, 2′ *O*-MeRNA, native RNA and native DNA (Vianini, Palumbo et al. 2001). Native RNA was degraded in 50 % human serum within ten minutes while the 2′ FluoroRNA and 2′ *O*-MeRNA had half-lives of 53.2 minutes and 187 minutes respectively. The best performing modification was the 2′-*O*-Me-4′thioRNA with a half-life of 1 631 minutes in 50 % human serum. Although the 2′ *O*-MeRNA and 2′-*O*-Me-4′thioRNA modifications can increase the RNA half-life greater than that of the 2′ FluoroRNA, there is no commercially available RNA polymerase able to incorporate these modified bases during an *in vitro* transcription experiment. As such, 2′ fluorinated pyrimidines were included in this work to protect against nuclease degradation and to allow for *in vitro* transcription of the various RNA molecules. Further modification and stabilisation can be investigated once a putative aptamer has been identified.

Once the library composition and complexity has been determined it can be used in the selection of specific aptamers (Figure 1-2). For the first step, the library is incubated with a target molecule in an appropriate buffer. The target molecule may be a recombinant protein, a whole cell or whole bacterium amongst others. This is an important consideration, as it will impact on the potential downstream applications of the aptamer. The bound and unbound molecules are partitioned from the target and the bound molecules are amplified by PCR (Sampson 2003). The first selection to introduce cell culture was in 1997, almost a decade after the initial introduction of aptamer selection. This approach used RNA processing signals in culture to identify splicing enhancer sites *in vivo* (Coulter, Landree et al. 1997). More recently a method of selection specific for aptamers able to internalise into cells was described (Thiel, Hernandez et al. 2012). In this internalising whole cell SELEX method, internalised molecules are separated out and amplified by PCR. A similar method has been used in this thesis to develop potential therapeutic delivery aptamers.

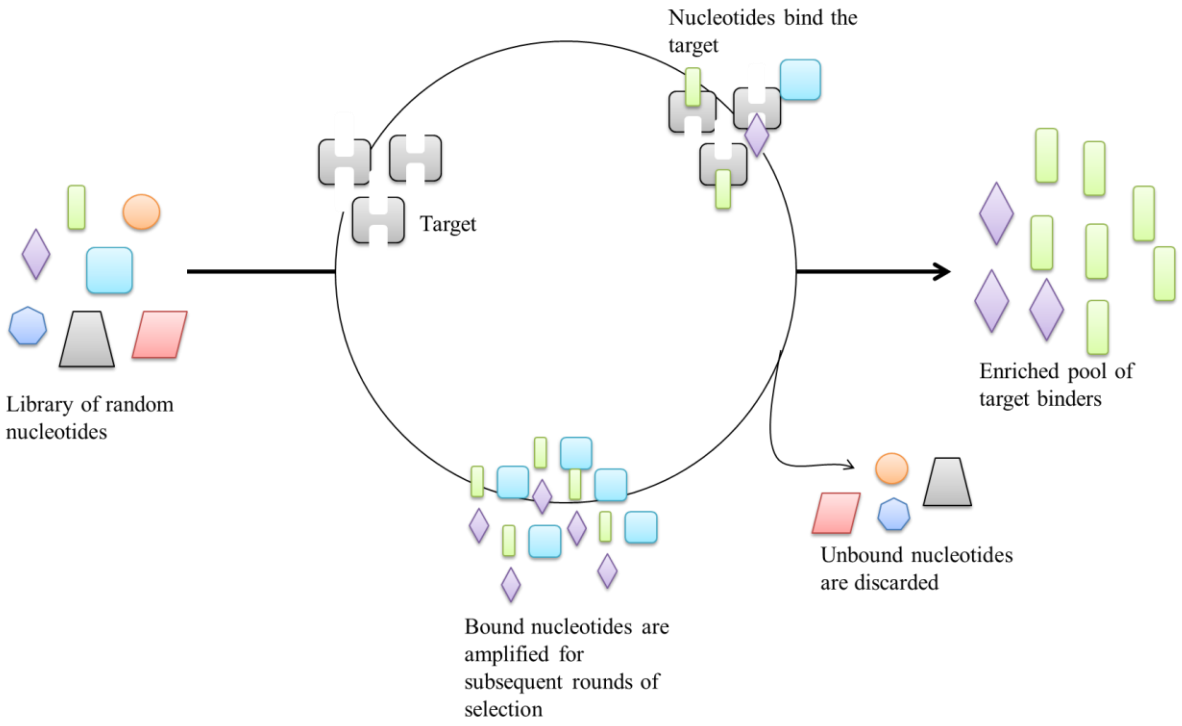

FIGURE 1-2: SELECTION OF APTAMERS BY SELEX

A library of random oligonucleotides is incubated with the target molecule. The unbound nucleotides are partitioned and discarded while the bound nucleotides are retained for amplification. The amplified nucleotide pool is used as the input for the next round of selection. After a number of rounds of selection an enriched pool of target binding aptamers is recovered.

Cycles of selection and amplification are continued until aptamers that strongly interact with the protein are selected. A bioinformatics analysis of aptamer sequences found

that the number of unique sequences identified per round decreases dramatically after four rounds of selection with sequence enrichment reaching a plateau after five rounds of selection (Thiel, Bair et al. 2012). This highlights the evolution of the aptamer pool during the selection process where the complexity decreases as the specificity increases. By sequencing after each round of selection, the true complexity of the pool can be monitored. Using this method the saturation point of the SELEX can be identified and the selection stopped at the point with greatest enrichment and lowest diversity. This direct approach is both labour intensive and high cost and as such may not be the most efficient for monitoring the selection. The enrichment of the aptamer pool can be determined indirectly by calculating the percentage of input library that bound the target of interest. As the aptamer pool increases in specificity the recovery percentage increases.

A number of modified selection methods have been developed including *in silico* methods, whole cell aptamer selection, internalising aptamer selection and an automated SELEX platform amongst others (Table 1-1). An overview of some of these, more prominent, SELEX methods will be discussed in detail in section 1.3. These selection methods have led to the development of a variety of aptamers capable of binding an array of macromolecules with varied functional characteristics. Aptamers have been developed against a number of clinically relevant disease markers including Protein Tyrosine Kinase 7 (PTK7) receptor highly expressed in colon carcinomas (Huang, Shangguan et al. 2009); transcription factor NF-κB which when blocked enhances the activity of anticancer and antiviral agents (Lebruska and Maher 1999); culture filtrate protein 10 (CFP10) an important virulence factor protein expressed by *Mycobacterium* Tuberculosis (Rahimi, Murakami et al. 2009); the trans-activating response (TAR) RNA element of HIV-1 (Watrin, Von Pelchrzim et al. 2009); the extracellular matrix protein Tenascin-C highly expressed in various solid tumours (Hicke, Stephens et al. 2006); the HIV surface glycoprotein gp120 (Khati 2003; Zhou, Swiderski et al. 2009); nucleolin, a BCL2 mRNA binding protein overexpressed on the surface of breast cancer cells (Cao, Tong et al. 2009) amongst many others. To date, no aptamers have been selected against the CD7 receptor found on the surface of T lymphocytes. This work is the first to develop such aptamers and made use of a modified selection method to select for internalising aptamers.

TABLE 1-1: THE HISTORY OF APTAMER SELECTION METHODS

Year	SELEX Name	Major Modification / Improvement	Reference
1990	Classical Selection	Aptamers selected against recombinant proteins	(Ellington and Szostak 1990; Teurk and Gold 1990)
1994	Counter selection	Negative selection using an analogue of the target for increased sensitivity	(Jenison, Gill et al. 1994; Geiger, Burgstaller et al. 1996)
1995	Blended SELEX	Improved the nuclease resistance of the starting library by including non-nucleic acid regions to the 3′end	(Smith, Kirschenheuter et al. 1995)
1995	Photo SELEX	Modified the library to include photosensitive nucleotides that react under UV light to covalently crosslink with molecules, increasing aptamer specificity	(Jensen, Atkinson et al. 1995)
1996	Spiegelmers	Generates mirror image RNA aptamers that are nuclease resistant	(Klussmann, Nolte et al. 1996)
1997	*In vivo* SELEX	Selected aptamers within mammalian cells	(Coulter, Landree et al. 1997)
1998	Chimeric SELEX	Generated bi-functional aptamers by generating chimeras of different aptamers	(Burke and Willis 1998)
1999	SELEX against live organism	Describe the selection of aptamers against the surface protein of live *Trypanosoma brucei* parasites. Highlighted use of selection method in diagnostic development	(Homann and Goringer 1999)
2000	Signalling Aptamer	Incorporated fluorescent dyes in aptamer sequence to detect molecules in solution	(Jhaveri, Rajendran et al. 2000)
2001	Toggle SELEX	Change target during selection to produce a “polyclonal” aptamer with cross reactivity	(Bianchini, Radrizzani et al. 2001; White, Rusconi et al. 2001)
2003	Flow cell SELEX	Aptamers were generated by surface plasmon resonance technology	(Khati 2003)
2003	Beacon Aptamer SELEX	Incorporated a fluorophore and quencher system to identify aptamer beacons	(Rajendran and Ellington 2003)
2003	Tailored SELEX	Reduced the constant regions by ligation and removal of primer sites allowing for shorter aptamers to be	(Vater, Jarosch et al. 2003)

Year	SELEX Name	Major Modification / Improvement	Reference
		selected	
2004	CE-SELEX	Capillary electrophoresis based selection reduced number of rounds needed for selection of high specificity aptamers	(Mendonsa and Bowser 2004)
2005	FluMag SELEX	Used magnetic beads for rapid and efficient partitioning	(Stoltenburg, Reinemann et al. 2005)
2005	Automated SELEX	Making use of microfluidics and magnetic beads to generate an automated SELEX machine	(Eulberg 2005)
2006	TECS-SELEX	Described a method to select for aptamers specific to cell surface expressed proteins	(Ohuchi, Ohtsu et al. 2006)
2006	Non-SELEX (adapted from CE-SELEX)	Removed the amplification step and used rounds of capillary electrophoresis to select for specific molecules.	(Berezovski, Musheev et al. 2006)
2007	MonoLEX	Selection of aptamers in a single round of selection (describe a protocol using microscopy and a protocol using capillary chromatography)	(Nitsche, Kurth et al. 2007; Peng, Stephens et al. 2007)
2008	Cell Specific SELEX	Selection of aptamers to specific cell receptors incorporating mass spectrometry and flow cytometry (adapted from Homann 1999)	(Shangguan, Cao et al. 2008)
2009	*In silico* SELEX	Selection of aptamers by computational modelling of aptamer structures	(Chushak and Stone 2009)
2012	Internalising cell SELEX	Specifically selects for internalising aptamers	(Thiel, Bair et al. 2012)

1.3 SYSTEMATIC EVOLUTION OF LIGANDS BY EXPONENTIAL ENRICHMENT

1.3.1 RECOMBINANT PROTEIN SELECTION

The traditional SELEX method selects aptamers against recombinant proteins. The first descriptions of this method selected for RNA aptamers (Ellington and Szostak 1990; Teurk and Gold 1990) and DNA aptamers were only described two years later (Ellington and Szostak 1992). In this later publication, Ellington et al isolated DNA aptamers in a similar

way to the previously described RNA aptamer selection method. This study identified that the DNA aptamer binding was sequence and ligand specific and depended on specific folding of the single stranded DNA. When *in vitro* transcribed to RNA, the aptamers no longer bound their target. Ellington et al proposed the use of DNA aptamers for pharmaceutical applications in place of the RNA aptamers due to the inherent instability of RNA. However, the addition of 2′ stabilising nucleotides has made RNA aptamers easier to work with. In addition, RNA aptamers have more potential for structural diversity with more non-canonical RNA-RNA interactions. As such, a number of aptamers being developed for pharmaceutical application are RNA aptamers including, amongst others, the only commercially available aptamer therapeutic, Macugen®. The traditional selection method was improved a couple of years later when Jenison et al proposed a counter selection method to improve aptamer sensitivity (Jenison, Gill et al. 1994). The study proposed making use of an analogue to the target for the negative selection to ensure that the resulting aptamers are capable of distinguishing minor differences in structure. Additional modifications to the traditional method have occurred over the years to improve on aptamer nuclease resistance (Smith, Kirschenheuter et al. 1995; Klussmann, Nolte et al. 1996), to increase aptamer specificity (Jensen, Atkinson et al. 1995) as well as improved partitioning methods (Mendonsa and Bowser 2004; Stoltenburg, Reinemann et al. 2005).

An appropriate partitioning method is essential for specific, high affinity aptamers to be selected. The evolution of the random oligonucleotide pool towards an enriched high specificity and affinity library of aptamers is directly dependent on the ability to remove non-specific aptamers from each round of selection. The failure of the partitioning method to remove all unwanted sequences results in a final aptamer pool containing non-specific aptamer sequences and leads to increased post SELEX characterisation. The partitioning method chosen depends on the optimal conditions of the target protein and can help determine the appropriate negative selection to be used. The aptamer protein complex can be separated from unbound DNA by passing the reaction through an electrophoresis capillary. The electrophoretic mobility of aptamer alone is greater than that of a complex allowing for elution at different time points (Javaherian, Musheev et al. 2009; Tran, Janssen et al. 2010). When making use of a nitrocellulose membrane for partitioning it is essential to negatively select the library against the membrane before starting the selection (Rahimi, Murakami et al. 2009). This helps to prevent the selection of aptamers specific to the membrane, diluting out the target specific aptamers. Aptamer selection using surface plasmon resonance (SPR)

makes use of an empty flow cell for negative selection. Protein is immobilised on a flow cell and an empty flow cell is activated and blocked in the same way. The oligonucleotide library is injected over both flow cells but binding aptamers are recovered only from the chip with immobilised protein (Jones, Clancy et al. 2006). Another aptamer partitioning method involves the use of magnetic beads (Murphy, Fuller et al. 2003). Protein is loaded onto the magnetic beads and incubated in a solution with the library. The reaction tubes can be placed against a magnet allowing for easy removal of the supernatant containing unbound sequences. As the application for aptamers in diagnostics and therapeutics increased, new methods of selection have been developed. Whole cells over expressing receptors were introduced in place of selecting against the recombinant receptor protein in order to select for aptamers using a target that more closely resembles the natural form, computational modelling has been used to preselect aptamers with affinity to a target protein, the selection process has been automated to increase turn over and reduce labour intensity amongst others. These adaptions to the selection process will be discussed further in the following sections.

1.3.2 IN SILICO SELECTION

In silico selection of small peptide inhibitors has been described in which modelling software has been used to predict a structure able to bind a preferred target (Yagi, Terada et al. 2007). The available modelling software makes use of the inherent properties of proteins provided by their amino acid side chains (hydrophobicity, acidity, charge and energy) to predict the interaction between two molecules and the possibility of different bonds. While these programs are quite well defined for small molecules and peptides, no such modelling software is available for nucleic acids. Recent developments in RNA modelling have introduced methods for 3D structure prediction of short RNA molecules (Das and Baker 2007; Ding, Sharma et al. 2008; Parisien and Major 2008). These however, are computationally intensive and not yet simple to use. Nucleic acid modelling is generally limited to the prediction of secondary structures based on one or multiple mathematical algorithms. The minimum free energy algorithm determines a single structure with the lowest free energy and identifies it as the optimal structure (Zuker 2003). The partial function algorithm predicts the base pairs according to thermodynamic properties of the binding (McCaskill 1990). The suboptimal folding algorithm provides a number of structure possibilities with free energies within a defined energy range (Wuchty, Fontana et al. 1999).

A recent publication highlighted the selection of aptamers by *in silico* modelling of aptamer structures (Chushak and Stone 2009). This approach used both the secondary structure prediction and 3D modelling to identify possible aptamer candidates. The RNA was docked to the target protein *in silico* to validate the selection according to known aptamer binding crystal structures. This *in silico* selection is proposed as a method to generate a library for a traditional SELEX that is conditioned towards the target. Although a novel approach, this method has not been widely adopted. The reduction of the complexity of the randomised pool before selection may hamper the evolution of the selection. This elaborate method of generating a directed library increases the complexity of the SELEX process while adding limited benefit as even a complex library will bias towards the target after the first round of selection. A number of other *in silico* methods have been more widely accepted in the evolution of optimal aptamers. As the traditional SELEX can result in a number of molecules with limited binding affinity, an *in silico* maturation step after selection has been proposed (Brunhouse 1971; Levere 1971; Pindyck, Kappas et al. 1971). For this, aptamers shown to have activity are ranked and are used as "parent strands" for the evolution. The activity is measured depending on the characteristics, dissociation constants calculated by a binding assay (usually SPR) and ranked according to the tightness of fit. Inhibition is determined by an inhibition assay and ranked according to the 50 % inhibitory concentration (IC_{50}). These "parent" aptamers are then mutated *in silico* to produce new aptamers with features from the best binders. The new aptamers are screened for binding ability or inhibition and the *in silico* maturation process is continued until an improved aptamer is discovered (Figure 1-3).

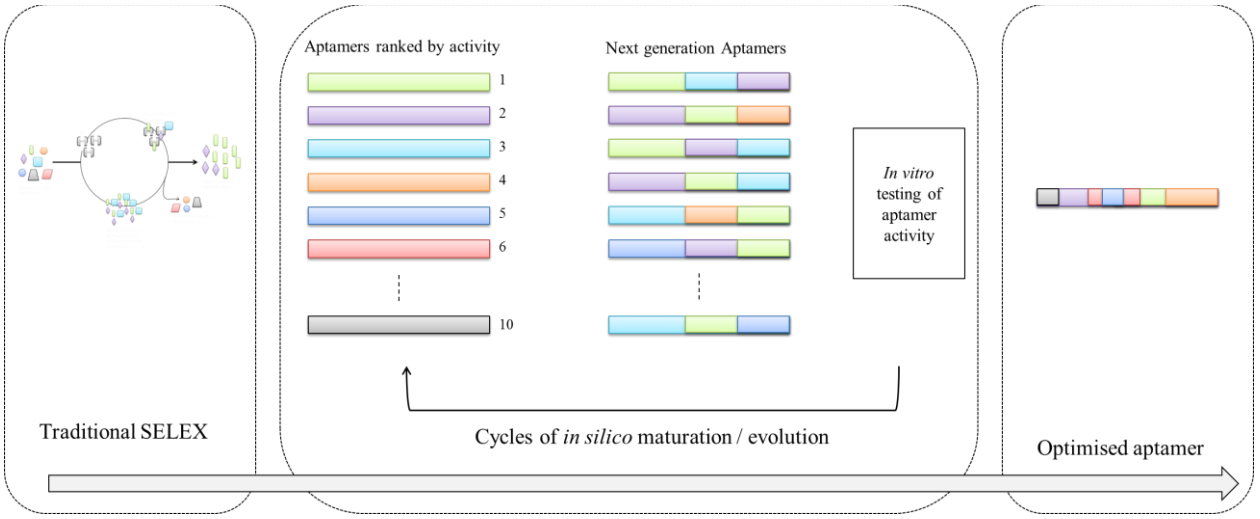

FIGURE 1-3: APTAMER SELECTION BY *IN SILICO* MATURATION

Following traditional selection, aptamers are ranked by activity. A second generation of aptamers is generated by *in silico* cross mutations and insertions from the identified active aptamer parent sequences. The newly generated aptamers are screened for activity and ranked for the next round of *in silico* maturation. After rounds of maturation and testing, a new optimised aptamer is developed.

A DNA aptamer known to bind to vascular endothelial growth factor (VEGF) with a K_d of 4.7 nM was improved 16 fold using this method to have a K_d of 300 pM (Pindyck, Kappas et al. 1971). The binding of an aptamer to prostate specific membrane antigen (PSMA) was improved 48 fold using *in silico* maturation and was subsequently used to detect PSMA at concentrations between 40 nM and 100 nM (Brunhouse 1971). Although this is classified as an *in silico* method, there is still the need for wet lab assessment at each round of maturation. This is essential to identify the "parent" strands that should be used in subsequent rounds of selection. The method is proposed as an addition to the traditional SELEX however, with the generation of new molecules at each round and the subsequent evolution of these molecules towards higher affinity it may be seen as a SELEX method in itself.

An *in silico* modelling technique using secondary structure prediction and energy landscape analysis has been used to identify possible aptazyme sequences (Brunhouse 1971). An aptazyme is formed by joining an aptamer to a ribozyme such that the ribozyme is activated in the presence of a molecule that binds to the aptamer. In the unbound form, the aptamer inhibits the catalytic core of the ribozyme, preventing the endonucleolytic cleavage of the phosphodiester backbone (Figure 1-4). When the aptamer target is added, the aptamer structure is stabilised by binding and the catalytic core of the ribozyme is formed. These molecular switches have a number of uses but are difficult to produce empirically. A comparison between aptazymes selected using *in silico* methods to those generated randomly revealed that although the directed selection did not necessarily increase the number of hits identified, the selected aptazymes performed better. The success rates differed for different aptamers and may indicate that further refinement is required to use this method on a broad scale. An anti-flavin (FMN) aptamer was used to generate aptazymes that respond to FMN. Of 23 selected aptazymes tested, three were highly activated (maximum at 60 fold) in the presence of FMN while eight were constitutively inactive and 12 were constitutively active (Brunhouse 1971). Of the 23 randomly generated aptazymes again three were activated by FMN (maximum at fivefold), 12 were constitutively active, three were constitutively inactive and five were inhibited by FMN (Brunhouse 1971). However, when the theopholine (Theo) aptamer was linked to the ribozyme, the randomly selected aptazymes all failed to respond to the addition of Theo. Of the selected aptazymes roughly 10 % were activated by the addition of Theo (Brunhouse 1971). Thus the *in silico* selection method may help to reduce the number of molecules tested before finding a hit.

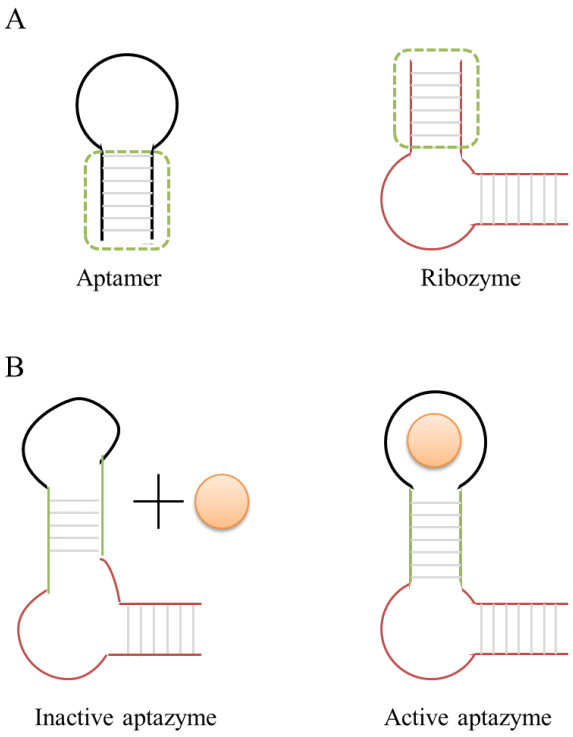

FIGURE 1-4: APTAMER CONTROLLED RIBOZYME (APTAZYME)

A. An aptamer and a ribozyme are combined by complementary base pairing at a region shown in green to generate an aptazyme. B. The aptazyme is inactive in the unbound state of the aptamer as a slip in the structure changes the conformation of the catalytic region of the ribozyme. Upon ligand binding, the aptamer structure changes the ribozyme conformation to the active state.

In addition, an *in silico* approach has been used to analyse and refine aptamer binding in a high throughput manner. Thousands of potential aptamer sequences are printed to slides and screened for target binding. Binders are analysed to determine the "affinity landscape" of the sequences and reveal the regions of aptamer sequence directly involved in binding (Knight, Platt et al. 2009; Rowe, Platt et al. 2010). In this way the optimal aptamer sequences can be predicted. Advances in *in silico* techniques have come a long way as a complementary science in nucleic acid research. However, the unpredictable nature of nucleic acid tertiary structure and molecular interactions result in its dependence on traditional methods for validation. As such, while *in silico* methods may continue as a supplement, a complete *in silico* aptamer selection method is unlikely to outperform traditional SELEX.

1.3.3 AUTOMATION OF SELECTION

Aptamer selection is time consuming and labour intensive with multiple stages and rounds of selection to complete. To overcome these challenges, a number of groups have developed automated SELEX platforms. The new aptamer selection methods make use of automated machines to complete the selection. These machines can use microfluidics and magnetic beads (Eulberg 2005; Huang, Lin et al. 2010) or affinity chromatography and high performance liquid chromatography (Zhang, Hamasaki et al. 2000) to partition and select for highly specific aptamers with no direct manual intervention. As such, this can result in multiple selections run in parallel decreasing selection time and thereby allowing for high throughput applications. The first demonstration of an automated platform generated aptamers against lysozyme that were able to inhibit cell lysis (Cox and Ellington 2001). The same group went on to develop an automated *in vitro* transcription and translation process for the protein targets to be transcribed straight from individual genes (Cox, Hayhurst et al. 2002). Further refinement of this method included the development of a monitoring system, to identify the optimal time to increase stringency in the selection, and ultrafiltration to remove low molecular weight contaminants such as salt and nucleotides from the RNA, allowing for free choice of buffer conditions in each reaction (Eulberg 2005). Further development of the automated platform has been to minimise the reaction size by making use of microfluidics (Hybarger, Bynum et al. 2006; Huang, Lin et al. 2010) and micromagentic separation (Lou, Qian et al. 2009; Oh, Qian et al. 2009).

1.3.4 WHOLE CELL SELECTION

While recombinant protein SELEX has been used to develop a large number of aptamers with clinical significance, conformational differences may exist between a recombinant protein and its naturally expressed receptor. The recombinant proteins used in selection are usually only small sections of the extracellular domain of the receptor and not the full length protein. This may result in the aptamer binding site (aptatope) on the recombinant protein being occluded when the receptor is properly folded. In addition, if the natural state of the receptor includes post translational modifications for activity, the structure of the proteins may vary dramatically. Aptamers were raised using traditional recombinant protein method against the extracellular domain of the epidermal growth factor receptor variant III (EGFRvIII) that had been expressed in *E. coli* (Liu, Kuan et al. 2009). These aptamers were found to have favourable kinetics to the recombinant protein in ELISA and SPR based *in vitro* tests with a

K_d in the nanomolar range. However, these aptamers failed to bind the EGFRvIII expressed on the surface of eukaryotic cells as the natural state of the receptor had modifications that could not be mimicked in a bacterial expression system.

To overcome these challenges with the traditional SELEX method, whole cell SELEX was developed that allows for the targeting of the receptor directly, in its natural form. The first selection to use mammalian cells was described in 1997 and was termed "*in vivo* SELEX" (Coulter, Landree et al. 1997). In this study, Coulter et al. used the intracellular machinery to identify novel exon splicing enhancers. A couple of years later, in 1999, a method to select for aptamers using live organisms was described (Homann and Goringer 1999). This study used live *Trypanosoma brucei* parasites as a target and was the first to illustrate aptamer selection to surface expressed molecules. It was not for another seven years, in 2006, that this was applied to mammalian cells in culture (Ohuchi, Ohtsu et al. 2006). The selection method was termed target expressed on cell surface-SELEX (TECS-SELEX) and made use of a recombinant cell line that expressed the target receptor. Ohuchi et al transformed Chinese Hamster Ovary (CHO) cells to express growth factor-β type III receptor and incubated them with an RNA library at 37 °C. The cells were washed and the bound RNA eluted using Ethylenediaminetetraacetic acid (EDTA) based phosphate buffered saline (PBS) buffer. A negative selection using un-transformed CHO cells was included where the unbound RNA was collected from the supernatant after incubation at 37 °C. This selection method resulted in an RNA aptamer with a dissociation constant in the 1 nM range. This, however, was determined using an SPR assay in which recombinant human soluble TGF-β receptor type III protein was used. As highlighted above, the differences in protein folding and expression may alter the aptamer binding and as such the dissociation constant calculated using the soluble recombinant protein may not be a true reflection of the binding kinetics to the surface expressed receptor. However, it was not until 2008 when the use of flow cytometry was introduced to monitor aptamer-cell interactions (Shangguan, Cao et al. 2008). The selection was then termed "cell specific SELEX" and later the term whole cell SELEX was adopted.

Whole cell SELEX has since been widely used to develop aptamers specific to cell types rather than specific proteins (Shangguan, Cao et al. 2007; Xiao, Shangguan et al. 2008). The selection procedure and the partitioning methods used for cell SELEX are more complex than those of the traditional SELEX method. Tissue culture techniques and sterility are important for whole cell SELEX as contamination of the target cells could confound the

selection as bacteria and fungi can take over the cell population rapidly. In addition, when selecting for a cell surface marker, the selection may be confounded by a highly expressed surface receptor that is not cell type or disease state specific. It is thus very important that an appropriate negative cell control is selected. The healthy cells of the same cell type as the disease cells are commonly used as a negative selection cell line. This approach has been used for cancerous cell selection in which the cancer causes a substantial increase in the expression of a receptor that is otherwise normally expressed on healthy cells. Members of the epidermal growth factor receptor (EGFR) family have been widely targeted, as they are associated with a number of tumours. They include but are not limited to breast cancer, lung cancer, and glioblastoma, head and neck cancer, bladder carcinoma, colorectal cancer, ovarian carcinoma, and prostate cancer (Salomon, Brandt et al. 1995). Although this strategy has been shown in a number of cases to produce aptamer specific for the diseased cell, as the receptor is present on healthy tissue there may still be a number of non-target cells treated by the aptamer. Where no disease specific marker is available, an abundantly expressed receptor is the best option. However, the whole cell SELEX method may also be used to identify novel targets that are specific to the diseased cell by negatively selecting against all normally expressed receptors. In the work presented in this thesis, the target of interest is not associated with disease. Aptamers were raised against CD7, a precursor T lymphocyte receptor (The receptor is discussed in detail in section 1.6). As the endogenous CD7 receptor expression level on commercial cell lines is not well documented, a recombinant cell line was generated for the aptamer selection. The un-transfected cells were used as a negative control to prevent the background selection of aptamers specific to cellular receptors that may be highly expressed on normal cells. By developing an exogenous cell line with the receptor of choice, the consensus sequence for the human receptor could be used which helped to ensure that receptor was clinically relevant.

The whole cell SELEX method can make use of adherent or suspension cells in mostly the same way (Figure 1-5). Cells are pre-blocked with yeast tRNA and or bovine serum albumen (BSA) to prevent the selection of non-specific binding interactions (Cerchia, Duconge et al. 2005). Blocked cells are exposed to the aptamer library and are in suspension or attached as a monolayer. Whole cell SELEX can be performed at 4 °C to enable aptamer binding without internalisation by membrane turnover (Daniels, Chen et al. 2003). The unbound aptamers are removed in the supernatant and the cells are washed to remove weakly bound molecules. Suspension cells would need to be pelleted by centrifugation for the

removal of the supernatant. The target aptamers will then be eluted from the cells by a heat denaturation step. A negative selection against non-target cells is included to remove cell type non-specific aptamers (Dwivedi, Smiley et al. 2010). The enriched aptamer pool is amplified and used in subsequent rounds of selection.

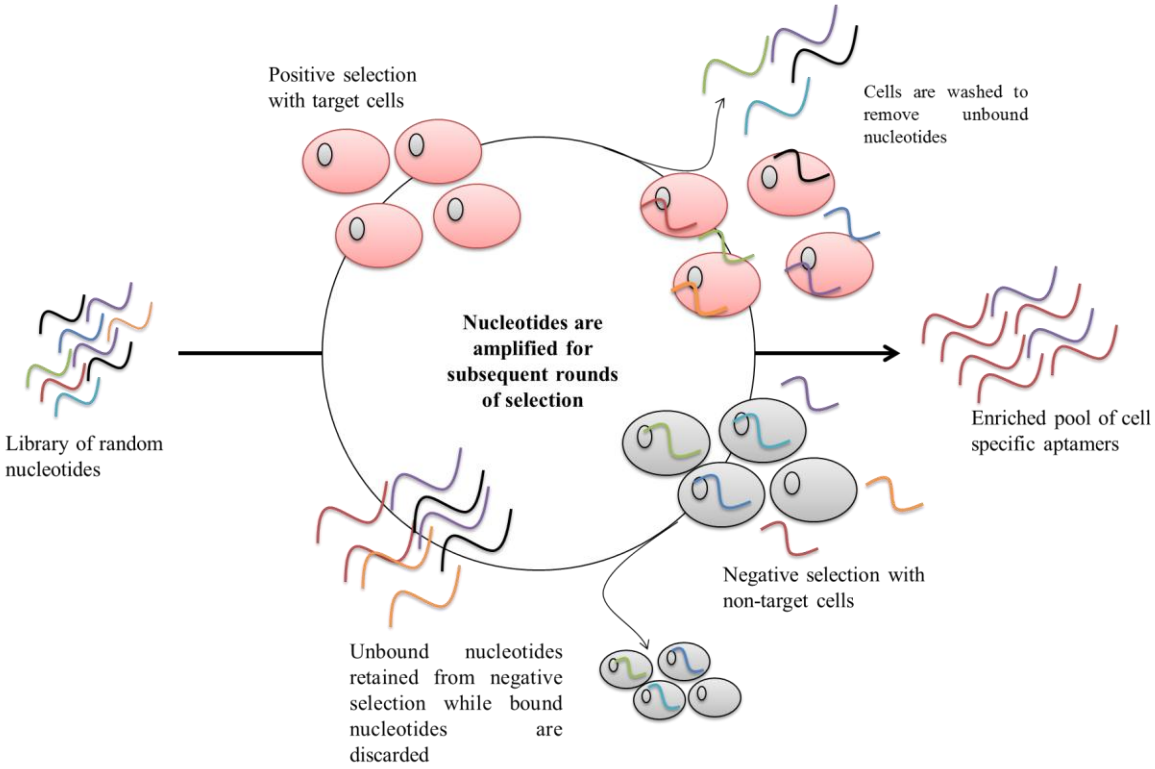

FIGURE 1-5: WHOLE CELL SELEX METHOD OVERVIEW

The whole cell SELEX method selects for aptamers specific to whole cells. The nucleotide library is incubated with target cells for the positive selection. Bound nucleotides are retained and amplified for use in subsequent rounds. A negative selection uses a closely related cell line and the unbound nucleotides are retained for amplification.

Aptamer enrichment at each round can be monitored in a number of ways including; determining the recovery as a percentage of the input library at each round; fluorescently labelling each pool of selection and monitoring cell binding by flow cytometry or high throughput sequencing to identify multi-copy sequences at each round with respect to pool complexity. The most cost effective method of monitoring is to determine the recovery percentage. As the recovery percentage increases per round it can be assumed that the complexity has decreased as the total number of input sequences that bind has increased. The other monitoring techniques inspect the aptamer evolution directly but are more labour intensive, reagent heavy and time consuming. The monitoring of enrichment by recovery percentage is the most efficient and was used in this thesis.

In the absence of a known target, the whole cell method allows for the development of aptamers and the identification of biomarkers for disease states. Using whole cells as a target in place of a recombinant protein allows for the selection of aptamers against an unknown marker of differentiation between two morphologically similar yet biologically distinct cell populations. The BNL cell line is an immortalised hepatocyte cell line that when injected into Balb/cJ mice, does not induce tumour growth. The MEAR cell line, derived from the BNL cell line by methylcholanthrene epoxide treatment is morphologically similar to the BNL cell line but does cause tumour growth in Balb/cJ mice (Shangguan, Meng et al. 2008). The whole cell SELEX method was followed against the MEAR cells with the BNL cells as a negative selection control cell line. The selection resulted in liver cancer specific aptamers that have since been used *in vitro* and *in vivo* to deliver chemotherapeutics specifically and potently (Shangguan, Meng et al. 2008; Meng, Yang et al. 2012). Using this whole cell SELEX method, aptamers able to internalise specifically into cells have been identified (Xiao, Shangguan et al. 2008).

With an interest in developing aptamers as delivery tools able to internalise into cells a newly adapted internalising whole cell SELEX has recently been described (Thiel, Hernandez et al. 2012). A similar method was used in this thesis for the selection of T lymphocyte specific internalising aptamers. This internalising whole cell SELEX method selects for the aptamers within target cells rather than surface bound molecules. The rationale for the selection of internalising aptamers is for the development of drug delivery systems that get the therapeutics into target cells. Using the whole cell SELEX, aptamers were selected based on their binding ability and any subsequent internalisation was not well defined. The internalising whole cell SELEX method is directed at the selection of the optimal internalising aptamers and binding is given less emphasis. However, the mechanism by which the aptamers internalise is not yet clear. There are a number of theories that explain the internalisation mechanism including receptor turnover, membrane recycling, endosome trapping and endocytosis however; the true mechanism has yet to be determined. It is proposed that an aptamer bound to a surface receptor will be internalised via receptor mediated endocytosis (Zhou, Swiderski et al. 2009). Whether this is induced by the aptamer binding the receptor or is the natural turnover of the cell membrane is unclear. What is known is that low temperatures can influence the turnover of the cell membrane and as such force the aptamer to remain at the cell surface (Daniels, Chen et al. 2003). In a study using *Trypanosoma brucei*, the endocytosis and intracellular trafficking of an RNA aptamer was

studied after the aptamer bound its protein target within the flagella pocket of the parasite (Homann and Goringer 2001). The study showed that after binding, the aptamer was internalised by endocytosis and trafficked to the lysosome. Although the RNA aptamer was partially degraded by the lysosomal enzymes, this study illustrated that an aptamer can be used to deliver compounds to the intracellular compartment of the parasite and may represent a novel therapeutic strategy. Confocal fluorescence microscopy was used in this study to follow the fluorescently labelled aptamer through the different stages of endocytosis. Fluorescent microscopy images of internalised aptamers have been used in a number of studies to confirm aptamer internalisation predicted from flow cytometry analysis (Xiao, Levy-Nissenbaum et al. 2012). This method allows for the real-time tracking of aptamer internalisation by taking images at time intervals after the aptamer is added to the cell culture dish (Li, Yang et al. 2008). This method was employed in this thesis to track the internalisation of the aptamers over time. The resulting data was in turn used to calculate the kinetics of internalisation into target cells.

Aptamer internalisation has also been determined by functional assays using flow cytometry (Wheeler, Trifonova et al. 2011). In this case, the mechanism of internalisation was not characterised directly but rather the ability of the aptamer to deliver functional siRNA to the cytoplasm was confirmed. As siRNA is only functional within the cytoplasm and needs to undergo a number of processing steps involving a cascade of proteins, it is fair to confirm that the complex was released from an endosome or similar trapping vesicle after internalisation. A number of studies have shown *in vitro* and *in vivo* that the aptamer-siRNA chimera is successful at target gene knockdown (McNamara, Andrechek et al. 2006; Zhou, Li et al. 2008; Neff, Zhou et al. 2011; Thiel, Hernandez et al. 2012). This indicates that if not the whole aptamer chimera, at least the cargo is able to escape lysosomal degradation after internalisation. However, the efficiency of this release has to be optimised as very large concentrations of the aptamer chimera are required for the knock down to be seen (Wheeler, Trifonova et al. 2011). Further studies are required to characterise the internalisation process of aptamers as they may differ between cell type and cellular target.

Although the general procedure for internalisation whole cell SELEX is similar to traditional whole cell SELEX, there is a fundamental difference. When isolating the aptamers from the positive selection, cells are lysed and the whole cell RNA is extracted. As the RNA aptamer pool is generated using modified nucleotides, the total RNA can be nuclease treated to remove all cellular RNA and recover the aptamer pool. The cells are washed with a cold

high salt solution prior to cell lysis to remove bound aptamers from the cell's surface. This process is performed under biologically relevant conditions and may aid to expedite the selection process for an aptamer able to deliver therapeutics selectively into target cells. Although this novel method offers the ability to direct the selection to an internalising aptamer, it may be confounded by the presence of dead cells in the selection. Dead cells non-specifically internalise small strands of nucleic acids. As such, there are a number of techniques that can be used to ensure cells are viable before selection. These include monitoring adherent cells by light microscopy before selection for morphological changes and discarding detached cells, fluorescently labelling cells with viability stains and optimising the salt concentration in the cell culture medium for optimal cell growth. This serious consideration was taken in the conducting of the experiments in this thesis and the cells were monitored by light microscopy at every stage. In addition, the cells were maintained in the optimal cell culture medium at all times during the selection and experimentation.

1.4 APPLICATIONS OF APTAMERS AS TOOLS

1.4.1 APTAMERS AS THERAPEUTICS

Aptamers raised against clinically relevant targets have been used in a number of *in vitro* and *in vivo* models to determine their use as therapeutics. Monoclonal antibodies (MAbs) can protect cells from infection by viruses by binding to the virus and inhibiting cellular entry. Aptamers have been shown to work in the same way and in some cases, improve the efficacy seen by antibodies. An RNA aptamer was raised against hemagglutinin (HA) of human influenza B virus and was able to inhibit viral entry (Gopinath, Sakamaki et al. 2006). HA is essential for membrane fusion and entry of the virus into the host cell. The aptamer binding to HA blocked viral membrane fusion and subsequent viral entry *in vitro*. This aptamer was able to distinguish between HA from influenza A and influenza B indicating the high specificity of the aptamer. Another RNA aptamer raised against HA of influenza A virus subtype H3N2 was used to distinguish the target strain from other closely related viruses (Gopinath, Misono et al. 2006). Although this specificity may be beneficial for genotyping studies and tracking of viruses in populations, as a therapeutic it may have limited application as the virus could easily escape from neutralisation. Another study developed DNA aptamers against a conserved region of the HA which allowed for cross strain neutralisation both *in*

vitro and *in vivo* (Jeon, Kayhan et al. 2004). In a similar manner, RNA aptamers raised against the surface protein of HIV-1 have been used as an entry inhibitor. These aptamers have been shown *in vitro* to have broad neutralising activity against the different HIV-1 strains from different stages of infection (Khati 2003; London, Madiga et al. 2012; Mufhandu, Gray et al. 2012).

A recent publication has highlighted the potential for an aptamer based anti-HIV-1 microbicide making use of an entry inhibiting aptamer (Moore, Cookson et al. 2011). The RNA aptamer was made using 2′ Fluoro modified pyrimidines that protect it from nuclease digestion. However, within the vaginal and rectal compartments, the aptamer showed sensitivity to microbial nucleases. It was identified that addition of chemical modifications, such as 2′-O-Me-modified nucleotides could aid in aptamer stability without negatively impacting activity. In addition, the aptamer was protected from degradation by the addition of zinc ions that disrupt the microbial nuclease activity. Another RNA aptamer proposed for intra-vaginal application was described for the delivery of siRNA via the CD4 receptor (Wheeler, Trifonova et al. 2011). This aptamer showed efficacy for delivery both *in vitro*, in polarized cervicovaginal tissue explants, and in the female genital tract of humanized mice. This aptamer was also stabilised by 2′ Fluoro modified pyrimidines and they report no nuclease degradation in their study. This may indicate that nuclease digestion by microbial nucleases is a matter of incubation time. While a number of studies have shown that 2′ Fluoro modified pyrimidines provide nuclease resistance to RNA in serum, few studies have explored the nuclease resistance in the presence of bacteria. A study was conducted that compared the stability of oligonucleotide probes generated with 2′ Fluoro modified pyrimidines, 2′ *O*-Me modified pyrimidines and an aptamer with all bases 2′ *O*-Me modified in cell culture media contaminated by *Mycoplasma fermentans* (Hernandez, Stockdale et al. 2012). *Mycoplasma fermentans* is a very common species of mycoplasma, a common bacterial contaminant of mammalian cell culture. Although all three stabilised oligonucleotide probes were stable in uncontaminated media for up to four hours (longest time point tested), only the fully 2′ *O*-Me modified RNA remained undegraded after half an hour (earliest time point tested). As the oligonucleotide probes in this study were added to the media in the absence of a target, it is unclear if the degradation could have been prevented by the probe binding to its target. Also, the first time point in this study was measured after half an hour which is a relatively long time for the oligonucleotide probes to find the target protein and thus it is difficult to conclude if the degradation occurred immediately or had

only just started when the reading was taken. Either way, this study has implications for aptamer therapeutics expected to perform once applied topically to areas with a known high bacterial load. The efficiency of aptamer delivery would need to be very high to ensure adequate delivery before the aptamer is degraded. Delivery aptamers, as they are internalised into the target cells, may be less affected by degradation than those that remain bound to the viral surface. A number of RNA aptamers specific to the envelope glycoprotein (gD) of herpes simplex virus type 2 (HSV-2) were identified for use in a multivariate microbicide application (Moore, Bunka et al. 2011). As HSV-2 is a sexually transmitted virus that is commonly found co-infected with HIV-1, there is current interest in developing a broadly neutralising microbicide for a number of infections. Moore et al. (2011) found their aptamers were able to inhibit HSV-2 infection, by binding the envelope gD, with an IC_{50} in the nanomolar range.

Aptamers have also been used to inhibit the binding of other proteins, unrelated to viral infection. Sialyl Lewis X (sLeX) is a membrane protein known to interact with selectin proteins for cellular adhesion during an inflammation response. Over expression of sLeX is a characteristic of highly malignant cancer cells and RNA aptamers were raised against sLeX to inhibit cellular adhesion (Jeong, Eom et al. 2001). These RNA aptamers showed efficacy at inhibiting cellular adhesion *in vitro* to E and P selectins. In a similar application, RNA aptamers were raised against epithelial cell adhesion molecule (EpCAM), a cancer stem cell marker (Shigdar, Lin et al. 2011). EpCAM has been identified as an attractive target for cancer treatment however clinical trials of antibody based immunotherapy have not provided very positive results. These limitations have been attributed to antibody immunogenicity, antibody size and target affinity. As such, aptamers have been identified as a potential alternative to the monoclonal antibody based approaches (Shigdar, Lin et al. 2011). *In vitro* studies demonstrated that the aptamers bound to EpCAM with high specificity and affinity and may have potential as a therapeutic. Further characterisation and *in vivo* testing will need to be conducted to conclude if aptamers can outperform antibodies in this case. RNA aptamers have been developed as autoimmune modulators for the autoimmune disease Myasthenia gravis (MG). MG is characterised by an immune response to acetylcholine receptors in muscle cells. While a previous study making use of decoy RNA to bind to the autoantibodies failed to inhibit their action (Lee and Sullenger 1997), the newly developed RNA aptamers to the autoantibody protected human cells in an *in vitro* study (Hwang and Lee 2002). Aptamers have been isolated against autoantibodies associated with idiopathic

dilated cardiomyopathy (Haberland, Wallukat et al. 2011). These aptamers were shown to inhibit autoantibody binding *in vitro* and have potential for further characterisation in animal studies. Aptamers have been raised against bovine prion protein (bPrP) (Mashima, Matsugami et al. 2009) and mouse prion protein (mPrP) (Sekiya, Noda et al. 2006) and human prion protein (Proske, Gilch et al. 2002; Rhie, Kirby et al. 2003) with high affinity and specificity. Prions are infectious particles made up of misfolded proteins and no nucleic acid molecules. There are two forms of prions; one normal ordered cellular prion and the other is protease resistant and linked to a number of pathologies. These aptamers serve to further characterise the pathogenesis of prions and may aid in the identification of novel therapeutics and diagnostics (Mashima, Matsugami et al. 2009). These findings indicate that aptamers have potential as therapeutics in a wide range of diseases and may serve to replace antibodies where they have not been successful.

1.4.2 DIAGNOSTICS AND BIOMARKER DISCOVERY

Aptamers have been identified for use as diagnostic reagents to increase diagnostic sensitivity and specificity (Liu, Mazumdar et al. 2006; Lee, Youn et al. 2008; Polonschii, David et al. 2010; Wu, Zhang et al. 2010). Making use of their inherent properties for high specificity and easy modification technology, aptamers have been widely applied to various cancer diagnostic applications. Aptamers developed using whole cell SELEX against tumour cells have been used in the development and enhancement of tumour imaging technologies. The current limitations with cancer imaging can be somewhat overcome by linking specific aptamers to a number of detector molecules for high sensitivity screening. These include: luminescent nanocrystals (Chu, Shieh et al. 2006), fluorescently functionalised quantum dots (Bagalkot, Zhang et al. 2007) and radiolabelling the aptamer with ^{99m}Tc (Hicke, Stephens et al. 2006; Da Pieve, Perkins et al. 2009). Aptamers were developed to recognise CCRF-CEM cells, an acute leukemic cell line, and attached to fluorescent nanoparticles and magnetic nanoparticles for detection and partitioning of cancer cells from complex matrices, including blood (Feldman, Levere et al. 1971). A magnetic nano-sensor was developed by conjugating aptamers to magnetic nanoparticles and was able to detect cancer cells at the density of 4 cells / 100 µl (Levere, Swerdlow et al. 1971). These aptamer based diagnostic materials have shown potential as replacements for current technologies as well as a method to improve the sensitivity of current diagnostics. A gold nanoparticle (AuNP) loaded with contrast material was functionalised with a PSMA RNA aptamer was used in place of traditional contrast

material in computed topography (CT) test. The PSMA aptamer conjugated AuNP showed four-fold greater contrast that the dye alone (Leverett 1971).

Aptamers have shown the ability to replace, and in some cases outperform, antibodies in methods that have always been antibody dominated. Aptamers have been used in place of antibodies in an ELISA (enzyme linked immunosorbent assay) leading to the defining of a new technique, the enzyme linked oligonucleotide assay (ELONA) (Murphy, Fuller et al. 2003; Rahimi, Murakami et al. 2009). A DNA aptamer specific to thyroid transcription factor 1 (TTF1) was used in a number of assays previously dominated by antibodies including western blotting to identify whole and denatured TTF1 in complex solutions at a similar affinity and intensity as the monoclonal antibody; and single step affinity purification of TTF1 from bacterial lysates (Murphy, Fuller et al. 2003). Aptamer-facilitated isolation of protein from cells (AptaPIC) has been suggested where an aptamer is developed against protein from cell lysate and applied to affinity purification of that protein. Using this method an aptamer specific to MutS expressed in *E. coli* was developed. This aptamer successfully isolated the MutS protein from complex cell lysate samples in an affinity purification procedure (Javaherian, Musheev et al. 2009).

In addition, aptamers have been used to identify new biomarkers for disease conditions. Aptamer-facilitated biomarker discovery (AptaBiD) has been shown to overcome the major problems previously encountered with biomarker discovery such as false positives and false negatives due to sample processing and differences in localisation and modification of proteins (Berezovski 2008). Berezovski et al (2008) successfully identified biomarkers for immature and mature dentritic cells. They went further to highlight how the aptamers used could have far reaching applications including targeted delivery of therapeutics, cell visualisation, tracking cells *in vivo* and as drug candidates themselves.

1.4.3 LOGIC GATES AND MOLECULAR SIGNALLING

Aptamers have found a place in synthetic biology as molecular switches for allosteric regulation with *in vitro* and *in vivo* application. Allosteric regulation refers to the binding of an effector molecule to one site on a molecule that influences the activity of that molecule at a different site such as; altered enzyme activity or altered binding affinity to a second effector. In the context of aptamers, the inputs include small molecules, proteins or oligonucleotides and the outputs could be altered enzyme activity or ligand binding resulting

in fluorescence, colourimitry or luminescence, amongst others. Aptamers have been developed that can change conformation upon binding a target molecule which allows for a number of signalling applications (Yang and Ellington 2008; Huang, Pei et al. 2009). Aptamers have been used to develop modular sensors whereby the binding of one aptamer to its target induces the binding of another aptamer to its target. Stojanovic et al (2004) connected an adenosine triphosphate (ATP) binding aptamer to a malachite green binding aptamer by a "communication module". The ATP bound aptamer induced a change in the malachite green binding aptamer causing it to recruit malachite green resulting in green fluorescence (Stojanovic and Kolpashchikov 2004). This study found that the induction of fluorescence was specific to ATP and was not confounded by other nucleotide triphosphates. This cell free system would need optimisation for a cell based assay but highlighted the possibility of aptamer signalling. An alternative signalling output involves ligand binding inducing cleavage. Adenosine specific aptamers were bound to AuNPs causing them to aggregate and appear blue in colour. In the presence of adenosine, the aptamers dissociate from the AuNPs causing the aggregates to disperse changing the colour to red (Liu, Mazumdar et al. 2006). This has been applied to the development of a lateral flow "dip stick" device for the detection of cocaine (Liu, Mazumdar et al. 2006). This technology has the potential to develop fast, reliable and cost effective diagnostic tests by changing the aptamer target as needed.

Aptamers have also been used to develop logic gates that control the output of the device based on the input provided. There are six basic logic gates (AND, NAND, NOR, OR, XNOR and XOR) that compare inputs and make an output dependent on the function of the gate (Figure 1-6). The six logic gates are made up of two basic functions, "and" and "or" and their negatives. The AND gate requires both input A and B to be present for activation while the NAND, or Not AND, gate is active only when A or B are not present and not when presented together. The OR gate requires the presence of A or B for activation while the NOR gate, Not OR, requires neither to be present. The XOR and XNOR are similar but include "exclusivity" to the function. XOR, eXclusively OR, is active only when A or B are present, not when they are both there. In a similar way, the XNOR gate is only active when A and B are not present alone. In other words it is activated by the presence of both or neither.

Logic gates form the basics of computer programing and allow for information to be transmitted in a modular and systematic manner. Aptamers have been used to generate a logic gate system that acted as an autonomous player in a game of tick-tack-toe against a human

player (Stojanovic and Stefanovic 2003). By adding the position selection to a plate, the aptamer logic gate "made a decision" as to the next move and indicated this choice by fluorescence. In a total of 19 games the aptamer automaton won 18 games and drew only once. Aptamers with different targets were combined in different manners with quenchers and fluorophores to develop logic gates that responded to stimuli in solution (Yoshida, Sode et al. 2006; Yoshida and Yokobayashi 2007). The development of this biological computation has massive implications for gene expression control for human and environmental health. Although these systems presented here are cell free and optimisation would be required for these systems to work in *in vitro* cell culture and eventually *in vivo* they highlight the possibilities of aptamer technology. Aptazymes (highlighted in 1.3.2) are being investigated for their ability to modulate gene expression in cell culture and have shown to control gene expression in yeast (Win and Smolke 2007; Win and Smolke 2008). Aptazymes have also been used to program *E. coli* to move towards the herbicide astizine and metabolise the herbicide (Sinha, Reyes et al. 2010). Although the control of mammalian gene expression provides greater challenges due to complex signalling cascades and regulatory mechanisms, aptamer technology has the capacity to influence this field greatly.

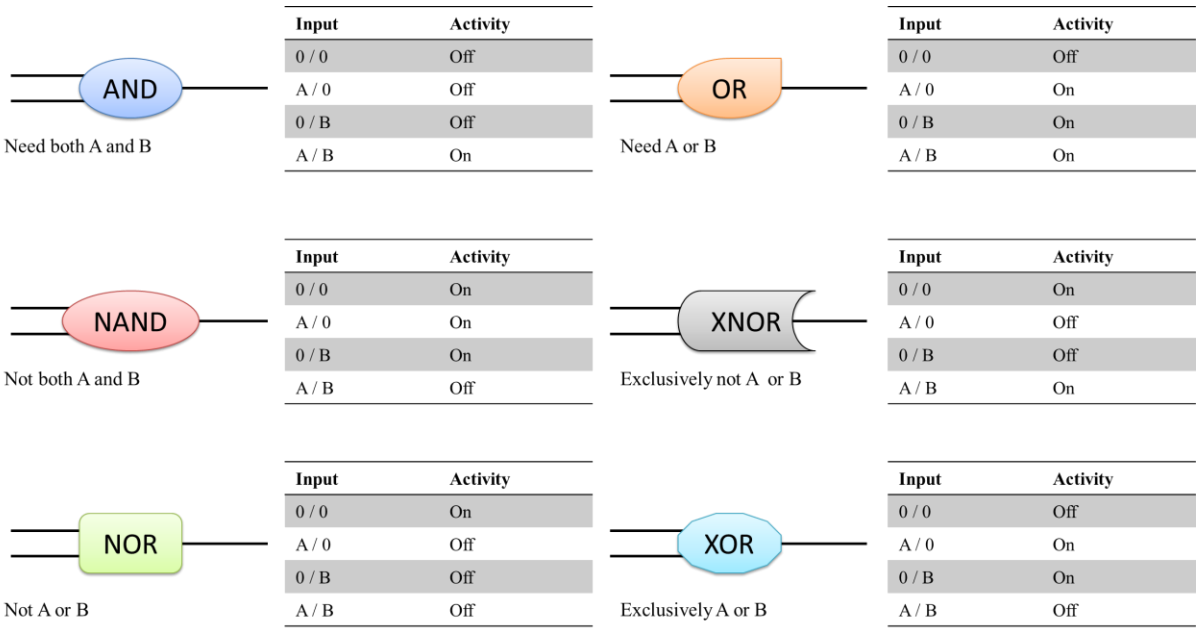

FIGURE 1-6: LOGIC GATES AND THEIR FUNCTIONS

Each logic gate has a function that determines the outcome based on the input. The logic gate function for each gate in response to four inputs is given: no input, A alone, B alone and A and B together.

1.5 APTAMERS FOR TARGET SPECIFIC DELIVERY

The specific delivery of therapeutics to target cells has eluded medical science for decades while the need for such tools has grown. This is especially true for highly toxic therapeutic treatments for which no feasible alternative is available, such as cancer chemotherapy and HIV-1 antiretroviral therapy. There are a number of mechanisms to deliver molecules into cells (e.g. Liposomes, viral vectors, polyplex reagents etc.) but these are limited in a number of ways, most notably their inability to deliver molecules specifically in a heterogeneous cell population, as would be found in human organs and tissues. In order to deliver molecules safely and effectively, a new alternative medical tool needs to be developed that is not only non-immunogenic but also capable of selectively identifying target cells in a mixed population. Aptamers selected against cell surface receptors have shown potential to fulfil this need, as they have shown to be non-immunogenic in *in vivo* studies, have great specificity and are relatively small in size. This thesis explores the use of the internalising whole SELEX (discussed in section 1.3.4) to develop aptamers able to target T lymphocytes through the CD7 receptor. These aptamers would have application in both diagnostics and therapeutics. The application of CD7 specific aptamers for treatment of HIV-1 and T lymphocyte diseases such as leukaemia is discussed in section 0.

Initially, delivery aptamers were raised against recombinant proteins and the extracellular domains of the target receptors. Recent selections have made use of the whole cell SELEX method to develop novel aptamers to specific cellular receptors, new biomarkers and disease state cells (Xiao, Shangguan et al. 2008; Li, Larson et al. 2010). The mechanism by which aptamers internalise into cells is not yet well understood (as explained in section 1.3.4) but this capability is being exploited in a number of ways, such as aptamer delivery of cancer chemotherapy. The cancer therapeutic candidates are usually highly effective but are limited by their inherent toxicity due to non-specific delivery or are not bioavailable without the aid of a delivery vector. By selectively delivering these cytotoxic compounds to the relevant tumour cells, the effective dose can be reduced and subsequently the toxic side effects can be avoided by reducing uptake by healthy tissue. This principle can be applied to any chemotherapy that is negatively impacted by toxicity due to off target delivery. A number of potential cancer chemotherapies are in various stages of development using aptamers to increase specificity and rate of delivery of the therapeutics to tumour cells (Chu, Marks et al. 2006; Cheng, Teply et al. 2007; Dhar 2008; Cao, Tong et al. 2009; Ferreira, Cheung et al. 2009; Huang, Shangguan et al. 2009; Yang, Meng et al. 2011).

The ease of aptamer modification has allowed for the attachment and delivery of a wide range of therapeutic molecules for cell specific delivery of therapeutic proteins, nanoparticles and other nucleic acids. The 3′ or 5′ end of aptamers can be functionalised to include a number of different chemical modifications allowing for the attachment of these effector molecules. Advancements in nanotechnology led to the development of nanoparticle drug delivery carriers called nanoparticles. These nanoparticles are < 100 nm in size, can be loaded with various therapeutic compounds and are used for cell specific delivery of drugs (Reviewed by Wang, Langer et al. 2012). Although nanoparticles have been used alone as delivery vectors and can be modified to target specific tissues, aptamer functionalised nanoparticles have become a widely researched topic. A number of aptamers have been covalently linked to different nanoparticles using a range of chemical modifications. A nanoparticle composition designed for slow release of therapeutics that had previously been approved by the United States Food and Drug Administration (FDA) for clinical use were functionalised with an aptamer and showed efficacy *in vitro* and *in vivo* (Farokhzad, Jon et al. 2004; Farokhzad, Cheng et al. 2006). The nanoparticle was synthesized from PEG copolymer with a terminal carboxylic acid functional group (PLA-PEG-COOH). The aptamer was modified with the addition of a 3′ NH_2 group that allowed for the direct covalent linkage of the aptamer to the nanoparticle. Not only did this result in a strong bond but as the aptamer was modified at the terminal end, the orientation was kept constant. This strategy is commonly used to attach aptamers to nanoparticles without diminished aptamer affinity but could be problematic if the proximity of the nanoparticle to the aptamer binding domain does not allow for the aptamer to bind its target. A similar strategy was used by Hu et al in the development of an aptamer delivered antidote to a toxic contaminant (Hu, Tulsieram et al. 2012). For this study, a 5′ NH_2 group was added to aptamer for conjugation to the polymeric nanoparticle functionalised with COOH groups. Mice were fed mercury contaminated food and intravenously administered aptamer guided antidote loaded nanoparticles. The aptamer-nanoparticles reduced the mercury toxicity *in vivo* and suggest a tool to reduce toxins and hazards to human health (Hu, Tulsieram et al. 2012). In addition to amino group modified aptamers, thiol modifications have been used to attach aptamers to AuNPs (Liu, Mazumdar et al. 2006). A thiol modified linker sequence has been used as a strategy to extend the distance between the aptamer and the AuNP. Kim et al made use of this strategy to bind an anti-PMSA aptamer to a AuNP (Leverett 1971). The linker sequence was 5′-SH-functionalised with a region of complementarity to an extended sequence on the aptamer 3′ region. The linker bound to the citrate-stabilised AuNPs by the 5′-SH group and formed a

short double stranded region with the aptamer. This strategy allowed for the aptamer being sufficiently far from the AuNP so as not to be affected by steric hindrance. However, the design on the extended sequence for complementarity has to be carefully considered, as it should not form interactions within the aptamer sequence. Adding additional flanking sequences can lead to modifications of the aptamer structure and may prevent the correct binding conformation to be generated.

An aptamer functionalised liposome was developed by generating the aptamer with a cholesterol molecule on the 5′ end that immobilised the aptamer by inserting into the liposome hydrophobic lipid membrane (Cao, Tong et al. 2009). This was a very interesting study as Cao et al demonstrated that the cDNA compliment of the aptamer could be used to inhibit the delivery of the drug loaded liposome. This was the first illustration of a reversible system for cell specific delivery. In addition to nanoparticles, aptamers can be conjugated to other oligonucleotides that act as therapeutics. The conjugation can be through direct hybridisation as with an RNA aptamer specific to epidermal growth factor receptor (EGFR) that was used to deliver Gemcitabine (Gem) specifically to MiaPaCa-2 cells, a pancreatic cell line (Ray, Cheek et al. 2012). Gem is a nucleoside analogue used for stand-alone treatment of pancreatic cancer and EGFR is over expressed on pancreatic cancer cells. In *in vitro* studies Gem is active against all pancreatic cancer cell lines however; the toxicity *in vivo* limits the success of Gem treatment as the effective concentration causes damage to healthy cells. When Gem was linked to an EGFR targeting aptamer, selective targeting of EGFR expressing cells was seen (Ray, Cheek et al. 2012). In addition, cellular inhibition caused by the aptamer linked Gem was greater than both that of the Gem linked to a random oligonucleotide and of Gem alone indicating that the aptamer played an important role in delivery of the compound.

Aptamer targeted delivery has been further explored for the delivery of siRNA and other members of the RNA interference (RNAi) pathway (Reviewed in section 5.3). A number of aptamer mediated RNAi delivery strategies have been tested *in vitro* and *in vivo* with success (McNamara, Andrechek et al. 2006; Zhou, Swiderski et al. 2009; Neff, Zhou et al. 2011). Different conjugation strategies have been explored to produce aptamer-siRNA chimeras. Biotinulated aptamers and siRNA have been combined using a streptavidin linker to generate a functional chimera (Chu, Twu et al. 2006). Making use of this strategy Chu et al. were able to link multiple PMSA specific aptamers and siRNA molecules in one complex. Although an efficient strategy for the simple production of chimeric molecules, this strategy

has limited application in therapeutics due to the immunogenicity of the streptavidin linker. McNamara et al. used the same PMSA aptamer to generate a chimera by covalently linking the aptamer to the sense strand of the siRNA (McNamara, Andrechek et al. 2006). While this approach is more simplistic in design, the aptamer folding and thus its function may be disrupted by the siRNA sequence if there is a region of complementarity within the aptamer. In addition, the highly structured aptamer region may impair the proper processing of the siRNA by the RNAi machinery. As a follow up design to this study, the authors truncated the aptamer to include only the essential regions and included a *UU* linker sequence between the aptamer and the sense strand of the siRNA to increase the accessibility of the RNAi machinery (Dassie, Liu et al. 2009). This linker sequence approach was further adapted by Zhou et al. in the generation of a so called "sticky bridge" chimera (Zhou, Li et al. 2008; Zhou, Swiderski et al. 2009). The "sticky bridge" approach makes use of a linker and bridge sequence attached to the 3′ end of the aptamer and siRNA. The bridge sequences are complementary and allow for the modular generation of a number of aptamer siRNA chimeras from a single design. Although simple in principle, this method of chimera generation is complicated by the possibility of the bridge region forming an interaction with the aptamer.

Aptamers can also be used to deliver intercalating molecules without affecting their binding affinity and specificity. An RNA aptamer was used to deliver Doxorubicin (Dox) specifically to a hepatocellular carcinoma cell line (Meng, Yang et al. 2012). Dox is an anthacycline antibiotic and acts by intercalating into DNA. It has been used in the treatment of liver cancers by local administration but its use is limited due to toxic side effects. Dox intercalated into an RNA aptamer specific to cancerous liver cells was shown to target tumour cells selectively without non-specific internalisation into healthy liver cells *in vitro* and *in vivo* (Meng, Yang et al. 2012). Kim et al. also delivered Dox to cancer cells using their AuNP-linker-aptamer therapeutic design (Leverett 1971). The double stranded region of linker and aptamer allowed for the Dox to intercalate into the RNA strand.

Aptamers have also been used to deliver alternative therapeutic agents such as proteins and enzymes. An aptamer attached to a viral capsid was shown to deliver the viral capsid in a cell specific manner (Tong, Hsiao et al. 2009). The viral capsid was modified to allow for the attachment of the aptamer functionalised with a phenylene diamine group. These aptamer-directed-viral-capsids were trafficked intracellularly to the liposome and thus could be useful delivery tools for acid-labile prodrugs. An aptamer was successfully used to

deliver lysosomal enzyme specifically to α-L-iduronidase-deficient mouse fibroblasts *in vitro* as an enzyme replacement therapy for lysosomal storage disease (Chen, Dellamaggiore et al. 2008). The aptamer was linked to the enzyme by a series of chemical reactions in which a linker region on the aptamer 3′ end comprising of 12 CH_2 groups and a glycerol was added to either α-L-iduronidase or its dephosphorylated form in a 10:1 molar ratio of aptamer to enzyme. In addition, aptamers have been developed to deliver therapeutics to specific organelles. An aptamer specific to nucleolin, able to deliver gene therapy interventions within the nucleus of a cell has been described (Kotula, Pratico et al. 2012). Kotula et al (2012) use the aptamer to deliver splice-switching oligonucleotides into cells that alter their gene expression by interfering with splice site recognition. This highlights the selective targeting ability of aptamers and the depth of their uses.

Finally, in addition to attaching molecules to single aptamers for delivery, aptamers have been linked to a lipid tail and have shown self-assembly into aptamer micelles capable of increased target affinity than that of the aptamer alone (Wu, Sefah et al. 2010). The examples outlined above indicate that, aptamers can be applied to a wide range of functions by making use of their inherent chemical simplicity for diverse modifications. The work covered in this thesis is aimed at generating a targeted delivery aptamer specific to T lymphocytes. T lymphocytes are the targets for therapeutic delivery for cancer, HIV-1 and other T tropic viruses. In this work, an aptamer specific to the T lymphocyte receptor CD7 was developed. This target will be discussed in greater detail in section 1.6 and the application of targeting this receptor for delivery of therapeutics in section 5.2.

1.6 TARGETING T LYMPHOCYTES THROUGH THE CD7 RECEPTOR

The human CD7 receptor is a 40 kDa transmembrane protein and a member of the immunoglobulin gene superfamily. The CD7 receptor has been shown to play a role in T cell and natural killer cell activation (Carrera 1988; Lazarovits, Osman et al. 1994). CD7 induced cell activation may be induced through interaction with lipid kinase phosphatidylinositol 3-kinase (PI 3-K), a well characterised enzyme involved in a number of important cellular functions (Lee, Patel et al. 1996). The CD7 receptor is one of the earliest receptors to be expressed and persists on the surface of T lymphocytes after CD4 and T cell receptor (TCR) activation (Lobac, Hensley et al. 1985; Cotta, Cintra et al. 2006) (Figure 1-7).

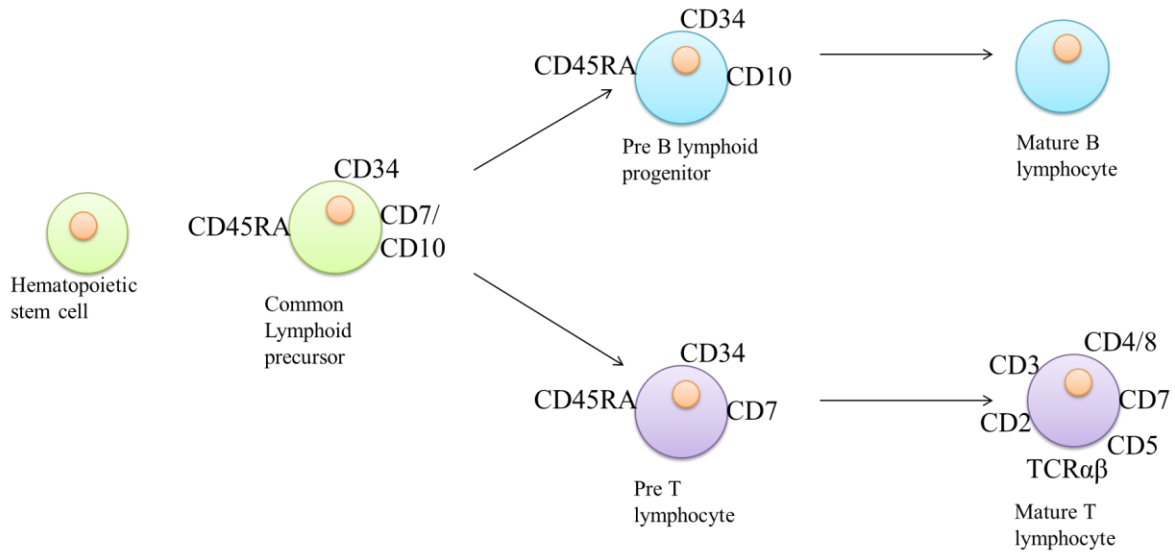

FIGURE 1-7: RECEPTOR EXPRESSION DURING LYMPHOCYTE DEVELOPMENT

The CD7 receptor is expressed on common lymphoid precursor cells with CD45RA and CD34. The presence of CD7 or CD10 dictates the development of T lymphocytes and B lymphocytes respectively. The CD7 receptor remains expressed on mature T lymphocytes after T cell receptor (TCR) activation.

The CD7 receptor has been implicated in the regulation of integrin adhesiveness in human T cells and is highlighted as a good candidate for targeting T cells (Shimizu, van Seventer et al. 1992; Rabinowich, Pricop et al. 1994; Chan, Mobley et al. 1997). The CD7 receptor has been widely studied as a target for delivery of cytotoxic molecules for the treatment of T lymphocyte diseases such as leukaemia, lymphoma and Rheumatoid Arthritis (RA) (Vallera, Burns et al. 1996; Frankel, Laver et al. 1997; Pauza, Doumbia et al. 1997; Waurzyniak, Schneider et al. 1997; Peipp, Kupers et al. 2002; Bremmer, Cate et al. 2006). These studies have made use of MAbs to target T lymphocytes for both preclinical and clinical trials. Recently it was shown that by targeting the CD7 receptor for delivery of HIV-1 therapeutics, there was a protective inhibition of viral infection (Kumar 2008). This study also made use of a MAb specific for the CD7 receptor for delivery. The protein nature of the antibody made the conjugation chemistry for the effector molecules complex and expensive. The therapeutic strategies using the CD7 receptor will be discussed in greater detail in section 0. We propose the use of aptamers in place of MAbs for the targeting of the CD7 receptor. As has been highlighted in the preceding chapters, aptamers have a number of inherent characteristics that make them ideal for use as delivery molecules. An aptamer targeting the CD7 receptor can be used for the targeted delivery of therapeutics for HIV-1 or certain lymphatic cell cancers. This project aims to develop aptamers to CD7 that may be used as a delivery molecule to target T lymphocytes selectively.

1.7 THESIS SCOPE AND OBJECTIVES

Aptamers can be developed against a wide range of molecules and applied to a number of applications. A newly developed aptamer selection protocol has been defined that selects for aptamers able to internalise into specific cells. This method has been used to develop aptamers specific for various cell types and applied to the delivery of cytotoxic therapeutics to diseased cells specifically. The overall aim of this thesis was to obtain highly sensitive and specific RNA aptamers that are capable of internalising into cells via the CD7 receptor. Therefore, the specific objectives of this thesis were:

1. To develop a stable cell line expressing CD7 receptor for the selection of CD7 specific aptamers
2. To select internalising anti-CD7 aptamers by a modified whole cell SELEX
3. To characterise anti-CD7 aptamer binding to the exogenously expressed CD7 receptor
4. To characterise anti-CD7 aptamer binding and internalisation in target T lymphocytes

Achieving these objectives contributed to the field of aptamer research by optimising a method to select for aptamers able to internalise into cells making use of a specific receptor not necessarily characteristic of disease. This optimised approach for selection against an exogenously expressed receptor could be widely applied to generate aptamers to any receptor of interest. The aptamers characterised in this thesis can be exploited for a number of applications including diagnostics and targeted therapeutic delivery. Targeted delivery of therapeutics using a T lymphocyte specific aptamer may be used in the development of novel therapeutics for HIV-1 and cancer.

Chapter 2. DEVELOPMENT OF INTERNALISING ANTI-CD7 APTAMERS

2.1 INTRODUCTION

The CD7 receptor is a marker for T cell development and is expressed on the surface of all T lymphocytes (Receptor detailed in section 1.6). The CD7 receptor has been identified by a number of groups as a suitable therapeutic target for T cell malignancies and T cell tropic viruses (highlighted in section 5.2). The CD7 receptor is expressed on immature and mature T lymphocytes and so is expressed before CD4 and T cell receptor activation. As such, the CD7 receptor can be targeted for prophylactic delivery of therapeutics for T tropic viruses that infect only mature T lymphocytes (Section 5.2.1). This can be achieved using internalising aptamers. In addition, as the CD7 receptor remains on mature CD4+ cells, the same receptor can be used to deliver therapeutics to mature infected cells. This wide range of potential targeting of CD7 makes the production of CD7 specific aptamers very valuable.

The selection of internalising aptamers by internalising whole cell SELEX has recently been described for vascular smooth muscle and HER2+ breast cancer cells aptamers (Thiel, Hernandez et al. 2012; Thiel, Bair et al. 2012). The selection of internalising aptamers may expedite the process of identifying internalising aptamers by starting with an enriched pool of internalising RNA. Previous aptamers used in delivery of various therapeutic molecules were selected against recombinant proteins and were found after selection to be internalised (Zhou, Swiderski et al. 2009). Aptamers selected with the internalising cell SELEX protocol are enriched for their ability to enter cells via a specific receptor. In addition, conformational differences between the recombinant ligand and a cell surface expressed receptor may bias recombinant protein selection away from the best internalising aptamers possible. A study has shown that making use of recombinant receptors for therapeutic studies may influence the overall outcome if there are stoichiometric differences between the natural receptor and the recombinant isoform (Chenna, Hu et al. 2012). In addition, the recombinant proteins commonly available are rarely of full length or the complete protein. Recombinant gp120 for example is a monomer while the surface expressed protein is in a trimeric form. The recombinant form of the CD7 receptor contains only the extracellular domain and thus may not fold to the same conformation as the surface expressed receptor with an intracellular and membrane domain. As such, aptamers were developed specific to the CD7 receptor by this

specialised internalising whole cell SELEX. The preparation for the selection as well as the selection of the CD7 specific aptamers will be discussed in detail in this chapter.

2.2.1 PRODUCTION OF A CD7 RECEPTOR GENE CLONING VECTOR

In order to perform cell SELEX to select for aptamers that internalise using CD7 receptor, a stable cell line expressing surface CD7 receptor had to be made. For this, CD7 receptor cDNA was ligated into the pcDNA 3.3-TOPO cloning vector (Invitrogen, CA, USA) to generate pcDNA-CD7. CD7 receptor cDNA of the CD7 receptor gene (GenBank® gene ID number: 924) was chemically synthesised (Integrated DNA Technologies, CA, USA) and made double stranded by PCR. The PCR contained: 1 × Taq buffer pH 8.5 (Supplied with the Go Taq polymerase; Promega, WI, USA), 1 mM $MgCl_2$ (Promega, WI, USA), 0.2 mM dNTPs (Fermentas, Thermo Fisher Scientific Inc., MA, USA), 1 μM forward primer (5′ GGAGGGGGTTGGTCATGGTCACT 3′) and 1 μM reverse primer (5′ TCGGAGCCTCCGGGCC**GGTATTG** 3′ Kozak translation sequence indicated in bold) (Integrated DNA Technologies, CA, USA), 1 U Go Taq Polymerase (Promega, WI, USA) and 40 ng DNA. The reaction was optimised for annealing temperature and cycle number with the following parameters: denaturation at 93 °C for one minute followed by cycles of 93 °C for 30 seconds, annealing for 30 seconds at 50.5 °C – 69.6 °C and extension for one minute at 72 °C. A final extension of ten minutes at 72 °C was included after the last cycle. Fifteen, 30 and 45 cycles were used to determine the optimal cycle number for band amplification. PCR fragments were resolved on a 2 % (w/ v) agarose gel stained with ethidium bromide (Merck, Darmstadt, Germany) and visualised under UV light using a Molecular Imager Chemidoc XRS+ Imaging System (BIORAD, CA, USA). An annealing temperature of 55.5 °C with 15 cycles produced the cleanest amplicon and was used for ligation into the pcDNA 3.3-TOPO cloning vector (Invitrogen, CA, USA). The pcDNA 3.3-TOPO cloning vector contains a TOPO-adapted expression vector that allows for cloning of a PCR product without prior modification. The cloning reaction mixture was set up using 90 ng PCR product, 200 mM NaCl, 10 mM $MgCl_2$, 40 ng pcDNA 3.3-TOPO Vector. The reaction was gently mixed and incubated at room temperature for five minutes before being placed on ice.

2.2.1.1 CLONING OF CD7 RECEPTOR GENE INTO CHEMICALLY COMPETENT CELLS

One Shot Competent *E. coli* cells (Invitrogen, CA, USA) were transformed with the pcDNA 3.3-TOPO cloning vector containing the CD7 receptor gene sequence. The pUC19 control plasmid was included to validate transformation and 10 pg was used for the 50 µl reaction. Cells were incubated on ice for five minutes and then heat-shocked for 30 seconds at 42 °C without shaking. Tubes were then transferred to ice and 250 µl of SOC medium (super optimal broth with Catabolite repression; Invitrogen, CA, USA) was added at room temperature. The tubes were capped tightly and placed in a shaker horizontally at 200 rpm at 37 °C for one hour. After incubation, 25 µl from each transformant was spread over pre-warmed selective nutrient agar plates (Sigma-Aldrich, MO, USA) supplemented with 200 µg/ ml ampicillin antibiotic (Sigma-Aldrich, MO, USA) and incubated over night at 37 °C.

From the transformation plates, ten colonies were picked and cultured overnight in LB broth ((10 % tryptone powder, 5 % yeast extract, 5 % NaCl (Sigma-Aldrich, MO, USA) containing 100 µg/ ml ampicillin antibiotic (Sigma-Aldrich, MO, USA)). Plasmid DNA was isolated using a commercially available mini prep kit **(**Qiagen, Hilden, Germany) as outlined in Appendix 6.1.1.

2.2.1.2 VALIDATION OF CD7 RECEPTOR CLONING REACTION AND PLASMID PRODUCTION

Plasmid DNA was quantified using a NanoDrop Spectrophotometer (Appendix 6.1.3) and was sequenced (Inqaba Biotech, Pretoria, South Africa) to ensure that the insert was in the correct orientation for CD7 receptor expression in mammalian cells. Primers included in the TOPO cloning kit were used to confirm the clones as insert positive (CMV forward 5′ CGCAAATGGGCGGTAGGCGTG 3′ and TK ploy A reverse 5′ CTTCCGTGTTTCAGTTAGC 3′). The plasmid sequences were analysed using CLUSTAL W multiple alignment application in BioEdit V7.1.3.0 software (Hall 1999) and aligned to the CD7 receptor consensus sequence (Entrez gene number: NP_006128.1). Clones with the correct insert in the correct orientation were used to generate glycerol stocks (Appendix 6.1.8).

2.2.2 TRANSFECTION TO GENERATE A STABLE CELL LINE EXPRESSING SURFACE CD7 RECEPTOR

To generate a stable cell line that constitutively expressed the CD7 surface receptor, HeLa cells were transfected with the pcDNA-CD7 cloning vector and placed under neomycin (Sigma-Aldrich, MO, USA) selection. Prior to the generation of a stable cell line the minimum inhibitory concentration of the neomycin was determined by kill curve analysis (Appendix 6.1.9). The minimum concentration of neomycin at which un-transfected cells were viable was 50 µg/ ml. The neomycin concentration chosen for generating stable cell lines was 100 µg/ ml. After selection, the cells were maintained in 50 µg/ ml neomycin concentration. To generate the stable cell line, 2×10^6 cells were seeded in a 6 cm dish (Nunc™, Thermo Fisher Scientific, Inc, MA, USA). After 24 hours at 37 °C with 5 % CO_2 seeded cells were transfected with the pcDNA-CD7 plasmid. After 48 hour incubation, the transfected cells were supplemented with 100 µg/ ml neomycin before splitting the cells over ten 6 cm dishes 48 hours later. Cells were collected and frozen in 10 % Dimethyl sulfoxide (DMSO) (Sigma-Aldrich, MO, USA), 20 % foetal bovine serum (FBS) (Sigma-Aldrich, MO, USA) in DMEM (Gibco, BRL, UK). A subset of cells was maintained in neomycin selection media (10 % FBS, 50 µg/ ml neomycin in Dulbecco's modified eagle's medium, DMEM) and analysed for CD7 receptor expression by flow cytometry and fluorescence microscopy.

2.2.3 FLOW CYTOMETRY ANALYSIS TO CONFIRM SURFACE EXPRESSION OF CD7 RECEPTOR ON GENERATED STABLE CD7-HELA CELL LINE

To confirm the surface expression of the CD7 receptor on transformed CD7-HeLa cells, CD7 receptor was detected by flow cytometry. CD7-HeLa cells and HeLa cells were seeded in a six well dish at 2×10^5 cells per well and incubated overnight at 37 °C with 5 % CO_2. The growth media (HeLa cell growth media contained 10 % FBS in DMEM and CD7-HeLa cell selection media contained 10 % FBS, 50 µg/ ml neomycin in DMEM) was then removed and the cells were washed three times with PBS with an extended, 10 minute, last wash. The cells were then washed an additional two times with 1 ml blocking buffer (PBS inoculated with 2 % FBS) before adding 0.5 µg FITC (fluorescein isothiocynate) labelled monoclonal mouse anti-human anti-CD7 antibody, clone CBC.37 (Milli-Mark™, Millipore, USA) in 1 ml blocking buffer and incubated at 37 °C for one hour. After incubation the antibody solution was removed and the cells were washed three times with 1 ml blocking buffer. Cells were suspended in 1 ml blocking buffer pre-warmed to 37 °C for analysis by flow cytometry using

a Guava Easy Cyte Flow cytometer (Guava Technologies Inc., CA, USA). The results were analysed and processed using FlowJo version 7.6.5 (Tree Star, Inc., OR, USA). For each run, 10 000 events were counted and cells gated according to forward and side scatter profiles. Antibody bound cells were compared to cells alone and the percentage cells stained was determined for each cell type. The mean and median fluorescence was calculated for cells alone as well as those stained with the monoclonal anti-CD7 antibody (FITC).

2.2.4 FLUORESCENT MICROSCOPY ANALYSIS TO CONFIRM SURFACE EXPRESSION OF CD7 RECEPTOR IN GENERATED STABLE CD7-HELA CELL LINE

To confirm the surface expression of the CD7 receptor on transformed CD7-HeLa cells, CD7 receptor was detected using fluorescent microscopy. CD7-HeLa cells and HeLa cells were grown on different coverslips (Sigma-Aldrich, MO, USA) in a six well dish to 80 % confluence. The growth medium was then removed and the cells were washed three times with PBS with an extended, ten minute, last wash. The cells were then washed an additional two times with 1 ml blocking buffer (PBS inoculated with 2 % FBS) before adding 0.5 µg anti-CD7-FITC monoclonal antibody, clone CBC.37 (Milli-Mark™, Millipore, USA) diluted in 1 ml blocking buffer and incubated at 37 °C for one hour. Control cells, without antibody, were incubated with PBS for the duration of the antibody binding step. After incubation the antibody solution was removed and the cells were washed three times with 1 ml blocking buffer. The coverslips were then mounted using VECTASHIELD mounting media (VECTOR laboratories, CA, USA) containing DAPI stain for nucleus localisation and sealed with clear nail varnish (Maybeline, USA). Slides were viewed using an Olympus BX41 Fluorescent Microscope (Olympus Corporation, Japan) under 100 × magnification and analysed using the AnalySIS LifeScience® software (Olympus Corporation, Japan).

2.2.5 SELECTION OF INTERNALISING ANTI-CD7 APTAMERS BY WHOLE CELL SELEX

2.2.5.1 RANDOM OLIGONUCLEOTIDE LIBRARY USED FOR APTAMER SELECTION

Aptamer selection made use of a 90 nucleotide ssDNA library with a 49 nucleotide random region (5′ GCCTGTTGTGAGCCTCCTAAC (N49) CATGCTTATTCTTGTCTCCC 3′)

custom synthesized by Integrated DNA Technologies (CA, USA). The single stranded DNA was made double stranded by PCR with the reverse primer containing the T7 polymerase promotor region (Forward primer: 5′ GCCTGTTGTGAGCCTCCTGTCGAA 3′ and T7 Reverse primer 5′ TAATACGACTCACTATAGGGAGACAAGAATAAGCATG 3′, T7 promotor region underlined). The double stranded DNA was transcribed to RNA to generate the RNA library used in the selection. The RNA library was transcribed to include 2′ fluorinated pyrimidines (2′ Fluoro) to increase RNA stability and prevent nuclease degradation.

2.2.5.2 SELECTION OF ANTI-CD7 APTAMERS BY WHOLE CELL SELEX

A modified whole cell SELEX was used to generate RNA aptamers capable of internalising into target cells using the human surface CD7 receptor. The SELEX included six rounds of positive selection in CD7-HeLa cells and a negative selection using un-transfected HeLa cells. Each round of positive selection was put into un-transfected HeLa cells to detect any background non-specific internalising aptamer selection. Positive selection in CD7-HeLa was achieved by growing cells in a six well dish to 90 % confluence for 48 hours. The growth media was removed from each well and cells were washed with 2 ml PBS. Non-specific RNA binding sites on the cells' surface were blocked by the addition of 100 µg/ ml yeast tRNA in 1 × HMCKN (10 mM Hepes pH 7.4, 1 mM $MgCl_2$, 1 mM $CaCl_2$, 2.7 mM KCl, and 150 mM NaCl) at 37 °C for 20 minutes. RNA was refolded by heating to 95 °C for three minutes followed by incubation at room temperature for ten minutes in 1 × HMCKN. The block was discarded before incubating the cells with 100 nM re-folded 2′ fluorinated RNA library in 1 × HMCKN at 37 °C for one hour. The selection stringency was increased per round by decreasing the amount of added RNA while keeping the cell number and volume constant.

The unbound RNA was discarded and cells were washed with 2 ml ice cold 0.5 M NaCl in PBS to remove any bound RNA on the cell surfaces. After washing, cells were solubilised using 1 ml Trizol (Sigma-Aldrich, MO, USA) per well and transferred into 2 ml eppendorf tubes. The samples were vortexed for 40 seconds to shear DNA before adding 200 µl of chloroform to each sample and vortexing again for 30 seconds. The samples were centrifuged at 12 000 × *g* for 15 minutes after which the aqueous phase was transferred to a new 2 ml eppendorf tube. To degrade and remove the cellular RNA and the blocking yeast tRNA, RNAse A (Fermentas, Thermo Fisher Scientific Inc., MA, USA) was added to each sample at a final concentration of 100 µg/ ml and incubated at 37 °C for 30 minutes. The

samples were then phenol: chloroform: isoamyl alcohol extracted (Appendix 6.1.6) and centrifuged at 12 000 × g at room temperature for ten minutes. The aqueous phase was retained following extraction with chloroform. Following this, 1 volume isopropanol and 0.1 volume 10 M sodium acetate was added to each sample which was incubated overnight at − 80 °C to precipitate the RNA. The RNA was then pelleted by centrifugation at 12 000 × g 4 °C for 30 minutes after which the supernatant was discarded. The pellets were washed with ice-cold 70 % ethanol and air dried. The dry pellets were re-suspended in 100 µl nuclease free water and passed through a NucAway™ Spin Columns (Ambion, NY, USA) (Appendix 6.1.5) to remove the free nucleotides before being quantified by NanoDrop-spectrophotometer at A_{260} (Appendix 6.1.3).

The recovered RNA was expressed as a percentage of the added RNA and was used to track the enrichment per round of selection. The recovered RNA was reverse transcribed into cDNA using a Verso cDNA Synthesis kit (Thermo Fisher Scientific Inc., MA, USA). The cDNA was used to generate a template for PCR amplification of the DNA for sufficient material to produce RNA for the next round of selection. The RNA (1 ng) was combined with 2.5 µM forward primer and incubated at 65 °C for ten minutes before chilling on ice. While on ice, the remaining reaction reagents were added in the following order according to the manufacturers protocol: 1 × cDNA synthesis buffer, 500 µM dNTP, 1.1 µl Verso Enzyme mix (Thermo Fisher Scientific Inc., MA, USA). As an extra precaution, 40 units RNAse inhibitor (Fermentas, Thermo Fisher Scientific Inc., MA, USA) was added to the reaction mix at a final volume of 20 µl and the mixture incubated at 45 °C for 30 minutes. The reverse transcription enzyme was deactivated before PCR by incubating the reaction at 85 °C for five minutes.

The resulting cDNA was used as the template for a mutagenic PCR (high salt concentration) to generate DNA for transcription to RNA for the next round of selection. The mutagenic PCR contained: 1 × Taq buffer (Promega, WI, USA), 7.5 mM $MgCl_2$ (Promega, WI, USA), 0.2 mM dNTPs (Fermentas, Thermo Fisher Scientific Inc., MA, USA), 1 µM forward primer (5′ AAGCTGTCCTCCGAGTGTTGTCCG 3′) and 1 µM reverse primer (5′ ATTATGCTGAGTGATATCCCTCTGTTCTTATTCGTAC 3′) (Integrated DNA Technologies, CA, USA), 1 U Go Taq Polymerase (Promega, WI, USA) and 100 ng DNA. The reaction was performed with the following parameters: an initial denaturation step at 93 °C for one minutes followed by cycles of 93 °C for 30 seconds for denaturation, 54 °C for 30

seconds for annealing and 72 °C for one minute for extension. A final extension of ten minutes at 72 °C was included after the last cycle. The PCR was optimised for optimal cycle number to generate a single band of PCR product at each round of selection.

The PCR product was purified by centrifugation using a PCR purification kit (Promega, WI, USA) according to manufacturer's specifications (Appendix 6.1.2). DNA was quantified as discussed in Appendix 6.1.3. Fractions of the clean DNA were resolved on a 2.5 % (w/ v) agarose gel stained with ethidium bromide (Merck, Darmstadt, Germany) in 1 × TBE running buffer. A Mass Ruler Low Range DNA Ladder (Fermentas, Thermo Fisher Scientific Inc., MA, USA) was used for DNA sizing and quantification by Molecular Imager Chemidoc XRS+ Imaging System (BIORAD, CA, USA). Purified DNA was used for RNA aptamer production by *in vitro* transcription. *In vitro* transcription followed the protocol previously described by Khati et al. (2003). Briefly, 100 µl reaction mixture contained: 1.5 ng DNA, 1 × transcription buffer (New England Biolabs® Inc., MA, USA) 2 mM spermidine, 1 mM rATP, 1 mM rGTP, 1.5 mM 2′F CTP, 1.5 mM 2′F UTP (Fermentas, Thermo Fisher Scientific Inc., MA, USA), 2 U T7 RNA Polymerase (New England Biolabs® Inc., MA, USA). Transcription reaction was incubated overnight at 37 °C. The reaction was stopped with the addition of 1 U RNAse free DNAse I in 1 × Reaction Buffer (Fermentas, Thermo Fisher Scientific Inc., MA, USA) and incubated at 37 °C for 25 minutes. RNA aptamers were purified from low molecular weight contaminants using NucAway™ Spin Columns (Ambion, NY, USA) as described in Appendix 6.1.5. RNA was quantified by Nanodrop spectrophotometry at A_{260} and was then used for subsequent rounds of selection.

Negative selection used un-transfected HeLa cells as these were the backbone for the production of CD7-HeLa cells used for the positive selection and as such will include all surface receptors excluding the target CD7. Cells were grown to 90 % confluence for 48 hours. The growth media was removed from each well and cells were washed with 2 ml PBS. Non-specific RNA binding sites on the cells' surface were blocked by the addition of 100 µg/ ml yeast tRNA in 1 × HMCKN at 37 °C for 20 minutes. The block was discarded before incubating the cells with 100 nM re-folded 2′ Fluoro enriched RNA in 1 × HMCKN at 37 °C for one hour. After incubation the cells were discarded and the RNA from the supernatant was collected and quantified. As a negative background control, the recovery from each round was incubated with HeLa cells and the RNA from within the cells was quantified (as described above for the positive selection rounds). This control served to confirm that the enrichment seen in CD7-HeLa cells was specific to the receptor positive cells.

2.2.5.3 CLONING AND SEQUENCING OF RNA ANTI-CD7 APTAMERS

The recovery from the final round of selection (round 6) was reverse transcribed to cDNA and amplified by PCR to generate the template for cloning. A non-mutagenic PCR with reduced magnesium conditions was used for the final amplification. Each 100 µl reaction mixture contained 1 × Taq buffer (Promega, WI, USA), 1 mM $MgCl_2$ (Promega, WI, USA), 0.2 mM dNTPs (Fermentas, Thermo Fisher Scientific Inc., MA, USA), 1 µM forward primer (5′ AAGCTGTCCTCCGAGTGTTGTCCG 3′) and 1 µM reverse primer (5′ ATTATGCTGAGTGATATCCCTCTGTTCTTATTCGTAC 3′) (Integrated DNA Technologies, CA, USA), 1 U Go Taq Polymerase (Promega, WI, USA) and 100 ng DNA. An eighteen cycle PCR was performed with the following parameters: an initial denaturation step at 93 °C for one minute followed by cycles of 93 °C for 30 seconds for denaturation, 54 °C for 30 seconds for annealing and 72 °C for one minute for extension. A final extension of ten minutes at 72 °C was included after the last cycle.

The PCR product was ligated into a pGEM-T Easy® vector (Promega, WI, USA) and transformed into TOP10 highly efficient chemically competent cells (Novagen, Merck, Darmstadt, Germany) (Appendix 6.1.10). Ninety six colonies were picked and spread onto two plates. One plate was used for colony PCR screening using M13 primers; pUC/M13 primer forward: 5′ CCCAGTCACGACGTTGTAAAACG 3′ and pUC/M13 reverse primer: 5′ AGCGGATAACAATTTCACACAGG 3′ (Integrated DNA Technologies, CA, USA) and to prepare overnight cultures for glycerol stocks. The other plate was sent to Inqaba Biotech (South Africa) for sequencing with the pUC/M13 forward and reverse primers. Sequence analysis and alignments were performed using BioEdit (Hall 1999). The full aptamer sequences were analysed using CLUSTAL W multiple alignment application in BioEdit V7.1.3.0 software (Hall 1999). A full multiple alignment was generated by bootstrapped neighbour joining tree with the bootstrap value set to 1000. Default gap penalties for gap opening and gap extension were used. The aligned sequences were assessed for conserved motifs and were used to generate a neighbour joining tree and was analysed for sequence similarity between aptamers.

2.2.6 MAMMALIAN CELL CULTURE

2.2.6.1 CEM T LYMPHOCYTES

CEM T lymphocytes were maintained at a density of 2×10^5 cells/ ml. The cells were maintained in Roswell Park Memorial Institute Medium (RPMI) 1640 with 2 mM L-glutamine (Gibco, BRL, UK), 1 mM sodium pyruvate (Gibco, BRL, UK), 4500 mg/ ml glucose (Gibco, BRL, UK), 1500 mg/ ml sodium- bicarbonate (Gibco, BRL, UK) supplemented with 10 % FBS (Gibco, BRL, UK) in a humidified incubator with 5 % CO_2 at 37 °C. Cell viability was determined by trypan exclusion under a light microscope after each passage.

2.2.6.2 JURKAT T LYMPHOCYTES

Jurkat T lymphocytes were maintained at a density of 1×10^5 cells/ ml. The cells were maintained in RPMI growth media as in section 2.2.6.1.

2.2.6.3 JEKO-1 B LYMPHOCYTES

JeKo-1 B lymphocytes were maintained at a density of 2×10^4 cells/ ml. The cells were maintained in RPMI growth media as in section 2.2.6.1.

2.2.6.4 HELA CELLS

HeLa mammalian cells were maintained at a density of 5×10^5 cells/ ml. The cells were maintained in DMEM with L-glutamine (Gibco, BRL, UK) supplemented with 10 % FBS (Gibco, BRL, UK) in a humidified incubator with 5 % CO_2 at 37 °C. Cell viability was determined by trypan exclusion under a light microscope after each passage.

2.2.6.5 CD7-HELA CELLS

CD7-HeLa mammalian cells were maintained at a density of 5×10^5 cells/ ml. The cells were maintained in DMEM with L-glutamine (Gibco, BRL, UK) supplemented with 10 % FBS (Gibco, BRL, UK) and 50 µg/ ml neomycin in a humidified incubator with 5 % CO_2 at 37 °C. Cell viability was determined by trypan exclusion under a light microscope after each passage.

2.3 RESULTS

2.3.1 PRODUCTION OF A STABLE CD7-HELA CELL LINE FOR SELECTION OF CD7 SPECIFIC APTAMERS

A recombinant CD7 expression cell line was generated to use as target cells for the CD7 aptamer selection. The recombinant CD7 expressing cell line needed to express the CD7 receptor stably over multiple generation and division cycles. A transiently transfected cell line would not be appropriate as the CD7 expressing cells are needed for multiple rounds of selection over a number of weeks. This section presents the results for the generation and selection of stable transfected HeLa cells and the characterisation of the CD7 receptor expressing cells.

A CD7 expression vector needed to be constructed, for this the cDNA of the human CD7 receptor gene (GenBank® gene ID number: 924) was chemically synthesised (Integrated DNA Technologies, CA, USA). The cDNA was made double stranded by PCR. The PCR was optimised for both cycle number and annealing temperature to determine the best conditions for gene amplification (Appendix 6.1.11). The CD7 receptor gene was amplified according to the optimised reaction conditions and cloned into a pcDNA 3.3-TOPO cloning vector (Invitrogen, CA, USA). Competent *E.coli* cells were transformed to express the pcDNA 3.3-TOPO cloning vector containing the CD7 receptor gene. Plasmids were isolated from the *E.coli* cells and sent for sequencing. The plasmid sequences were aligned with the CD7 receptor consensus sequence (Entrez gene number: NP_006128.1) to confirm the correct sequence for cloning (Appendix 6.1.11). A single plasmid was selected for the transfection of HeLa cells for the production of a stable CD7 receptor expressing cell line.

To generate a stable cell line that constitutively expressed the CD7 surface receptor, HeLa cells were transfected with the pcDNA-CD7 cloning vector and placed under neomycin antibiotic (Sigma-Aldrich, MO, USA) selection. The minimum inhibitory concentration of the neomycin was determined by kill curve analysis using transfected and non-transfected cells (Appendix 6.1.9). Cell viability was monitored for one week using light microscopy. The phenol red in the cell growth media changed colour as an indication of change in pH due to cell proliferation and death. Flow cytometry and fluorescence microscopy were used to confirm the presence of CD7 receptor on the surface of the stably transfected HeLa cells. When the CD7 receptor is expressed on the cell surface, FITC labelled anti-CD7 antibody

binding causes a right hand shift in green fluorescence (Figure 2-1). The base line level of fluorescence was determined using cells alone and the fluorescence shift due to antibody binding was determined for CD7-HeLa cells and un-transfected HeLa cells. A right hand shift after antibody incubation with the CD7-HeLa cells indicated antibody binding the surface expressed CD7 receptor (Figure 2-1 A). The un-transfected HeLa cells had no shift after incubation with the antibody indicating that there was no antibody binding and as such no CD7 receptor on the surface of the cells (Figure 2-1 B).

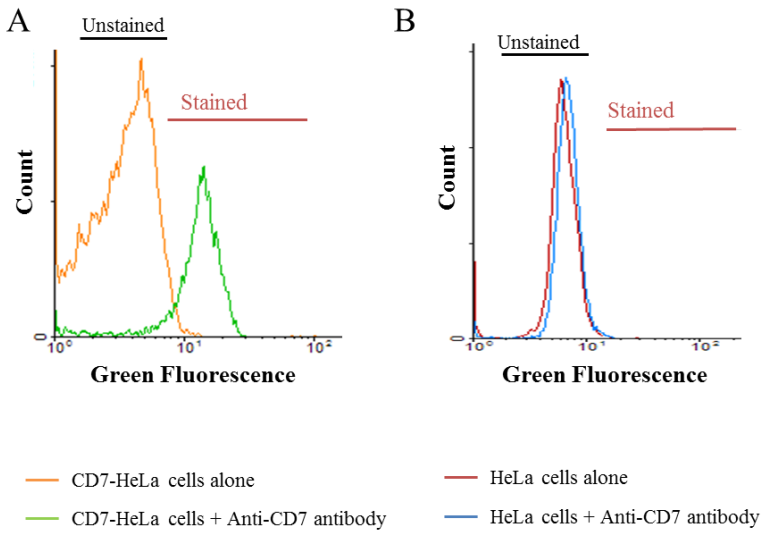

FIGURE 2-1: FLOW CYTOMETRY CONFIRMATION OF SURFACE CD7 RECEPTOR EXPRESSION
Un-transfected HeLa cells and CD7-HeLa cells were incubated with a FITC labelled mouse anti-human monoclonal anti-CD7 antibody. A right hand shift in green fluorescence is an indication of antibody binding. The shift is seen only in the transfected CD7-HeLa cells (A) and not for the un-transfected HeLa cells (B).

In addition to flow cytometry, fluorescence microscopy was used to confirm the presence of CD7 receptor on the surface of the stably transfected HeLa cells. Un-transfected HeLa cells were used as a negative control in all experiments. CD7-HeLa and un-transfected HeLa cells were fixed and incubated with a FITC labelled anti-CD7 antibody. A no antibody control was included to account for the autofluorescence of the CD7-HeLa cells. Antibody binding was seen for the CD7-HeLa cells as fluorescence around the surface of the cells while no fluorescence was detected for the un-transfected HeLa cells (Figure 2-2). The microscopy and flow cytometry data confirmed the surface expression of the CD7 receptor on the transduced CD7-HeLa cell line. The stably transfected CD7-HeLa cell line was used for positive selection rounds for the whole cell selection of CD7 specific internalising

aptamers. Un-transfected HeLa cells were confirmed for no CD7 receptor expression and were used for the negative selection.

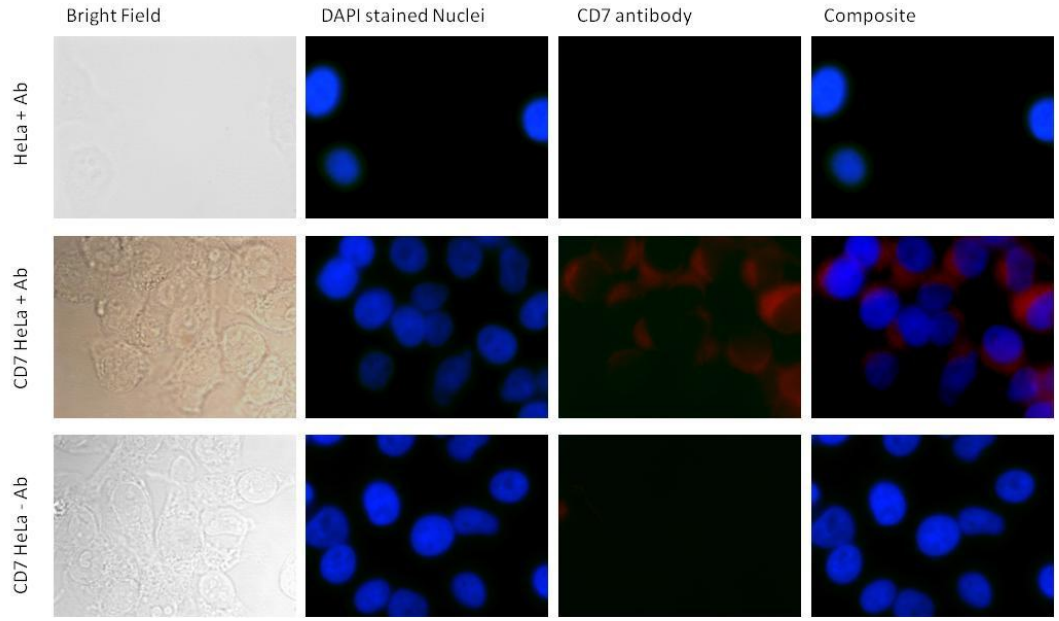

FIGURE 2-2: MICROSCOPY CONFIRMATION OF CELL SURFACE CD7 RECEPTOR EXPRESSION
Cells were stained with a FITC labelled anti-CD7 antibody and viewed using a wide field fluorescent microscope. CD7-HeLa cells showed antibody staining around the cells while un-transfected HeLa cells did not.

2.3.2 SELECTION OF INTERNALISING ANTI-CD7 APTAMERS BY WHOLE CELL SELEX

The aim of this section was to select for internalising aptamers specific to the human CD7 receptor. To generate these aptamers a specialised selection method against whole cells was used. This internalising whole cell SELEX made use of the CD7-HeLa cells generated in the previous section as target cells. The selection was optimised for RNA aptamers and as such made use of rounds of PCR and *in vitro* transcription to generate the input for each round.

Whole cell SELEX was used to generate RNA aptamers capable of internalising cells using the human surface CD7 receptor (Figure 2-3). The stably transfected CD7-HeLa cell line was used for positive selection of internalising aptamers. The un-transfected HeLa cells, that did not express the CD7 receptor, were used for negative selection to remove non-specific internalising RNA species. At each round of selection, the PCR was optimised for cycle number (Appendix 6.1.12) before DNA was transcribed to generate the RNA input. The PCR reaction used a high magnesium concentration to promote mutations and diversity in the

input RNA. A high magnesium concentration helps to stabilise non-complimentary base pairs (Ruigrok, van Duijn et al. 2012).

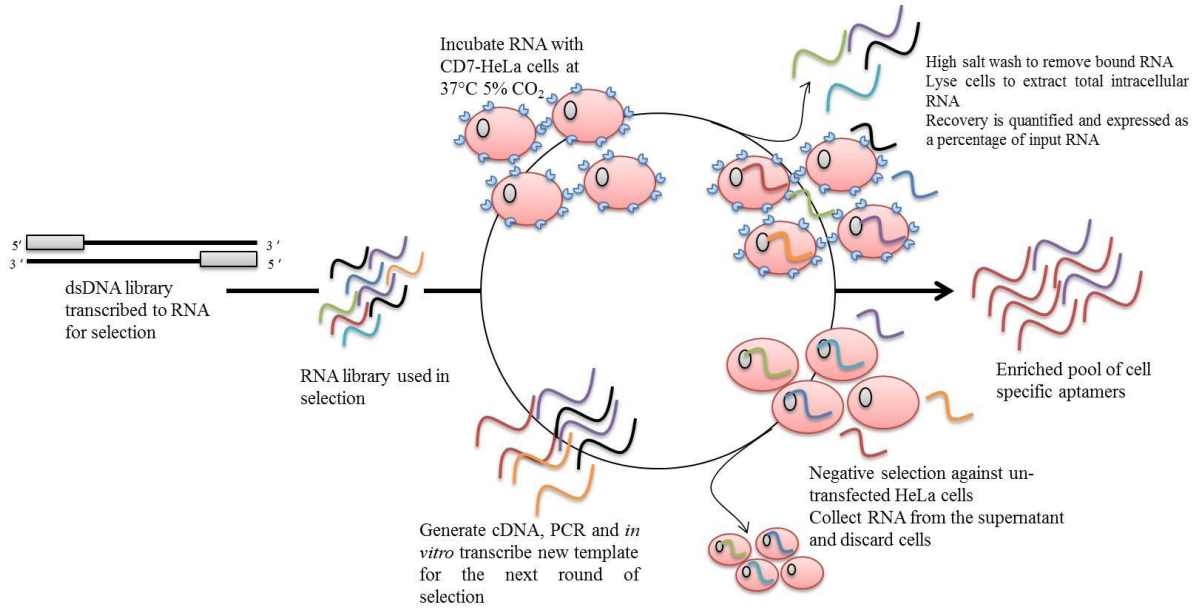

FIGURE 2-3: PROCEDURE OF WHOLE CELL SELEX TO SELECT INTERNALISING APTAMERS

The dsDNA library was transcribed to 2′-Fluoro RNA for use in the selection. Positive selection used CD7-HeLa cells and the internalised nucleotides were recovered for subsequent rounds of selection. The negative selection used un-transfected HeLa cells and the supernatant was retained to recover the unbound nucleotides for amplification. The selection was continued until the recovery from each round reached a plateau.

Three rounds of positive selection in CD7-HeLa cells were followed by a round of negative selection against un-transfected HeLa cells. The negative selection was followed by an additional two rounds of positive selection in CD7-HeLa cells. The selection pressure was increased during the selection by reducing the aptamer concentration from 100 nM in the first round to 70 nM in the last. Each round of selection in CD7-HeLa cells was repeated in un-transfected HeLa cells and the recovery from each cell type compared (Figure 2-4). The recovery from un-transfected HeLa cells remained constant at five per cent while that in CD7-HeLa cells showed enrichment at each round, indicating specificity for the expressed CD7 receptor (Figure 2-4). The initial recovery from CD7-HeLa cells was similar to the first round in transfected HeLa cells at 11 % but increased steadily at each round eventually plateauing at around 60 % after five rounds (Figure 2-4). The enriched pool (recovery from round 6) was tested for internalisation in the un-transfected HeLa cells and no increase in internalisation was seen (Figure 2-4). This indicated that the enriched pool showed specificity to the CD7 receptor and the internalisation into the un-transfected HeLa cells was non-specific internalisation. As the same level of background internalisation was seen in the

enriched pool, it was evident that the negative selection was not sufficient to remove all non-specific internalising RNA. Additional negative selection rounds could have been included which may have improved the removal of the background internalising RNA. However, as the background internalisation was at 5 %, it did not contribute significantly to the overall enriched pool and thus no additional rounds of negative selection were included. The recovery from each round in the un-transfected HeLa cells was checked for binding to CD7-HeLa cells and un-transfected HeLa cells using flow cytometry (Appendix 6.2). The binding assay confirmed that the un-transfected HeLa internalised RNA contained no CD7 specific binders, as the binding was similar for both cell types (Appendix 6.2). After six rounds of selection, the enriched pool of aptamers was amplified by PCR (Figure 2-5) and ligated into a pGEM-T Easy® vector (Promega, WI, USA) for cloning into chemically competent One Shot TOP10 *E.coli* cells (Novagen, Merck, Darmstadt, Germany).

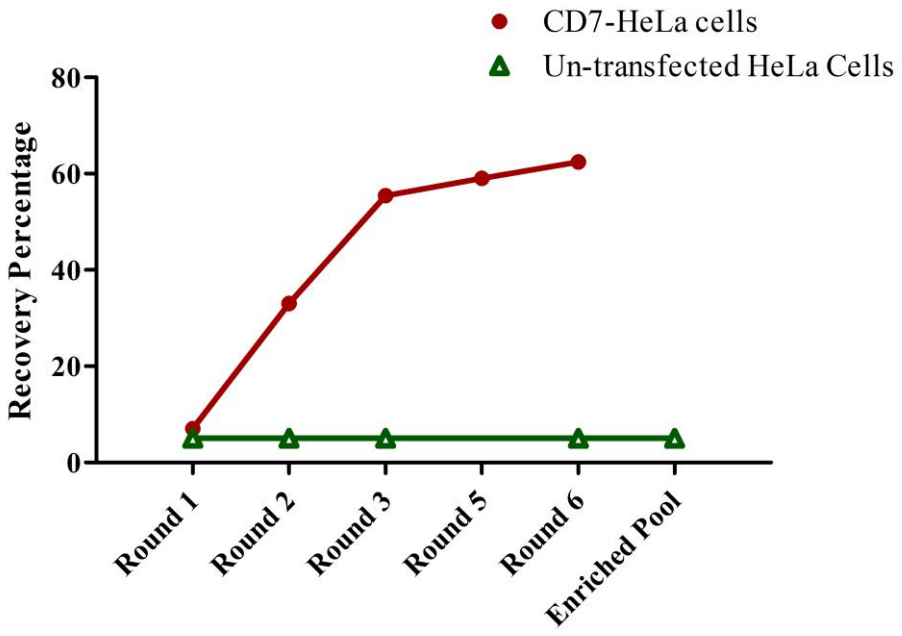

FIGURE 2-4: RECOVERY FROM INTERNALISING WHOLE CELL SELEX

CD7 specific internalising aptamers were selected after five rounds of positive selection in CD7-HeLa cells and one round of negative selection, at round 4, in un-transfected HeLa cells. Each round of recovery was repeated in un-transfected HeLa cells to confirm the enrichment of CD7 specific aptamers. The recovery from un-transfected HeLa cells remained constant while that in CD7-HeLa cells showed enrichment at each round.

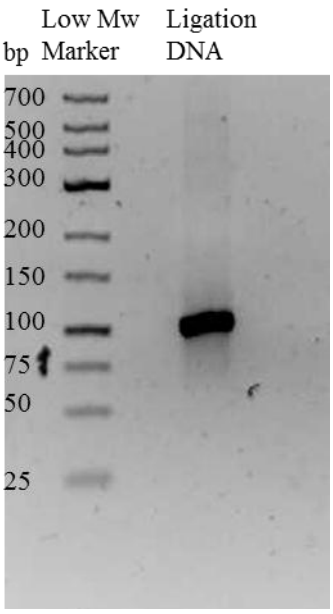

FIGURE 2-5: PCR AMPLIFICATION OF THE ENRICHED POOL OF CD7 SPECIFIC APTAMERS

The enriched pool of CD7 specific aptamers was amplified by PCR using a low magnesium concentration buffer. The PCR resulted in a single band at the correct size according to the molecular weight marker. Once confirmed as a single band at 100bp, the DNA was ligated into a pGEM-T Easy® vector.

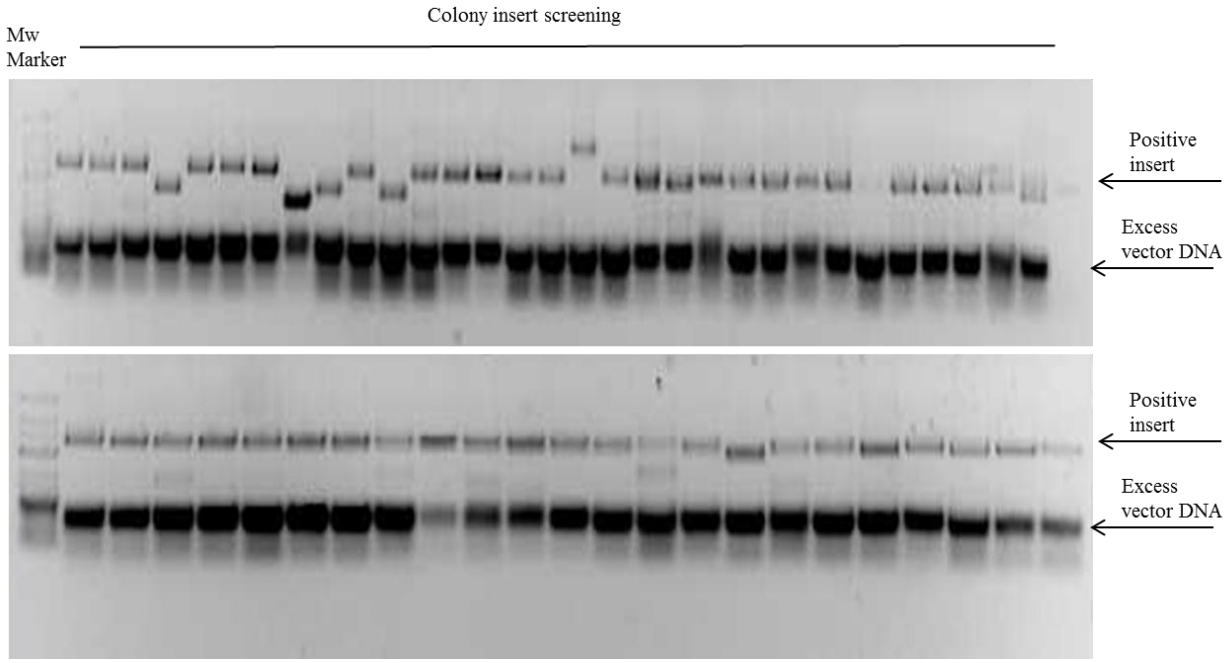

FIGURE 2-6: VECTOR INSERT SCREENING USING M13 PRIMERS

Ninety six colonies were amplified using M13 specific primers to determine the insert positive clones. The positive insert was confirmed by a band at the indicated arrow. The excess vector DNA can be seen as a band below the band of interest and indicates an overloading of template into the PCR.

Ninety six colonies were picked and analysed for positive inserts. To detect positive inserts, each clone was amplified by PCR using M13 specific primers to amplify the vector (Figure 2-6). Sixty-two clones were positive for an insert and were sent for sequencing at Inqaba Biotech (South Africa). Of the sequenced clones, fifty-nine clones were identified as full length with both primer sequences. The missing primer sequence in some clones may indicate why inserts of different sizes were observed (Figure 2-6). The three clones without primer sequences were excluded from the analysis while the remaining sequences were analysed for conserved motifs and sequence similarity using CLUSTAL W multiple alignment (Table 2-1). Aptamers were assigned names based on the order of their sequencing and the target number using CSIR nomenclature and so do not reflect their attributes. Of the 59 aptamer clones, three were pooled more than once, CSIR 3.3 and CSIR 3.53 were pooled twice and aptamer CSIR 3.23 was pooled three times (Figure 2-7). The remaining aptamer sequences were highly divergent. An unrooted maximum likelihood phylogenetic tree of the aptamer clones was generated and indicates the great diversity of the clones (Figure 2-7). An unrooted tree provides information about the relationship between the different sequences but does not assign ancestry to the sequences. The statistical information for the phylogenetic tree can be found in Appendix 6.3. Four clusters of sequences were seen in the phylogenetic tree with one main outlier, CSIR 3.1 (Figure 2-7). The clusters make up 35 % of the sequences while the remaining 65 % of the sequences were highly divergent or only coupled with one other sequence. The three aptamers pooled more than once were all found in different clusters (Cluster A, D and un-clustered) indicating that each cluster of similar sequences was favoured in the selection. Aptamers were selected for binding and internalisation screening using CD7-HeLa cells and un-transfected HeLa cells. The screening experiments are documented in Chapter 3.

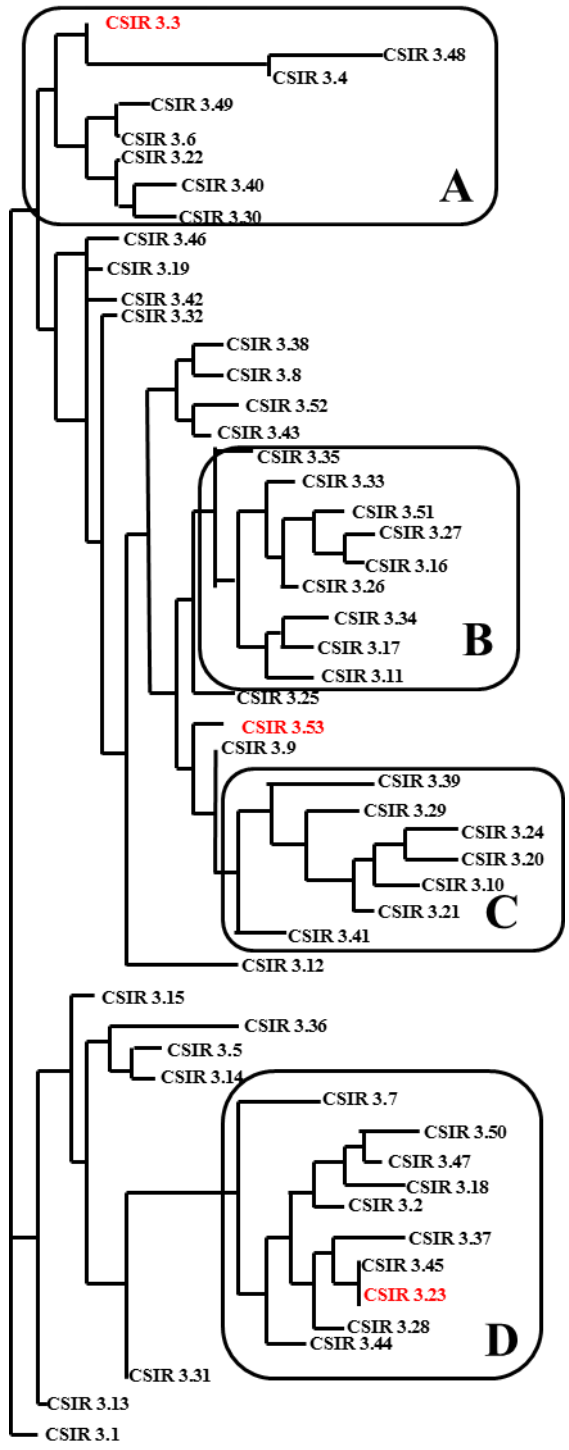

FIGURE 2-7: MAXIMUM LIKELIHOOD PHYLOGENETIC TREE OF APTAMER SEQUENCES

Aptamer sequences from the whole cell SELEX were aligned and plotted on a neighbour joining tree to identify similarity in the sequences. Aptamers CSIR 3.3, CSIR 3.23 and CSIR 3.53 were pooled more than once and are shown in red.

TABLE 2-1: CD7 SPECIFIC INTERNALISING APTAMER CLONE SEQUENCES

Cluster	Aptamer Name	Aptamer Sequences
A	CSIR 3.3	GGGAGACAAGAATAAGCATGGGACCCCAACTAGCGTGTCATTGTTCGAATCGACTGAGATTTCGGGTTCGACAGGAGGCTCACA ACAGGC
	CSIR 3.4	GGGAGACAAGAATAAGCATGAGACTGATCCAAATACGACACAAATACCCGGCACTAGACGTTCGACAGGAGGCTCACAACAGGC
	CSIR 3.6	GGGAGACAAGAATAAGCATGTAATTCCAGCATAAAAAAGATAGGTACTATTAATACACGACCAGAATTCGACAGGAGGCTCACA ACAGGC
	CSIR 3.22	GGGAGACAAGAATAAGCATGCGTTAGCAGATACATCGAGATTGCAAAGTCCAATACAGTTAATAAGTTCGACAGGAGGCTCACA ACAGGC
	CSIR 3.30	GGGAGACAAGAATAAGCATGCACGGATGACAGCAGAATAACTCCTACAGTCCATATATAAACGATTTTCGACAGGAGGCTCACA ACAGGC
	CSIR 3.40	GGGAGACAAGAATAAGCATGCCATGATATACCGATATTAACTTCCGCGTTGCACAAGAATACACTGTTCGACAGGAGGCTCACA ACAGGC
	CSIR 3.48	GGGAGACAAGAATAAGCATGCTGGCAATAAACGGCTATAAGTAAAGTTCGACAGGAGGCTCACAACAGGC
	CSIR 3.49	GGGAGACAAGAATAAGCATGCAAAATATACAAATAACAGACAGAATACTTTGCATCAATAGTTGGATTCGACAGGAGGCTCACA ACAGGC
B	CSIR 3.11	GGGAGACAAGAATAAGCATGGGATAGTTCTGCGTAGCTTAAGAGATGTTAAATCACACCCACGCCATTCGACAGGAGGCTCACA ACAGGC
	CSIR 3.16	GGGAGACAAGAATAAGCATGATCTAAAGACAGATTTAATACTACCCGTCGTATCCAACTCGGAACGGTCGACAGGAGGCTCACA ACAGGC
	CSIR 3.17	GGGAGACAAGAATAAGCATGTACGTAGACAAGAGATTTCCAGACCCTGTTACTAATACATTTCCCGTTCGACAGGAGGCTCACA ACAGGC
	CSIR 3.26	GGGAGACAAGAATAAGCATGTACAAATCCGCATATACACCCAACCACACCCAATCCTCTCAGTCCATTCGACAGGAGGCTCACA ACAGGC
	CSIR 3.27	GGGAGACAAGAATAAGCATGCCCTAGCAACATTCTATGCGCAAACCATAGTTATGACTATTGACTCTTCGACAGGAGGCTCACA ACAGGC
	CSIR 3.33	GGGAGACAAGAATAAGCATGGGGATAGCCGCACTTCTCACAGGAGTCGAGTCTTTTGATCGGTCTCTT CGACAGGAGGCTCACAACAGGC
	CSIR 3.34	GGGAGACAAGAATAAGCATGCGTGCGCCTATGATGAGTCTGGTTCACATAATTTGCGTTAGTTAGTTTCGACAGGAGGCTCACA ACAGGC
	CSIR 3.35	GGGAGACAAGAATAAGCATGGATCTTTCGACAGGAGGCTCACAACAGGC
	CSIR 3.51	GGGAGACAAGAATAAGCATGAGCAGATGTTGTGATTAGTTGAACAAGGTCCCCAAACATTGGAGGATTCGACAGGAGGCTCACA ACAGGC
C	CSIR 3.10	GGGAGACAAGAATAAGCATGGCCGATCCATCCTCCCCACGACCATCATGAATCCCAACAGGAACTTCGACAGGAGGCTCACAAC AGGC
	CSIR 3.20	GGGAGACAAGAATAAGCATGATATGTAGTAACCCCAATGATAAATAACTAAGACCGCAAGTCAGTTCGACAGGAGGCTCACAAC AGGC
	CSIR 3.21	GGGAGACAAGAATAAGCATGCCACTCCCACACTTCCTTAATCCGCGCTAACACACCATATGTACTTCGACAGGAGGCTCACAAC AGGC
	CSIR 3.24	GGGAGACAAGAATAAGCATGCCCCACCCCACTATTAGCCGAACCCGAACCCCATCTTACCCGGACCCGACAGGAGGCTCACAAC AGGC
	CSIR 3.29	GGGAGACAAGAATAAGCATGCCGCACCCGTACCTCCTTCCTCTCAGGTATTCACTCACATCATTTCGACAGGAGGCTCACAACA GG
	CSIR 3.39	GGGAGACAAGAATAAGCATGTTAGCTCCGTCAGGTATCCACAGATCATTGTTCAATACATTCGACAGGAGGCTCACAACAGGC
	CSIR 3.41	GGGAGACAAGAATAAGCATGCGAAATCATAGCCCACGGTTGCATCACCCGTTCTGATCATATACTTAAAGTTAGGAGGCTCACA ACAGGC
D	CSIR 3.2	GGGAGACAAGAATAAGCATGCCCTTCCCTAGAACGCAGGCAGCAGTTACTCGGAGAACCCTACCCTTCGACAGGAGGCTCACAA CAG
	CSIR 3.7	GGGAGACAAGAATAAGCATGATCTACGCGACCACAAAATTATCCGCGATTTGAATATTCGACAGGAGGCTCACAACAGGC
	CSIR 3.18	GGGAGACAAGAATAAGCATGCCTACATTCGACAGGAGGCTCACAACAGGC
	CSIR 3.23	GGGAGACAAGAATAAGCATGGAGTGCGTCGCCACTACTCCTCTCATTACCTCTTGCATTTCACTATTCGACAGGAGGCTCACAA CAGGC
	CSIR 3.28	GGGAGACAAGAATAAGCATGCACACCGGCTGAGTATCTGCCTGTGTAATCGAAACAACTGCGACATTCGACAGGAGGCTCACAA CAGGC
	CSIR 3.37	GGGAGACAAGAATAAGCATGAGAGATTTTGGGAAGGCTCAGGACTGCCTACTAACCCGATAAGAATTCGACAGGAGGCTCACAA CAGGC
	CSIR 3.44	GGGAGACAAGAATAAGCATGTTCCTGGAGACGCCTATAGTACCTTGCCCCGTAGTATCTGATCAATTCGACAGGAGGCTCACAA CAGGC
	CSIR 3.45	GGGAGACAAGAATAAGCATGTTACCTACAAAAAAGAAAAAGAATTAAACGGATTAAGAAGGGGAAAAAGTAGTTCGACAGGAGG CTCACAACAGGC
	CSIR 3.47	GGGAGACAAGAATAAGCATGACCGTGCTCTGTGACAGGACTTTACTTAGGGATAAGGGTTGAAACTTCGACAGGAGGCTCACAA CAGGC
	CSIR 3.50	GGGAGACAAGAATAAGCATGCGCGCATAAACCTAACGCGCTTTTCTCTAGGTTGATTAAACTGGGTTCGACAGGAGGCTCACAA CAGGC
Outlier	CSIR 3.1	GGGAGACAAGAATAAGCATGAAACCCCAACTCTGGCGCACATTTCCCCGCCACCACCGTAGAATACTTCGACAGGAGGCTCACA ACAGGC

Cluster	Aptamer Name	Aptamer Sequences
Un-clustered	CSIR 3.8	GGGAGACAAGAATAAGCATGCCCCTTGCGGTTCCCACATTATCTCTCTGCTATCCCGATGGCCCGATTCGACAGGAGGCTCACA ACAGGC
	CSIR 3.9	GGGAGACAAGAATAAGCATGAGACATTCTCTCCGCCCTCAACTCCGCCCGCTCCATCCAGTTCCCTGTCGACAGGAGGCTCACA ACAGGC
	CSIR 3.12	GGGAGACAAGAATAAGCATGGCTATCATACCCGAGACCGCTATCCCCCACCTTAATGTTCCTTCGACAGGAGGCTCACAACAGG C
	CSIR 3.13	GGGAGACAAGAATAAGCATGAGACCGTACACCTCGCTCGCCATCCGACTTTGAATAAGCATAGACCTTCGACAGGAGGCTCACA ACAGGC
	CSIR 3.14	GGGAGACAAGAATAAGCATGAGCGCCAATATGACCGCGACATCGTTTGAATAGTTCCTGGGGATCTTTCGACAGGAGGCTCACA ACAGG
	CSIR 3.15	GGGAGACAAGAATAAGCATGCCGGATAAGGTCGTCCGTAGTACCGGTTAACGTACCAGCCTTACTCTTCGACAGGAGGCTCACA ACAGGC
	CSIR 3.19	GGGAGACAAGAATAAGCATGCTCTGACAATCCTGCAACAATTACATTCATTAACGGGCTAATTCATATCGACAGGAGGCTCACA ACAGGC
	CSIR 3.5	GGGAGACAAGAATAAGCATGAGCATCAATCTAGACTAGACTCAGATTACCAGCGAACTAGTGTATCTTCGACAGGAGGCTCACA ACAGGC
	CSIR 3.25	GGGAGACAAGAATAAGCATGTTCTCTGCGGTCTAGGTCACGATATACCCGTTACATATCATTCCTGTTCGACAGGAGGCTCACA ACAGGC
	CSIR 3.31	GGGAGACAAGAATAAGCATGCAATTTATCGAGACCCAGATAACCGATTTATACGCAGACGATAAGTTTCGACAGGAGGCTCACA ACAGGC
	CSIR 3.32	GGGAGACAAGAATAAGCATGAGCCCCACATCCTACGCCACTCACCCACGCATCCCGATTGATCAAATTCGACAGGAGGCTCACA ACAGGC
	CSIR 3.36	GGGAGACAAGAATAAGCATGGGCAGCGATAGACTGTTAACTACAGACGGGAGTCCGCGTTTCGACAGGAGGCTCACAACAGGC
	CSIR 3.38	GGGAGACAAGAATAAGCATGCATCCCCAGGCTCTTCCATCAAGCAATTAATACAATCACAACCCCCTTCGACAGGAGGCTCACA ACAGGC
	CSIR 3.42	GGGAGACAAGAATAAGCATGCGTCCCACACCCTCCGATTCCGACCAGGACTGGATACTTACACTTTTTCGACAGGAGGCTCACA ACAGGC
	CSIR 3.43	GGGAGACAAGAATAAGCATGCCCCCTTCGCCCAAAACATATCGCTTCGACCTTCCACACCCTATCATTCGACAGGAGGCTCACA ACAGGC
	CSIR 3.46	GGGAGACAAGAATAAGCATGATTGAGCCCTCCGCCCAAACTCACTCTCAACAAACCGCTGGAACGCTTCGACAGGAGGCTCACA ACAGGC
	CSIR 3.52	GGGAGACAAGAATAAGCATGCCTCATTAACCCCGCTGTGCCCTGCATCACTTCTCATAGTCCGACACTCGACAGGAGGCTCACA ACAGGC
	CSIR 3.53	GGGAGACAAGAATAAGCATGCAGGTCCCACCGCCCCGCTCCCTTATCAGCTTGGAATACGTTTTCATTCGACAGGAGGCTCACA ACAGGC
	CSIR 3.54	GGGAGACAAGAATAAGCATGTCATCTCACCGCCATAATCCTCAACATTCTCCCCACCCGATTCCCGTTCGACAGGAGGCTCACA ACAGGC

2.4 DISCUSSION

The human CD7 receptor was identified as a good target for delivery of therapeutics due to its expression pattern on T lymphocytes progenitors and CD4+ cells (Discussed in detail in section 5.2). As such, aptamers specific to the CD7 receptor were isolated. The aptamers were selected against whole cells so that the correctly folded CD7 receptor structure was used. Selection using the recombinant protein of a receptor can lead to aptamers not functional against the surface expressed receptor due to conformational differences (as discussed in section 2.1). The whole cell SELEX technique is typically used to develop aptamers specific to disease cells overexpressing a specific receptor (Section 1.3.4). For the selection used here a cell line overexpressing the CD7 receptor had to be generated as using a T cell lymphoma cell line would introduce the complexity of selecting an appropriate negative selection cell line. T and B cell lymphoma cell lines were found to express the same level of the CD7 receptor even though it is a marker for T cell development (Appendix 6.4). However, it has been noted that B cell lymphomas may aberrantly express T cell receptors (Kaleem, White et al. 2001). In addition, when selecting for aptamers against a whole cell, there are a number of receptors and surface markers that may confound the selection. This may result in aptamers with unknown surface targets. The aptamer selection protocol included a step to remove non-CD7 specific aptamers by selecting for aptamers that did not bind or internalise into un-transfected HeLa cells. This approach was important to prevent the selection of RNA sequences able to non-discriminately internalise into cells or specifically internalise via a different receptor. Also, as opposed to a standard whole cell SELEX that selects for aptamers able to bind to a specific receptor, our approach was to select for aptamers internalised into cells via a specific receptor; a fundamental and important difference.

The enriched pool of selected aptamers was characterised computationally for sequence similarity. Three aptamers were isolated multiple times (aptamers CSIR 3.3, CSIR 3.23 and CSIR 3.53) from the selection and as such were identified as the most highly enriched aptamers. The aptamers pooled more than once were not clustered together in the maximum likelihood phylogenetic tree. The unrooted maximum likelihood phylogenetic tree plotted the sequence similarity and as such, by being in different clusters, the most enriched aptamers were not closely related. As this analysis is focussed on the sequences, it has no insight into the structures favoured by selection. Aptamers bind in a conformation dependent manner and thus an inspection into the conformational landscape of the RNA pool during

selection may provide insight into the evolutional pull for particular structures rather than sequence.

Minimal conservation identified in this selection may have been the consequence of sequencing only a subset of the enriched pool. Greater conservation may have been identified from sequencing of the whole enriched pool rather than the selected clones. A recent study made use of next generation sequencing of each round of selection allowing for the selection to be tracked according to sequence diversity (Thiel, Bair et al. 2012). It was seen that after the first three rounds of selection the sequence diversity reduced four fold while the enrichment increased 3 fold (Thiel, Bair et al. 2012). This effect plateaued from the fifth round of selection. Future internalising aptamer selections using the next generation sequencing method should be considered as it may present a more accurate measure of aptamer enrichment than the increase in percentage recovery at each round (Discussed further in section 5.1). It will also allow for the stopping point of selection to be more accurately identified. As such, the conservation within the enriched pool may be an under representation of the actual sequence similarity. In addition, without the knowledge of the entire enriched pool of sequences it is difficult to assign statistical significance to the repeated sequences. The most "enriched aptamer identified, CSIR 3.23 was identified three times making up 5.6 % of the sequenced pool. The other aptamers pooled more than once, CSIR 3.3 and CSIR 3.53 make up 3.7 % of the sequenced pool. In a recent study it was shown that a highly enriched aptamer identified by high throughput sequencing, made up 90 % of the sequenced pool can be missed by sequencing of random clones (Ngubane 2012, Personal communication). Thus, although the three sequences pooled more than once in this method appear more highly enriched than the other sequences, this may not be the case. However, as a starting point, the aptamers pooled more than once in the selection will be the first to be tested for binding and internalisation into target cells followed by the remaining aptamers. The following chapter will cover the characterisation of aptamer binding and internalisation in CD7-HeLa and un-transfected HeLa cells.

Chapter 3. CHARACTERISATION AND OPTIMISATION OF ANTI-CD7 APTAMERS BINDING EXOGENOUSLY EXPRESSED CELL SURFACE CD7 RECEPTOR

3.1 INTRODUCTION

A modified whole cell SELEX was performed for the selection of aptamers able to internalise into cells using the T lymphocyte receptor CD7. The enriched pool of selected aptamers was sequenced and analysed for sequence similarity by phylogenetic analysis. Although three aptamers were identified more than once, the statistical significance of the repetition is difficult to assess, as the entire enriched pool was not sequenced (as discussed in section 2.4). Although the enriched pool is assumed to contain largely specific aptamers, and a negative selection was included to remove non-specific aptamers from the selection pool, a number of non-specific binders can be selected. These unwanted aptamers may come through the selection process due to inefficient partitioning of non-specific protein interactions, termed background partitioning (Djordjevic 2007). This chapter will cover the characterisation of aptamer binding to the CD7 receptor expressed on CD7-HeLa cells.

Aptamer binding and internalisation was compared between the un-transfected HeLa cells and the receptor positive CD7-HeLa cells. A number of binding and internalisation methods have been used for aptamer characterisation including, but not limited to; binding by SPR (Di Primo, Dausse et al. 2011), binding by aptamer based ELISA commonly referred to as ELONA (Baldrich, Restrepo et al. 2004), internalisation by confocal microscopy (Zhou, Swiderski et al. 2009) and binding and internalisation by flow cytometry (Wheeler, Trifonova et al. 2011). Both the SPR and ELONA methods make use of recombinant protein while confocal microscopy and flow cytometry assess interactions with whole cells. SPR technology has an advantage over ELONA as it allows for label free, real time assessment of ligand-analyte interaction while using relatively small sample volumes (Johnsson 1991; Crouch 1999). The SPR method was selected for characterisation of aptamer binding to recombinant protein however failed to produce significant results due to the low capacity binding of the protein (Appendix 6.5).

As the eventual application of the CD7 aptamers is cell specific delivery, the aptamers were characterised for cell specific association. Cell surface receptor binding characterisation

is commonly performed at controlled temperatures to prevent membrane turn over and molecule internalisation (Coffey, Stefanich et al. 2004). After binding at reduced temperature, the cells can be warmed to physiological temperature for internalisation of the attached molecules. This method was employed in this chapter to characterise both cell specific binding and internalisation using both flow cytometry and confocal microscopy. Aptamers showing CD7 receptor specificity were analysed computationally to identify the secondary structure for each aptamer. The secondary structures were assessed for identification of possible binding region and structural conservation. This chapter covers characterisation of aptamer interaction with exogenously expressed CD7 receptor and recombinant CD7 protein and the identification of candidate aptamers for further study.

3.2 MATERIALS AND METHODS

3.2.1 ANTI-CD7 APTAMER PRODUCTION BY PCR AND IN VITRO TRANSCRIPTION

Each selected aptamer was generated by *in vitro* transcription of double stranded DNA. For this, plasmid DNA of each aptamer was amplified using PCR. Each 100 µl reaction mixture contained 1 × Taq buffer (Promega, WI, USA), 1 mM $MgCl_2$ (Promega, WI, USA), 0.2 mM dNTPs (Fermentas, Thermo Fisher Scientific Inc., MA, USA), forward primer (5′ AAGCTGTCCTCCGAGTGTTGTCCG 3′) and reverse primer (5′ ATTATGCTGAGTGATATCCCTCTGTTCTTATTCGTAC 3′) (Integrated DNA Technologies, CA, USA), 1 U Go Taq Polymerase (Promega, WI, USA) and 100 ng DNA. An eighteen cycle PCR was performed with the following parameters: 93 °C for 30 seconds for denaturation, 54 °C for 30 seconds for annealing and 72 °C for one minute for extension. A final extension of 10 minutes at 72 °C was included in the last cycle.

The PCR product was purified by centrifugation using a PCR purification kit (Promega, WI, USA) according to manufacturer's specifications (Appendix 6.1.2). DNA was quantified as discussed in Appendix 6.1.3. Purified DNA was used for RNA aptamer production by *in vitro* transcription. *In vitro* transcription followed the protocol previously described by Khati et al. (2003) as outlined in section 2.2.5.2. RNA aptamers were purified from low molecular weight contaminants using NucAway™ Spin Columns (Ambion, NY, USA) as described in Appendix 6.1.5.

3.2.2 FLUORESCENT LABELLING OF ANTI-CD7 APTAMERS

Aptamers were end labelled with 6-carboxy-fluorescein (FAM, excitation 494 nm and emission 518 nm) so that they could be tracked using microscopy and flow cytometry for internalisation and binding. A Silencer® siRNA Labelling Kit (Ambion, NY, USA) was used according to manufacturer's protocol. The labelling reaction was prepared with 5 µg single stranded RNA, 1 × labelling buffer and 15 % FAM Labelling Reagent and was incubated at 37 °C for one hour in the dark. The labelled RNA was then ethanol precipitated to remove excess labelling reagent as it may cause short term toxicity of transfected cells. To precipitate the RNA, 0.1 vol 5 M NaCl and 2.5 vol 100 % ethanol were added to the end labelling reaction and after mixing well, the reaction was incubated at -20 °C for one hour. The RNA

was pelleted by centrifugation at 80 000 × g for 15 minutes after which the supernatant was removed and by this stage the RNA was visible as a green pellet. The RNA pellet was washed in 70 % ethanol before being air dried at room temperature in the dark. The pellet was then re-suspended in 1 × HMCKN buffer and quantified using the microarray assay to detect fluorescence concentration on a NanoDrop 1000 spectrophotometer (Thermo Fisher Scientific Inc., MA, USA) (Appendix 6.1.4).

3.2.3 FLOW CYTOMETRY ANALYSIS OF CELL SURFACE BINDING OF ANTI-CD7 APTAMERS

Aptamer binding to the CD7 receptor, expressed on the cell surface, was assessed using flow cytometry. CD7-HeLa and un-transfected HeLa cells were suspended at a concentration of 1 × 10^5 cells/ ml in serum free DMEM. A portion of the CD7-HeLa cells was incubated with an 0.5 µg anti-CD7 monoclonal antibody (CD7 (H-7): sc-28332; Santa Cruz Biotechnology, Inc., CA, USA) antibody at 4 °C for 20 minutes after which all cells were incubated with 400 nM FAM labelled aptamer for 20 minutes. The cells were then washed three times in 500 µl PBS at 4 °C before being re-suspended in 100 µl serum free DMEM at 4 °C for analysis by flow cytometry using a Guava Easy Cyte Flow cytometer (Guava Technologies Inc., CA, USA). The results were analysed and processed using FlowJo version 7.6.5 (Tree Star, Inc., OR, USA). For each run, 10 000 events were counted and cells gated according to forward and side scatter profiles. Aptamer bound cells were compared to cells alone and the percentage cells stained was determined. Aptamer binding to CD7-HeLa cells was compared to binding of un-transfected HeLa cells by normalising aptamer binding to each cell alone control set to 1 using the following formula:

$$Aptamer\ binding = \frac{Aptamer\ percentage\ shift}{Cell\ alone\ percentage\ shift}$$

Aptamer binding to CD7-HeLa cells in the presence of the anti-CD7 monoclonal antibody was compared by normalising CD7-HeLa cells with aptamer to 100% using the following formula:

$$Aptamer\ binding = \frac{Aptamer\ with\ antibody\ percentage\ shift}{Aptamer\ no\ antibody\ percentage\ shift} \times 100$$

As the same cell type was used, the data was not pre-normalised to the cell alone control.

3.2.4 CONFOCAL MICROSCOPY ANALYSIS OF ANTI-CD7 APTAMER INTERNALISATION

Initial screening of aptamer CSIR 3.3, CSIR 3.53 and CSIR 3.23 internalisation was conducted by incubating the fluorescently labelled aptamer with CD7-HeLa cells and un-transfected HeLa cells at 37 °C for 20 minutes. CD7-HeLa cells and un-transfected HeLa cells were seeded at a density of 2×10^5 cells / ml onto 14 mm glass coverslips and incubated overnight at 37 °C with 5 % CO_2. Following incubation, the aptamers were added to the cells at a final concentration of 20 nM and incubated for two hours at 37 °C. Coverslips were washed with pre-warmed PBS (Gibco, BRL, UK) and fixed using 4 % (w/ v) paraformaldehyde (PFA) at room temperature for 30 minutes. The fixed cells were washed three times with PBS at room temperature and stained using HCS CellMask™ Blue Whole Cell Stain, excitation 346 nm and emission 442 nm (Invitrogen, CA, USA) at room temperature for 30 minutes. Staining was followed by another three washes with PBS (Gibco, BRL, UK) after which the coverslip was mounted using 50 % glycerol in PBS mounting media. Slides were imaged using a Nikon T_1 eclipse (Nikon Corporation, Japan) with an Andor enccd 16 bit camera (Andor Technology plc., UK). A Z-stack of images was taken from within the cell, excluding the cell surface. This was to ensure that only aptamer within the cell and not those attached to the cell surface were imaged. ImageJ 1.45 software was used to analyse the images and to flatten the stack images into a single image selecting for "maximum Intensity". Cellular staining stack was flattened using the "average Intensity" command. Both images were processed by subtracting the background and normalised using "enhance contrast" with 0.01 % saturated pixels before generating a montage of the images. Green pseudo colour was assigned to the aptamer stain while grey scale was used for the cellular staining.

3.2.5 CONFOCAL MICROSCOPY ANALYSIS OF ANTI-CD7 APTAMER INTERNALISATION AFTER PRE-BLOCKING OF THE CD7 RECEPTOR

Aptamer CSIR 3.42 shown to bind more in the presence of the anti-CD7 monoclonal antibody was tested to determine if cellular internalisation will increase when CD7-HeLa cells were pre-blocked with an anti-CD7 monoclonal antibody by confocal microscopy. CD7-HeLa cells were seeded at a density of 2×10^5 cells / ml onto four 14 mm glass coverslips and incubated overnight at 37 °C with 5 % CO_2. Following incubation, a subset (two coverslips) of CD7-HeLa cells were blocked using 0.5 µg anti-CD7 monoclonal antibody

(CD7 (H-7): sc-28332; Santa Cruz Biotechnology, Inc., CA, USA) for 20 minutes at 4 °C. The block was removed and all CD7-HeLa cell coverslips were incubated with 70 nM FAM labelled aptamer (in serum free media) for 20 minutes at 4 °C. After incubation, the coverslips were washed three times with PBS (Gibco, BRL, UK) at 4 °C and two coverslips were fixed with 4 % PFA (Sigma-Aldrich, MO, USA) at room temperature for 30 minutes. These were used to assess aptamer binding to the cell surface receptor in the presence and absence of the anti-CD7 antibody. The remaining coverslips were incubated for a further hour at room temperature in serum free DMEM at 37 °C. This is to allow for the bound aptamer to internalise into the cells via the receptor. After incubation, these coverslips were washed three times with PBS (Gibco, BRL, UK) and fixed with 4 % PFA (Sigma-Aldrich, MO, USA) at room temperature for 30 minutes. The fixed cells were stained with 1 µg/ ml Hoechst (33342) nuclear stain for 30 minutes at room temperature. Staining was followed by another three washes with PBS (Gibco, BRL, UK) after which the coverslips were mounted using 50 % Glycerol in PBS mounting media. Slides were imaged as in section 3.2.4. ImageJ version 1.45 software (Schneider, Rasband et al. 2012) was used to analyse the images. Images were processed by subtracting the background and normalised before making the montage. Red pseudo colour was assigned to the aptamer stain, blue pseudo colour was assigned to the nuclear stain and grey scale was used for the bright field images.

3.2.6 COMPUTATIONAL PREDICTION OF THE ANTI-CD7 APTAMER SECONDARY STRUCTURE

MFOLD (http://mfold.bioinfo.rpi.edu/) was used to identify secondary structures possible within the aptamer using the sequence information (Zuker 2003). The nucleotide sequences were added in FASTA format as linear RNA molecules. Secondary structure predictions were made at 37 °C with no divalent ions, 1 M NaCl, 5 % suboptimality, an upper limit of 50 computed folding, a maximum interior / bulge loop size of 30 base pair and maximum asymmetry of interior / bulge loop of 30 base pair. No limits were defined for the distance between base pairs.

3.2.7 MAMMALIAN CELL CULTURE

CD7-HeLa and HeLa cells were maintained as detailed in section 2.2.6.

3.3 RESULTS

3.3.1 ANTI-CD7 APTAMER BINDING AND INTERNALISATION SPECIFICITY TO RECOMBINANT CELL LINE, CD7-HELA

Aptamer binding and internalisation was characterised using the recombinant CD7-HeLa cell line used in selection. This section covers the characterisation of aptamer affinity and internalisation into CD7-HeLa cells. The un-transfected HeLa cells were used to make a comparison for receptor CD7 specificity. In addition, a monoclonal anti-CD7 antibody was used to block the CD7 receptor to confirm receptor specificity. Aptamer RNA was fluorescently labelled using a labelling kit for tracking of internalisation and binding by flow cytometry and confocal microscopy. The labelled RNA was quantified using a nanodrop spectrophotometer. The reading provides a spectrum of the RNA as well as the fluorescent label (Appendix 6.1.4) and the concentration of the labelled RNA is given. The average labelling efficiency was seen to be 80 % for all aptamer clones. The labelled concentration was used for the calculations for all aptamer incubations for flow cytometry and microscopy experiments.

Aptamers were screened for specificity to CD7-HeLa cells using flow cytometry and confocal microscopy. The flow cytometry assay tested binding specificity by incubating the cells with aptamers at 4 °C to prevent membrane trafficking and thus prevent internalisation of the aptamer. This method is commonly used when characterising receptor mediated internalisation as it allows for surface binding to the receptor (Coffey, Stefanich et al. 2004). Warming of the cells after binding allows for internalisation via the receptor (Wassenberg, Dezfulian et al. 1999; Man, Lin et al. 2000). Aptamer specificity was also assessed by blocking the CD7-HeLa cells with an anti-CD7 monoclonal antibody before aptamer incubation. Aptamer binding was identified as a right hand shift in green fluorescence when the aptamer was bound as compared to the cells alone (Figure 3-1 A). Aptamer binding was determined for the different cells by normalising the aptamer binding parentage to each cell alone control set to 1. A student's t test identified that all the aptamers bound significantly ($p < 0.05$) more to CD7-HeLa cells than the un-transfected HeLa cells (Figure 3-1 B). It is not immediately evident whether aptamer binding corresponds to the surface expression of the CD7 receptor. However, other studies have noted that aptamer binding corresponded to cell surface expression of the target (Hernandez, Flenker et al. 2013) which may be the case here. As this was not the main concern for this experiment, the analysis was not included. Multiple

replicates for aptamers CSIR 3.37 and CSIR 3.39 were not achieved so no statistics could be generated. On average a fivefold increase in binding was seen for CD7-HeLa cells with respect to the un-transfected HeLa cells (Figure 3-1).

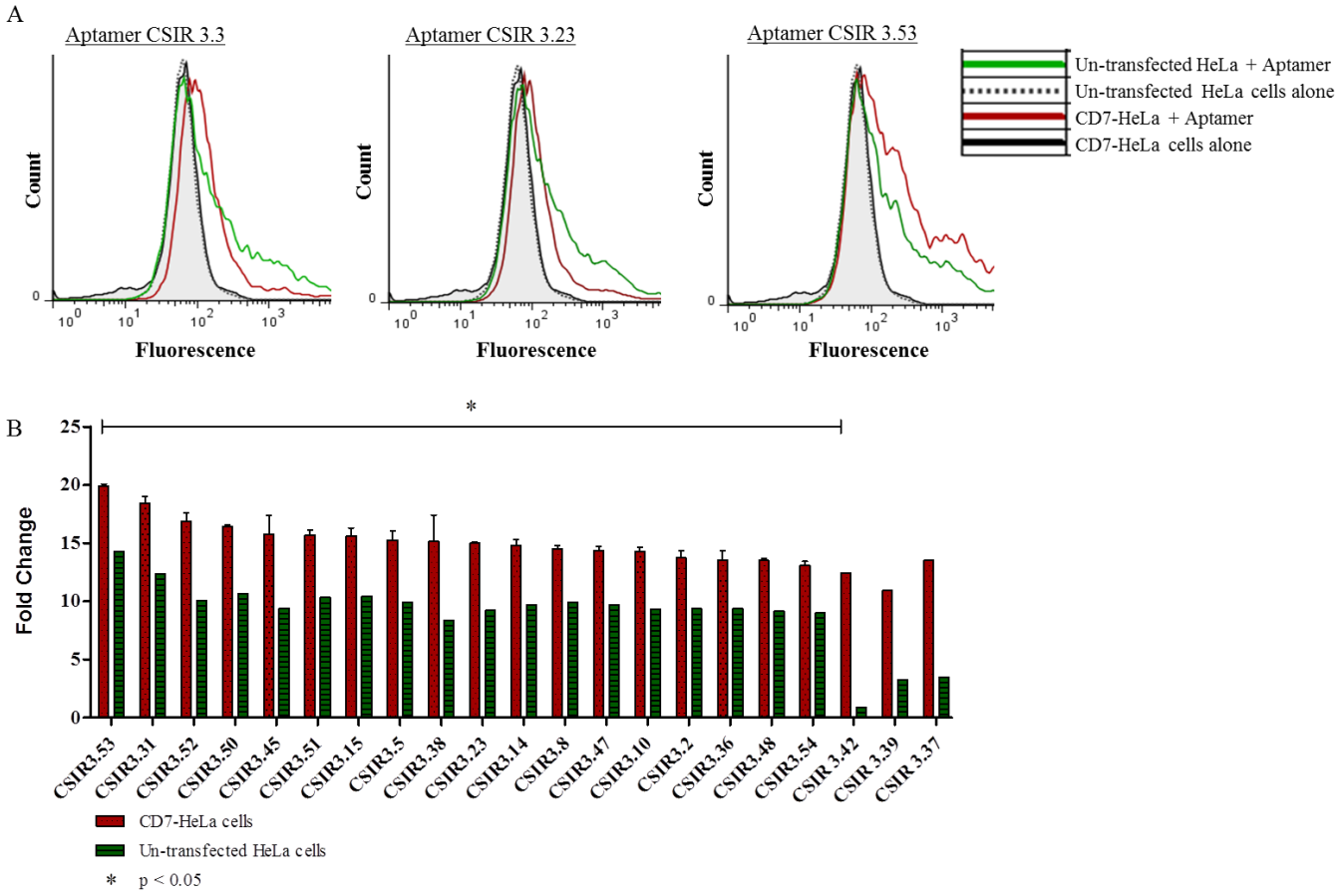

FIGURE 3-1: APTAMER SPECIFICITY TO CD7-HELA CELLS OVER HELA CELLS

A. Overlay histogram of aptamer CSIR 3.3, CSIR 3.23 and CSIR 3.53 binding to CD7-HeLa and un-transfected HeLa cells. The cell alone controls are shaded in grey while aptamer binding CD7-HeLa cells and un-transfected HeLa cells are a red and green line respectively. B. Aptamer binding normalised to the cell alone control set to 1 (n = 4).

For the confocal microscopy analysis aptamers were incubated with the cells at 37 °C and so aptamer internalisation was assessed. Aptamer CSIR 3.23 showed internalisation specificity for CD7-HeLa cells while CSIR 3.3 and CSIR 3.53 did not (Figure 3-2). However, the flow cytometry indicated that the aptamers showed greater affinity for the CD7-HeLa cells.

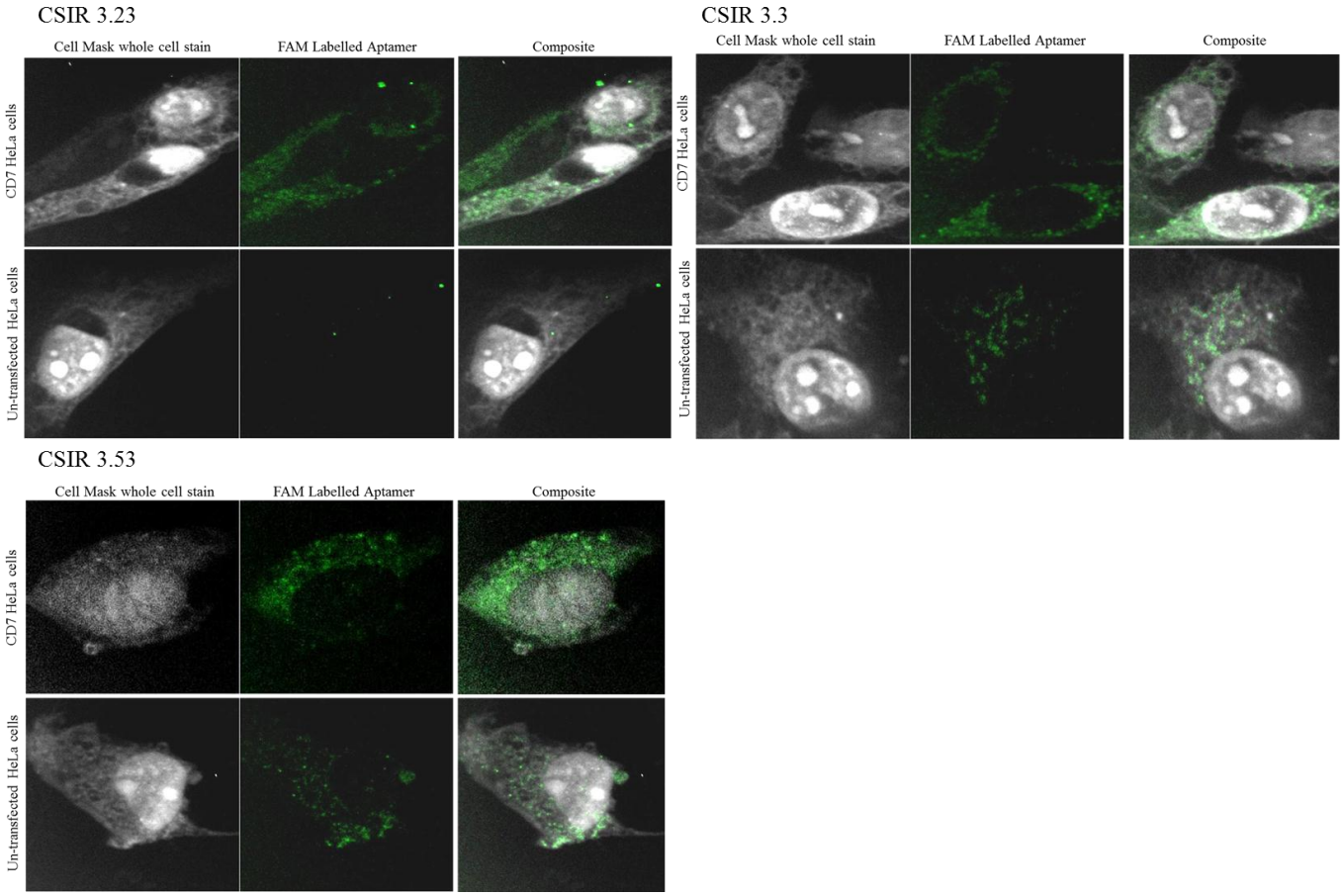

FIGURE 3-2: APTAMER CSIR 3.23, CSIR 3.3 AND CSIR 3.53 INTERNALISATION SPECIFICITY

CD7-HeLa and un-transfected HeLa cells were incubated with FAM labelled aptamer. Cell Mask whole cell stain was used to visualise the cells and localise the aptamer staining. A composite of cell and aptamer stain was generated.

To test specificity of binding to the receptor, the aptamers were bound to the CD7-HeLa cells in the presence of a CD7 antibody. The binding of each aptamer in the presence of the anti-CD7 antibody was normalised to its comparative CD7-HeLa binding assay set to 100 %. All aptamers except CSIR 3.8 had reduced binding in the presence of the antibody (Figure 3-3). A student's t test was used to determine the significance of the change with a 95 % confidence level. Multiple replicates for aptamers CSIR 3.37 and CSIR 3.39 were not achieved so no statistics could be generated, however, these aptamers showed a marked decrease in binding in the presence of the anti-CD7 MAb. Aptamer CSIR 3.8 had significantly increased binding ($p < 0.05$) while aptamers CSIR 3.5, CSIR 3.10, CSIR 3.14, CSIR 3.23, CSIR 3.38, CSIR 3.42, CSIR 3.45, CSIR 3.48, CSIR 3.50 and CSIR 3.53 had significantly reduced binding. These aptamers were representatives of different sequence clusters as described in section 2.3.2.

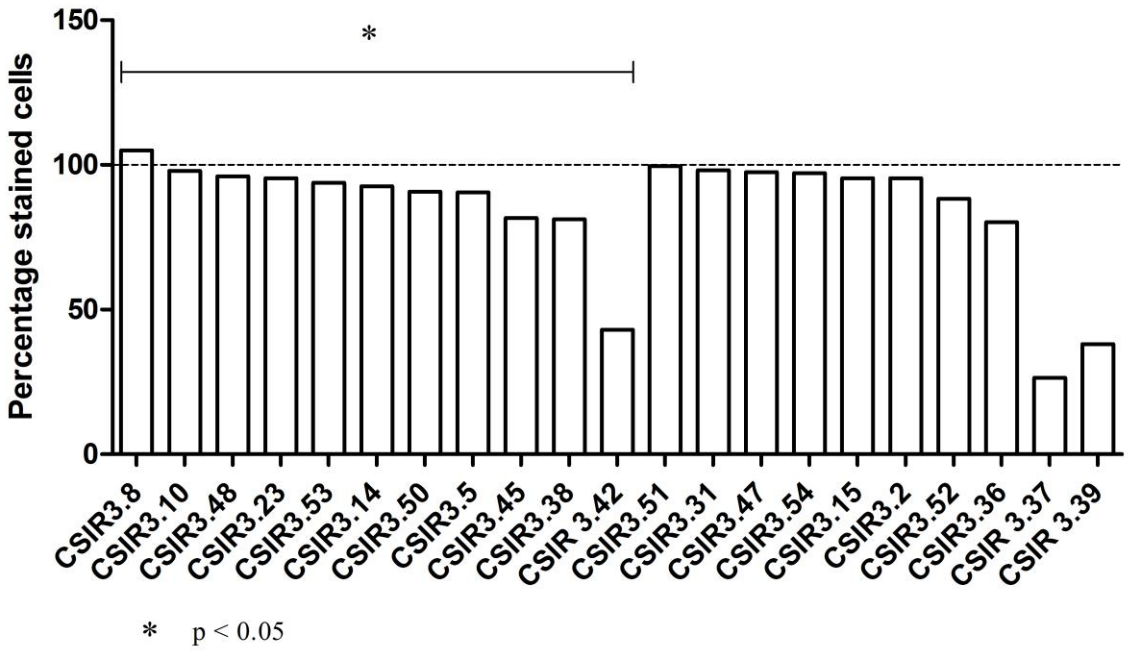

FIGURE 3-3: APTAMER BINDING COMPETITION WITH THE ANTI-CD7 MONOCLONAL ANTIBODY

Aptamer binding to CD7-HeLa cells in the presence of the anti-CD7 antibody was normalised to its CD7-HeLa binding assay set to 100 % indicated by the dashed line. Some aptamer binding increased while other aptamers showed reduced binding after antibody blocking (n = 4).

Eight aptamers were selected for further characterisation in Jurkat cells. These included aptamers from each of the sequence clusters identified in section 2.3.2, three of which showed significantly reduced binding in the presence of the monoclonal CD7 antibody. The aptamers selected for further characterisation were CSIR 3.14, CSIR 3.31, CSIR 3.48, CSIR3.35, CSIR 3.42, CSIR 3.28, CSIR 3.37 and CSIR 3.39. Aptamer CSIR 3.42 showed the lowest binding to un-transfected HeLa cells and significant decrease in binding in the presence of the anti-CD7 monoclonal antibody (Figure 3-1 and Figure 3-3). As such, aptamer CSIR 3.42 was assessed to determine if decrease in aptamer internalisation as well as binding was seen in the presence of the antibody. The aptamer CSIR 3.42 was bound to the CD7 receptor at 4 °C to prevent non-specific endocytosis and to ensure that the aptamer bound the receptor. Aptamer binding was competed with an anti-CD7 antibody to have visual confirmation of the flow cytometry analysis. Aptamer CSIR 3.42 bound to CD7-HeLa cells with more intensity in the presence of the anti-CD7 antibody (Figure 3-4). Stained cells were warmed to 37 °C with serum free DMEM and incubated at room temperature for one hour. By warming up the cells, membrane turn over and endocytosis was able to occur. As the cells were washed prior to replacing with media, any weakly bound aptamer or unbound aptamer

in solution was removed. This allows for the tracking of only receptor bound aptamer internalisation. Aptamer CSIR 3.42 internalised into the CD7-HeLa cells only when not blocked by the anti-CD7 antibody (Figure 3-5). This indicates aptamer binding in the presence of the anti-CD7 antibody is only a weak association and does not improve aptamer internalisation.

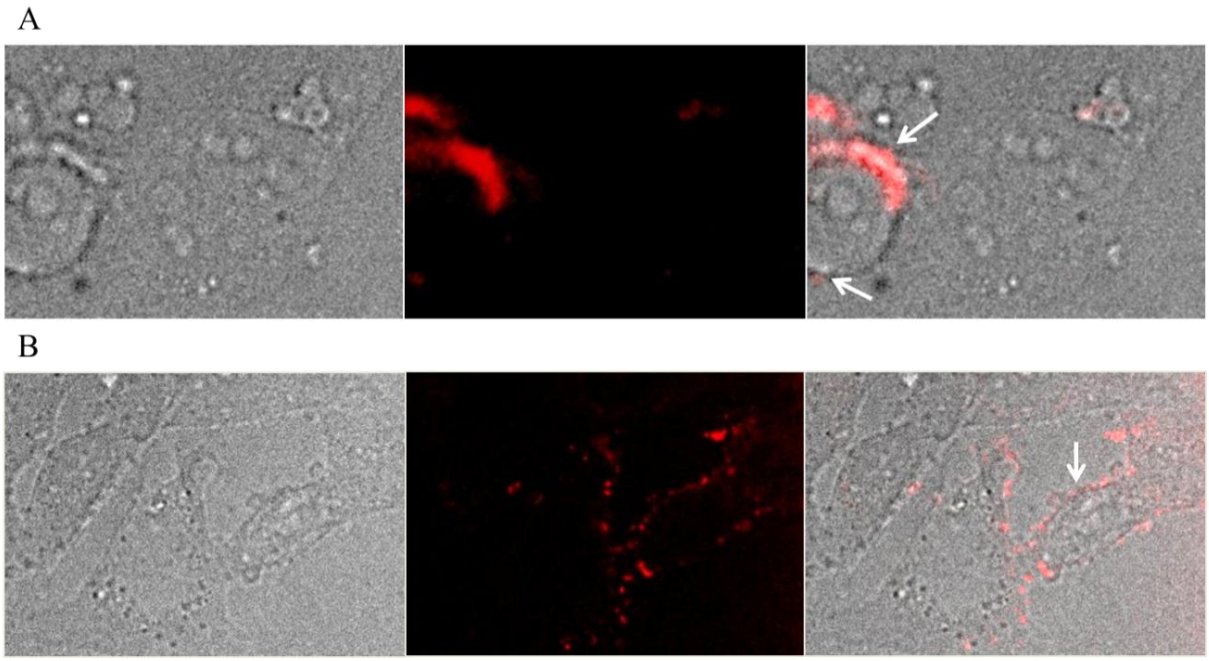

FIGURE 3-4: MICROSCOPY ANALYSIS OF APTAMER CSIR 3.42 BINDING TO CD7 RECEPTOR ON CD7-HELA CELLS

The first panel is a bright field image, the second is the aptamer stain (assigned a pseudo colour, red) and the last panel is the composite of the first two images. A. CD7-HeLa cells incubated with CSIR 3.42 at 4 °C. Aptamer staining can be seen localised to the cell periphery (white arrows). B. CD7-HeLa cells were blocked with an anti-CD7 antibody prior to incubation with CSIR 3.42 at 4 °C. Aptamer can be seen localised to the periphery of the cells (white arrows).

A

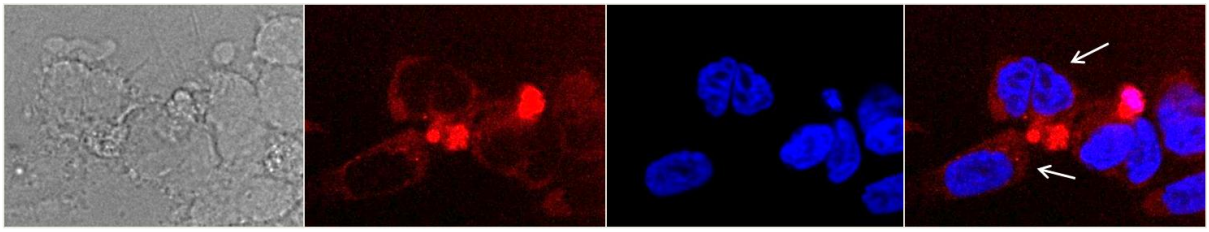

B

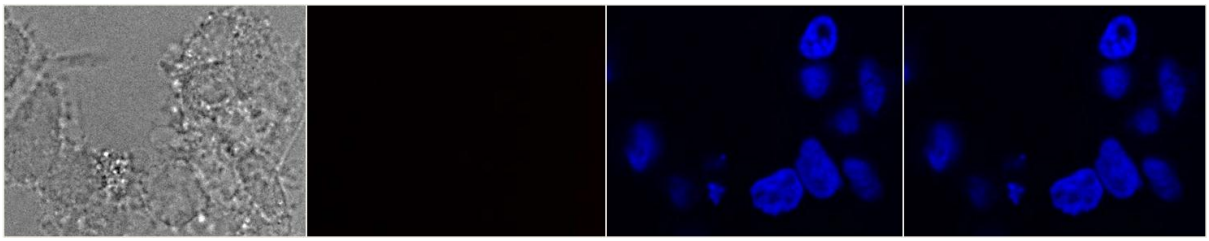

FIGURE 3-5: RECEPTOR MEDIATED INTERNALISATION OF APTAMER CSIR 3.42 INTO CD7-HELA CELLS

The first panel is a bright field image, the second is the aptamer stain (assigned a pseudo colour, red); the third panel is the nuclear stain (assigned a pseudo colour, blue) and the last panel is the composite of the aptamer stain and the nuclear stain images. A. CD7-HeLa cells were incubated with CSIR 3.42 at 4 °C, washed and warmed to 37 °C to allow aptamer internalisation. Aptamer staining can be seen localised to the cell interior, surrounding the nucleus (white arrows). B. CD7-HeLa cells were blocked with an anti-CD7 antibody prior to incubation with CSIR 3.42 at 4 °C, washed and warmed to 37 °C with serum free media. No aptamer stain is evident.

3.3.2 STRUCTURE COMPARISON OF CD7 SPECIFIC APTAMERS

The secondary structures of aptamers taken forward for characterisation in Jurkat cells were analysed using MFOLD (Zuker 2003). The computational prediction of secondary structure for each aptamer was analysed for conserved structures. The MFOLD analysis revealed that only CSIR 3.39 had a single predicted structure, ΔG -14 (Figure 3-6). A single predicted structure may indicate increased stability as the aptamer would not be expected to change conformation in solution and thus the binding structure should always be present.

The remaining aptamers were predicted to have multiple structures and these were analysed to identify conserved structures within the predicted structures for each aptamer. Two aptamers analysed had only two predicted structures, aptamers CSIR 3.35 (ΔG -5.9 and ΔG -4.7) and CSIR 3.28 (ΔG -12.45 and ΔG -12.77) (Figure 3-6). Both aptamers had regions of similarity between the predicted structures that is depicted by a box. As the random region for aptamer CSIR 3.35 is relatively small (19 nucleotides), the regions of similarity incorporated parts of the primer sequences. This aptamer is difficult to analyse at the

secondary structure level, as the predicted unpaired region is unlikely to remain single stranded in solution. More likely a complex tertiary structure could form. However, from the secondary structure information it can be predicted that the hairpin loop would play a role in target binding. Aptamer CSIR 3.28 has a much longer random region and has two regions of similarity between the predicted structures.

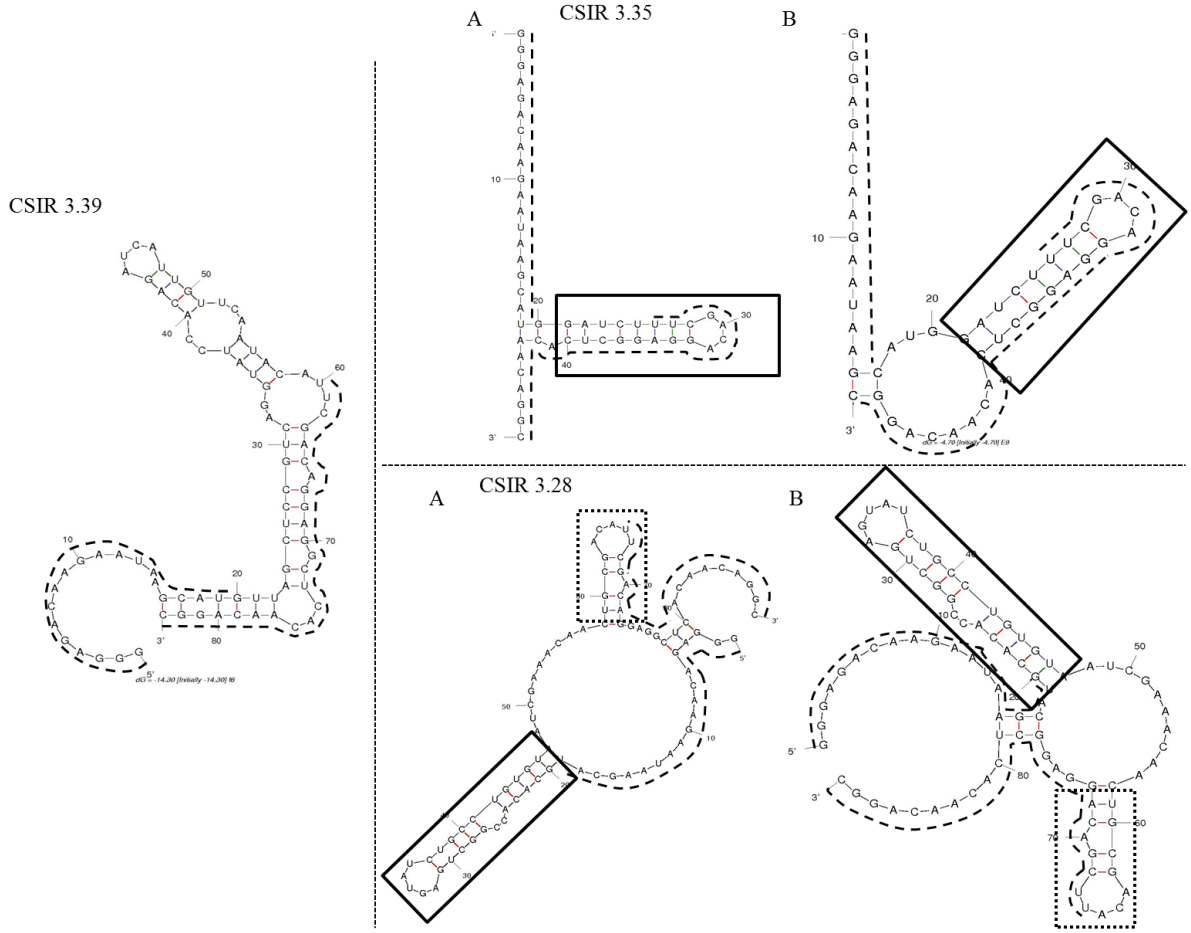

FIGURE 3-6: COMPUTATIONAL SECONDARY STRUCTURE PREDICTION FOR APTAMER CSIR 3.39, CSIR 3.35 AND CSIR 3.28

A computational secondary structure prediction for the aptamers was done using MFOLD. The primer regions are indicated by a dashed line. The dotted box indicates an area of similarity within the predicted structures.

Aptamers CSIR 3.42, CSIR 3.48 and CSIR 3.37 had three predicted structures (Figure 3-7). The three predicted structures of aptamer CSIR 3.42 (ΔG -12.45, ΔG -15.6 and ΔG -15) have no structural similarity and thus may negatively influence the functionality of this aptamer should one of the possible structures have the ability to bind. This may lead to non-binding aptamer forms competing and diluting out binding aptamer forms resulting in a reduction in apparent binding ability. Two of the three predicted structures for aptamer CSIR

3.48 (ΔG -7.3, ΔG -4.47 and ΔG -3.05) share a large area of similarity between nucleotide 20 and 57 (indicated by the solid line). This larger area includes a portion of the primer sequence. A smaller region, indicated by a dotted box, is common to all three structures and does not include the primer regions (Figure 3-7). Aptamer CSIR 3.37 (ΔG -11.33, ΔG -9.75 and ΔG -9.67) had three structures predicted with an area of similarity within two predicted structures indicated by the dotted box. The solid box in A has partial similarity with the dotted box of B and C (Figure 3-7).

Aptamer CSIR 3.14 (ΔG -15.38, ΔG -15.95, ΔG -13.93 and ΔG -15.05) had four predicted structures (Figure 3-8). Two structures showed areas of structural similarity with the third having partial similarity to that area. The fourth structure shared no similarity with the other structures (Figure 3-8). This may affect the binding kinetic of the aptamer as it is expected to alternate between the predicted structures in solution. If the binding conformation is in structure C it may be outcompeted by non-binding conformations. However, if the binding site is within the area of similarity, the predominant folding pattern would include the binding site. Aptamer CSIR 3.31 (ΔG -3.4, ΔG -3.62, ΔG -8.7, ΔG -4.75, ΔG -3.48, ΔG -5.12 and ΔG -7.8) had six structures predicted with only two of the six showing a region of structural similarity (Figure 3-8). Even if the binding conformation is in the region of similarity it may be outcompeted by non-binding conformations.

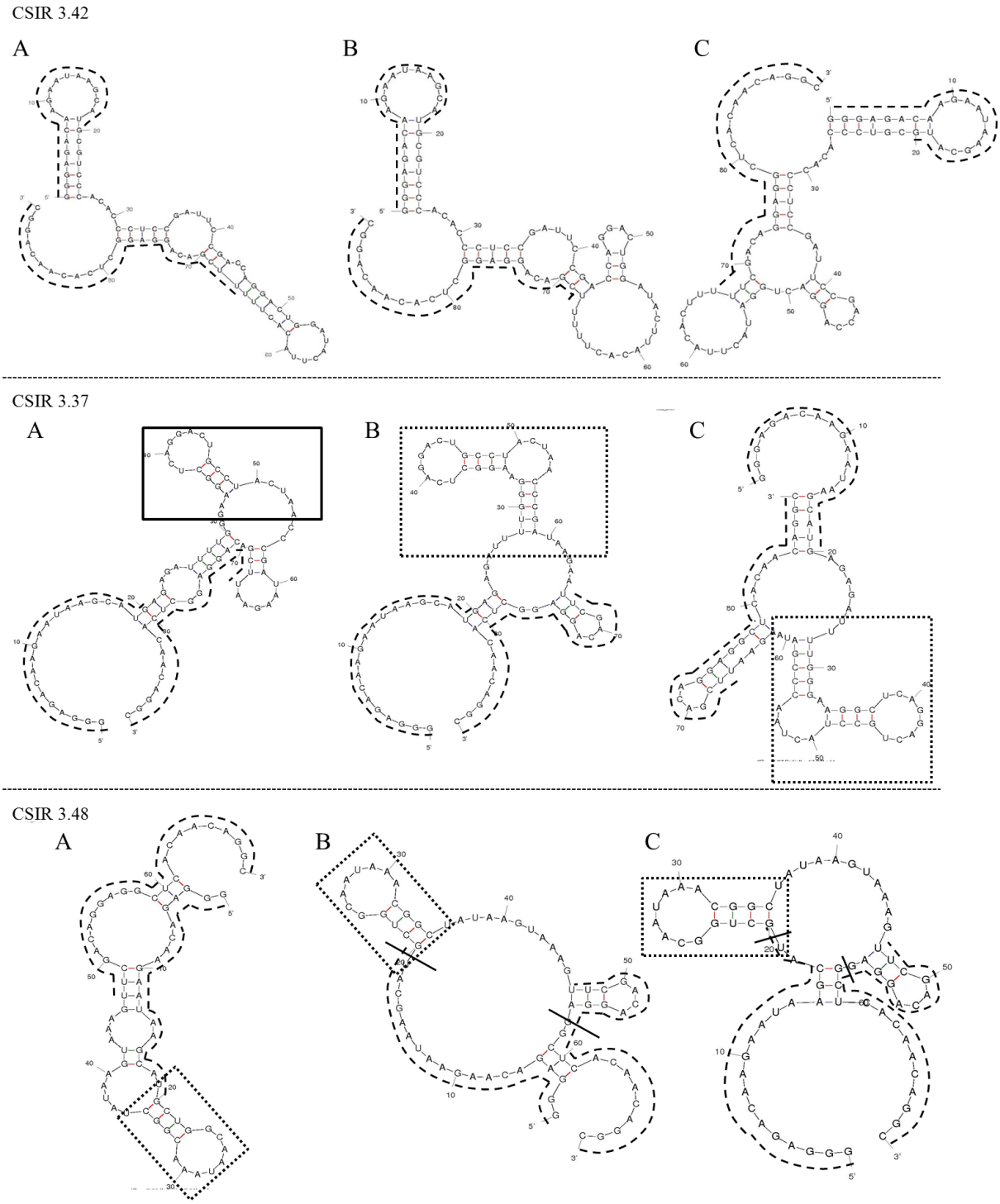

FIGURE 3-7: COMPUTATIONAL SECONDARY STRUCTURE PREDICTION FOR APTAMER CSIR 3.42, CSIR 3.37 AND CSIR 3.48

A computational secondary structure prediction for the aptamers was done using MFOLD. Three structures were predicted with different free energy values. The primer regions are indicated by a dashed line. The dotted box indicates an area of similarity within the predicted structures.

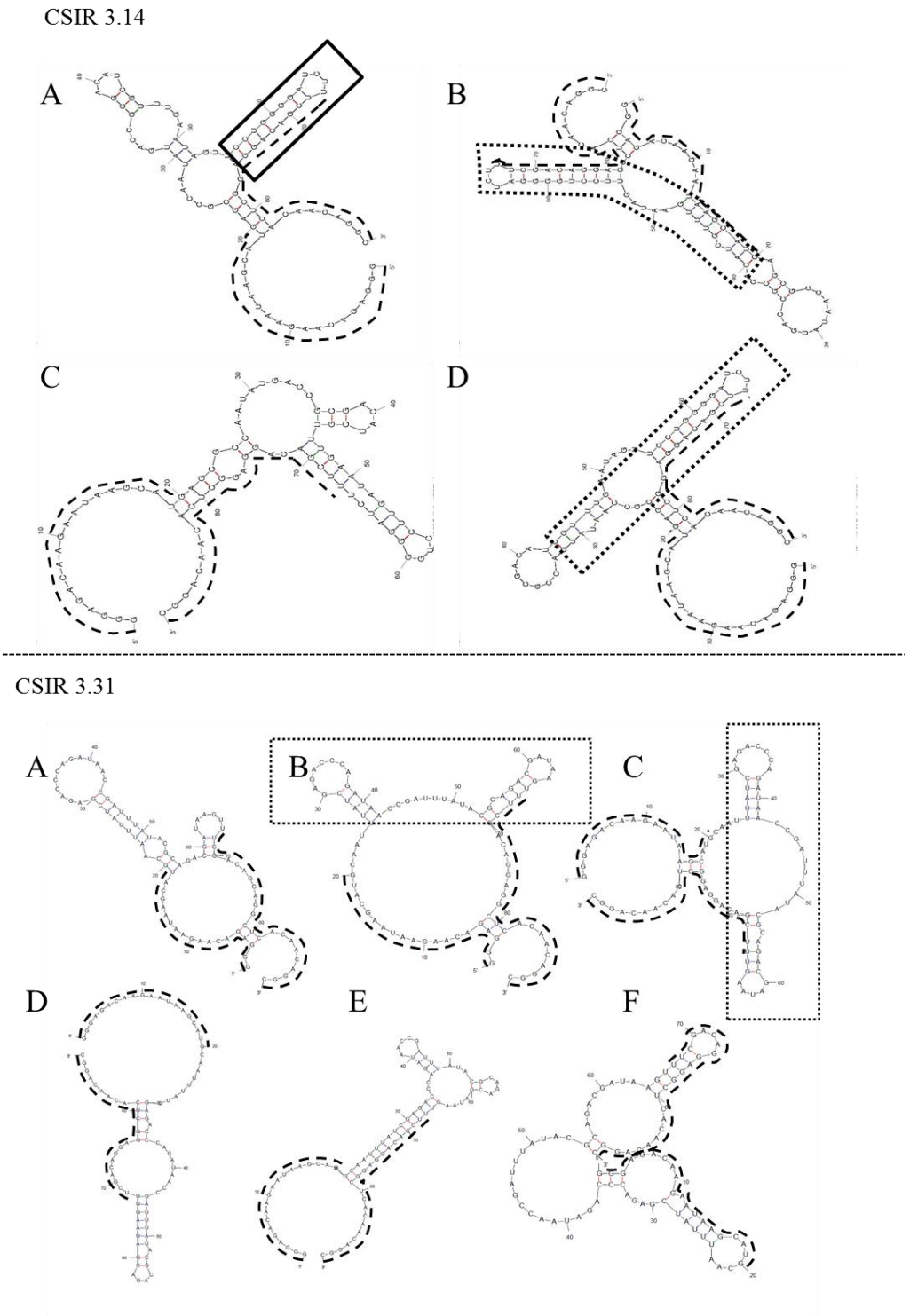

FIGURE 3-8: COMPUTATIONAL SECONDARY STRUCTURE PREDICTION FOR APTAMER CSIR 3.14 AND CSIR 3.31

A computational secondary structure prediction for the aptamers was done using MFOLD. Multiple structures were predicted with different free energy values. The primer regions are indicated by a dashed line. The dotted box indicates an area of similarity within the predicted structures.

3.4 DISCUSSION

Twenty-seven anti-CD7 aptamers were characterised for binding and internalisation using the transgenic cell line generated for aptamer selection that express the CD7 receptor, CD7-HeLa cells. All aptamers showed preferential association with the CD7-HeLa cells over the un-transfected HeLa cells. However, this result did not indicate internalisation specificity as confocal microscopy of aptamer CSIR 3.3 and CSIR 3.23 internalisation at 37 °C showed a lack of cell specificity. Temperature reduction is a common method for analysing receptor mediated internalisation, there is evidence to suggest that changes in temperature can cause fluctuations in aptamer binding affinity (Hu, Tulsieram et al. 2012). It was shown that for both RNA and DNA aptamers, binding affinity of the aptamer increased with increased temperature and this change was attributed to conformational changes of the aptamer (Hu, Tulsieram et al. 2012). This same phenomenon may have played a role here in the apparent differences in aptamer specificity at different temperatures. It may also be the result of incubation time. In the preparation of the microscope slides, the cells were incubated with the aptamer for two hours, double the time used for aptamer selection (Method outlined in section 2.2.5.2). As noted in the selection, roughly 5 % of the enriched pool was able to internalise into HeLa cells which may represent the aptamers shown here. This may indicate that some aptamers appear specific in binding but are able to internalise into cells non-specifically. As discussed in section 1.3.4, the specific mechanism by which aptamers are internalised is not known. A closer look at the cellular localisation of the internalised aptamers may reveal subcellular localisation differences between receptor mediated and non-specifically internalised aptamers. This consideration will need to be addressed in further studies.

Receptor specificity was characterised by comparing aptamer binding to CD7-HeLa cells in the presence and absence of an anti-CD7 monoclonal antibody. Half the aptamers tested were significantly affected by the presence of the anti-CD7 monoclonal antibody. One aptamer, CSIR 3.8 had increased binding while the remaining aptamers showed reduced binding. The increased binding of aptamer CSIR 3.8 may be due to an increase in epitope exposure after anti-CD7 monoclonal antibody binding. Aptamer binding was reduced on average by less than 20 %. The reduction in binding may be due to direct competition of the aptamer and antibody for a binding epitope or could be due to conformational changes in the receptor due to antibody binding occluding the aptamer binding epitope.

Eight aptamers were selected for further characterisation in Jurkat cells which included aptamers from each of the sequence clusters identified in section 2.3.2. Three of the aptamers showed significantly reduced binding in the presence of the monoclonal CD7 antibody. A computational secondary structure prediction was conducted for the chosen aptamers. This *in silico* method is discussed in section 1.3.2 and predicts structures with the lowest free energy using a minimum free energy algorithm (Zuker 2003). The optimal structures are provided with the Gibbs free energy (ΔG) associated with the structures. The ΔG gives an indication of the structure's stability as it implies the energy available for random movement. A negative ΔG indicates a release of energy by the reaction indicating it to be more favourable. Thus the structure with the lowest (most negative) ΔG is provided as the optimal structure. Interestingly the aptamers with three predicted structures had the lowest ΔG values while aptamer CSIR 3.31 with six predicted structures has the least negative ΔG structures. This provides evidence for the rationalisation that more predicted structures may indicate an unfavourable aptamer. Structures with similar ΔG values have similar chance of being formed in solution and so a number of the different predicted structures may be possible in a single reaction. However, the ΔG does not provide insight into the energy required to change between structures. For this an energy landscape analysis would need to be performed. Using an energy landscape analysis, energies of single structures are assigned and the relationship between the structures analysed. The probability of the change in structure is then determined based on the difference in energy between the structures and the energy requirement of the change (Reviewed by Washietl, Will et al. 2012). Further computational analysis of the aptamers may be important once a candidate aptamer has been selected but this is beyond the scope of this thesis. In the following chapter, the eight selected aptamers will be characterised in a T lymphocyte cell line, Jurkat cells.

Chapter 4. ANTI-CD7 APTAMERS CHARACTERISATION IN T LYMPHOCYTES

4.1 INTRODUCTION

Anti-CD7 aptamers were selected against whole cells exogenously expressing the CD7 receptor (Chapter 2). Twenty-seven aptamers were assessed for specific binding to CD7-HeLa cells over un-transfected HeLa cells (Chapter 3) and eight aptamers were brought forward for further characterisation in Jurkat cells, a T lymphocyte cell line closely resembling the intended target cells for these aptamer carriers. Previous studies have reported differences between exogenously expressed receptors and their endogenous counterparts (Kuteykin-Teplyakov, Luna-Tortós et al. 2010) which highlights the importance of further characterisation of the aptamers in a relevant cell line. As the density and distribution of the CD7 receptor may play a role in the eventual application of the aptamers as delivery vectors, their ability to target T lymphocytes was used to select for the best performing aptamers.

Aptamer internalisation rather than binding was assessed by flow cytometry and confocal microscopy. Target cells were incubated with the cells at 37 °C to allow for cellular membrane turn over and aptamer internalisation to identify the best aptamer candidate for kinetic study. Aptamer kinetics is an important tool for the characterisation of candidate aptamers and is usually assessed using SPR (Primo, Dausse et al. 2011; González-Fernández, de-los-Santos-Álvarez et al. 2012; Ruigrok, van Duijn et al. 2012). The aptamer kinetics gives insight into the dynamic association and dissociation of the aptamer target complex. Aptamers form strong associations with their targets and thus have small associated K_d in the nanomolar range (Dey 2005; Li, Nguyen et al. 2011). An aptamer with a relatively fast rate of association and slow dissociation is advantageous, as it will allow for rapid and maintained binding to the target receptor (Discussed in detail in section 1.2.2). As SPR had failed to characterise aptamer binding, a different method of kinetic analysis had to be used. The kinetics were determined using confocal microscopy and flow cytometry and in this way, kinetics of internalisation rather than kinetics of binding were determined. The kinetics of internalisation is an important consideration for targeting the CD7 receptor. As discussed in section 1.6, the CD7 receptor is associated with a number of regulatory pathways including the PI-3K pathway. The cross linking of the CD7 receptor with a monoclonal antibody leads to an association with CD3, a T lymphocyte specific receptor, and CD45, a common

Lymphocyte precursor receptor (Lazarovits, Osman et al. 1994). This, in turn, leads to the stimulation of signalling cascades within the cell. It is unclear whether an aptamer that is able to internalise quickly via the CD7 receptor will cause this same effect or not. However, an aptamer able to enter cells rapidly will allow for fast delivery of therapeutics to target cells. This chapter covers the further characterisation of eight CD7 specific aptamers in Jurkat cells. The specific internalisation of an aptamer is tracked by confocal microscopy to reveal the rapid internalisation of the aptamer to target cells. A candidate aptamer is identified in this chapter for which a number of applications are highlighted in Chapter 5.

4.2 MATERIALS AND METHODS

4.2.1 ANTI-CD7 APTAMER PRODUCTION BY PCR AND IN VITRO TRANSCRIPTION

Each selected aptamer was generated by *in vitro* transcription of double stranded DNA using a similar method as described in section 3.2.1. The PCR primers were specific for the anti-CD7 aptamers and were as follows: forward primer 5′ AAGCTGTCCTCCGAGTGTTGTCCG 3′ and reverse primer 5′ ATTATGCTGAGTGATATCCCTCTGTTCTTATTCGTAC 3′ (Integrated DNA Technologies, CA, USA).

4.2.2 FLUORESCENT LABELLING OF ANTI-CD7 APTAMERS

Aptamers were labelled with cyanine 3 (Cy3) or 6-carboxy-fluorescein (FAM) using a Silencer® siRNA Labelling Kit (Ambion, NY, USA) as detailed in section 3.2.2 and quantified as in Appendix 6.1.4.

4.2.3 CHARACTERISATION OF ENDOGENOUS SURFACE EXPRESSION OF CD7 RECEPTOR ON JURKAT CELLS

As a closer model of the *in vivo* condition, a T lymphoblast cell line was used to characterise anti-CD7 aptamer binding and internalisation. Jurkat cells are a T lymphoblast derived from peripheral blood buffy coat of a 14 year old male with acute lymphoblastic leukaemia (ATCC #TIB-152). Surface expression of CD7 on Jurkat cells was confirmed using fluorescent microscopy with a PE/Cy5 anti-CD7 antibody (NBP1-43102; Novus Biologicals, CO, USA) and flow cytometry using a FITC labelled anti-CD7 monoclonal antibody clone CBC.37 (Milli-Mark™, Millipore, USA) and an isotype control antibody Alexa fluor 488 anti-Connexin43 Clone CX1B1 (Invitrogen, CA, USA).

4.2.3.1 MICROSCOPY ANALYSIS

Cells were grown to a density of 1×10^6 cells /ml in RPMI growth media (Detailed in section 2.2.6.1). Cells were pelleted at 200 × *g* for five minutes then re-suspended in 100 µl PBS supplemented with 0.5 µg PE/Cy5 anti-CD7 antibody and incubated at room temperature for 40 minutes. Cells were then pelleted as previously described and were washed three times

with 200 µl PBS. Once washed, the cells were stained with 3 µM DAPI (Invitrogen, CA, USA) for ten minutes at room temperature. A 10 µl sample from each cell preparation was spotted onto a slide and covered with a cover slip for imaging. Slides were imaged under a 40 × objective using an Olympus AX70 fluorescence microscope with Image-ProPlus V6.3.542 and processed using ImageJ software version 1.45 (Schneider, Rasband et al. 2012).

4.2.3.2 FLOW CYTOMETRY ANALYSIS

Jurkat cells were grown to a density of 1×10^6 cells /ml in RPMI growth media (Detailed in section 2.2.6.1). Three samples were removed and cells were pelleted at 200 × *g* for five minutes. Cells were split then re-suspended in 80 µl binding buffer (10 % FBS in 1 × PBS). One cell sample remained unstained and the others were supplemented with 0.5 µg FITC labelled anti-CD7 monoclonal antibody clone CBC.37 (Milli-Mark™, Millipore, USA) or isotype control antibody Alexa fluor 488 anti-Connexin43 Clone CX1B1 (Invitrogen, CA, USA).and incubated at room temperature for 40 minutes. Cells were pelleted as before and washed three times with 200 µl binding buffer. After washing, cells were re-suspended in 400 µl PBS and analysed on a Guava Easy Cyte Flow cytometer (Guava Technologies Inc., CA, USA) and the results analysed using FlowJo version 7.6.5 (Tree Star, Inc., OR, USA). For each run, 10 000 events were counted with cells gated according to forward and side scatter profiles. Antibody bound cells were compared to cells alone and to each other. Specific binding of the anti-CD7 antibody was determined by accounting for non-specific antibody association and cell alone auto-fluorescence.

4.2.4 ANTI-CD7 APTAMER ASSOCIATION TO ENDOGENOUSLY EXPRESSED SURFACE CD7 RECEPTOR ON T LYMPHOCYTES

Jurkat cells were selected to be used as the T lymphocyte cell line for aptamer association characterisation. Jurkat cells were grown to a density of 4×10^6 cells/ ml in RPMI growth media (Detailed in section 2.2.6.1) and seeded into a 96 well dish (Nunc™, Thermo Fisher Scientific, Inc., MA, USA) at a density of 2×10^5 cells per well. Anti-CD7 aptamers (CSIR 3.14, CSIR 3.28, CSIR 3.31, CSIR 3.35, CSIR 3.37, CSIR 3.39, CSIR 3.42 and CSIR 3.48) selected from binding studies with CD7-HeLa cells were tested for binding to Jurkat T lymphocytes. Cy3 labelled aptamer (Generated according to section 4.2.2) was incubated over night with Jurkat cells in RPMI growth media (Detailed in section 2.2.6.1) at 37 °C and 5 % CO_2 at a final concentration of 400 nM. As a positive control for aptamer internalisation,

aptamers were transfected into cells using Lipofectamine RNAiMAX reagent (Invitrogen, CA, USA). Following incubation, cells were pelleted and washed three times with PBS. After washing, cells were re-suspended in 400 µl PBS and analysed using a CyAn flow cytometer (Beckman Coulter Inc., CA, USA); the data were analysed using FlowJo version 7.6.5 (Tree Star, Inc., OR, USA). For each run, 10 000 events were collected with cells gated according to forward and side scatter profiles. Aptamer bound cells were compared to cells alone and the percentage cells stained was determined. Each aptamer alone association was normalised to its transfection control set to 100 % using the following equation:

$$Percentage\ Stained\ Cells = \frac{Aptamer\ percentage\ shift}{Transfected\ aptamer\ percentage\ shift} \times 100$$

A student's t test was conducted to determine a significant difference between the transfection control and the aptamer alone. The average of two experiments was used to validate the association of anti-CD7 aptamers.

4.2.5 ANTI-CD7 APTAMER ASSOCIATION RATES AND BINDING CHARACTERISATION

4.2.5.1 KINETIC ANALYSIS BY TIME COURSE ASSAY

Aptamers CSIR 3.14, CSIR 3.37 and CSIR3.42 shown to bind Jurkat cells were further analysed to determine their kinetic rate constants. Jurkat cells were grown to a density of 4×10^6 cells/ ml in RPMI growth media (Detailed in section 2.2.6.1) and seeded into a 96 well dish (Nunc™, Thermo Fisher Scientific, Inc., MA, USA) at a density of 2×10^5 cells per well. Cy3 labelled aptamers (Section 4.2.2) were incubated for different time periods (1 hour, 3 hours, 6 hours, 12 hours and 24 hours) with Jurkat cells in complete media at 37 °C and 5 % CO_2 at a final concentration of 400 nM. Following incubation, cells were pelleted and washed three times with PBS. After washing, cells were re-suspended in 400 µl PBS and analysed using a CyAn flow cytometer (Beckman Coulter Inc., CA, USA) as detailed in section 4.2.4. The average of two experiments was used to validate the association of anti-CD7 aptamers with surface expressed CD7 receptor. The percentage stained cells was analysed across time periods and a non-linear regression line was fitted (GraphPad Prism Software Inc., CA, USA) to determine the association and dissociation rate constants using the following formula:

$$Y = Ymax \times (1 - e^{-kob.X})$$

kob = observed rate constant (min^{-1})

Ymax = maximum Y value (specific binding)

X = time (min)

4.2.5.2 LIMIT OF DETECTION FOR APTAMER ASSOCIATION WITH JURKAT CELLS

Aptamers CSIR 3.14 and CSIR 3.37 were analysed to determine the limit of detection for aptamer-cell association. Jurkat cells were grown to a density of 4×10^6 cells/ ml in RPMI growth media (Detailed in section 2.2.6.1) and seeded into a 96 well dish (Nunc™, Thermo Fisher Scientific, Inc., MA, USA) at a density of 2×10^5 cells per well. Cy3 labelled aptamers were incubated for 12 hours with Jurkat cells in RPMI growth media at 37 °C and 5 % CO_2 at 2 fold diluted concentrations (10.9 nM, 21.9 nM, 43.8 nM, 87.5 nM, 175 nM, 350 nM and 700 nM). Following incubation, cells were pelleted and washed three times with PBS. After washing, cells were re-suspended in 400 µl PBS and analysed for fluorescence using a CyAn flow cytometer (Beckman Coulter Inc., CA, USA) as detailed in section 4.2.4. The average of two experiments was used to validate the concentration gradient association of anti-CD7 aptamers. Aptamer binding was normalised to the cell alone control set to 1 according to the following formula:

$$Fold\ change = \frac{Aptamer\ percentage\ shift}{cell\ alone\ percentage\ shift}$$

4.2.6 ANTI-CD7 APTAMER INTERNALISATION CHARACTERISATION AND LOCALISATION

Aptamer CSIR 3.14 was selected for further characterisation of internalisation in Jurkat T lymphocytes. A glass bottom cell chamber (Mateck, MA, USA) was coated with Poly-L-lysine solution 0.1 % (w/ v) in water (Sigma-Aldrich, MO, USA) to allow for the suspension cells to attach to the chamber's surface. Jurkat cells (2×10^5 cells) were added to the centre of the dish and allowed to settle and attach for 20 minutes at 37 °C with 5 % CO_2. Live cells were placed in an incubation chamber attached to a Zeiss LSM 510 confocal microscope (Carl ZeissAG, Oberkochen, Germany) for live cell imaging using a 40 × objective. A Z-stack of images through the cell section was performed with 1 µm sections. These images

were analysed using Zeiss LSM Image Browser version 3.5 (Carl ZeissAG, Oberkochen, Germany) to generate a three dimensional projection of the stack. These tools were used to localise the aptamer fluorescence to the inside the cells.

4.2.7 ANTI-CD7 APTAMER KINETICS OF INTERNALISATION

Aptamer CSIR 3.14 was selected for further kinetic internalisation characterisation in Jurkat T lymphocytes by confocal microscopy. A glass bottom cell chamber (Mateck, MA, USA) was coated with Poly-L-lysine solution 0.1 % (w/ v) in water (Sigma-Aldrich, MO, USA) to allow for the suspension cells to settle and attach to the chamber's surface. Jurkat cells (2×10^5 cells) were added to the centre of the dish and allowed to settle and attach for 20 minutes at 37 °C with 5 % CO_2. Live cells were placed in an incubation chamber attached to a Zeiss LSM 510 confocal microscope (Carl ZeissAG, Oberkochen, Germany) set for the detection of Cy3 fluorescence with an excitation of 550 nm and an emission of 570 nm. The time course imaging was conducted over a six hour period with images captured using a 40 × objective at 15 minutes intervals. Zeiss LSM Image Browser version 3.5 (Carl ZeissAG, Oberkochen, Germany) was used to analyse images. Two regions of interest (ROI 1 and ROI 2) were selected including the whole field of view and a single cell respectively. These regions were analysed for an accumulation of fluorescence signal over time. This data was analysed using GraphPad Prism version 5 (GraphPad Prism Software Inc., CA, USA) and a non-linear regression line was fitted to the data to determine the association and dissociation rate constants using the same equation as in section 4.2.5.1.

4.2.8 APTAMER CSIR 3.14 BINDING SITE MUTATION CHARACTERISATION

Aptamer CSIR 3.14 secondary structure prediction highlighted a region of conservation that may attribute to CD7 binding. This prediction was tested by removing ten nucleotide sections of the binding region and assessing association to Jurkat cells. The DNA of aptamer CSIR 3.14 was also assessed for Jurkat cell association. Jurkat cells were grown to a density of 4×10^6 cells/ ml in RPMI growth media (Detailed in section 2.2.6.1) and seeded into a 96 well dish (Nunc™, Thermo Fisher Scientific, Inc., MA, USA) at a density of 2×10^5 cells per well. FAM labelled aptamer (Generated according to section 3.2.2) was incubated over night with Jurkat cells in complete media at 37 °C and 5 % CO_2 at a final concentration of 400 nM. As a positive control for aptamer association, full length aptamer CSIR 3.14 was included. Following incubation, cells were pelleted and washed three times with PBS. After washing,

cells were re-suspended in 400 µl PBS and analysed on a Guava Easy Cyte Flow cytometer (Guava Technologies Inc., CA, USA) as detailed in section 4.2.4 Each aptamer mutation and the DNA was normalised to the association of full length CSIR 3.14 set to 100 % using the following formula:

$$Specific\ Association = \frac{Aptamer\ percentage\ shift}{CSIR\ 3.14\ RNA\ percentage\ shift} \times 100$$

A student's t test was conducted to determine a significant difference between the transfection control and the aptamer alone ($p < 0.05$). Two independent experiments were used to calculate the association of each aptamer. A computation analysis of aptamer CSIR 3.14 mutants and DNA was conducted to predict the secondary structure according to the protocol outlined in section 3.2.6.

4.2.9 MAMMALIAN CELL CULTURE

Jurkat T lymphocytes were maintained as described in section 2.2.6.2.

4.3.1 ANTI-CD7 APTAMER INTERNALISATION SPECIFICITY AND KINETICS TO T LYMPHOCYTE CELL LINE, JURKAT CELLS

The association of the anti-CD7 aptamers to transgenic CD7 receptor expressing cells was established. To confirm this association with endogenously expressed CD7 receptor, a lymphoblast cell line was selected. Jurkat cells have previously been utilised for the characterisation of anti-leukemic treatments due to the expression of surface CD7 (Peipp, Kupers et al. 2002; Bremer, ten Cate et al. 2006). In this section, the endogenous surface expression of the CD7 receptor on Jurkat cells was confirmed before the characterisation of anti-CD7 aptamer internalisation and kinetics. As there may be differences in the expression and folding of an endogenous receptor to the exogenous receptor that the aptamers were raised against, it is possible some aptamers will fail to internalise into Jurkat cells. Since the eventual usability of the aptamers relies on their specificity to T lymphocytes, characterisation of internalisation using a T lymphocyte cell line was important.

The endogenous surface expression was confirmed by flow cytometry and fluorescence microscopy using an FITC labelled anti-CD7 monoclonal antibody. Alexa Fluor 488 anti-connexin43 monoclonal antibody was used as an isotype control to determine the binding attributable to non-specific antibody interactions. The cells alone and the anti-connexin43 accumulated below 10^1 on the Log scale of fluorescence indicating minimal cellular auto-fluorescence and anti-connexin43 binding. Cells stained with anti-CD7 shifted to the right, between 10^1 and 10^2 on the Log scale of fluorescence indicating binding of the antibody (Figure 4-1 A). The percentage stained cells was determined by gating to the right of the cells alone. The percentage cells stained per treatment was plotted and a horizontal line plotted to indicate the level of non-specific fluorescence due to cellular auto-fluorescence and non-specific antibody interactions. The anti-connexin43 stained cells accounted for 12 % and the cells alone 5 % (Figure 4-1 A). The anti-CD7 antibody treated cells showed an 88 % shift in fluorescence. As such, the specific binding of the anti-CD7 antibody can be determined as a 76 % cell shift.

Jurkat cells treated with PE/Cy5 anti-CD7 monoclonal antibody were imaged using fluorescence microscopy. Cells were stained with DAPI to locate the nuclei and a composite image was made of the nuclear staining and the PE/Cy5 anti-CD7 antibody staining (Figure

4-1 B). Surface CD7 receptor expression on Jurkat cells was confirmed and these cells were then used for aptamer binding and internalisation characterisation.

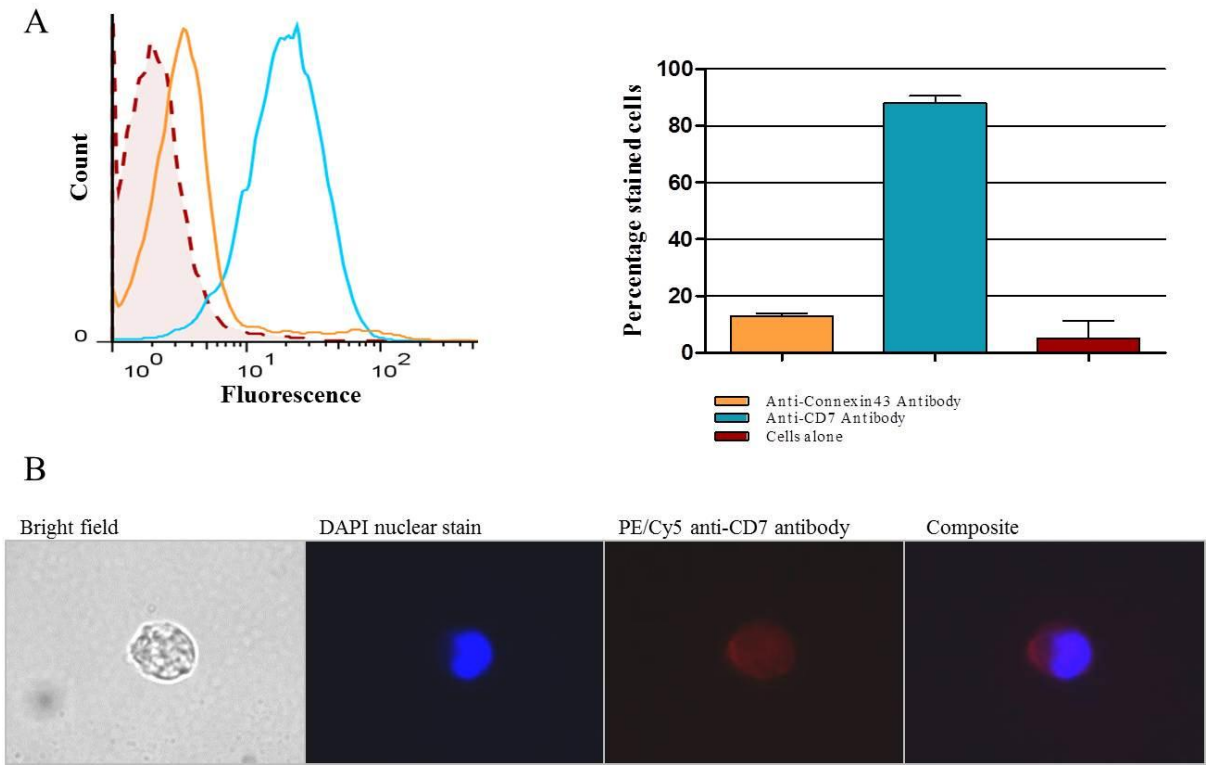

FIGURE 4-1: VALIDATION OF SURFACE CD7 RECEPTOR EXPRESSION ON JURKAT CELLS

A. Jurkat cells treated with FITC anti-CD7 antibody, Alexa Fluor 488 anti-connexin43 antibody and Jurkat cells alone plotted as an overlaid histogram. Antibody binding gate was selected to the right of the cells alone. Percentage stained cells was plotted on a bar graph (n = 4). B. Jurkat cell treated with PE/Cy5 anti-CD7 monoclonal antibody imaged by fluorescence microscopy. Bright field panel shows the whole cell under white light, the DAPI nuclear stain shows only the cell nucleus and the PE/Cy5 anti-CD7 antibody shows presence of surface CD7. A composite image was made using the nuclear staining and the PE/Cy5 anti-CD7 antibody images.

Eight aptamers (CSIR 3.14, CSIR 3.28, CSIR 3.31, CSIR 3.35, CSIR 3.37, CSIR 3.39, CSIR 3.42 and CSIR 3.48) brought forward from binding studies (Section 3.3.2) using the CD7-HeLa recombinant cell line were assessed for internalisation into Jurkat cells endogenously expressing CD7 on the surface by flow cytometry. As the aptamers were incubated with the cells overnight, it was presumed that the aptamers would internalise into the cells rather than only bind to the surface. However, flow cytometry does not differentiate between surface associated and internalised signal and so this assay was used to determine association of the aptamer to Jurkat cells. Further characterisation of internalisation after association studies was required to confirm internalisation of the aptamer. As a positive control for internalisation, aptamers were transfected into cells. The percentage stained cells

was determined by gating cells positive for Cy3 fluorescence when compared to the cells alone control. The maximum transfection efficiency as a percentage of cells stained was around 60 % for all aptamers transfected. The cell specific association of each aptamer was normalised to the transfection control set to 100 %. A student's t test was conducted to determine a significant difference between the transfection control and the aptamer alone (n = 2). CSIR 3.42 and CSIR 3.14 were the only aptamers not significantly different to their transfection control, indicating that the aptamer alone is able to internalise into cell at a similar efficiency as with a specialised reagent (Figure 4-2). Aptamers CSIR 3.14, CSIR 3.42 and CSIR 3.37 had a higher aptamer association than their respective transfection controls and were selected for further characterisation of internalisation kinetics.

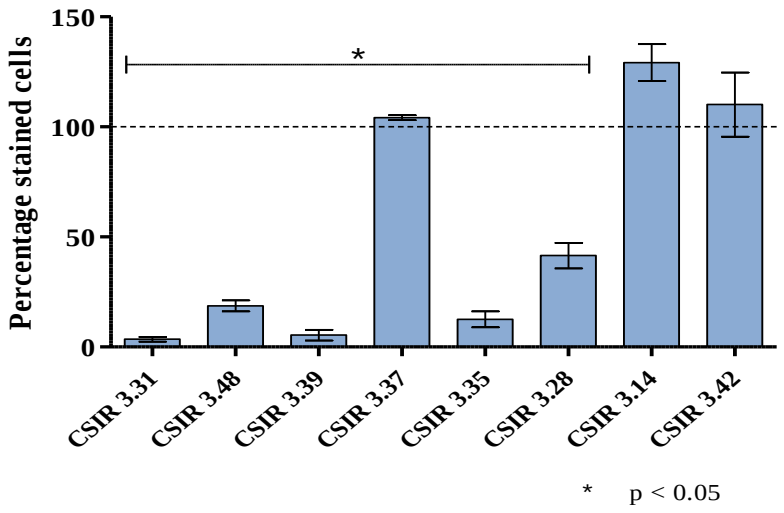

FIGURE 4-2: APTAMER ASSOCIATION WITH ENDOGENOUSLY EXPRESSED CD7 RECEPTOR ON JURKAT CELLS

Association of each aptamer alone was normalised to its respective transfection control set to 100 % indicated by a dashed line. A students t test was used to determine significance ($p < 0.05$) between the aptamer alone and its transfection control (n = 2).

The kinetic analysis was done using flow cytometry in which the aptamer concentration was kept constant and incubated with cells for different time periods. Non-binding aptamer CSIR 3.31 was included as a negative control to illustrate that aptamers do not non-specifically internalise after a 24 hour incubation period (Appendix 6.6). Aptamer CSIR 3.31 binding did not increase significantly at the maximum incubation period with an increase from 1.97 % after six hours to 7.6 % after 24 hours. Since no association was detected the data could not be plotted. The percentage shift for all aptamers was determined by gating only the Cy3 stained cells as compared to the cell alone control. Specific

association plotted for aptamers CSIR 3.14, CSIR 3.37 and CSIR 3.42 was calculated as a function of the non-binding aptamer CSIR 3.31 at the same incubation time. A non-linear regression line was fitted to the specific association of the aptamers to determine the kinetic parameters (Figure 4-3). Aptamer CSIR 3.14 showed a threefold increase in specific association with an increase in incubation time up to six hours (Figure 4-3). The combined analysis from two independent experiments attributed CSIR 3.14 with a cell binding constant of 2.1 fM and an association rate of $4.7 \pm 2.4 \times 10^5$ $Molar^{-1}minute^{-1}$. The specific association was seen to plateau at the last time points measured and the majority of internalisation occurred within the first two measured time points (Figure 4-3). Aptamer CSIR 3.37 showed a twofold increase in specific association with an increase in incubation time from one to six hours. However, much like with CSIR 3.14, when plotted the non-linear regression line had plateaued for all later time points measured. Two independent experiments corresponded exactly with no deviation between points (Figure 4-3). The cell binding constant calculated for CSIR 3.37 was 0.23 fM with an association rate of $4.3 \pm 3.3 \times 10^6$ $Molar^{-1}minute^{-1}$ and is evidence for the rapid internalisation of the aptamer before the one hour time point. Aptamer CSIR3.42 showed a twofold increase in specific association with an increase in incubation time. When the non-linear regression line was fit it was evident that, like for CSIR 3.14 and CSIR 3.37, the plateau of aptamer association was reached early on in the incubation times (Figure 4-3). The aptamer cell binding constant was calculated from the non-linear regression fit as 1.1 fM with an association rate of $7.9 \pm 5.1 \times 10^5$ $Molar^{-1}minute^{-1}$. The maximum association was reached by six hours incubation and was in line with CSIR 3.14 with a similar cell binding constant.

The kinetic calculations illustrated that the association and uptake is rapid for aptamers CSIR 3.14, CSIR 3.37 and CSIR 3.42 as the cell binding constants were in the femtomolar range. It is important to note however, that the specific calculation was of the association rate and the dissociation constant provided was as an additional output. As such, the dissociation constant provided by the calculation has been referred to as the cell binding constant. The association calculation at different aptamer concentrations should be included in further studies to validate the true dissociation constant provided. In addition, it was unclear if the rapid plateau was due to the aptamer concentration or the CD7 expression being rate limiting. As such, Jurkat cells were incubated with different concentrations of aptamer CSIR 3.14 and CSIR 3.37 for 12 hours. An increase in binding with increased concentration would indicate that the aptamer concentration was rate limiting while a plateau of binding

over 400 nM would indicate saturation of the aptamer binding sites on the cellular CD7 receptors. Lower concentrations were included to determine the limit of detection to compensate for receptor saturation.

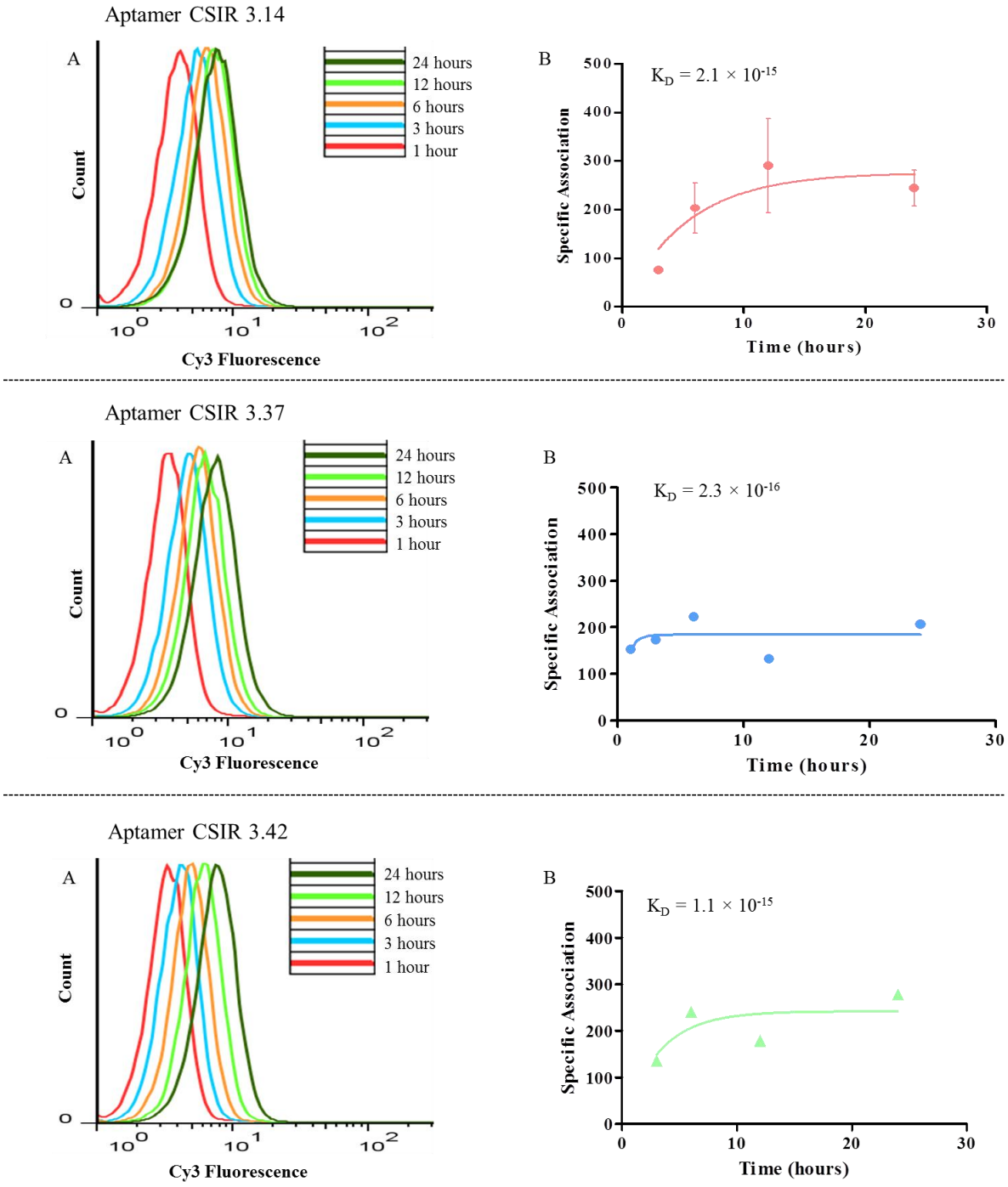

FIGURE 4-3: TIME COURSE ASSOCIATION OF APTAMER CSIR 3.14, CSIR 3.37 AND CSIR 3.42

Aptamers were incubated at a 400 nM final concentration with Jurkat cells for variable times (1 hour, 3 hours, 6 hours, 12 hours and 24 hours). A: Overlay histogram of aptamer binding after different incubation times. B: Non-linear regression fit of aptamer binding over time.

Aptamer association was determined as a shift in Cy3 fluorescence when compared to cells alone control. The specific association of aptamer CSIR 3.14, CSIR 3.37 and CSIR 3.42 was calculated as a function of the cell alone control set to 1. Aptamer CSIR 3.14 and aptamer CSIR 3.37, had a steady increase in binding concentrations up to 175 nM (Figure 4-4). On average binding increased by 60 % with each doubling in aptamer concentration. Binding increased by 260 % for CSIR 3.14 and 180 % for CSIR 3.37 when the concentration was increased from 175 nM to 350 nM. From 350 nM to 700 nM binding increased by 240 % for CSIR 3.14 and 500 % for CSIR 3.37 (Figure 4-4). This indicates that the aptamer concentration at 400 nM did not saturate all binding sites. The maximal RNA concentration for both aptamers was not determined as the highest concentration tested was 700nM. In addition, a comparison was not made with the negative control aptamer to account for the contribution of non-specific internalisation on saturation. This is because, non-specific internalisation is assumed to be not through the CD7 receptor, and as such it should not have an effect on the saturation of the receptor.

The best candidate aptamer for pharmaceutical application would have a low dissociation constant and a high specificity to the target. As such, aptamer CSIR 3.14 was selected for further characterisation as the kinetics data showed the best fit and a low dissociation constant. Characterisation of aptamer binding by concentration revealed that the plateau reached with the kinetics analysis was due to aptamer depletion and not saturation of the binding sites.

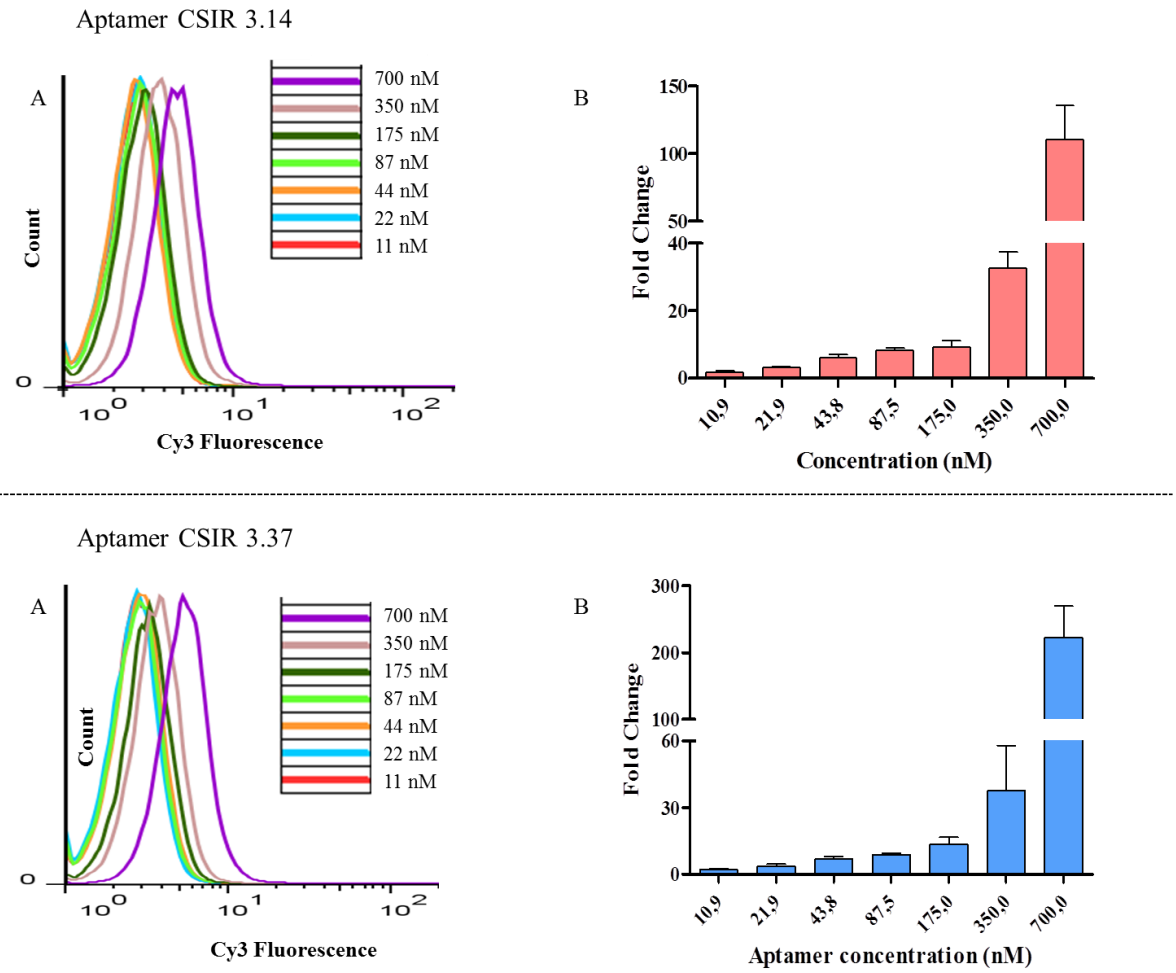

FIGURE 4-4: CONCENTRATION GRADIENT BINDING ANALYSIS OF APTAMERS CSIR 3.14 AND CSIR 3.37

Aptamer CSIR 3.14 and CSIR 3.37 were incubated with Jurkat cells for 12 hours at variable concentrations (11 nM, 22 nM, 44 nM, 87 nM, 175 nM, 350 nM and 700 nM). A. Overlay histogram of aptamer binding at different concentrations. B. Specific association of aptamer to Jurkat cells at different concentrations.

4.3.2 ANTI-CD7 APTAMER CSIR 3.14 INTERNALISATION LOCALISATION AND KINETICS

All data up to now have characterised the aptamer interaction with whole cells using flow cytometry. This method, although sensitive, does not differentiate between fluorescence at the cell surface and fluorescence from within the cell. For the cellular localisation of aptamer staining, confocal microscopy was used. Aptamer CSIR 3.14 internalisation was localised by taking images through the cell at 1 µm intervals along the Z axis (Figure 4-5 A). These images were compiled to generate a Z stack, a compilation of images that dissects the cells

visually from below the cell surface, through the cytoplasm to above the top of the cell surface (Figure 4-5 B). .

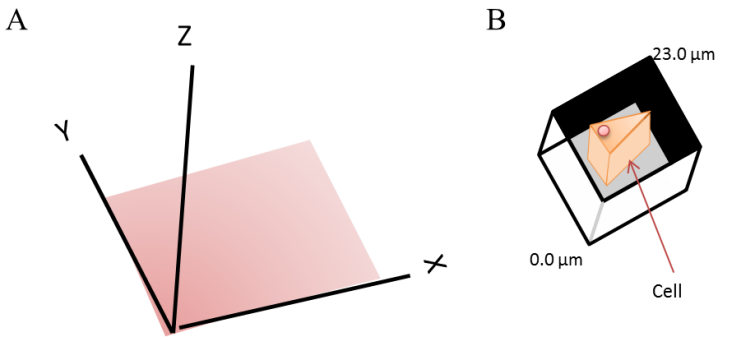

FIGURE 4-5: DIAGRAMMATIC REPRESENTATION OF A Z STACK THROUGH AN IMAGE SECTION

A: A diagrammatic representation of the X, Y and Z planes of view. B: A diagrammatic representation of the visible plane dissected every 1 µm to generate a Z stack

Below the cell, at 0.0 µm, no fluorescence can be seen (Figure 4-6). As the images travel upward through the cell surface (2 µm to 8 µm) some fluorescence becomes evident. Once inside the cell (9 µm to 15 µm) the fluorescence is very bright. The fluorescence dims again as the images are moving through the top of the cell to above the cell (16 µm to 23 µm) (Figure 4-6). From this is it clear that the fluorescence associated with the cells is coming from within the cells and thus the aptamer has internalised and is not attached at the cell surface.

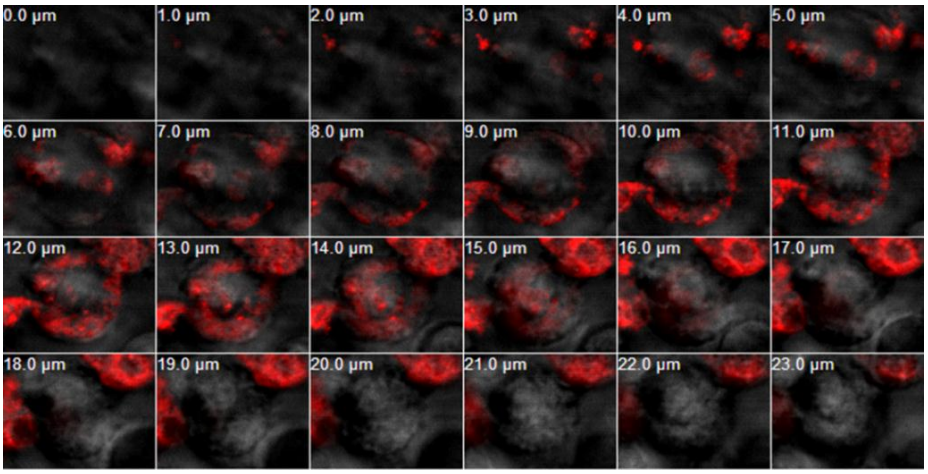

FIGURE 4-6: IMAGE SLICES THROUGH AN INDIVIDUAL CELL ALONG THE Z AXIS FOR LOCALISATION OF APTAMER CSIR 3.14

Image slices at 1 µm intervals along the Z axis from below the cell to above the cell. The first image at 0.0 µm is below the cell and the final image at 23.0 µm is above the cell. Images between 9.0 µm and 15.0 µm are from within the cell.

Kinetics of aptamer CSIR 3.14 internalisation was determined by confocal microscopy. Images were taken every 15 minutes for six hours (Full set of images can be found in Appendix 6.7) and the fluorescence intensity of all cells measured. Aptamer CSIR 3.14 was added to the live Jurkat cells and the first image recorded within a minute. At the first time point some cells were starting to take up the aptamer (Figure 4-7). Cells already saturated at this point may be dead cells that took up the stain due to porous membranes rather than active uptake through the CD7 receptor. An increased number of cells have taken up the stain by the second time point (15 minutes) and at 30 minutes the maximum fluorescence appears to have been reached (Figure 4-7). Images from the different time points were combined to generate an orthogram depicting the cellular localisation of the aptamer stain on the different planes of view (Figure 4-8). The cell can be seen to move in the X plane over time, as it appears elongated. The red fluorescence of aptamer CSIR 3.14 is within the cell on all visible planes confirming the aptamer internalisation (Figure 4-8).

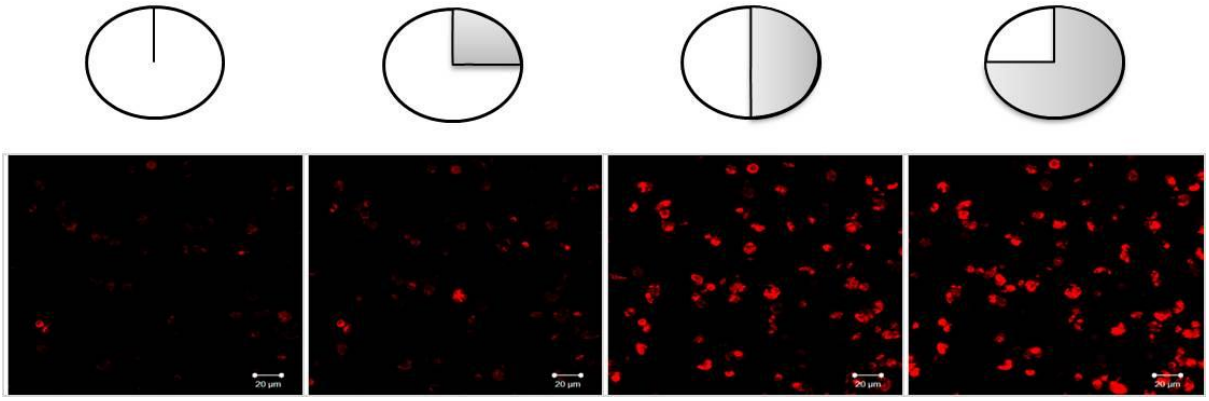

FIGURE 4-7: TIME COURSE OF APTAMER CSIR 3.14 INTERNALISATION

Images of aptamer CSIR 3.14 internalisation up to 45 minutes post addition of aptamer. Images were taken at 15 minute intervals for six hours.

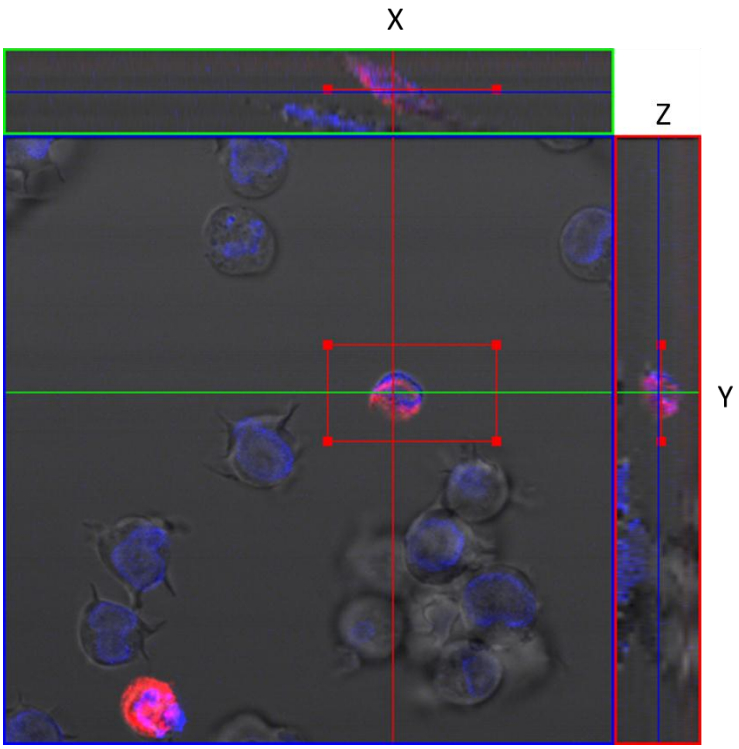

FIGURE 4-8: ORTHOGRAM ILLUSTRATING CSIR3.14 CELLULAR LOCALISATION

Images were captured over time and compiled to illustrate the cellular localisation of the aptamer over time. The X plane indicates how the cell moved over the time course. The red fluorescence of the aptamer can be seen to localise within the cell on all planes of view. The red box visible on the Y axis is indicated on the X and Z axis by a red line.

A quantitative analysis of the fluorescence over time was carried out with the selection of two regions of interest chosen to study. The first region of interest (ROI 1) included the whole visible plane while region of interest two (ROI 2) included only a single cell. The single cell selected was not one that showed fluorescence at time zero but rather one that lit up later. The fluorescence intensity per region of interest was plotted and a non-linear regression line fit from which the association rate constant and the dissociation constant was calculated. Even though the cells were attached to the slide surface by Poly-L-Lysine, some cell movement was still recorded. As such, in making use of the whole visible plane for the calculation of the internalisation kinetics, two basic assumptions were made, namely:

1. Cells contributing to the mean fluorescence are those attached to the slide surface

2. Cells drifting in and out of the frame are at a constant and equal rate and have no significant influence on signal accumulation over time

The association rate constant for ROI 1 was calculated at 4.2×10^4 $Molar^{-1}Minute^{-1}$ with a dissociation constant of 23 fM and an R^2 of 0.88 (Figure 4-9). For the second region of interest (ROI 2), a single cell was selected that did not move over the time period. As with the whole visible plane, the fluorescence within the single cell plateaued within one hour. The association rate constant for ROI 2 was calculated at 6.3×10^4 $Molar^{-1}Minute^{-1}$ with a dissociation constant of 15 fM (Figure 4-9).

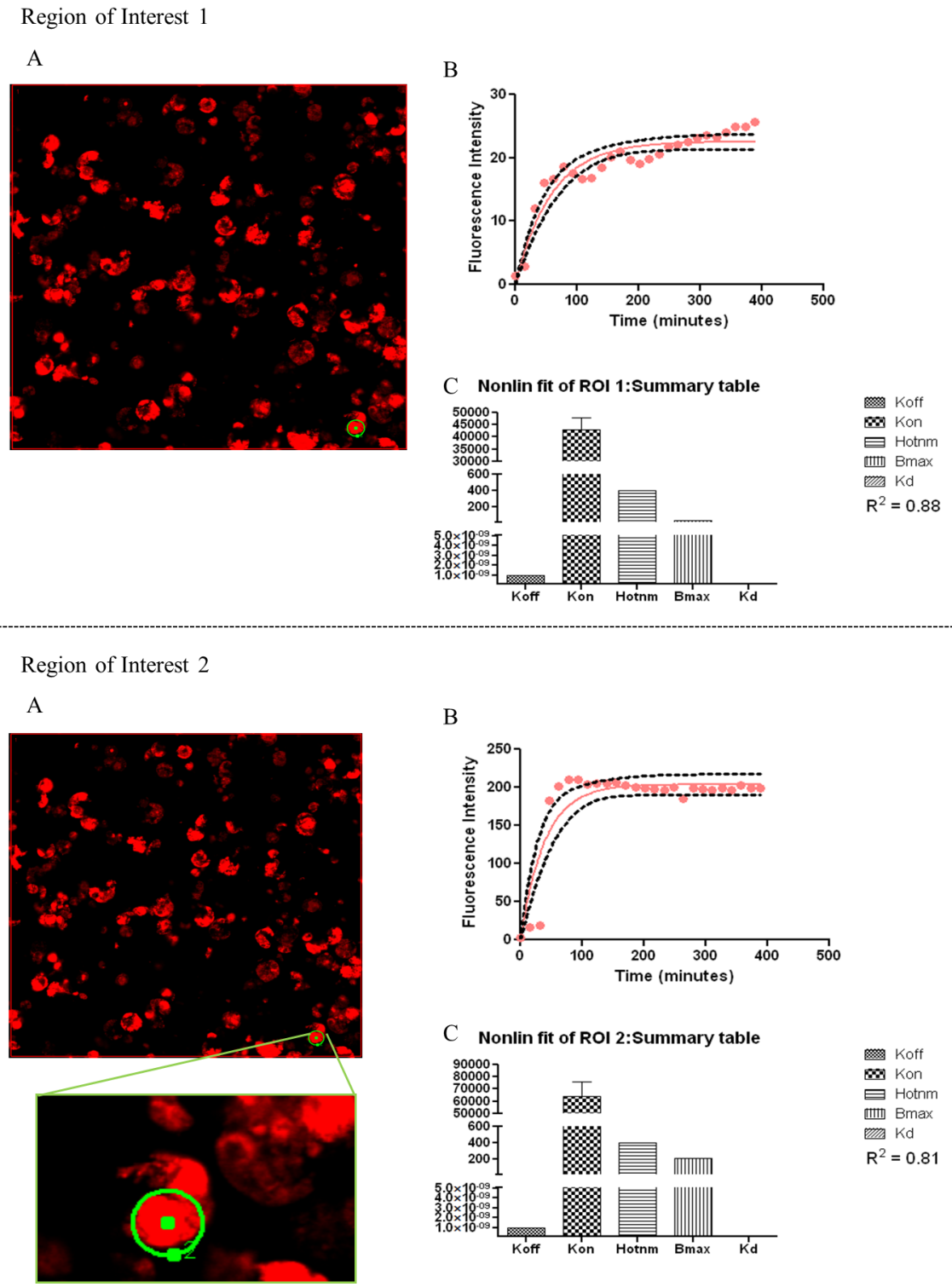

FIGURE 4-9: KINETICS OF INTERNALISATION FOR CSIR 3.14

ROI1 and ROI2 were selected for the calculation of internalisation kinetics. A. The area making up the ROI selected. B. Fluorescence intensity over time fitted with a non-linear regression line. The 95 % confidence interval for the line is indicated by a dashed line. C. The calculation parameters for the non-linear regression line.

4.3.3 ANTI-CD7 APTAMER CSIR 3.14 BINDING SITE MUTATION CHARACTERISATION

Aptamer CSIR 3.14 was the best internalising aptamer based on the internalisation and kinetics so far. As aptamers are known to fold and form specific structures it was important to identify if the binding capacity of aptamer CSIR 3.14 is based on secondary structure or sequence specific interaction. It is expected that when the folding of the aptamer is disrupted, the binding will be negatively affected. This section covers the characterisation of aptamer binding when the structure was disrupted by mutations.

Aptamer CSIR 3.14 was mutated to remove ten nucleotide sections of the proposed binding region based on Mfold predicted structure analysis (Section 3.3.2). The mutated sequences were analysed by flow cytometry for association to Jurkat cells to determine if the aptamer was still able to bind. In addition, the DNA of aptamer CSIR 3.14 was analysed for binding. Previous studies have reported the use of the DNA form of an RNA aptamer for successful targeted delivery of siRNA (Zhu, Shibata et al. 2012). DNA aptamers are intrinsically easier to truncate, as they are not restricted by the 3′ regions T7 polymerase promoter. A DNA aptamer can be chemically synthesised at the desired length and at low cost and tested for activity while the chemical synthesis of RNA can be prohibitively expensive. Aptamer secondary structure was predicted for the mutants and the CSIR 3.14 DNA to confirm the deleted proposed binding structure. All predicted structures did not contain the proposed binding region of CSIR 3.14 (Figure 4-10 A).

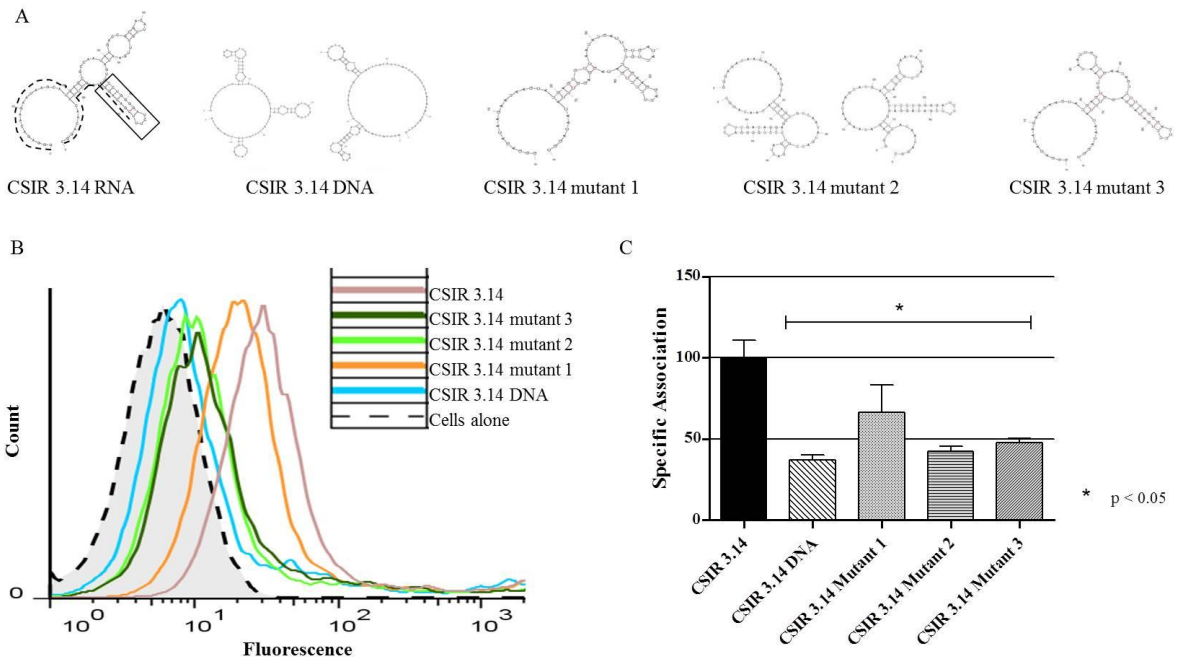

FIGURE 4-10: ASSOCIATION OF APTAMER CSIR 3.14 FULL LENGTH, MUTANTS AND CSIR 3.14 DNA TO JURKAT CELLS

Aptamer CSIR 3.14 RNA, mutants and DNA were incubated with Jurkat cells at a final concentration of 400 nM overnight. A. Computational prediction of aptamer secondary structure, proposed binding region of CSIR 3.14 RNA is indicated by a solid box. B. Overlay histogram of aptamer binding at different concentrations (Cell alone control shaded in grey). C. Specific association of aptamer isoforms to Jurkat cells (n = 5).

Aptamer association was determined by gating a shift in fluorescence when compared to the cell alone control. Aptamer CSIR 3.14 DNA and mutations were normalised to the full length CSIR 3.14 RNA (set to 100 %). A minimal shift in fluorescence was seen for CSIR 3.14 DNA, CSIR 3.14 mutant 2 and CSIR 3.14 mutant 3. A one log shift in fluorescence was seen for CSIR 3.14 mutant 1 and CSIR 3.14 full length RNA (Figure 4-10 B). A student's t test was used to determine the significance of the association differences (n = 5) and found all mutants and CSIR 3.14 DNA bound significantly less than the full length CSIR 3.14 aptamer ($p < 0.05$) (Figure 4-10 C). The DNA isoform of aptamer CSIR 3.14 was not able to bind significantly and so could not be used for truncation optimisation.

Eight aptamers (CSIR 3.141, CSIR 3.28, CSIR 3.31, CSIR 3.35, CSIR 3.37, CSIR 3.39, CSIR 3.42 and CSIR 3.48) were brought forward from binding characterisation with CD7-HeLa cells for characterisation using Jurkat cells. Aptamer internalisation was initially characterised using flow cytometry to determine if the aptamers were able to internalise through the endogenously expressed receptor. Three aptamers were shown to internalise into the T lymphocyte cell line, illustrating how specific aptamers for an exogenously expressed receptor may not be suitable for *in vivo* application. As aptamers are known to bind with high specificity, even slight alterations in protein folding and epitope presentation could result in an aptamer losing activity. The three aptamers able to bind the Jurkat T lymphocytes were characterised for kinetic parameters. The calculated cell binding constants of the aptamers were 2.1 fM, 0.23 fM and 1.1 fM for CSIR 3.14, CSIR 3.37 and CSIR 3.42 respectively. Future studies should investigate the aptamer association relative to a negative control aptamer as a means to calculate the dissociation constant. As saturation was not reached at low concentrations it could be argued that the calculated dissociation constant may not be within the femtomolar range but rather in the high nanomolar range.

Aptamer CSIR 3.14 kinetics was visualised by confocal microscopy and the internalisation of the aptamer validated. Although the calculated dissociation constant was higher from this experiment than the previous calculation using flow cytometry, it was within the same molar range. In addition, independent research reporting kinetic analysis of RNA binding using methods with intrinsic differences have noted differences in predicted and/or calculated constants (Arraiano, Barbas et al. 2008; Rockey, Hernandez et al. 2011). The internalisation kinetic constant for the confocal microscopy for CSIR 3.14 was calculated as 19 ± 5 fM. Previously isolated aptamers selected against whole cells have internalisation rate constants in the Nano molar range (Xiao, Shangguan et al. 2008; Rockey, Hernandez et al. 2011; Huang, Hernandez et al. 2012) indicating that these aptamers may be potential candidates for lymphocyte specific delivery. As recent *in vivo* studies of aptamer delivery have reported different levels of nuclease resistance which may be the result of incubation time (As discussed in section 1.3.4), a quickly internalised aptamer may have an advantage over slower aptamers.

Aptamer CSIR 3.14 was mutated to remove section of the proposed binding region identified in section 3.3.2. All modifications to the structure resulted in significantly reduced

binding to Jurkat T lymphocytes. This data illustrates the importance of structural conservation in aptamer functioning. This is a characteristic common to aptamers and has been exploited for the generation of aptamers with unique characteristics. An example of this is an aptamer that forms two structures that work synergistically to inhibit their target (Huang, Pei et al. 2009). Further characterisation of aptamer CSIR 3.14 will be required to identify the minimal sequence required for binding such that a truncated aptamer can be generated.

A limit of detection study for aptamers CSIR 3.14 and CSIR 3.37 showed that a doubling of aptamer concentration caused a 60 % increase in binding at lower concentrations. In addition, it was shown that the cells had greater capacity to bind the aptamer thus indicating that the rapid plateau was due to aptamer depletion and not binding site saturation. This is an important characteristic as it implies that the aptamer concentration can be increased beyond 300 nM for increased delivery of a therapeutic molecule should it be necessary. However, it is important to note that the therapeutic value of the aptamer decreases as the concentration needed for efficacy increases as the cost becomes prohibitive. Taken together, the data shown here suggests that CSIR 3.14 has potential to be developed for selective targeting of T lymphocytes.

Chapter 5. GENERAL DISCUSSION

5.1 NEXT GENERATION SEQUENCING AND APTAMER SELECTION

As highlighted previously in section 2.4, the aptamer monitoring approach used in this thesis may not be the most efficient and informative. Next generation sequencing allows for the whole pool of aptamers to be monitored after each round for enrichment and diversity. The traditional SELEX approach relies on multiple rounds of selection and maturation to identify enriched aptamer sequences. The selection can be monitored indirectly by assessing the binding affinity of the pools at each round or the level of enrichment by percentage recovery (as used in this thesis). Although these methods will provide insight into the development of the selection pool, the process may bias the aptamer selection by excessive PCR and transcription reactions. The high throughput sequencing (HTS) of each round allows for the identification of not only highly represented sequences but those that are enriched round by round as well. Although concerns for PCR bias have been raised in the past, the first experimental monitoring of it was conducted by Zimmerman et al in 2010. The experimental approach made use of a "Natural SELEX" in which the library was amplified and transcribed over successive rounds but not enriched for any target in particular (Zimmermann, Gesell et al. 2010). At each round, the pool was sequenced to identify changes in represented sequences. Zimmerman et al noted that successive rounds of amplification favour shorter sequences with lower structural stability and to some extent specific nucleotide content (Zimmermann, Gesell et al. 2010). The nucleotide bias was later noted by Theil et al in 2011 where HTS of successive rounds saw the inclusion of more adenosines (Thiel, Bair et al. 2011). A recent study using HTS in the SELEX highlighted how a number of sequences that were highly represented across all rounds of selection were not highly enriched (Cho, Xiao et al. 2010). In other words, although the sequences were present in abundance at all rounds of selection, the copy number did not increase as rounds increased. The authors attributed this to a bias in the PCR allowing for certain sequences to be amplified more than others (Cho, Xiao et al. 2010). This highlights how arbitrary sequences may appear as enriched aptamers by virtue of PCR bias without the monitoring of aptamer enrichment by sequencing. This may have been the case in this thesis where the three aptamers identified more than once in the sequencing were not the most enriched for the target (Section 3.3.2).

In addition to PCR bias, the monitoring of enrichment by HTS allows for a more rapid and cost effective aptamer selection. The cost savings can come in two forms, firstly fewer rounds are needed to identify enriched sequences and secondly arbitrary sequences and background can be identified and ruled out without the need for characterisation experiments. Cho et al (2010) highlight how aptamers identified after three SELEX rounds using HTS had up to eight fold greater affinity and up to four fold greater specificity than aptamers identified using the standard cloning and sequencing technique (Cho, Xiao et al. 2010). Since then, other groups have shown by making use of melting curve analysis that the pool diversity decreases after three rounds and remains constant to the end of selection (Schutze, Wilhelm et al. 2011). HTS has shown to be an invaluable tool minimising the time and cost of aptamer selection and in identifying the most specific aptamers with the highest affinity. Hoon et al (2011) proposed a novel SELEX method with a single round followed by a bioinformatic analysis of HTS data. This method, Aptamer Selection by K-mer Analysis of Sequences (ASKAS), was shown to select for known and novel thrombin aptamers in a single round (Hoon, Zhou et al. 2011). The ASKAS method analyses the frequency of aptamers based on their length and K is set to a predetermined range. In this case, K ranged from 15 to 33 bases. A doubling in frequency of different K-mers identified between 15 and 16 nucleotides was identified. These 15mer sequences were further characterised using SPR to determine the K_d which were shown to be within nano and micro molar range (Hoon, Zhou et al. 2011). They propose using this method to identify high affinity aptamers of varied length with limited hands on time. Although this method may be promising for selection of aptamers against recombinant proteins, it may not be as simple for cell based selections. Additional rounds of selection and negative selection would need to be included to remove aptamer sequences that are not specific to the receptor of interest. However, with that said, HTS has a place in all aptamer selection methods as it allows for direct monitoring of the selection and enrichment. All aptamer selections in the future would benefit from including HTS to identify the best aptamers in the shortest possible time.

5.2 THERAPEUTIC APPLICATION OF A LYMPHOCYTE SPECIFIC APTAMER

5.2.1 T LYMPHOCYTE TROPIC VIRUS TREATMENT: HIV-1

Aptamers have been developed against various HIV-1 components including: reverse-transcriptase (Andreola 2001), surface glycoprotein gp120 (Khati 2003), integrase (de Soultrait 2002), and the *trans*-activation response (TAR) RNA (Duconge 1999) for development into aptamer based HIV-therapeutics. Aptamers have also been raised against drug resistant strains of HIV-1 in an attempt to overcome challenges associated with drug resistance (Li 2008). A range of aptamers have been developed that bind within the co-receptor binding region of gp120 and effectively block HIV-1 binding and entry into the cell (Sayer, Ibrahim et al. 2002; Khati 2003; Dey 2005; Cohen 2008; Mufhandu, Gray et al. 2012). These aptamers have been highlighted for use as entry inhibitors and studies have explored their use in microbicides (Moore, Cookson et al. 2011). While aptamers as therapeutics has been discussed in detail in section 1.4.1, this section will focus on the use of aptamers for delivery of HIV-1 therapeutics. The HIV-1 genomic organisation and life cycle will be described as well as the current antiretroviral (ARV) strategies and mode of action. A role for the CD7 specific internalising aptamers in the development of novel therapeutics will be described.

HIV-1 is the causative agent of acquired immune deficiency syndrome (AIDS), a global public health issue as the virus infects an estimated 33 million people worldwide (UNAIDS 2009). HIV-1 is a lentivirus that infects CD4+ cells and integrates its genome into the host. The HIV-1 genome is roughly 9 Kb and is comprised of two copies of positive sense RNA encoding for nine overlapping genes (Figure 5-1). These genes can be classed into three broad categories, namely: Structural genes Gag, Pol and Env; Regulatory genes Rev and Tat and Accessory genes Nef, Vir, Vpr and Vpu (Li, Hui et al. 1992). These genes are processed by alternate splicing and encode all the viral proteins required for the production of new virus particles. In order to produce the new, complex virus particles, the virus relies on host machinery. The virus enters the cellular host making use of the CD4 receptor and co-receptor CCR5 or CXCR4. Once inside the cell, the viral capsid is released and the viral RNA genome is reverse transcribed into DNA and integrated into the host genome making use of viral enzymes reverse transcriptase and integrase. Once integrated into the host genome, the viral

particles are produced and packaged using cellular machinery. As such, to prevent infection successfully, the events prior to genome integration need to be inhibited.

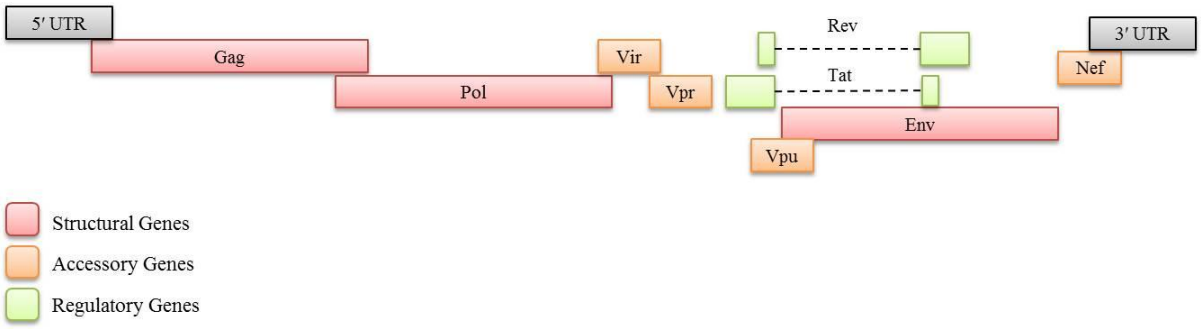

FIGURE 5-1: HIV-1 GENOME ORGANISATION

The HIV genome is comprised of nine genes that can be classed into three categories: Structural, accessory and regulator genes. As the genome is very small (± 9 Kb) the overlapping genes are spliced to form all the HIV proteins required for viral particle production.

To date numerous treatments are available that can effectively increase the life expectancy of an infected individual. ARV therapies interact with various stages of the viral life cycle (Figure 5-2) and can be defined by four different treatment classes: entry or fusion inhibitors (EI), reverse transcriptase inhibitors either non-nucleoside (NNRTI) or nucleoside (NRTI), protease inhibitors (PI) and integrase inhibitors (II). EI inhibit viral entry to $CD4^+$ cells by blocking binding of the virus to the receptors or co-receptors, or by blocking fusion of the membranes (Wild, Shugars et al. 1994). NNRTI inhibit reverse transcriptase activity indirectly by stopping elongation of nascent DNA while NRTI inhibit reverse transcription directly by physically binding to the enzyme (Hang, Li et al. 2007). PI inhibits protease enzymes required to cleave nascent proteins for assembly of new virions (Flexner 1998). II prevent provirus integration into the host chromosome (Sato, Motomura et al. 2006).

The current HIV-1 treatments both on the market and in development were designed against HIV-1 subtype B, a strain prevalent in Europe and America. Subtype C however, is the most prevalent subtype in Sub Saharan Africa and is the fastest spreading worldwide. As ARV treatments are targeted toward viral function they are hampered by viral strain differences and non-subtype B resistance can occur rapidly. To combat viral resistance, highly active antiretroviral therapy (HAART) was introduced that uses a PI coupled with either NRTI or NNRTI (Baxter 2006). Although HAART is generally successful , it is limited by: toxicity with prolonged use, cost (Murphy 2002; Baxter 2006; Stenger 2009), non-compliance since over 95 % compliance is required for successful treatment (Penedoa 2003),

accessibility to treatment and viral resistance resulting in cross class resistance. Thus, there is a need for a novel HIV-1 treatment option with reduced side effects that is cost effective. The toxicity caused by non-target effects can be significantly reduced by specific targeting of relevant cells. Aptamers represent novel, non-toxic, non-immunogenic molecules that can be directed to bind a variety of targets with great specificity.

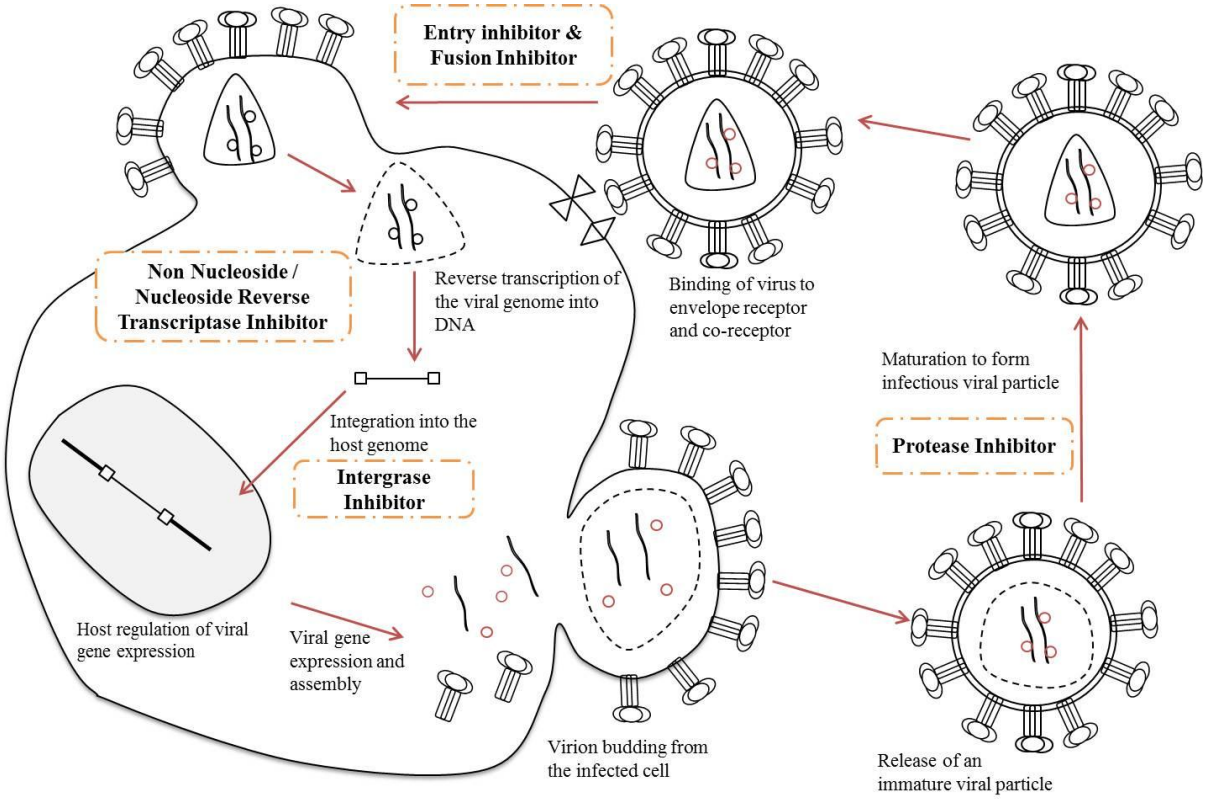

FIGURE 5-2: THE HIV-1 LIFECYCLE PRESENTED WITH ANTIRETROVIRAL INTERACTIONS

The current antiretroviral therapies interact with various aspects of the viral life cycle. Entry and Fusion inhibitors prevent viral entry by blocking the binding of the viral and host membrane proteins. Reverse transcriptase inhibitors prevent the reverse transcription of the viral genome into DNA before the integrase inhibitor can prevent the integration of the viral DNA into the host genome. Viral gene expression is under the control of the host once the viral genome has been integrated into the host DNA. Viral proteins accumulate at the cell membrane during assembly of the virion. Viral membrane proteins are trafficked to the cell surface and the immature viral particles bud from the cell, taking the cell membrane as their own. The protease inhibitor acts at the point of viral maturation to prevent processes essential to virion virility.

As HIV-1 makes use of CD4 to enter cells, the selective targeting of cells expressing CD4 is necessary. However, targeting of CD4 allows for only mature cells to be targeted and as such could not be used for delivery of a prophylaxis. The need for life long HIV-1

treatment, the toxicity of the current treatment and the inability of current therapeutics to clear the viral infection are considered obstacles for novel therapeutics to overcome. Aptamer-siRNA chimeras have been designed with different cellular and viral targets in an attempt to prevent and or eradicate HIV-1 infection (Discussed in greater detail in section 5.3). The CD7 specific aptamers described in this thesis could be applied to the delivery of HIV-1 therapeutics prophylactically. As the CD7 receptor is expressed on progenitors of T lymphocytes, natural killer cells and dendritic cells (Hao, Zhu et al. 2001) the cells could be targeted for gene therapy before HIV-1 infection.

5.2.2 T LYMPHOCYTE DISEASE TARGETING: RHEUMATOID ARTHRITIS AND LEUKAEMIA

The CD7 receptor has been widely studied as a target for delivery of cytotoxic molecules for the treatment of T lymphocyte diseases such as leukaemia, lymphoma and Rheumatoid Arthritis (RA) (Vallera, Burns et al. 1996; Frankel, Laver et al. 1997; Pauza, Doumbia et al. 1997; Waurzyniak, Schneider et al. 1997; Peipp, Kupers et al. 2002; Bremmer, Cate et al. 2006). RA is an autoimmune disease characterised by chronic inflammation of the joints. CD4+ T lymphocytes have been identified as the key component for the perpetual inflammation resulting from auto activation or cytokine activation (Moore, Walters et al. 1988; Morimoto, Romain et al. 1988). As such, a number of strategies have been identified to induce apoptosis in these cells as a potential therapy. These therapies have looked at targeting a number of different T lymphocyte receptors including CD4, CD28, CD40L, RANKL and CD7 (Kirkham, Thien et al. 1992; Moreland, Pratt et al. 1995; Bremer, ten Cate et al. 2006). Many of the early monoclonal antibody targeting strategies have shown limited success in clinical trials including those targeting the CD4 receptor (Moreland, Sewell et al. 1995) and the CD7 receptor (Kirkham, Thien et al. 1992). In the study by Moreland et al, a positive clinical response was determined by $\geq$ 50 % improvement in tender and swollen joints. Patients treated with the anti-CD4 monoclonal antibody, in combination with a stable low dose of methotrexate showed no difference to the placebo at all concentrations despite significant CD4+ T lymphocyte depletion (Moreland, Pratt et al. 1995). This apparent contradiction in treatment outcome highlights the complexity of RA and the need for improved targeting therapeutics. In a recent study, an alternative pathway was targeted for apoptosis induction in T lymphocytes. Bremer et al targeted the Activation Induced Cell Death (AICD) pathway to deplete the auto activated T lymphocytes at the site of

inflammation. AICD is a tightly controlled negative feedback mechanism that regulates the apoptosis of T lymphocytes after activation for inflammation. In this study, the Fas signalling pathway was induced to activate cell death using the FasL protein fused to a monoclonal antibody specific to various T cell receptors (Bremer, ten Cate et al. 2006). The Fas receptor is a transmembrane receptor that forms part of the death receptor family. Once activated by FasL, it induces a signalling cascade that results in apoptosis. This *in vitro* study identified the CD7 receptor targeted fusion protein (ScFvCD7:sFasL) as the most potent inducer of apoptosis with induction of up to 80 % apoptosis in CD3-positive inflammation associated T-cells. The internalising aptamer described in this thesis may highlight another mechanism for inducing apoptosis for treatment of RA. As highlighted previously (Section 1.5) aptamers can be linked to a number of effector molecules for efficient delivery into target cells. This could be applied to gene therapy approaches to deactivate the autoimmune reaction or the delivery of apoptosis inducing chemicals that are only active once inside the cell.

Fas mediated apoptosis induction has also been applied to leukaemia therapy. The same CD7 targeted FasL molecule identified for RA treatment, ScFvCD7:sFasL, was tested for activity against a T lymphoblastic leukaemia cell line, patient-derived T-cell lymphoma and acute myeloid leukaemia cells (Bremer, ten Cate et al. 2006). The ScFvCD7:sFasL was shown to be a potent inducer of apoptosis in target cells while normal peripheral-blood lymphocytes and epithelial cells were unaffected. A similar construct was also produced by the same group that induces cell death through the tumour necrosis factor (TNF)–related apoptosis-inducing ligand (TRAIL) (Bremer, Samplonius et al. 2005). In this study, TRAIL was linked to a CD7 specific monoclonal antibody, scFvCD7:sTRAIL, and was able to induce apoptosis in leukemic cells with no toxicity in epithelial and normal cells *in vitro* (Bremer, Samplonius et al. 2005). The CD7 receptor has been used as a target for a number of leukaemia treatments including those under pre-clinical testing, clinical testing and in clinical use that deliver a number of different cytotoxic compounds (Frankel, Laver et al. 1997; Peipp, Kupers et al. 2002). The aptamers described in this thesis have shown high affinity for the T lymphocyte cell line, Jurkat cells, which are commonly used in the characterisation of potential T cell malignancy therapeutics. As such, these aptamers may have potential as delivery vectors for apoptotic therapeutics in place of the monoclonal antibodies commonly used.

5.3 APTAMER-SIRNA CHIMERAS

There is a persistent need for novel HIV-1 therapeutics with reduced toxicity with sustained anti-HIV activity, resistant to viral escape (Section 5.3.1). The reliance of the virus on host factor proteins allow for the regulation of viral gene expression without directly targeting the virus. Genetic modulation of host proteins required by HIV-1 for replication has been identified as a possible strategy for HIV-1 treatment (Reviewed by Rossi, June et al. 2007). The identification that a Δ 32 CCR5 mutation confers resistance to R5-tropic HIV-1 strains lead to the successful treatment of an HIV-1 positive individual with acute myelogenous leukemia by a bone marrow transplant (Hutter 2009). The donor was homozygous for the Δ 32 CCR5 mutation and now years after the transplant the recipient has shown no viral rebound. This protective mutation causes no known detrimental effects and suggests that it may be possible to treat HIV-1 by targeting host proteins required for viral replication without toxic side effects. A number of studies have been conducted that have identified hundreds of host genes required by HIV-1 to replicate (Li, Nguyen et al. 2011; Primo, Dausse et al. 2011; González-Fernández, de-los-Santos-Álvarez et al. 2012; Hernandez, Flenker et al. 2013).

An aptamer specific to HIV-1 gp120 has been used as a delivery vehicle for targeted delivery of Dicer substrate anti-HIV-1 siRNA to HIV-1 infected cells (McNamara 2006; Zhou, Swiderski et al. 2009). The anti-gp120 aptamer and anti-*tat/rev* siRNA chimera reduced viral replication and helper $CD4^+$ T cell depletion in humanized mice (Neff, Zhou et al. 2011). The chimera did not elicit an interferon response, unlike what has been seen with liposome or polyplex regent mediated delivery of siRNA (Zhou, Swiderski et al. 2009). A similar approach can be used with the CD7 specific aptamer to deliver dicer substrate siRNA against host factors require by HIV-1 such as CCR5. Making use of the progenitor expression of CD7, the CD7 specific aptamers can be used to deliver anti-CCR5 siRNA to cells before they mature to express CD4. In this way, the cells are immunised against HIV-1 infection and should survive to protect the individual from secondary infections.

The gp120 aptamer anti-*tat/rev* siRNA chimera had dual function as it not only delivered siRNA to specific cells but was able to act as an entry inhibitor by binding gp120 on the viral surface blocking entry. Although this aptamer chimera has shown great potential as a therapeutic intervention for HIV-1 infection, there are a number of concerns with this approach. A major challenge when working with gp120 is its probable unstable conformation

and the large conformational change seen when gp120 binds CD4 (Kelker 2010). In addition, gp120 is mostly shielded from immune response by a cover of negatively charged carbohydrate groups (Sayer, Ibrahim et al. 2002). These inhibit the binding of molecules not only by reducing immunogenicity but by steric hindrance of immunogenic epitopes on the gp120 molecule. The effects of steric hindrance against the aptamer binding can be reduced by identifying the minimal sequence required for its binding, an aptamer can be reduced in size to contain only the essential binding sequence (Dey 2005). In addition, the hyper-variable nature of gp120 may not make it a suitable target for aptamer delivery. Although the ability of aptamers to be able to discriminate between targets with subtle structural differences such as isoforms of a protein (Jenison 1994; Gopinath 2006) is highlighted as an advantage as great specificity, it may allow viral escape to occur with relatively minor protein modifications. In addition, the dual ability of the aptamer as a delivery molecule and an entry inhibitor may increase the selection pressure for the viral gp120 to escape leading to faster rates of resistance mutations. Using the CD7 specific aptamers to target a cellular receptor may help to overcome these challenges.

Aptamers have been selected against the CD4 receptor and have been used to deliver siRNA successfully to inhibit HIV-1 infection in explants in humanised mice (Wheeler, Trifonova et al. 2011). It is important to note that this study highlighted two important drug delivery characteristics, namely: 1. a human immune cell receptor (CD4) was able to be targeted by aptamers without stimulating lymphocytes or activating innate immunity and 2. targeted delivery of an aptamer-siRNA to a human immune cell receptor has the ability to inhibit HIV-1 infection. Although this successful study has shown important advancements in therapeutic delivery, targeting of CD4+ cells cannot be used to deliver a prophylactic treatment. By selectively targeting cells before they are CD4+, they can be targeted before HIV-1 infection is possible. This would allow for a prophylactic treatment of viral infection. It has been shown that siRNA delivered before HIV-1 challenge caused a reduction in infection due to a reduction in viral integration (Jacque, Triques et al. 2002). This mode of action would allow for a number of therapeutic interventions such as the knock down of HIV-1 dependency factors required for successful infection, such as co-receptor CCR5. By preventing new infections within an infected individual is it believed that the active viral reservoir could be eradicated giving the individuals immune system a chance to rebuild. As the CD7 receptor remains expressed on CD4+ cells, it is also possible to treat infected cells with targeted therapeutics. Targeting of therapeutics to infected cells has been widely studied

to overcome high toxicity of therapeutics and to reduce dosages (Chen, Dellamaggiore et al. 2008). As such, aptamers were selected against the CD7 receptor with the potential application of the aptamers in HIV-1 therapeutic delivery. As such, the targeting of CD7 not only improves HIV-1 treatment delivery by overcoming challenges with viral targeting but may provide a system of prophylactic delivery of HIV-1 inhibitors allowing for viral reproduction to be halted.

Additional characterisation, beyond the scope of this project, will be required to attach the candidate aptamer to a siRNA. The internalisation kinetics will need to be determined for the chimera and the activity of the aptamer and siRNA assessed. As the aptamer and siRNA are composed of the same molecule (namely RNA) there is possibility for the two sequences to lose their individual structure and form a new structure all together. This design consideration is essential as the aptamer binding is structurally determined and any obstruction of the binding pocket significantly reduces binding capacity (Shown in section 4.3.3). In addition, chemical modification may be explored for increased stability of the chimera for therapeutic application.

5.4 CONCLUDING REMARKS

Taken together, the results presented in this thesis identify the first CD7 receptor specific aptamers that can be used for T lymphocyte targeting. Making use of the internalising whole cell SELEX, a panel of CD7 receptor specific aptamers were selected. One aptamer in particular, CSIR 3.14, showed great potential as a delivery vector with the lowest reported dissociation kinetics for an RNA aptamer. This aptamer can be applied to a number of applications, most notable the delivery of prophylactic therapy for HIV-1 (as discussed above). Although the selection method used was not without potential optimisations (as discussed in section 5.1), constant iterations are always necessary in order to identify the best possible scientific methods. This thesis adds to the current knowledge in the aptamer field by providing evidence for lymphocyte specific targeting molecules and identifies their application in medical science and therapeutic applications.

Chapter 6. APPENDIX

6.1 GENERAL METHODS AND OPTIMISATION RESULTS

6.1.1 MINI PREP KIT PREPARATION

Transformed *E.coli* cultures were grown in LB broth until log phase as measured by OD_{600} of 0.4 followed by centrifugation for 20 minutes at 16 000 × g. The pellets were re-suspended in 250 µl of Buffer P1 [50 mM Tris-HCl pH 8.0, 10 mM EDTA and 100 µg/ ml RNAse A]. An equal volume of Buffer P2 [200 mM NaOH, 1 % SDS (w/ v)] was added and mixed by inversion for one minute. An equal volume (350 µl) of pre-chilled Buffer P3 (3.0 M potassium acetate pH 5.5) was added and mixed by inversion for one minute prior to centrifugation for 20 minutes at 16 000 × g. The supernatant was pipetted into a QIAprep spin column, centrifuged for 60 seconds at 16 000 × g and the flow through was discarded. Following this, 750 µl of Buffer PE (wash buffer, composition not provided) was added and centrifuged for a further 60 seconds at 16 000 × g. Flow-through was discarded and samples were centrifuged for 60 seconds at 16 000 × g. QIAprep columns were transferred to new 1.5 ml centrifuge tubes and plasmid DNA eluted with 100 µl of double distilled water by centrifugation for 60 seconds at 16 000 × g.

6.1.2 PCR CLEAN UP KIT PROTOCOL

The PCR products were purified by centrifugation using a PCR purification kit (Promega, WI, USA). Briefly, the PCR product was prepared for clean up by adding equal volume Membrane Binding Solution (Provided in the kit) and added to an SV mini-column inside a Collection Tube and incubated for one minute. The SV mini-column assembly was centrifuged at 16 000 × *g* for one minute and the flow through was discarded. The SV mini-column was washed with 700 µl Membrane Wash Solution (previously diluted with 95 % ethanol) and again centrifuged at 16 000 × *g* for one minute. Flow through was again discarded and the column washed with 500 µl of Membrane Wash Solution and centrifuged at 16 000 × *g* for five minutes. The flow through was discarded and the assembly centrifuged at 16 000 × *g* for one minute to evaporate remaining ethanol. The SV mini-column was transferred to a 1.5 ml microfuge tube the cleaned product was eluted in 50 µl nuclease-free water by centrifugation at 16 000 × *g* for one minute.

6.1.3 DNA / RNA QUANTIFICATION BY SPECTROPHOTOMETRY

DNA and RNA were quantified by spectrophotometry using a NanoDrop Spectrophotometer at A_{260}. The absorbance ratio at A_{260} and A_{280} was used to determine the purity of the nucleic acid. The expected ration for pure RNA is 2.0 and for pure DNA it is > 1.8.

6.1.4 QUANTIFICATION OF FLUORESCENT LABELLING BY SPECTROPHOTOMETRY

Labelled RNA was quantified using a NanoDrop Spectrophotometer. The reading provides a spectrum of the RNA as well as the fluorescent label and the concentration of the labelled RNA is given (Figure 6-1). The average labelling efficiency was seen to be 80 % for all aptamer clones.

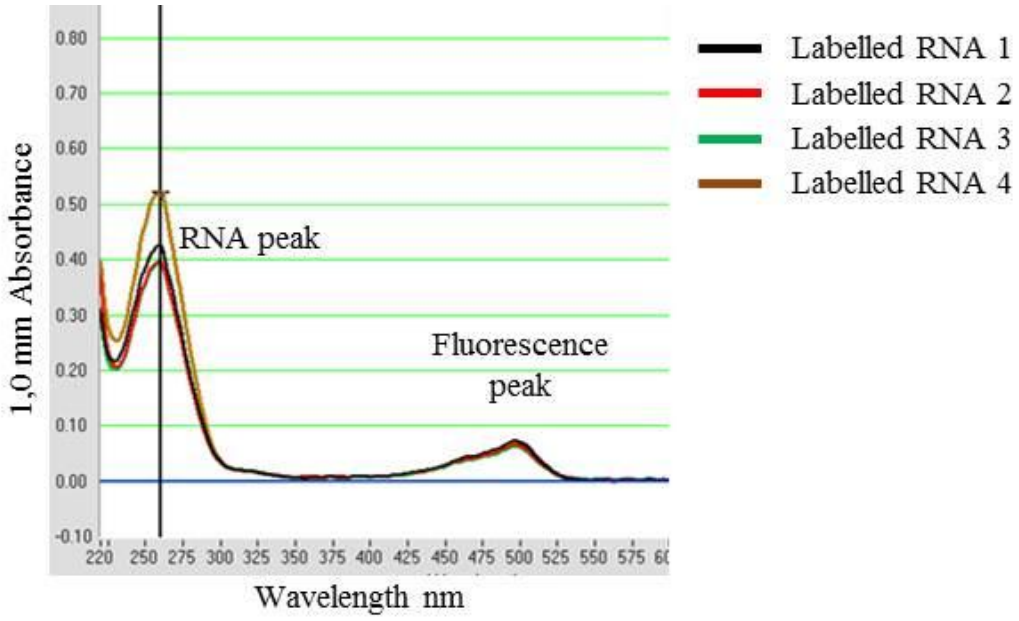

FIGURE 6-1: SPECTROPHOTOMETER QUANTIFICATION OF LABELLED APTAMER RNA

Quantification of RNA labelled with a fluorophore using spectrophotometry. The spectrum of the RNA and the label is shown labelled and the quantification of the labelled RNA is calculated.

6.1.5 RNA PURIFICATION USING THE NUCAWAY CLEAN UP KIT

RNA aptamers were purified from low molecular weight contaminants using NucAway™ Spin Columns (Ambion, NY, USA). Columns were hydrated using 650 µl 1 × HMCKN buffer for five minutes at room temperature. The columns were placed in collection tubes and spun for two minutes at 750 × g to remove excess interstitial fluid. The flow through was

discarded and the *in vitro* transcription product was added directly to the centre of the gel bed. The columns were placed into supplied collection tubes and spun for two minutes at 750 × *g*. The flow through contained the clean RNA ready for use and the spin columns were discarded. RNA was quantified using a NanoDrop 1000 spectrophotometer.

6.1.6 PHENOL CHLOROFORM EXTRACTION OF RNA

RNA was precipitated in 5:1 phenol-chloroform-isoamyl alcohol pH 4.7 and extracted with chloroform. The extract was incubated at -80 °C for 2 hours in 0.1 vol 3 M NaAc pH 5.2 and 1 vol Isopropanol. After incubation, it was centrifuged at 4 °C for 30 minutes (190 × *g*). Supernatant was discarded and the pellet washed with 70% Ethanol. Ethanol was removed and RNA pellets were left to air dry. The pellet was re-suspended in 50 µl nuclease-free water (Fermentas, Thermo Fisher Scientific Inc., MA, USA).

6.1.7 POLYACRYLAMIDE GEL ELECTROPHORESIS OF RNA

RNA fractions were resolved on a 12 % polyacrylamide 8 M urea gel in 1 × TBE running buffer at 200 V, to validate the RNA production quality. RNA was prepared for electrophoresis by incubation with 1 × RNA loading dye [95% formamide, 0.025% SDS, 0.025% bromophenol blue, 0.025% xylene cyanol FF, 0.025% ethidium bromide, 0.5 mM EDTA (Fermentas, Thermo Fisher Scientific Inc., MA, USA)] and heated to 95 °C for three minutes. Visualisation was achieved by ethidium bromide staining under UV light with a Molecular Imager Chemidoc XRS+ Imaging System (BIORAD, CA, USA).

6.1.8 GLYCEROL STOCK PRODUCTION

Single colonies were isolated and inoculated into 5 ml LB containing 100 µg/ ml ampicillin antibiotic (Sigma-Aldrich, MO, USA). Cultures were grown to stationary phase in a shaking incubator at 37 °C. At this stage 0.85 ml culture was added to 0.15 ml sterile glycerol and transferred to a cryovile for long term storage at – 80 °C.

6.1.9 KILL CURVE ANALYSIS AND OPTIMISATION

A kill curve analysis using transfected and un-transfected cells was used to determine the optimal antibiotic concentration for the selection and maintenance of transfected CD7-HeLa cells. Cells were seeded at 8×10^4 cells per well in a six well dish (Nunc™, Thermo Fisher

Scientific, Inc., MA, USA) and incubated overnight at 37 °C with 5 % CO_2. Cells were counted on a haemocytometer using a 1:1 mixture of Trypan Blue stain (Sigma-Aldrich, MO, USA) and cells that had been washed in PBS (Gibco, BRL, UK) and re-suspended in DMEM. One plate was then transfected with the pcDNA-CD7. For the transfection 3 µg of plasmid DNA was incubated in 500 µl OptiMem (Gibco, BRL, UK) with 24 µl FuGene 6 (Promega, WI, USA) for 45 minutes before adding to one plate of seeded HeLa cells. After 48 hours neomycin (Sigma-Aldrich, MO, USA) was added to both plates at different concentrations per well: 10 µg/ ml, 50 µg/ ml, 100 µg/ ml, 200 µg/ ml and 500 µg/ ml. A no antibiotic control well was included on both plates. Cell viability was monitored for one week using light microscopy.

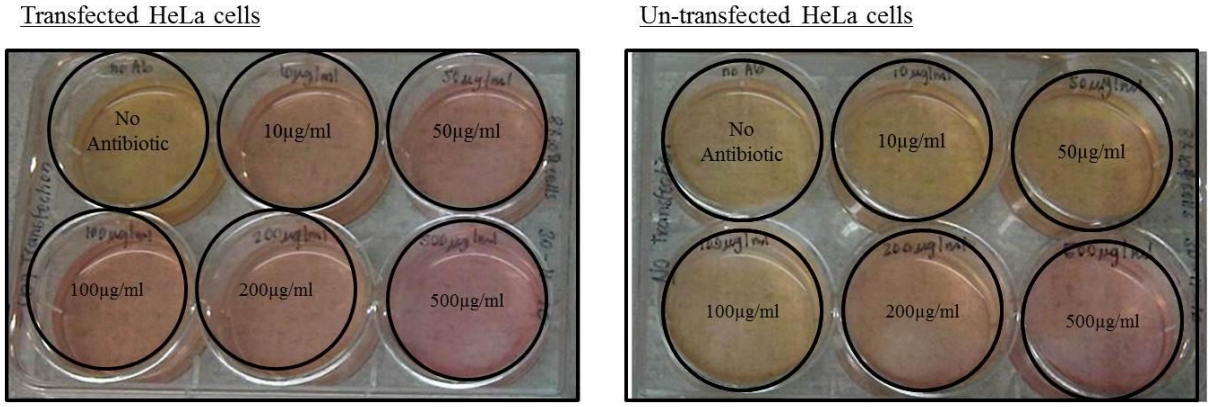

FIGURE 6-2: ANTIBIOTIC GRADIENT FOR MINIMUM CONCENTRATION SELECTION

HeLa cells were seeded in two six well plates and either transfected with the pcDNA-CD7 cloning vector or not. Each well was loaded with a different antibiotic concentration (from zero to 500 µg/ ml) and incubated at 37 °C for one week. Cell viability was monitored by light microscopy for one week. The minimum concentration to cause 50 % cell death in non-transfected cells was 50 µg/ ml.

With no antibiotic, both transfected and un-transfected cells proliferated excessively causing a change in media colour from red to yellow (Figure 6-2). With an increase in antibiotic concentration the level of cell growth was reduced in non-transfected cells. At the highest concentration, all un-transfected cells had died. The transfected cells were able to survive all but the highest concentration of antibiotic but thrived best at concentrations below 200 µg/ ml. The minimum concentration of neomycin at which un-transfected cells were 50 % viable was 50 µg/ ml. The concentration of neomycin chosen for generating the stable CD7-HeLa cell line was 100 µg/ ml after which, the cells were maintained in 50 µg/ ml neomycin in complete media.

6.1.10 LIGATION AND TRANSFORMATION METHODS

Ligation was done by adding 100 ng of double stranded PCR product to 50 ng of pGEM-T Easy® vector and 3 units of T4 enzyme. The reaction was incubated at 37 °C for one hour. For the transformation, frozen TOP10 highly efficient chemically competent cells (Novagen, Merck, Darmstadt, Germany) were thawed on ice. Two microliters of the ligation reaction was added to 50 µl competent cells and incubated on ice for 20 minutes. A cell control (without the vector) was included and treated the same as the transformed cells. After incubation, the cells were heat shocked at 42 °C for 45 seconds and immediately placed on ice for two minutes. To each vial of cells, 950 µl of SOC (Super Optimal broth with Catabolite repression, Invitrogen, CA, USA) was added and the samples were incubated at 37 °C for 90 minutes shaking at 200 rpm. After incubation, 25 µl from each transformant was spread over pre-warmed selective nutrient agar plates (Sigma-Aldrich, MO, USA) supplemented with 100 µg/ ml ampicillin antibiotic (Sigma-Aldrich, MO, USA) and incubated over night at 37 °C.

6.1.11 PCR OPTIMISATION FOR CD7 GENE VECTOR PRODUCTION

The PCR for amplification of the CD7 gene sequence was optimised for both cycle number and annealing temperature to determine the best conditions for gene amplification. The PCR product from each reaction was separated by electrophoresis on a 2 % agarose gel and analysed for optimal conditions (Figure 6-3). A 15 cycle PCR with annealing temperature of 55.5 °C was determined as the optimal reaction condition. Amplified DNA was sent for sequencing and confirmed for the correct sequence by aligning them with the genbank consensus sequence for human CD7 receptor (Figure 6-4).

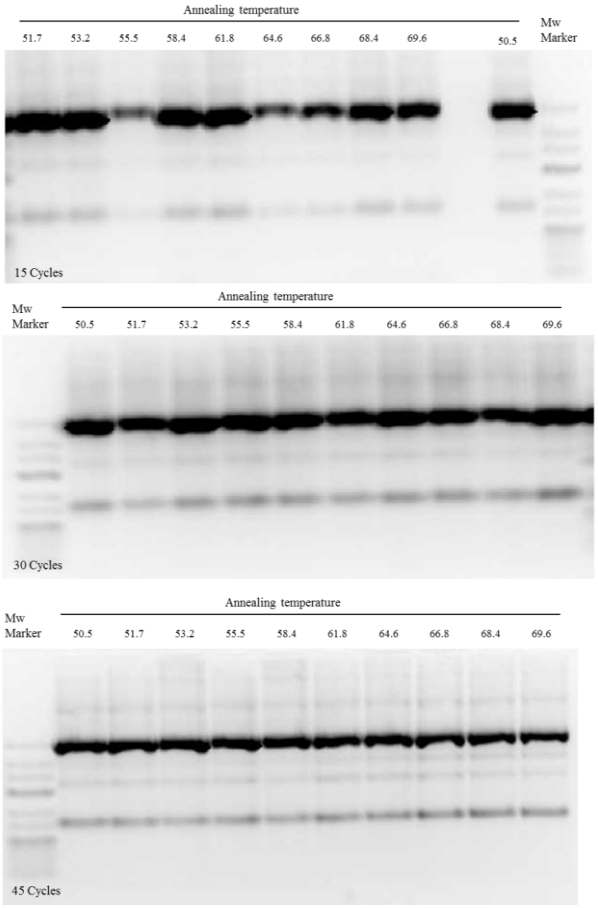

FIGURE 6-3: PCR OPTIMISATION FOR CD7 RECEPTOR GENE AMPLIFICATION

CD7 receptor gene was amplified by PCR which was optimised for annealing temperature and cycle number to identify the best reaction conditions to produce a single band of interest. Fifteen, 30 and 45 cycles were used and the annealing temperature was varied from 50.5 °C to 69.6 °C. A 15 cycle PCR with annealing temperature of 55.5 °C was determined as the optimal reaction condition.

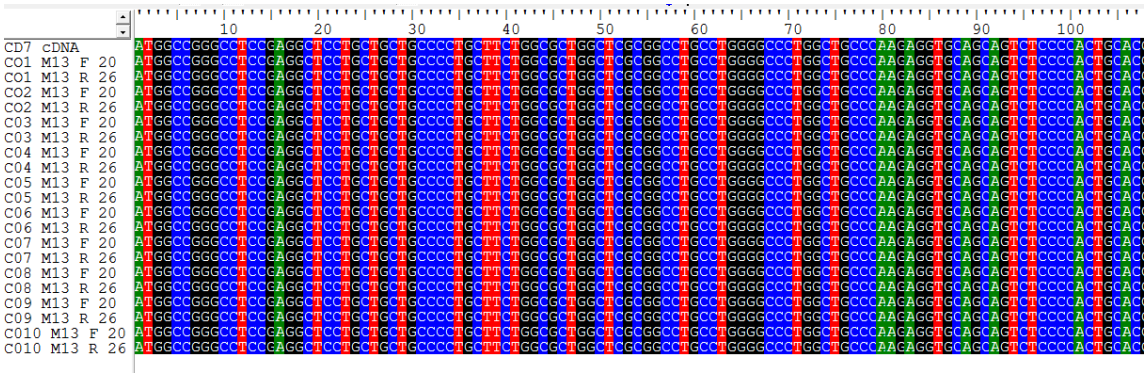

FIGURE 6-4: ALIGNMENT OF CD7 RECEPTOR PLASMID SEQUENCES TO THE GENBANK CONSENSUS SEQUENCE FOR HUMAN CD7 RECEPTOR

Plasmid sequences were aligned using the CLUSTAL W multiple alignment application in BioEdit V7.1.3.0 to the CD7 receptor consensus sequence (Entrez gene number: NP_006128.1). All sequences aligned fully to the consensus sequence indicated by the colouring of the matched sequences.

6.1.12 PCR OPTIMISATION IN SELEX

At each round of selection, the PCR was optimised for cycle number (Figure 6-5). The maximum PCR cycle number was chosen such that the PCR fragment would over amplify (higher bands after 24 cycles, Figure 6-5). At higher number of cycles, the primer dimers start to amplify and can be seen as a band at roughly 75 nucleotides. The band of interest can be seen in line with the 100 nucleotide band of the molecular weight marker. The cycle number that generated a single band was chosen as the optimal cycle number for PCR amplification of the DNA for that round of selection.

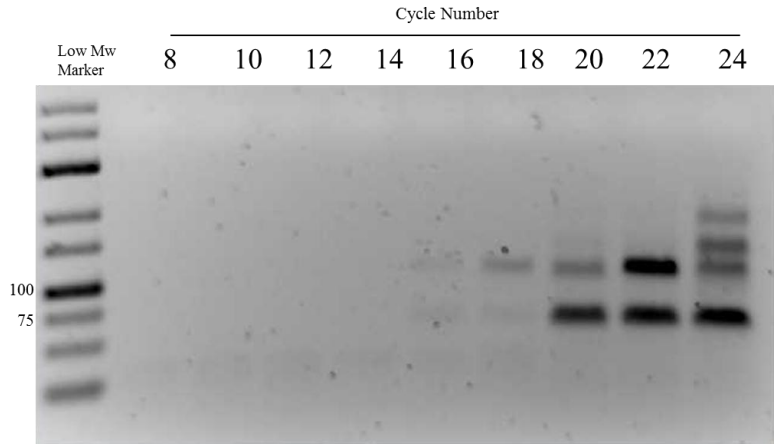

FIGURE 6-5: PILOT PCR TO OPTIMISE CYCLE NUMBER FOR SELEX DNA AMPLIFICATION

PCR amplification of DNA at each round of selection was optimised for cycle number. The band of interest at 100 nucleotides was evident from 16 cycles. The optimal cycle number produced the band of interest without any aberrant bands.

6.2 CONFIRMATION OF NEGATIVE SELECTION BY FLOW CYTOMETRY

The recovered RNA from the HeLa control selection was fluorescently labelled and used in a flow cytometry assay to determine the binding capacity of this RNA to both CD7-HeLa and HeLa cells. This is the RNA recovered from inside the HeLa cells after each round. It is expected that this RNA should not contain CD7 specific aptamers but rather have limited binding to CD7 HeLa cells. The relative fluorescence of binding per round was plotted on a graph and compared between CD7-HeLa and HeLa cells (Figure 6-6). For comparison, the fluorescence was calculated relative to the cell alones control set to 1. The relative fluorescence of the CD7-HeLa cells and un-transfected HeLa cells did not deviate much from the cells alone control. The greatest binding was seen at round two with 25 % increase in fluorescence for the CD7-HeLa cells and a doubling in fluorescence for the HeLa cells. This indicates that the un-transfected HeLa cell internalising aptamers were most likely not internalising through a receptor mediated process. Should the aptamers have used a receptor on the un-transfected HeLa cells, they would have had the same binding affinity to the CD7-HeLa cells. Passive internalisation through membrane turn over at physiological temperature would explain the internalisation at a constant level regardless of enrichment for the CD7 receptor.

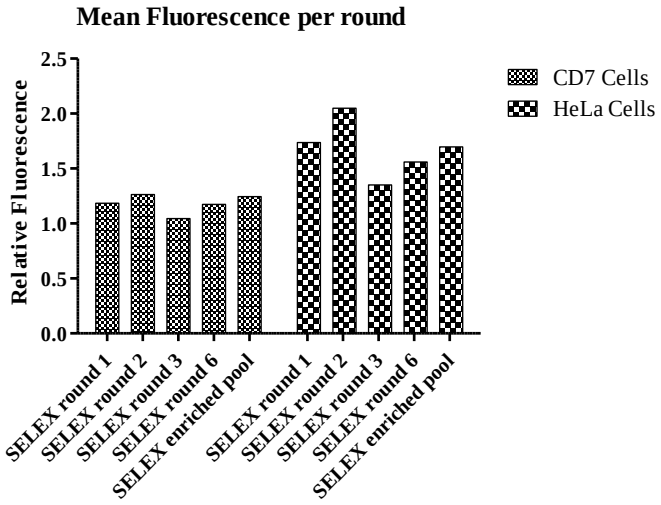

FIGURE 6-6: CONFIRMATION OF CONTROL HELA SELECTION USING FLOW CYTOMETRY

RNA recovered from the HeLa control selection was fluorescently labeled and assessed for binding ability to CD7-HeLa and HeLa cells. Relative fluorescence was calculated relative to the cell alone controls.

6.3 STATISTICAL INFORMATION FOR THE PHYLOGENETIC TREE OF APTAMER SEQUENCES

Between	And	Length	Approx. Confidence Limits
6	CSIR_3.1	0.19800	(0.06798, 0.32805) **
6	3	0.01987	(zero, 0.08946)
3	4	0.14064	(0.01578, 0.26562) **
4	2	0.02294	(zero, 0.13474)
2	CSIR_3.3	0.11211	(zero, 0.22639) **
2	46	1.26912	(0.58129, 1.95621) **
46	CSIR_3.48	0.82179	(0.42433, 1.21867) **
46	CSIR_3.4	0.00371	(zero, 0.29757)
4	28	0.18626	(0.03520, 0.33737) **
28	47	0.12377	(zero, 0.25011) **
47	CSIR_3.49	0.29515	(0.12680, 0.46342) **
47	CSIR_3.6	0.14374	(0.01763, 0.26985) **
28	20	0.10186	(zero, 0.23360) *
20	CSIR_3.22	0.14723	(0.01652, 0.27782) **
20	38	0.20422	(0.05399, 0.35457) **
38	CSIR_3.40	0.22175	(0.07826, 0.36513) **
38	CSIR_3.30	0.18229	(0.04577, 0.31887) **
3	17	0.13602	(0.01538, 0.25670) **
17	44	0.11407	(zero, 0.23054) **
44	CSIR_3.46	0.25559	(0.10093, 0.41032) **
44	CSIR_3.19	0.18549	(0.05023, 0.32066) **
17	40	0.06164	(zero, 0.16699)
40	CSIR_3.42	0.23707	(0.09322, 0.38098) **
40	7	0.09291	(0.00118, 0.18472) **
7	CSIR_3.32	0.11641	(0.01807, 0.21467) **

Between	And	Length	Approx. Confidence Limits
7	30	0.01617	(zero, 0.11932)
30	10	0.12809	(0.01199, 0.24409) **
10	41	0.05953	(zero, 0.15408)
41	36	0.13527	(0.01860, 0.25198) **
36	CSIR_3.38	0.26794	(0.11332, 0.42253) **
36	CSIR_3.8	0.18012	(0.05284, 0.30739) **
41	50	0.03487	(zero, 0.11239)
50	CSIR_3.52	0.30871	(0.15053, 0.46681) **
50	CSIR_3.43	0.15323	(0.04049, 0.26603) **
10	23	0.09986	(zero, 0.20674) **
23	9	0.06353	(zero, 0.16445)
9	33	0.10684	(zero, 0.23563) **
33	CSIR_3.35	0.26432	(0.02753, 0.50110) **
33	14	0.13083	(zero, 0.26273) **
14	31	0.07340	(zero, 0.18098) *
31	CSIR_3.33	0.26439	(0.10934, 0.41941) **
31	24	0.09601	(zero, 0.21123) *
24	49	0.18996	(0.04084, 0.33915) **
49	CSIR_3.51	0.26966	(0.09347, 0.44587) **
49	25	0.13224	(zero, 0.26684) **
25	CSIR_2.27	0.30020	(0.12734, 0.47316) **
25	CSIR_3.16	0.18416	(0.04014, 0.32816) **
24	CSIR_2.26	0.13713	(0.00929, 0.26493) **
14	32	0.08998	(zero, 0.20190) *
32	15	0.00006	(zero, 0.09658)
15	CSIR_3.34	0.34074	(0.16595, 0.51554) **
15	CSIR_3.17	0.23645	(0.08900, 0.38381) **
32	CSIR_3.11	0.39258	(0.19829, 0.58693) **

Between	And	Length	Approx. Confidence Limits
9	CSIR_3.25	0.22515	(0.08128, 0.36899) **
23	51	0.07372	(zero, 0.17100) *
51	CSIR_3.53	0.20744	(0.07453, 0.34032) **
51	8	0.14193	(0.02111, 0.26279) **
8	CSIR_3.9	0.05903	(zero, 0.14986)
8	39	0.08567	(zero, 0.21260)
39	37	0.20632	(zero, 0.45129) *
37	CSIR_3.39	0.73270	(0.33340, 1.13209) **
37	27	0.23797	(zero, 0.49491) **
27	CSIR_3.29	0.38906	(0.14356, 0.63455) **
27	19	0.28878	(0.06305, 0.51460) **
19	18	0.01169	(zero, 0.14159)
18	22	0.19836	(0.03807, 0.35854) **
22	CSIR_3.24	0.37348	(0.15867, 0.58838) **
22	CSIR_3.20	0.34089	(0.13352, 0.54818) **
18	CSIR_3.10	0.23699	(0.09046, 0.38345) **
19	CSIR_3.21	0.13558	(0.02151, 0.24957) **
39	CSIR_3.41	0.36582	(0.17289, 0.55886) **
30	CSIR_3.12	0.75308	(0.40776, 1.09841) **
6	11	0.14924	(0.02318, 0.27538) **
11	13	0.22169	(0.06391, 0.37953) **
13	CSIR_3.15	0.19010	(0.05407, 0.32615) **
13	29	0.06642	(zero, 0.17747)
29	34	0.14186	(zero, 0.28502) **
34	CSIR_3.36	0.90170	(0.46564, 1.33766) **
34	12	0.07413	(zero, 0.19575)
12	CSIR_3.5	0.20339	(0.06537, 0.34130) **
12	CSIR_3.14	0.21863	(0.07518, 0.36214) **

Between	And	Length	Approx. Confidence Limits
29	1	0.22527	(0.07673, 0.37383) **
1	5	0.73144	(0.33218, 1.13070) **
5	CSIR_3.7	0.53913	(0.19784, 0.88041) **
5	42	0.17098	(zero, 0.44260)
42	26	0.18311	(0.00957, 0.35667) **
26	16	0.09914	(zero, 0.21546) **
16	45	0.18408	(0.02212, 0.34611) **
45	48	0.09085	(zero, 0.23429)
48	CSIR_3.50	0.41757	(0.21291, 0.62215) **
48	CSIR_3.47	0.11337	(zero, 0.23291) **
45	CSIR_3.18	0.42822	(0.14509, 0.71142) **
16	CSIR_3.2	0.18267	(0.03833, 0.32700) **
26	21	0.04481	(zero, 0.13693)
21	35	0.16346	(0.01807, 0.30894) **
35	CSIR_3.37	0.47639	(0.24180, 0.71106) **
35	43	0.15550	(0.01275, 0.29822) **
43	CSIR_3.45	0.00006	(zero, infinity)
43	CSIR_3.23	0.00006	(zero, infinity)
21	CSIR_3.28	0.22091	(0.07456, 0.36736) **
42	CSIR_3.44	0.23696	(0.05994, 0.41389) **
1	CSIR_3.31	0.00006	(zero, 0.10286)
11	CSIR_3.13	0.15948	(0.02924, 0.28962) **

* = significantly positive, P < 0.05

** = significantly positive, P < 0.01

6.4 CHARACTERISATION OF ENDOGENOUS SURFACE EXPRESSION OF CD7 RECEPTOR ON T AND B LYMPHOCYTE CELL LINES

As the CD7 receptor is a T cell specific receptor, the use of T cells as target cells for the selection of CD7 specific aptamers, would be preferable. However, this was not immediately possible as the surface expression of CD7 on commercial cell lines is not well characterised. Three lymphoblast cell lines were characterised for the CD7 receptor expression level to determine if a lymphocyte cell line could be used for the selection of CD7 specific aptamers.

6.4.1 METHODS

6.4.1.1 MICROSCOPY ANALYSIS

Jurkat, JeKo-1 and CEM cells were grown to a density of 1×10^6 cells/ ml in complete media. A sample from each cell type was removed and cells were pelleted at 200 × *g* for five minutes. Cells were re-suspended in 100 µl PBS supplemented with 0.5 µg PE/Cy5 anti-CD7 antibody and incubated at room temperature for 40 minutes. Cells were then pelleted as before and washed three times with 200 µl PBS. Once washed, the cells were stained with 3 µM 4',6-diamidino-2-phenylindole (DAPI) (Invitrogen, CA, USA) for ten minutes at room temperature. A 10 µl sample from each cell preparation was spotted onto a slide and covered with a cover slip for imaging. Slides were imaged under a 40 × objective using an Olympus AX70 fluorescence microscope with Image-ProPlus V6.3.542 and processed using ImageJ software V1.45.

6.4.1.2 FLOW CYTOMETRY ANALYSIS

Jurkat, JeKo-1 and CEM cells were grown to a density of 1×10^6 cells/ ml in complete media. Two samples from each cell type were removed and cells were pelleted at 200 × *g* for five minutes. Cells were split then re-suspended in 80 µl binding buffer (10 % foetal calf serum in 1 × PBS). A sample of each cell type was incubated with 0.5 µg PE/Cy5 anti-CD7 antibody at room temperature for 40 minutes. A cell alone control was included for each cell type. Cells were pelleted as before and washed three times with 200 µl binding buffer. After washing, cells were re-suspended in 400 µl PBS and analysed on a CyAn Flow cytometer (Beckman Coulter Inc., CA, USA) and the results analysed using FlowJo version 7.6.5 (Tree Star, Inc., OR, USA). For each run, 50 000 events were counted and cells gated according to forward and side scatter profiles. Antibody bound cells were compared to cells alone and the

percentage cells stained was determined. The mean and median fluorescence was calculated for cells alone as well as those stained with the anti-CD7 antibody (PE/Cy5). The average of three independent experiments was used to validate the surface expression of CD7 receptor.

6.4.2 RESULTS AND DISCUSSION

A T lymphocyte cell line for the selection of CD7 specific aptamers was preferable as the downstream application for the aptamers is for pharmacological targeting of immune cells. To identify if a commercial T lymphocyte cell line could be used in the selection, T lymphoblast cells, CEM and Jurkat, and B lymphoblasts, JeKo, were analysed for endogenous CD7 receptor expression. This was achieved using fluorescence microscopy and flow cytometry using a PE/Cy5 labelled anti-CD7 monoclonal antibody. The cell lines used were: CCRF-CEM, a T lymphoblast cell line derived from peripheral blood buffy coat of a 4 year old Caucasian female with acute lymphoblastic leukaemia (ATCC #CCL-119); Jurkat, a T lymphoblast derived from peripheral blood buffy coat of a 14 year old male with acute lymphoblastic leukaemia (ATCC #TIB-152) and JeKo-1, B lymphoblast derived from the peripheral blood mononuclear cells of a 78 year old female with a large cell variant of mantel cell lymphoma showing leukemic conversion (ATCC #CRL-3006).

It was expected that the T lymphocyte cell lines would express CD7 while the B cell lymphoma cell line would not. However, microscopy screening of the three cell lines showed a high level of receptor expression on CEM, JeKo-1 and Jurkat cells (Figure 6-7). This was later confirmed by flow cytometry. The flow cytometry analysis was done in three independent assays. The percentage cells stained was averaged from the three assays and resulting in CEM, Jurkat and JeKo-1 cells showing 98.4 %, 98.4 % and 99.1 % staining respectively (Figure 6-8). As the expression level appeared to be similar between the two cell types, a recombinant cell line was used in the selection. The recombinant cell line would allow for un-transfected cells to be used as a negative control cell line.

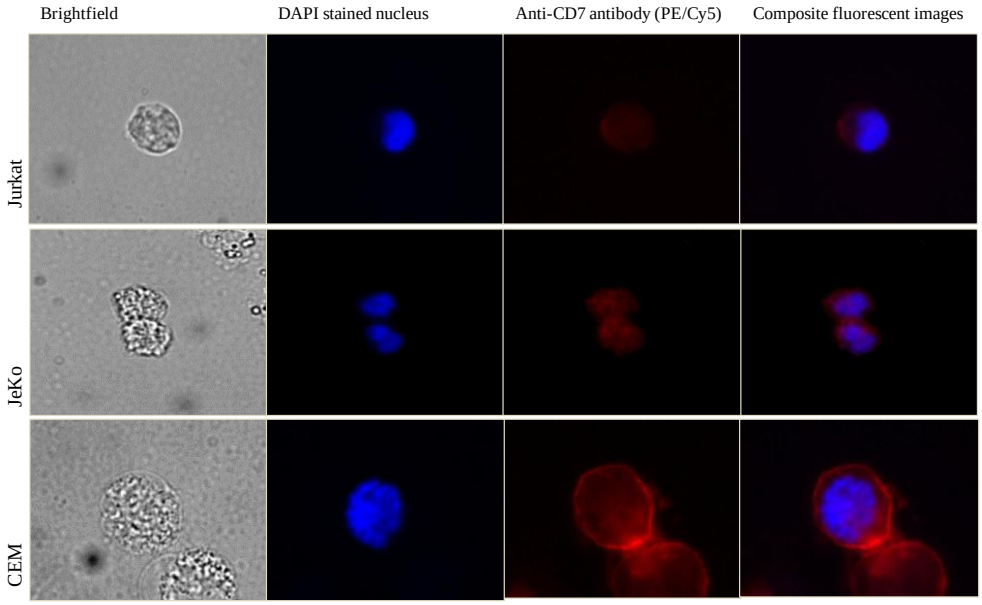

FIGURE 6-7: CONFIRMATION OF CELL SURFACE EXPRESSION OF CD7 RECEPTOR ON LYMPHOCYTES

CEM, Jurkat and JeKo cells were incubated with PE/Cy5 anti-CD7 monoclonal antibody and viewed through a fluorescent microscope at 40 × magnification. Bright field images for each cell are shown in the left most panel followed by the DAPI stained nuclei, the PE/Cy5 anti-CD7 antibody and finally the composite of fluorescent images on the right most panel.

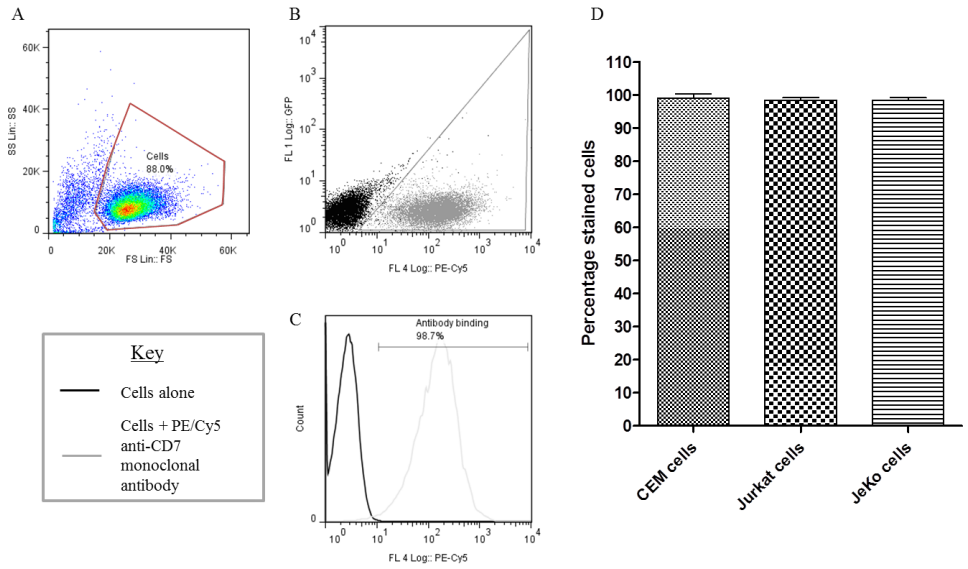

FIGURE 6-8: FLOW CYTOMETRY CONFIRMATION OF SURFACE CD7 RECEPTOR EXPRESSION

A. **Whole cell population gated according to forward and side scatter profiles. B. Gated cells plotted according to PE/Cy5 fluorescence and GFP auto-fluorescence. Cells alone are shown in black while the grey indicates PE/Cy5 anti-CD7 monoclonal antibody stained cells. C. Histogram representation of the data shown in panel B. Unstained cells are in black and PE/Cy5 anti-CD7 monoclonal antibody stained cells are shown in grey. D. Percentage stained cells from three independent antibody binding (n =3).**

6.5 SURFACE PLASMON RESONANCE ANALYSIS OF APTAMER – CD7 PROTEIN INTERACTION

To determine the binding capacity of each aptamer to recombinant human CD7 protein a BIAcore 3000 (BIAcore AB Inc., GE Healthcare, Buckinghamshire, UK) surface plasmon resonance (SPR) assay was used. SPR allows for a highly sensitive real time analysis of molecule interactions.

6.5.1 METHODS

6.5.1.1 RECOMBINANT CD7 PROTEIN PREPARATION AND QUANTIFICATION

The extracellular domain of the human CD7 receptor was sourced (#11028-H08H, Sino Biological, China) and was validated for size and concentration in two independent assays. Human recombinant CD7 protein was re-suspended according to manufacturer's instruction in distilled water to an apparent concentration of 250 µg/ ml. To confirm the integrity of the protein, a sample was resolved on a SDS-PAGE with a 12 % acrylamide resolving gel and a 5 % stacking gel. The protein was prepared for electrophoresis by the addition of 2 × SDS sample buffer (62.5 mM Tris pH6.8, 10 % glycerol, 2 % sodium dodecyle sulphate (SDS), 10 % (w/ v) acetic acid and 1:20 2-βmercaptoethanol bromophenol blue) and heating to 95 °C for three minutes. The gel was run at 25 mA in 1 × SDS running buffer (0.3 % (w/v) Tris, 1.44 % (w/ v) glycine and 0.1 % (w/ v) SDS). Once resolved, the gel was transferred to a staining container and stained with Coomasie blue stain (10 % (v/ v) acetic acid, 0.006 % (w/ v) coomasie blue dye) at room temperature for two hours. The gel was then de-stained using 10 % acetic acid at room temperature on a shaker overnight. The gel was then imaged under white light using a Molecular Imager Chemidoc XRS+ Imaging System (BIORAD, CA, USA).

Protein concentration was validated using a bicinchoninic acid (BCA) protein assay kit (Thermo Fisher Scientific Inc., MA, USA) according to manufacturer's instructions. Briefly, a bovine serum albumen (BSA) concentration series was prepared (25 µg/ ml to 2000 µg/ ml). Using a microplate, 25 µl of each prepared standard, unknown concentration test solution and the blank control was added to the plate. A further 200 µl of working solution (1:1 BCA solution A: BCA solution B, supplied) was added to each well and mixed thoroughly on a shaker for 30 seconds. The plate was covered and incubated at 37 °C for 30

minutes before reading absorbance at 562 nm on a MultiscanGo plate reader (Thermo Fisher Scientific Inc., MA, USA).

6.5.1.2 RECOMBINANT HUMAN CD7 PROTEIN IMMOBILISATION, PH SCOUTING AND REGENERATION OPTIMISATION

In preparation for SPR analysis of aptamer – protein interaction, the pH required for the protein to be immobilised to the chip sensor surface was determined. At a low pH, the protein is electrostatically attracted to the sensor surface and the highest pH at which the protein attaches is chosen for subsequent amine coupling. In brief, 50 µg/ ml of recombinant CD7 protein was prepared in 10 mM NaAc at different pH (3.5, 4, 4.5 and 5). The protein was injected over the un-activated sensor chip at a flow rate of 10 µl per minute. The electrostatically bound protein was washed off with of 1 M ethanolamine-HCl before and after injections. Three immobilisation pH conditions were assessed for their stability by regenerating with the wash buffer (20 mM NaOH) and checking for a reduction in bound protein. Recombinant CD7 protein (50 µg/ ml) was prepared in 10 mM NaAc at pH 3.5, pH 4 and pH 5. Five micrograms of the CD7 recombinant protein was injected over a CM5 sensor chip activated by injection of 0.2 M 1-Ethyl-3-(3-dimethylaminopropyl) Carbodiimide hydrochloride (EDC) and 0.5 M N-Hydroxysuccinimide (NHS) for 10 minutes at a flow rate of 10 µl per minute. After protein immobilisation, the remaining activated carboxymethyl groups were blocked with 1 M ethanolamine-HCl for seven minutes. Non-specifically bound protein was removed with 10 mM Glycine-HCl injected for three minutes. An anti-CD7 monoclonal antibody (CD7 (H-7): sc-28332; Santa Cruz Biotechnology, Inc., CA, USA) was bound to the protein and removed using a two minute wash with 20 mM NaOH. The resultant sensorgrams were analysed using BIAevaluation 4.1 software (BIAcore AB Inc., GE Healthcare, Buckinghamshire, UK).

6.5.1.3 APTAMER BINDING ANALYSIS TO RECOMBINANT HUMAN CD7 PROTEIN INTERACTION

Research grade CM5 chips, EDC (1-Ethyl-3-(3-dimethylaminopropyl) Carbodiimide hydrochloride), NHS (N-Hydroxysuccinimide), Ethanolamine and HBS-N running buffer used in all the SPR experiments were obtained from BIAcore AB Inc., GE Healthcare, Buckinghamshire, UK. For the preparation of CM5 chips, 1 × HBS-N (10 mM Hepes, 150 mM NaCl, pH 7.4) running buffer was injected at a flow rate of 10 µl per minute. CM5 sensor chips were activated with 0.2 M EDC and 0.5 M NHS for ten minutes at a flow rate of

10 µl per minute. By amine coupling chemistry 5 µg recombinant human CD7 protein (buffer exchanged in 10 mM NaAc pH 5) was immobilised to the experimental flow cell. A flow cell with no protein bound was included as a negative control allowing for the deduction of non-specific background binding during analysis. After protein immobilisation, the remaining activated carboxymethyl groups were blocked with 1 M ethanolamine for seven minutes. Non-specifically bound protein was removed with 10 mM glycine-HCl injected for three minutes. Aptamers were refolded as previously described and prepared to a concentration of 100 nM in 1 × HMCKN. The aptamers were injected over the prepared sensor chip at a flow rate of 5 µl per minute with a contact time of four minutes. The bound aptamer was dissociated with a two minute 20 mM NaOH wash. The resultant sensorgrams were analysed using BIAevaluation 4.1 software (BIAcore AB Inc., GE Healthcare, Buckinghamshire, UK).

6.5.2 RESULTS

6.5.2.1 HUMAN RECOMBINANT CD7 PROTEIN PREPARATION AND QUANTIFICATION

Aptamers were selected against a surface expressed human CD7 receptor. The aptamer sequences were analysed and individual clones identified. Aptamer binding specificity and affinity to the human CD7 receptor will be covered in this chapter. The initial screening method identified was to use SPR to screen aptamer clones rapidly for binding to the human CD7 recombinant protein. This section covers the protein quality assurance steps before SPR, the aptamer quality assurance steps and the optimisation of the protein for SPR analysis.

The recombinant CD7 protein was sourced from Sino Biological and was received lyophilized. The lyophilized protein was re-suspended in water as per the manufacturer's instructions. Before aptamer binding was assessed using the BIAcore 3000, the protein was resolved on a denaturing polyacrylamide gel to verify the correct size and was quantified using a BCA Assay. Under reducing conditions in a SDS-PAGE (Sodium dodecyl sulphate polyacrylamide gel electrophoresis) the apparent molecular mass of the recombinant protein is 30 – 35 kDa due to glycosylation. This corresponded with the SDS-PAGE (Figure 6-9) in which a single clear band was seen that indicated that the protein was not degraded. The protein concentration was then verified before it was used in subsequent experiments.

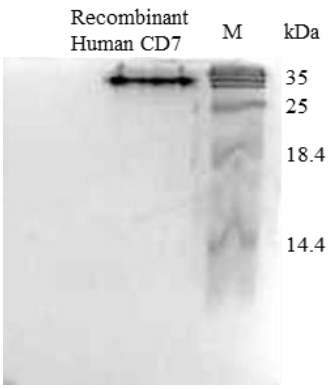

FIGURE 6-9: RECOMBINANT HUMAN CD7 PROTEIN SIZE VERIFICATION

Recombinant human CD7 was resolved in a SDS-PAGE under reducing conditions. The expected apparent size was 30-35 kDa which corresponded with the result.

The protein was quantified using a BCA Protein Assay Kit (Thermo Scientific, USA), a colorimetric assay (Figure 6-10 A) where a standard curve was generated using known concentrations of bovine serum albumin (BSA) and the concentration of the recombinant CD7 protein was extrapolated from the standard curve ($R^2 = 0.99$) (Figure 6-10 B). The stock concentration was calculated to be 375 µg/ ml and this was used for all subsequent calculations. The protein was thus determined to be fit for binding analysis using the SPR and the protein binding conditions were then optimised. The RNA aptamers used in all experiments were produced by PCR and *in vitro* transcription. PCR was used to amplify the aptamer DNA before transcribing the aptamer to RNA for use. Aptamer DNA and RNA were separated by gel electrophoresis to determine the quality and ensure the fragment generated is of the correct length (Figure 6-11).

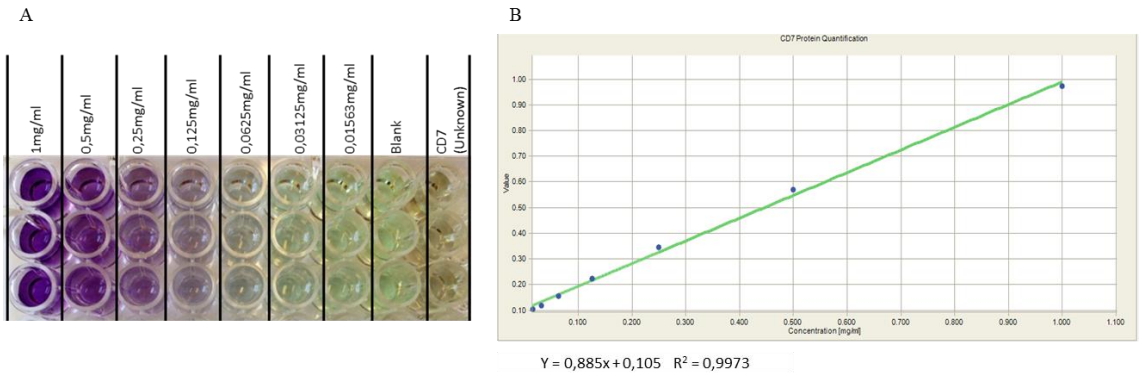

FIGURE 6-10: RECOMBINANT HUMAN CD7 PROTEIN QUANTIFICATION

Recombinant human CD7 was sourced from Sino Biological (China) and reconstituted in water according to manufacturer's recommendations. A. BCA colorimetric assay was performed to verify the protein concentration. Known concentration standards of BSA protein were used to construct a standard curve B. Standard curve generated from the dilution of standards ($R^2 = 0.99$).

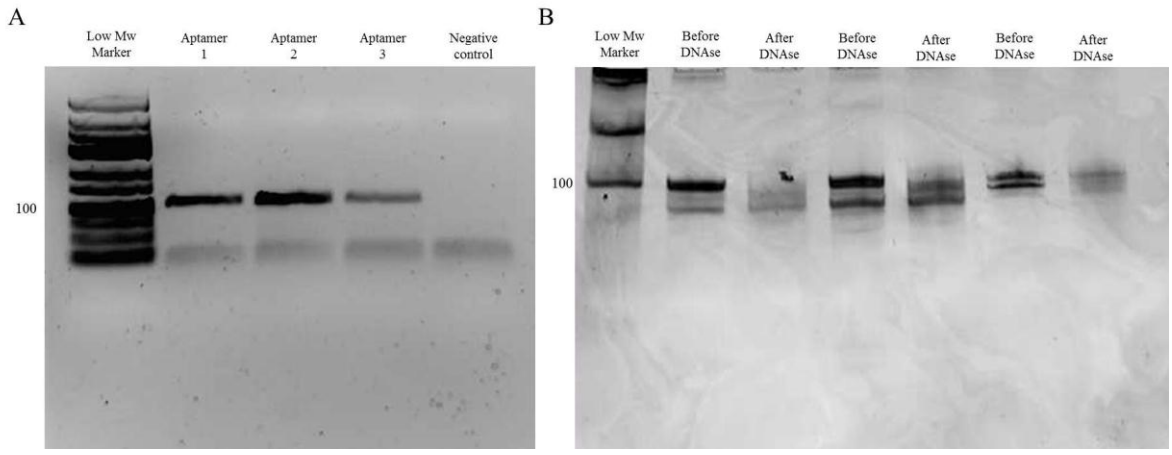

FIGURE 6-11: PRODUCTION OF CD7 APTAMERS

A. **Aptamers are amplified by PCR before transcribing to their active RNA. Aptamers (90bp in size) can be seen aligned with the molecular marker at 100 nucleotides. B. Aptamers amplified by PCR are transcribed to their active RNA. Fractions before DNAse (BD) and After DNAse (AD) are separated on an 8M denaturing polyacrylamide gel. Multiple bands in the BD indicate DNA and RNA molecules**

6.5.2.2 OPTIMISATION OF PROTEIN IMMOBILISATION

Two factors are essential for adequate amine coupling of the ligand to the sensor surface and binding analysis are; 1. efficient amine coupling at the highest pH showing electrostatic interaction of the protein with an un-modified sensor chip and 2. stable attachment of the ligand to the sensor surface after rounds of binding and washing. The optimal pH to immobilise the recombinant CD7 protein by amine coupling to the CM5 chip was identified by pH scouting. An un-activated and un-modified sensor chip is exposed to the protein buffer exchanged in sodium-acetate to different pH (3.5, 4, 4.5 and 5) and the protein association is observed. Under low ionic strength and with the pH lower than the isoelectric point of the protein, the protein is electrostatically attracted to the chip surface. The electrostatic interaction is the greatest at the lowest pH however; a higher pH is required for efficient amine coupling. The highest interaction was seen at pH 3.5; however, pH 4.5 and pH 5 were more appropriate for efficient amine coupling (Figure 6-12).

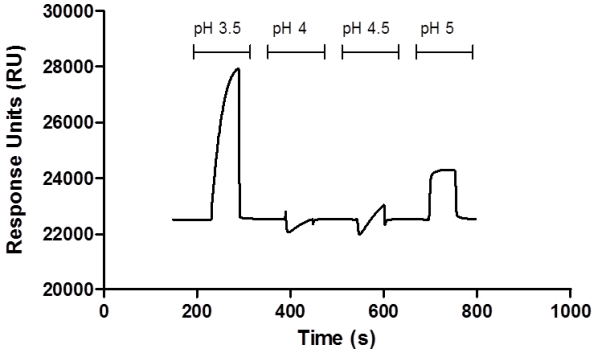

FIGURE 6-12: RECOMBINANT HUMAN CD7 PROTEIN IMMOBILISATION PH SCOUTING

CD7 protein buffer exchanged to different pH values (3.5 to 5) was injected over an un-modified and un-activated sensor chip. The electrostatic interaction of the protein with the chip surface at different pH was compared. The greatest interaction was seen for pH 3.5, pH 4.5 and pH 5.

To ensure the most stable interaction was achieved, the three pH identified with the highest electrostatic interaction were characterised for binding stability after washing. The protein was immobilised to a sensor chip at pH 3.5, pH 4.5 and pH 5. The protein bound at pH 3.5 showed the highest response units of immobilised protein, 5136 RU, followed by pH 5 with 4812 RU and pH 4.5 with 3600 RU. The anti-CD7 monoclonal antibody was bound to the immobilised protein at all three pH and the highest response units of binding was for protein immobilised at pH 5 (Figure 6-13). The binding response units are determined by subtracting the non-specific binding response units to a flow cell without protein. The binding of the monoclonal antibody to the protein was under 100 response units for all protein pH tested.

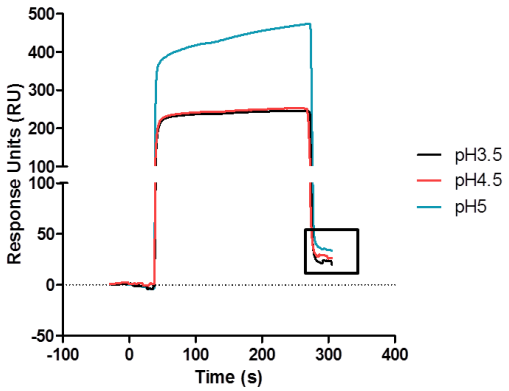

FIGURE 6-13: ANTI-CD7 ANTIBODY BINDING RECOMBINANT HUMAN CD7 PROTEIN

Anti-CD7 monoclonal antibody was bound to recombinant CD7 protein immobilised at different pH. The association of the antibody to the chip was greatest for the protein immobilised at pH 5 and the final binding response units was higher at this pH. Binding response units were determined by subtracting non-specific response units of binding to an empty flow cell.

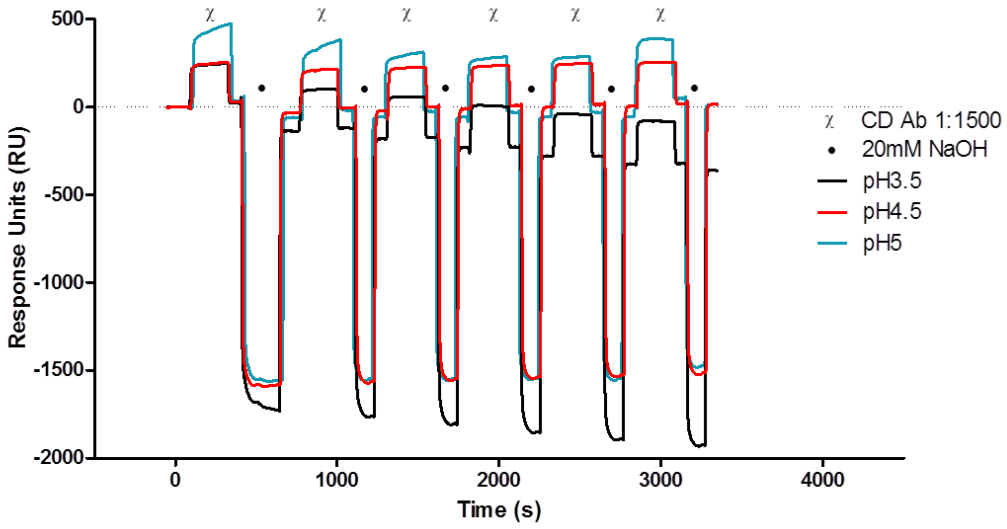

FIGURE 6-14: RECOMBINANT HUMAN CD7 PROTEIN IMMOBILISATION STABILITY TEST

Recombinant CD7 protein was immobilised to the sensor chip at pH 3, pH 4.5 and pH 5. Anti-CD7 antibody was bound to the chip a number of times after which the sensor chip was regenerated with a 20mM Sodium Hydroxide (NaOH). Protein immobilised at pH 4.5 and pH 5 remained stably bound after 6 rounds of binding and regeneration. Protein immobilised at pH 3.5 started to dissociate after a single regeneration

To remove the bound antibody, the sensor chip was washed with 20 mM NaOH. Although immobilisation of the protein was the greatest at pH 3.5, the interaction was not stable and the protein was removed with every wash cycle (Figure 6-14). Protein immobilised at pH 4.5 and pH 5 were the most stable as the protein was not removed with rounds of antibody binding and washing (Figure 6-14). The protein was immobilised at pH 5 for subsequent aptamer binding analyses but the response units for aptamer binding were too low to make any conclusions of protein binding.

6.5.2.3 APTAMER BINDING TO RECOMBINANT HUMAN CD7 RECEPTOR

Aptamers were assessed for their ability to bind recombinant CD7 protein by surface plasmon resonance on the BIAcore 3000. The recombinant protein was sourced and re-suspended according to the manufacturer's instructions. The protein was immobilised on the sensor chip following the standard protocol (Figure 6-15). The aptamers were injected over the protein at a final concentration of 100 nM in 1 × HMCKN binding buffer and a contact time of 200 seconds (Figure 6-16 A). Buffer alone was injected over the protein and the buffer response was subtracted from the injected aptamer response (Figure 6-16 B). Most aptamers tested bound more to the protein than the empty flow cell however, binding was very low for all but one aptamer (CSIR 3.23) (Figure 6-17). Aptamer binding response units were too low to be

significant and so BIAcore binding was not used to select aptamers for further characterisation.

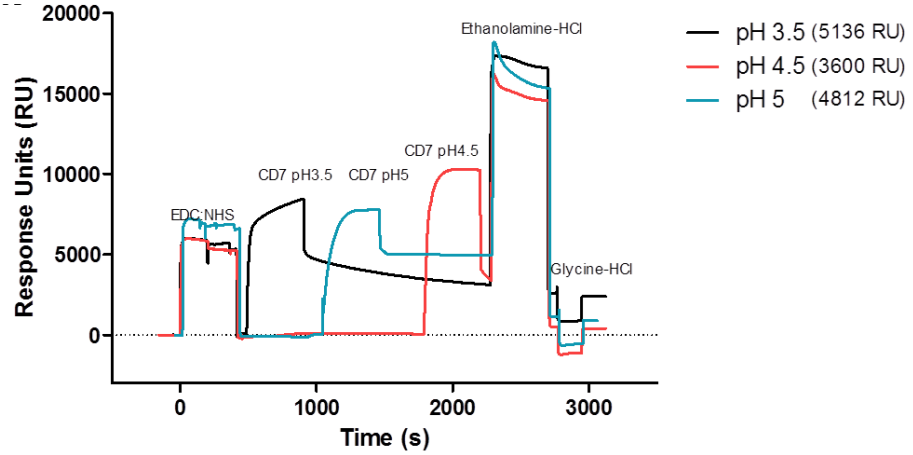

FIGURE 6-15: IMMOBILISATION OF RECOMBINANT CD7 PROTEIN

Recombinant CD7 protein was buffer exchanged at different pH to test binding stability of the protein to the sensor chip after rounds of regeneration. The chip surface was activated with EDC: NHS after which CD7 protein was bound to three different flow cells. Remaining active sites were blocked using Ethanolamine-HCl and weakly bound protein was removed with a glycine-HCl wash.

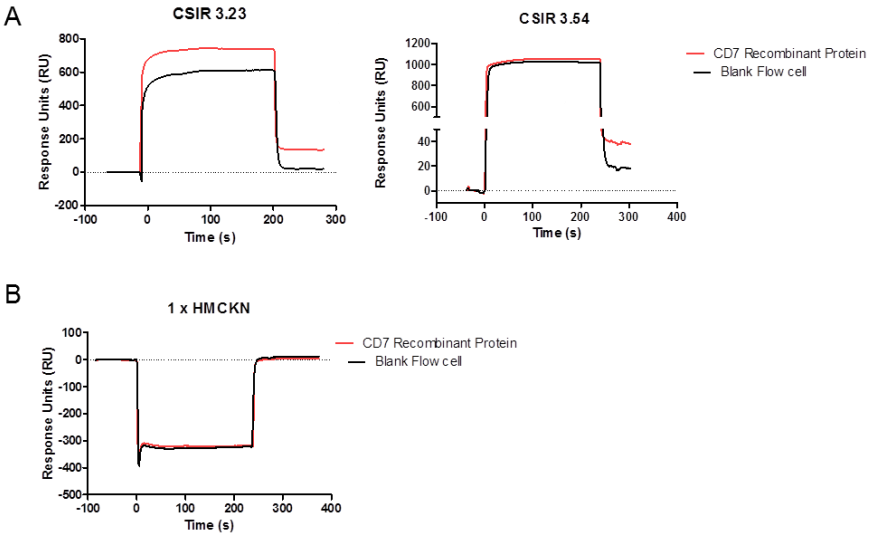

FIGURE 6-16: ANTI-CD7 APTAMER BINDING RECOMBINANT PROTEIN

A. Aptamer CSIR 3.23 and CSIR 3.54 binding to the immobilised recombinant protein and the empty flow cell. B. Binding response of the buffer alone to the immobilised CD7 protein and the empty flow cell

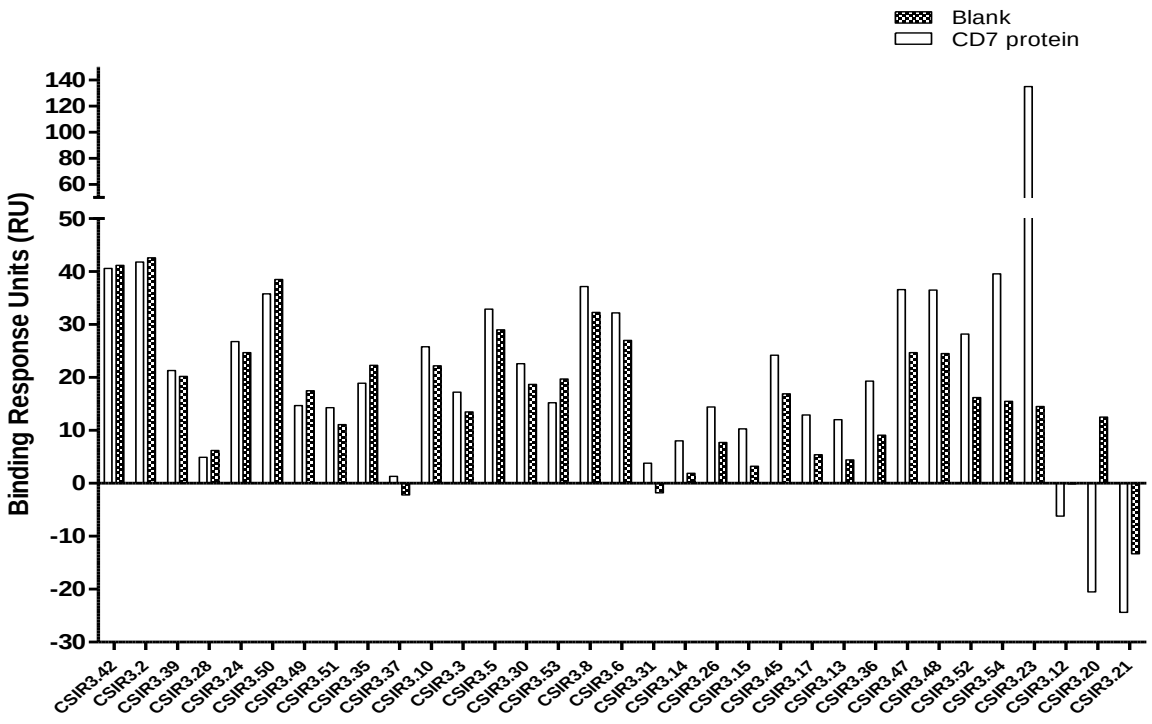

FIGURE 6-17: APTAMER BINDING RESPONSE UNITS TO RECOMBINANT CD7 PROTEIN

Aptamers were injected over the immobilised CD7 protein and an empty flow cell. Binding response units were determined by subtracting the binding response of the buffer alone. Aptamer binding response was similar between the protein and the empty flow cell for most aptamers tested.

6.5.3 DISCUSSION

Twenty-seven anti-CD7 aptamers were characterised for binding specificity to the CD7 receptor making use of various experimental methods. Surface plasmon resonance was used to assess aptamer binding to the recombinant protein. This method failed to produce valuable data as the binding capacity of the aptamers to the recombinant human CD7 protein was very low. The recombinant human CD7 protein consisted of 166 amino acids with a predicted mass of 18 kDa and contained only the extracellular domain of the receptor, not the entire receptor protein. As such, the conformation of the extracellular domain of the recombinant protein may not match that of the fully expressed surface receptor extracellular domain. As the response units of binding were very low, a meaningful contribution to the analysis could not be made by the BIAcore data. As such, BIAcore analysis was not used for the selection of aptamers for further characterisation.

6.6 NEGATIVE CONTROL FOR APTAMER ASSOCIATION AT 24 HOUR INCUBATION

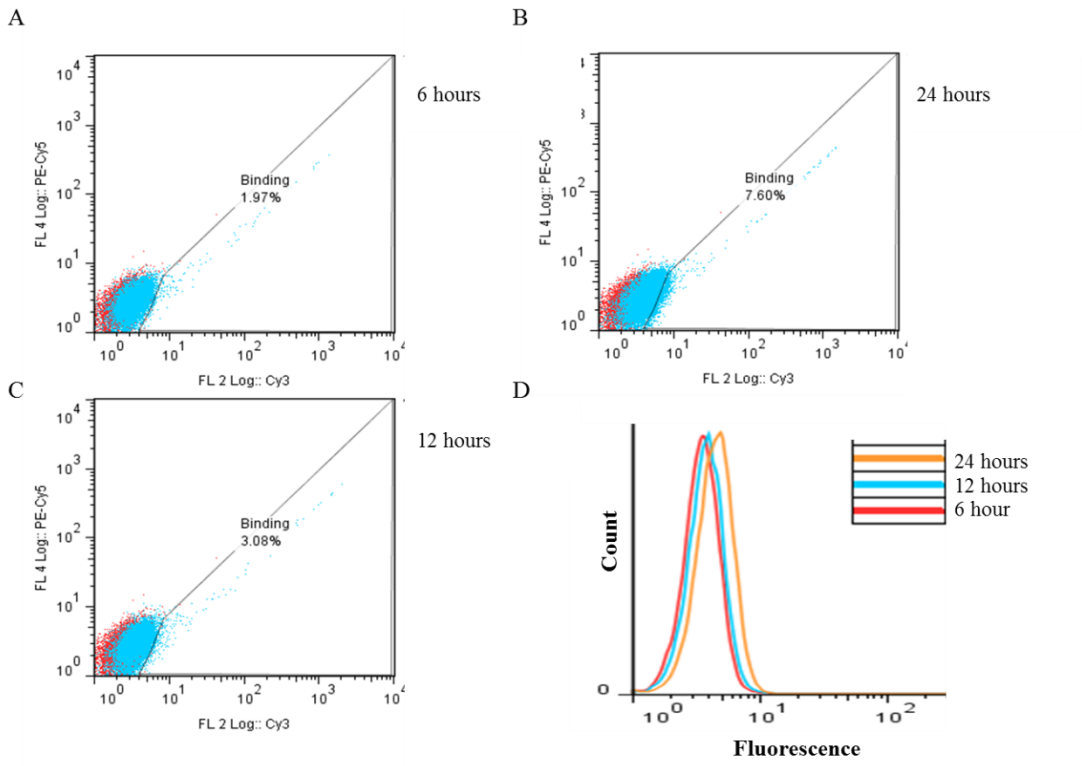

FIGURE 6-18: TIME COURSE ASSOCIATION OF APTAMER CSIR 3.31

Aptamer CSIR 3.31 was incubated at a 400 nM final concentration with Jurkat cells for variable times (6 hours, 12 hours and 24 hours). A: Dot plot of events at 6 hour incubation plotted against Cy3 fluorescence (X axis) and PE/Cy5 auto-fluorescence (Y axis). Binding gate was taken from the right of unstained cells. B: Dot plot of events at 24 hour incubation plotted against Cy3 fluorescence (X axis) and PE/Cy5 auto-fluorescence (Y axis). Binding gate was taken from the right of unstained cells. C: Dot plot of events at 12 hour incubation plotted against Cy3 fluorescence (X axis) and PE/Cy5 auto-fluorescence (Y axis). Binding gate was taken from the right of unstained cells. D: Histogram of aptamer binding after different incubation times.

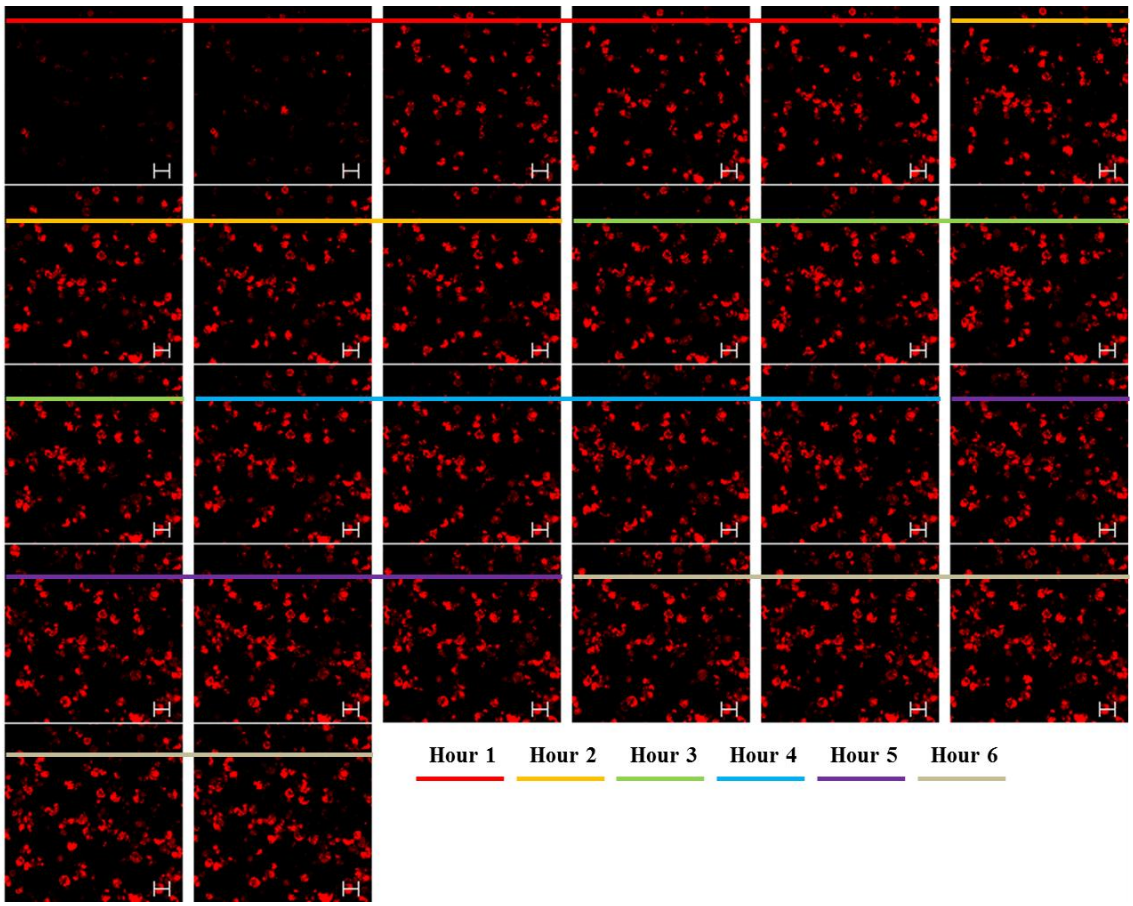

FIGURE 6-19: APTAMER CSIR 3.14 TIME COURSE INTERNALISATION

Aptamer CSIR 3.14 was added to Jurkat cells at a final concentration of 400 nM and imaged over a 6 hour period at 15 minute intervals. Aptamer can be seen as red fluorescence and time intervals are represented by coloured lines.

Chapter 7. REFERENCES

Agrawal, S., J. Temsamani, et al. (1991). "Pharmacokinetics, biodistribution, and stability of oligodeoxynucleotide phosphorothioates in mice." Proc Natl Acad Sci U S A **88**(17): 7595-7599.

Andreola, M., Pileur, F., Calmels, C., Ventura, M., Tarrago-Litvak, L., Toulme, J., and Litvak, S. (2001). "DNA aptamers selected against the HIV-1 RNAse H display in vitro antiviral activity." Biochemistry **40**: 10087-10094.

Arraiano, C. M., A. Barbas, et al. (2008). Chapter 8 Characterizing Ribonucleases In Vitro: Examples of Synergies between Biochemical and Structural Analysis. Methods in Enzymology. E. M. Lynne and M. A. Cecilia, Academic Press. **Volume 447:** 131-160.

Bagalkot, V., L. Zhang, et al. (2007). "Quantum Dot−Aptamer Conjugates for Synchronous Cancer Imaging, Therapy, and Sensing of Drug Delivery Based on Bi-Fluorescence Resonance Energy Transfer." Nano Letters **7**(10): 3065-3070.

Baldrich, E., A. Restrepo, et al. (2004). "Aptasensor development: elucidation of critical parameters for optimal aptamer performance." Anal Chem **76**(23): 7053-7063.

Balogh, Z., G. Lautner, et al. (2010). "Selection and versatile application of virus-specific aptamers." The FASEB Journal **24**(11): 4187-4195.

Baxter, J. D., Schapiro, J.M., Boucher, C.A.B., Kohlbrenner, V.M., Hall, D.B., Scherer, J.R., and Mayers D.L. (2006). "Genotypic Changes in Human Immunodeficiency Virus Type 1 Protease Associated with Reduced Susceptibility and Virologic Response to the Protease Inhibitor Tipranavir." Journal of Virology **80**(21): 10794-10801.

Berezovski, M. V., Lechmann, M., Musheev, M.U., Mak, T.W., and Krylov, S.N. (2008). "Aptamer-Facilitated Biomarker Discovery (AptaBiD)." American Chemical Society **130**(9137-9143).

Berezovski, M. V., M. U. Musheev, et al. (2006). "Non-SELEX: selection of aptamers without intermediate amplification of candidate oligonucleotides." Nat Protoc **1**(3): 1359-1369.

Bianchini, M., M. Radrizzani, et al. (2001). "Specific oligobodies against ERK-2 that recognize both the native and the denatured state of the protein." J Immunol Methods **252**(1-2): 191-197.

Bremer, E., D. F. Samplonius, et al. (2005). "Target cell-restricted apoptosis induction of acute leukemic T cells by a recombinant tumor necrosis factor-related apoptosis-inducing ligand fusion protein with specificity for human CD7." Cancer Res **65**(8): 3380-3388.

Bremer, E., B. ten Cate, et al. (2006). "CD7-restricted activation of Fas-mediated apoptosis: a novel therapeutic approach for acute T-cell leukemia." Blood **107**(7): 2863-2870.

Bremmer, E., B. Cate, et al. (2006). "CD7-Restricted Activation of Fas-Mediated Apoptosis: A Novel Therapeutic Approach for Acute T Cell Leukemia." Blood **107**: 2863-2870.

Brunhouse, R. L. (1971). The counter-revolution in Pennsylvania, 1776-1790. New York,, Octagon Books.

Brunhouse, R. L. (1971). Sylvanus G. Morley and the world of the ancient Mayas. Norman,, University of Oklahoma Press.

Burke, D. H. and J. H. Willis (1998). "Recombination, RNA evolution, and bifunctional RNA molecules isolated through chimeric SELEX." RNA **4**(9): 1165-1175.

Burmeister, P. E., S. D. Lewis, et al. (2005). "Direct in vitro selection of a 2'-O-methyl aptamer to VEGF." Chem Biol **12**(1): 25-33.

Cao, Z., R. Tong, et al. (2009). "Reversible cell-specific drug delivery with aptamer-functionalized liposomes." Angew Chem Int Ed Engl **48**(35): 6494-6498.
Cao, Z., R. Tong, et al. (2009). "Reversible Cell-Specific Drug Delivery with Aptamer-Functionalized Liposomes." Angewandte Chemie International Edition **48**(35): 6494-6498.
Carrera, A. C., Rincon, M., Sanchez-Madrid, F., Lopez-Botet, M., and de Landazuri, M.O. (1988). "Triggering of Co-Mitogenic Signals in T Cell Proliferation by Anti-LFA-1 (CD18, CDIIa), LFA-3 and CD7 Monoclonal Antibodies." Journal of Immunology **141**(6): 1919-1924.
Cerchia, L., F. Duconge, et al. (2005). "Neutralizing aptamers from whole-cell SELEX inhibit the RET receptor tyrosine kinase." PLoS Biol **3**(4): e123.
Chan, A. S., J. L. Mobley, et al. (1997). "CD7-mediated regulation of integrin adhesiveness on human T cells involves tyrosine phosphorylation-dependent activation of phosphatidylinositol 3-kinase." J Immunol **159**(2): 934-942.
Chen, C. H., K. R. Dellamaggiore, et al. (2008). "Aptamer-based endocytosis of a lysosomal enzyme." Proc Natl Acad Sci U S A **105**(41): 15908-15913.
Cheng, J., B. A. Teply, et al. (2007). "Formulation of functionalized PLGA–PEG nanoparticles for in vivo targeted drug delivery." Biomaterials **28**(5): 869-876.
Chenna, V., C. Hu, et al. (2012). "A polymeric nanoparticle encapsulated small-molecule inhibitor of Hedgehog signaling (NanoHHI) bypasses secondary mutational resistance to Smoothened antagonists." Mol Cancer Ther **11**(1): 165-173.
Cho, M., Y. Xiao, et al. (2010). "Quantitative selection of DNA aptamers through microfluidic selection and high-throughput sequencing." Proc Natl Acad Sci U S A **107**(35): 15373-15378.
Chu, T. C., J. W. Marks, et al. (2006). "Aptamer:Toxin Conjugates that Specifically Target Prostate Tumor Cells." Cancer Research **66**(12): 5989-5992.
Chu, T. C., F. Shieh, et al. (2006). "Labeling tumor cells with fluorescent nanocrystal–aptamer bioconjugates." Biosensors and Bioelectronics **21**(10): 1859-1866.
Chu, T. C., K. Y. Twu, et al. (2006). "Aptamer mediated siRNA delivery." Nucleic Acids Res **34**(10): e73.
Chushak, Y. and M. O. Stone (2009). "In silico selection of RNA aptamers." Nucleic Acids Res **37**(12): e87.
Coffey, G. P., E. Stefanich, et al. (2004). "In vitro internalization, intracellular transport, and clearance of an anti-CD11a antibody (Raptiva) by human T-cells." J Pharmacol Exp Ther **310**(3): 896-904.
Cohen, C., Forzan, M., Sproat, B., Pantophlet, R., McGowan, I., Burton, D., and James, W. (2008). "An aptamer that neutralises R5 strains of HIV-1 binds to core residues of gp120 in the CCR5 binding site " Virology **381**(1): 46-54.
Cotta, A. C., M. L. Cintra, et al. (2006). "Diagnosis of Mycosis Fungoides: A Comparitive Immunohistochemical Study of T Cell Markers Using a Novel Anti-CD7 Antibody." Applied Immunohistochemistry and Molecular Morphology **14**(3): 291-295.
Coulter, L. R., M. A. Landree, et al. (1997). "Identification of a new class of exonic splicing enhancers by in vivo selection." Mol Cell Biol **17**(4): 2143-2150.
Cox, J. C. and A. D. Ellington (2001). "Automated selection of anti-protein aptamers." Bioorg Med Chem **9**(10): 2525-2531.
Cox, J. C., A. Hayhurst, et al. (2002). "Automated selection of aptamers against protein targets translated in vitro: from gene to aptamer." Nucleic Acids Res **30**(20): e108.
Crick, F. (1970). "Central dogma of molecular biology." Nature **227**(5258): 561-563.
Crick, F. H. (1968). "The origin of the genetic code." J Mol Biol **38**(3): 367-379.

Crouch, R. J., Wakasa, M., and Haruki, M. (1999). Detection of Nucleic Acid Interactions Using Surface Plasmon Resonance. RNA-Protein Interaction Protocols. S. R. Haynes. New York, Humana Press. **118**.

Da Pieve, C., A. C. Perkins, et al. (2009). "Anti-MUC1 aptamers: radiolabelling with 99mTc and biodistribution in MCF-7 tumour-bearing mice." Nuclear Medicine and Biology **36**(6): 703-710.

Daniels, D. A., H. Chen, et al. (2003). "A tenascin-C aptamer identified by tumor cell SELEX: systematic evolution of ligands by exponential enrichment." Proc Natl Acad Sci U S A **100**(26): 15416-15421.

Darfeuille, F., Hansen, J.B., Orum, H., Di Primo, C., and Toulme, J. (2004). "LNA/DNA chimeric oligomers mimic RNA aptamers targeted to the TAR RNA element of HIV-1." Nucleic Acids Research **32**(10): 3101-3107.

Das, R. and D. Baker (2007). "Automated de novo prediction of native-like RNA tertiary structures." Proc Natl Acad Sci U S A **104**(37): 14664-14669.

Dassie, J. P., X. Y. Liu, et al. (2009). "Systemic administration of optimized aptamer-siRNA chimeras promotes regression of PSMA-expressing tumors." Nat Biotechnol **27**(9): 839-849.

De Clercq, E., E. Eckstein, et al. (1969). "[Interferon induction increased through chemical modification of a synthetic polyribonucleotide]." Science **165**(3898): 1137-1139.

de Soultrait, V. R., Lozach, P., Altmeyer, R., Tarrago-Litvak, L., Litvak, S., and Andreola, M.L. (2002). "DNA aptamers derived from HIV-1 RNase H inhibitors are strong integrase agents." Journal of Molecular Biology **324**: 195-203.

Dey, A. K., Griffiths, C., Lea, S.M., and James, W. (2005). "Structural characterisation of an anti-gp120 RNA aptamer that neutralises R5 strains of HIV-1." RNA **11**: 873-884.

Dhar, S., Gu, F.X., Langer, R., Farokhzad, O.C., and Lippard, S.J. (2008). "Targeted Delivery of Cisplatin to Prostate Cancer Cells by Aptamer Functionalized Pt(IV) Prodrug-PLGA-PEG Nanoparticles." Proceedings of the National Academy of Sciences **105**(45): 17356-17361.

Di Primo, C., E. Dausse, et al. (2011). Surface Plasmon Resonance Investigation of RNA Aptamer–RNA Ligand Interactions. Therapeutic Oligonucleotides. J. Goodchild, Humana Press. **764:** 279-300.

Ding, F., S. Sharma, et al. (2008). "Ab initio RNA folding by discrete molecular dynamics: from structure prediction to folding mechanisms." RNA **14**(6): 1164-1173.

Djordjevic, M. (2007). "SELEX experiments: New prospects, applications and data analysis in inferring regulatory pathways." Biomolecular Engineering **24**: 179-189.

Duconge, F., and Toulme, J.J. (1999). "In vitro selection identifies key determinants for loop-loop interactions: RNA aptamers selective for the TAR RNA element of HIV-1." RNA **5**: 1605-1614.

Dwivedi, H. P., R. D. Smiley, et al. (2010). "Selection and characterization of DNA aptamers with binding selectivity to Campylobacter jejuni using whole-cell SELEX." Appl Microbiol Biotechnol **87**(6): 2323-2334.

Ellington, A. D. and J. W. Szostak (1990). "In vitro selection of RNA molecules that bind specific ligands." Nature **346**(6287): 818-822.

Ellington, A. D. and J. W. Szostak (1992). "Selection in vitro of single-stranded DNA molecules that fold into specific ligand-binding structures." Nature **355**(6363): 850-852.

Eulberg, D., Buchner, K., Maasch, C., and Klussmann, S. (2005). "Development of an automated in vitro selection protocol to obtain RNA-based aptamers: identification of a biostable substance P antagonist." Nucleic Acid Research **33**(4): e45.

Farokhzad, O. C., J. Cheng, et al. (2006). "Targeted nanoparticle-aptamer bioconjugates for cancer chemotherapy in vivo." Proc Natl Acad Sci U S A **103**(16): 6315-6320.
Farokhzad, O. C., S. Jon, et al. (2004). "Nanoparticle-aptamer bioconjugates: a new approach for targeting prostate cancer cells." Cancer Res **64**(21): 7668-7672.
Feldman, D. S., R. D. Levere, et al. (1971). "Presynaptic neuromuscular inhibition by porphobilinogen and porphobilin." Proc Natl Acad Sci U S A **68**(2): 383-386.
Ferreira, C. S. M., M. C. Cheung, et al. (2009). "Phototoxic aptamers selectively enter and kill epithelial cancer cells." Nucleic Acids Research **37**(3): 866-876.
Flexner, C. (1998). "HIV-protease inhibitors." N Engl J Med **338**(18): 1281-1292.
Frankel, A. E., J. H. Laver, et al. (1997). "Therapy of patients with T-cell lymphomas and leukemias using an anti-CD7 monoclonal antibody-ricin A chain immunotoxin." Leuk Lymphoma **26**(3-4): 287-298.
Frankel, A. E., J. H. Laver, et al. (1997). "Therapy of Patients with T Cell Lymphomas and Leukemas Using an Anti-CD7 Monoclonal Antibody-Rich Chain Immunotoxin." Leukemia and Lymphoma **26**(3): 287-298.
Geiger, A., P. Burgstaller, et al. (1996). "RNA aptamers that bind L-arginine with sub-micromolar dissociation constants and high enantioselectivity." Nucleic Acids Res **24**(6): 1029-1036.
Gilbert, W. (1986). "Origin of life: The RNA world." Nature **319**(618).
González-Fernández, E., N. de-los-Santos-Álvarez, et al. (2012). "SPR evaluation of binding kinetics and affinity study of modified RNA aptamers towards small molecules." Talanta **99**(0): 767-773.
Gopinath, S. C., Y. Sakamaki, et al. (2006). "An efficient RNA aptamer against human influenza B virus hemagglutinin." J Biochem **139**(5): 837-846.
Gopinath, S. C. B., Balasundaresan, D., Akitomi, J., and Mizuno, H. (2006). "An RNA Aptamer That Discriminates Bovine Factor IX from Human Factor IX." Journal of Biochemistry **140**(5): 667-676.
Gopinath, S. C. B., T. S. Misono, et al. (2006). "An RNA aptamer that distinguishes between closely related human influenza viruses and inhibits haemagglutinin-mediated membrane fusion." Journal of General Virology **87**(3): 479-487.
Guerrier-Takada, C., K. Gardiner, et al. (1983). "The RNA moiety of ribonuclease P is the catalytic subunit of the enzyme." Cell **35**(3 Pt 2): 849-857.
Haberland, A., G. Wallukat, et al. (2011). "Aptamer binding and neutralization of beta1-adrenoceptor autoantibodies: basics and a vision of its future in cardiomyopathy treatment." Trends Cardiovasc Med **21**(6): 177-182.
Hage, D. S. (1999). "Affinity chromatography: A review of clinical applications." Clinical Chemistry **45**(5): 593-615.
Hall, T. A. (1999). "BioEdit: a user-friendly biological sequence alignment editor and analysis program for Windows 95/98/NT. ." Nucl. Acids. Symp. Ser. **41** 95-98. .
Hang, J. Q., Y. Li, et al. (2007). "Substrate-dependent inhibition or stimulation of HIV RNase H activity by non-nucleoside reverse transcriptase inhibitors (NNRTIs)." Biochem Biophys Res Commun **352**(2): 341-350.
Hao, Q., J. Zhu, et al. (2001). "Identification of a Novel, Human Multilymphoid Projenitor in Cord Blood." Blood **97**: 3683-3690.
Hernandez, F. J., K. R. Stockdale, et al. (2012). "Degradation of nuclease-stabilized RNA oligonucleotides in Mycoplasma-contaminated cell culture media." Nucleic Acid Ther **22**(1): 58-68.
Hernandez, L. I., K. S. Flenker, et al. (2013). "Methods for Evaluating Cell-Specific, Cell-Internalizing RNA Aptamers." Pharmaceuticals (Basel) **6**(3): 295-319.

Hicke, B. J., A. W. Stephens, et al. (2006). "Tumor Targeting by an Aptamer." Journal of Nuclear Medicine **47**(4): 668-678.
Homann, M. and H. U. Goringer (1999). "Combinatorial selection of high affinity RNA ligands to live African trypanosomes." Nucleic Acids Res **27**(9): 2006-2014.
Homann, M. and H. U. Goringer (2001). "Uptake and intracellular transport of RNA aptamers in African trypanosomes suggest therapeutic "piggy-back" approach." Bioorg Med Chem **9**(10): 2571-2580.
Hoon, S., B. Zhou, et al. (2011). "Aptamer selection by high-throughput sequencing and informatic analysis." Biotechniques **51**(6): 413-416.
Hu, X., K. L. Tulsieram, et al. (2012). "Polymeric nanoparticle-aptamer bioconjugates can diminish the toxicity of mercury in vivo." Toxicol Lett **208**(1): 69-74.
Huang, C. J., H. I. Lin, et al. (2010). "Integrated microfluidic system for rapid screening of CRP aptamers utilizing systematic evolution of ligands by exponential enrichment (SELEX)." Biosens Bioelectron **25**(7): 1761-1766.
Huang, Y.-F., D. Shangguan, et al. (2009). "Molecular Assembly of an Aptamer–Drug Conjugate for Targeted Drug Delivery to Tumor Cells." ChemBioChem **10**(5): 862-868.
Huang, Y., F. Eckstein, et al. (1997). "Mechanism of ribose 2'-group discrimination by an RNA polymerase." Biochemistry **36**(27): 8231-8242.
Huang, Y. Z., F. J. Hernandez, et al. (2012). "RNA Aptamer-based Functional Ligands of the Neurotrophin Receptor, TrkB." Molecular Pharmacology.
Huang, Z., W. Pei, et al. (2009). "One RNA aptamer sequence, two structures: a collaborating pair that inhibits AMPA receptors." Nucleic Acids Res **37**(12): 4022-4032.
Hutter, G., Nowak, D., Mossner, M., Ganepola, S., Mubig, A., Allers, K., Schneider, T., Hofmann, J., Kucherer, C., Blau, o., Blau, I.W., Hoffmann, W.K., and Thiel, E. (2009). "Long-term control of HIV by CCR5 delta32/delta32 stem-cell transplantation." The New England Journal of Medicine **360**: 692-698.
Hwang, B. and S. W. Lee (2002). "Improvement of RNA aptamer activity against myasthenic autoantibodies by extended sequence selection." Biochem Biophys Res Commun **290**(2): 656-662.
Hybarger, G., J. Bynum, et al. (2006). "A microfluidic SELEX prototype." Anal Bioanal Chem **384**(1): 191-198.
Jacque, J. M., K. Triques, et al. (2002). "Modulation of HIV-1 replication by RNA interference." Nature **418**(6896): 435.
Javaherian, S., M. U. Musheev, et al. (2009). "Selection of aptamers for a protein target in cell lysate and their application to protein purification." Nucleic Acids Res **37**(8): e62.
Jenison, R. D., S. C. Gill, et al. (1994). "High-resolution molecular discrimination by RNA." Science **263**(5152): 1425-1429.
Jenison, R. D., Gill, S.C., Pardi, A., and Polisky, B. (1994). "High-resolution Molecular Discrimination by RNA." Science **263**(5152): 1425-1429.
Jensen, K. B., B. L. Atkinson, et al. (1995). "Using in vitro selection to direct the covalent attachment of human immunodeficiency virus type 1 Rev protein to high-affinity RNA ligands." Proc Natl Acad Sci U S A **92**(26): 12220-12224.
Jeon, S. H., B. Kayhan, et al. (2004). "A DNA Aptamer Prevents Influenza Infection by Blocking the Receptor Binding Region of the Viral Hemagglutinin." Journal of Biological Chemistry **279**(46): 48410-48419.
Jeong, S., T. Eom, et al. (2001). "In vitro selection of the RNA aptamer against the Sialyl Lewis X and its inhibition of the cell adhesion." Biochem Biophys Res Commun **281**(1): 237-243.

Jhaveri, S., Olwin, B., and Ellington, A.D. (1998). "In vitro selection of phophorothiolated aptamers." Bioorganic and medicinal chemistry letters **8**: 2285-2290.

Jhaveri, S., M. Rajendran, et al. (2000). "In vitro selection of signaling aptamers." Nat Biotechnol **18**(12): 1293-1297.

Johnsson, B., Löfås, S., and Lindquist, G. (1991). "Immobilization of proteins to a carboxymethyldextran-modified gold surface for biospecific interaction in surface plasmon resonance sensors." Analytical Biochemistry **198**: 268-277.

Jones, L. A., L. E. Clancy, et al. (2006). "High-affinity aptamers to subtype 3a hepatitis C virus polymerase display genotypic specificity." Antimicrob Agents Chemother **50**(9): 3019-3027.

Kaleem, Z., G. White, et al. (2001). "Aberrant expression of T-cell-associated antigens on B-cell non-Hodgkin lymphomas." Am J Clin Pathol **115**(3): 396-403.

Kelker, H. C., Itri, V.R., and Valentine, F.T. (2010). "A Strategy for Eliciting Antibodies against Cryptic, Conserved, Conformationally Dependent Epitopes of HIV Envelope Glycoprotein." PLOS one **5**(1): e8555.

Khati, M., Schuman, M., Ibrahim, J., Sattentau, Q., Gordon, S., and James, W. (2003). "Neutralisation of Infectivity of Diverse R5 Clinical Isolates of Human Immunodeficiency Virus Type 1 by gp120-Binding 2'F-RNA Aptamers." Journal of Virology **77**(23): 12692-12698.

Kirkham, B. W., F. Thien, et al. (1992). "Chimeric CD7 monoclonal antibody therapy in rheumatoid arthritis." J Rheumatol **19**(9): 1348-1352.

Klussmann, S., A. Nolte, et al. (1996). "Mirror-image RNA that binds D-adenosine." Nat Biotechnol **14**(9): 1112-1115.

Knight, C. G., M. Platt, et al. (2009). "Array-based evolution of DNA aptamers allows modelling of an explicit sequence-fitness landscape." Nucleic Acids Res **37**(1): e6.

Kotula, J. W., E. D. Pratico, et al. (2012). "Aptamer-mediated delivery of splice-switching oligonucleotides to the nuclei of cancer cells." Nucleic Acid Ther **22**(3): 187-195.

Kruger, K., P. J. Grabowski, et al. (1982). "Self-splicing RNA: autoexcision and autocyclization of the ribosomal RNA intervening sequence of Tetrahymena." Cell **31**(1): 147-157.

Kumar, P., Ban, H., Kim, S., Wu, H., Pearson, T., Greiner, D.L., Laour, A., Yao, J., Haridas, V., Habiro, K., Yang, Y., Jeong, J., Lee, K., Kim, Y., Kim, S.W., Peipp, M., Fey, G.H., Manjunath, N., Shultz, L.D., Lee, S., and Shankar, P. (2008). "T Cell- Specific siRNA Delivery Suppressed HIV-1 Infection in Humanised Mice." Cell **134**: 577-586.

Kuteykin-Teplyakov, K., C. Luna-Tortós, et al. (2010). "Differences in the expression of endogenous efflux transporters in MDR1-transfected versus wildtype cell lines affect P-glycoprotein mediated drug transport." British Journal of Pharmacology **160**(6): 1453-1463.

Lazarovits, A. I., N. Osman, et al. (1994). "CD7 is associated with CD3 and CD45 on human T cells." J Immunol **153**(9): 3956-3966.

Lazarovits, A. I., N. Osman, et al. (1994). "CD7 is Associated with CD3 and CD45 on Human T Cells." Journal of Immunology **153**(9): 3956-3966.

Leavy, O. (2010). "Therapeutic antibodies: past, present and future." Nat Rev Immunol **10**(5): 297.

Lebruska, L. L. and L. J. Maher (1999). "Selection and Characterization of an RNA Decoy for Transcription Factor NF-Î°Bâ€ " Biochemistry **38**(10): 3168-3174.

Lee, D. M., D. D. Patel, et al. (1996). "Functional association of CD7 with phosphatidylinositol 3-kinase: interaction via a YEDM motif." Int Immunol **8**(8): 1195-1203.

Lee, S. J., B.-S. Youn, et al. (2008). "ssDNA Aptamer-Based Surface Plasmon Resonance Biosensor for the Detection of Retinol Binding Protein 4 for the Early Diagnosis of Type 2 Diabetes." Analytical Chemistry **80**(8): 2867-2873.
Lee, S. W. and B. A. Sullenger (1997). "Isolation of a nuclease-resistant decoy RNA that can protect human acetylcholine receptors from myasthenic antibodies." Nat Biotechnol **15**(1): 41-45.
Levere, R. D. and J. Pindyck (1971). "Porphyric diseases in man." Ann Clin Lab Sci **1**(2): 101-112.
Levere, R. D., F. Swerdlow, et al. (1971). "Measurement of human plasma hemoglobin by difference spectrophotometry." J Lab Clin Med **77**(1): 168-176.
Levere, T. H. (1971). Affinity and matter: elements of chemical philosophy, 1800-1865. Oxford,, Clarendon Press.
Leverett, D. H. (1971). "Developing dental programs within Model Cities." Am J Public Health **61**(5): 943-948.
Leverett, D. H. (1971). "The operation of a community dental clinic in a health center; an evaluation." J Public Health Dent **31**(1): 27-31.
Li, N., T. Larson, et al. (2010). "Directed evolution of gold nanoparticle delivery to cells." Chemical Communications **46**(3): 392-394.
Li, N., H. H. Nguyen, et al. (2011). "Inhibition of Cell Proliferation by an Anti-EGFR Aptamer." PLoS ONE **6**(6): e20299.
Li, N., Wang, Y., Pothukuchy, A., Syrett, A., Husain, N., Gopalakrisha, S., Kosaraju, P., and Ellington, A.D. (2008). "Aptamers that Recognize Drug-Resistant HIV-1 Reverse Transcriptase." Nucleic Acids Research **36**(21): 6739-6751.
Li, W., X. H. Yang, et al. (2008). "Real-time imaging of protein internalization using aptamer conjugates." Anal Chem **80**(13): 5002-5008.
Li, Y., H. Hui, et al. (1992). "Complete nucleotide sequence, genome organization, and biological properties of human immunodeficiency virus type 1 in vivo: evidence for limited defectiveness and complementation." J Virol **66**(11): 6587-6600.
Liu, J., D. Mazumdar, et al. (2006). "A simple and sensitive "dipstick" test in serum based on lateral flow separation of aptamer-linked nanostructures." Angew Chem Int Ed Engl **45**(47): 7955-7959.
Liu, Y., C. T. Kuan, et al. (2009). "Aptamers selected against the unglycosylated EGFRvIII ectodomain and delivered intracellularly reduce membrane-bound EGFRvIII and induce apoptosis." Biol Chem **390**(2): 137-144.
Lobac, D. F., L. L. Hensley, et al. (1985). "Human T Cell Antigen Expression During Early Stages of Fetal Thymic Maturation." Journal of Immunology **135**(3): 1752-1759.
London, G., M. Madiga, et al. (2012). "Inhibition of HIV-1 subtype C by 2'F-RNA aptamers isolated against enveloped pseudovirus." Retrovirology **9**(Suppl 2): P222.
Lou, X., J. Qian, et al. (2009). "Micromagnetic selection of aptamers in microfluidic channels." Proc Natl Acad Sci U S A **106**(9): 2989-2994.
Ma, S. K., A. K. Lie, et al. (1997). "CD7+ acute myeloid leukaemia with 'mature lymphoid' blast morphology, marrow basophilia and t(4;12)(q12;p13)." Br J Haematol **99**(4): 978-980.
Man, H. Y., J. W. Lin, et al. (2000). "Regulation of AMPA receptor-mediated synaptic transmission by clathrin-dependent receptor internalization." Neuron **25**(3): 649-662.
Mashima, T., A. Matsugami, et al. (2009). "Unique quadruplex structure and interaction of an RNA aptamer against bovine prion protein." Nucleic Acids Res **37**(18): 6249-6258.
Matsukura, M., K. Shinozuka, et al. (1987). "Phosphorothioate analogs of oligodeoxynucleotides: inhibitors of replication and cytopathic effects of human immunodeficiency virus." Proc Natl Acad Sci U S A **84**(21): 7706-7710.

McCaskill, J. S. (1990). "The equilibrium partition function and base pair binding probabilities for RNA secondary structure." Biopolymers **29**(6-7): 1105-1119.
McNamara, J. O., E. R. Andrechek, et al. (2006). "Cell type-specific delivery of siRNAs with aptamer-siRNA chimeras." Nat Biotech **24**(8): 1005-1015.
McNamara, J. O., Andrechek, E.R., Wang, Y., Viles, K.D., Rempel, R.E., Gilbpa, E., Sullenger, B.A., and Giangrande, R.H. (2006). "Cell type-specific delivery of siRNAs with siRNA chimeras." Nature Biotechnolgy **24**(8): 1005-1015.
Mendonsa, S. D. and M. T. Bowser (2004). "In vitro selection of high-affinity DNA ligands for human IgE using capillary electrophoresis." Anal Chem **76**(18): 5387-5392.
Meng, L., L. Yang, et al. (2012). "Targeted delivery of chemotherapy agents using a liver cancer-specific aptamer." PLoS ONE **7**(4): e33434.
Miller, P. S., L. T. Braiterman, et al. (1977). "Effects of a trinucleotide ethyl phosphotriester, Gmp(Et)Gmp(Et)U, on mammalian cells in culture." Biochemistry **16**(9): 1988-1996.
Mills, D. R., R. L. Peterson, et al. (1967). "An extracellular Darwinian experiment with a self-duplicating nucleic acid molecule." Proc Natl Acad Sci U S A **58**(1): 217-224.
Moore, K., M. T. Walters, et al. (1988). "An immunohistological study of CD4+ lymphocyte subsets within inflammatory lesions with special reference to rheumatoid arthritis and inflammatory bowel disease." Immunology **65**(3): 457-463.
Moore, M. D., D. H. J. Bunka, et al. (2011). "Generation of neutralizing aptamers against herpes simplex virus type 2: potential components of multivalent microbicides." Journal of General Virology **92**(7): 1493-1499.
Moore, M. D., J. Cookson, et al. (2011). "Protection of HIV Neutralizing Aptamers against Rectal and Vaginal Nucleases." Journal of Biological Chemistry **286**(4): 2526-2535.
Moreland, L. W., P. W. Pratt, et al. (1995). "Double-blind, placebo-controlled multicenter trial using chimeric monoclonal anti-CD4 antibody, cM-T412, in rheumatoid arthritis patients receiving concomitant methotrexate." Arthritis Rheum **38**(11): 1581-1588.
Moreland, L. W., K. L. Sewell, et al. (1995). "Interleukin-2 diphtheria fusion protein (DAB486IL-2) in refractory rheumatoid arthritis. A double-blind, placebo-controlled trial with open-label extension." Arthritis Rheum **38**(9): 1177-1186.
Morimoto, C., P. L. Romain, et al. (1988). "Abnormalities in CD4+ T-lymphocyte subsets in inflammatory rheumatic diseases." Am J Med **84**(5): 817-825.
Mufhandu, H. T., E. S. Gray, et al. (2012). "UCLA1, a synthetic derivative of a gp120 RNA aptamer, inhibits entry of human immunodeficiency virus type 1 subtype C." J Virol **86**(9): 4989-4999.
Murphy, M. B., S. T. Fuller, et al. (2003). "An improved method for the in vitro evolution of aptamers and applications in protein detection and purification." Nucleic Acids Res **31**(18): e110.
Murphy, R. L., and Smith, W.J. (2002). "Switch studies: a review." Reviews in Antiretroviral Therapy **3**: 146-155.
Neff, C. P., J. Zhou, et al. (2011). "An aptamer-siRNA chimera suppresses HIV-1 viral loads and protects from helper CD4(+) T cell decline in humanized mice." Sci Transl Med **3**(66): 66ra66.
Neff, C. P., J. Zhou, et al. (2011). "An Aptamer-siRNA Chimera Suppresses HIV-1 Viral Loads and Protects from Helper CD4+ T Cell Decline in Humanized Mice." Science Translational Medicine **3**(66): 66ra66.
Ngubane, N. (2012).
Nitsche, A., A. Kurth, et al. (2007). "One-step selection of Vaccinia virus-binding DNA aptamers by MonoLEX." BMC Biotechnol **7**: 48.
O'Sullivan, C. K. (2002). "Aptasensors- the future of biosensing?" Analytical and Bioanalytical Chemistry **372**: 44-48.

Oh, S. S., J. Qian, et al. (2009). "Generation of highly specific aptamers via micromagnetic selection." Anal Chem **81**(13): 5490-5495.
Ohuchi, S. P., T. Ohtsu, et al. (2006). "Selection of RNA aptamers against recombinant transforming growth factor-beta type III receptor displayed on cell surface." Biochimie **88**(7): 897-904.
Orgel, L. E. (1968). "Evolution of the genetic apparatus." J Mol Biol **38**(3): 381-393.
Padilla, R. and R. Sousa (1999). "Efficient synthesis of nucleic acids heavily modified with non-canonical ribose 2'-groups using a mutantT7 RNA polymerase (RNAP)." Nucleic Acids Res **27**(6): 1561-1563.
Parisien, M. and F. Major (2008). "The MC-Fold and MC-Sym pipeline infers RNA structure from sequence data." Nature **452**(7183): 51-55.
Paterson, B. M., B. E. Roberts, et al. (1977). "Structural gene indentification and mapping by DNA mRNA hybrid arrested cell-free translation." Proceedings of the National Academy of Sciences **74**: 4370-4374.
Pauza, M., S. Doumbia, et al. (1997). "Construction and characterization of human CD7-specific single-chain Fv immunotoxins." The Journal of Immunology **158**(7): 3259-3269.
Peipp, M., H. Kupers, et al. (2002). "A recombinant CD7-specific single-chain immunotoxin is a potent inducer of apoptosis in acute leukemic T cells." Cancer Res **62**(10): 2848-2855.
Peipp, M., H. Kupers, et al. (2002). "A Recombinant CD7- Specific Single-Chain Immunotoxin is a Potent Inducer of Apoptosis in Acute Leukemic Cells." Cancer Research **62**: 2848-2855.
Penedoa, F. J., Gonzaleza, J.S., Dahna, J.R., Antonia, M., Malowb, R., Costac, P., and Schneidermana, N. (2003). "Personality, quality of life and HAART adherence among men and women living with HIV/AIDS." Journal of Psychosomatic Research **54**: 271-278.
Peng, L., B. J. Stephens, et al. (2007). "A combined atomic force/fluorescence microscopy technique to select aptamers in a single cycle from a small pool of random oligonucleotides." Microsc Res Tech **70**(4): 372-381.
Pindyck, J., A. Kappas, et al. (1971). "Recent advances in porphyrin metabolism." CRC Crit Rev Clin Lab Sci **2**(4): 639-657.
Polonschii, C., S. David, et al. (2010). "A novel low-cost and easy to develop functionalization platform. Case study: Aptamer-based detection of thrombin by surface plasmon resonance." Talanta **80**(5): 2157-2164.
Primo, C. D., E. Dausse, et al. (2011). Surface Plasmon Resonance Investigation of RNA Aptamer–RNA Ligand Interactions. **764:** 279-300.
Proske, D., S. Gilch, et al. (2002). "Prion-protein-specific aptamer reduces PrPSc formation." ChemBioChem **3**(8): 717-725.
Rabinowich, H., L. Pricop, et al. (1994). "Expression and Function of CD7 Molecule on Human Natural Killer Cells." Journal of Immunology **152**(2): 517-526.
Rahimi, F., K. Murakami, et al. (2009). "RNA Aptamers Generated against Oligomeric Aβ40 Recognize Common Amyloid Aptatopes with Low Specificity but High Sensitivity." PLoS ONE **4**(11): e7694.
Rajendran, M. and A. D. Ellington (2003). "In vitro selection of molecular beacons." Nucleic Acids Res **31**(19): 5700-5713.
Ray, P., M. A. Cheek, et al. (2012). "Aptamer-mediated delivery of chemotherapy to pancreatic cancer cells." Nucleic Acid Ther **22**(5): 295-305.

Rhie, A., L. Kirby, et al. (2003). "Characterization of 2'-fluoro-RNA aptamers that bind preferentially to disease-associated conformations of prion protein and inhibit conversion." J Biol Chem **278**(41): 39697-39705.
Rockey, W. M., F. J. Hernandez, et al. (2011). "Rational truncation of an RNA aptamer to prostate-specific membrane antigen using computational structural modeling." Nucleic Acid Ther **21**(5): 299-314.
Rossi, J. J., C. H. June, et al. (2007). "Genetic therapies against HIV." Nature Biotechnolgy **25**(12): 1444-1453.
Rowe, W., M. Platt, et al. (2010). "Analysis of a complete DNA-protein affinity landscape." J R Soc Interface **7**(44): 397-408.
Ruigrok, V. J. B., E. van Duijn, et al. (2012). "Kinetic and Stoichiometric Characterisation of Streptavidin-Binding Aptamers." ChemBioChem **13**(6): 829-836.
Saffhill, R., H. Schneider-Bernloehr, et al. (1970). "In vitro selection of bacteriophage Q-beta ribonucleic acid variants resistant to ethidium bromide." J Mol Biol **51**(3): 531-539.
Salomon, D. S., R. Brandt, et al. (1995). "Epidermal growth factor-related peptides and their receptors in human malignancies." Crit Rev Oncol Hematol **19**(3): 183-232.
Sampson, T. (2003). "Aptamers and SELEX: the technology." World Patent Information **25**: 123-129.
Sato, M., T. Motomura, et al. (2006). "Novel HIV-1 integrase inhibitors derived from quinolone antibiotics." J Med Chem **49**(5): 1506-1508.
Sayer, N., J. Ibrahim, et al. (2002). "Structural characterization of a 2'F-RNA aptamer that binds a HIV-1 SU glycoprotein, gp120." Biochemical and Biophysical Research Communications **293**: 924-931.
Schneider, C. A., W. S. Rasband, et al. (2012). "NIH Image to ImageJ: 25 years of image analysis." Nat Methods **9**(7): 671-675.
Schutze, T., B. Wilhelm, et al. (2011). "Probing the SELEX process with next-generation sequencing." PLoS ONE **6**(12): e29604.
Sekiya, S., K. Noda, et al. (2006). "Characterization and application of a novel RNA aptamer against the mouse prion protein." J Biochem **139**(3): 383-390.
Shangguan, D., Z. Cao, et al. (2008). "Cell-specific aptamer probes for membrane protein elucidation in cancer cells." J Proteome Res **7**(5): 2133-2139.
Shangguan, D., Z. C. Cao, et al. (2007). "Aptamers evolved from cultured cancer cells reveal molecular differences of cancer cells in patient samples." Clin Chem **53**(6): 1153-1155.
Shangguan, D., L. Meng, et al. (2008). "Identification of liver cancer-specific aptamers using whole live cells." Anal Chem **80**(3): 721-728.
Shigdar, S., J. Lin, et al. (2011). "RNA aptamer against a cancer stem cell marker epithelial cell adhesion molecule." Cancer Sci **102**(5): 991-998.
Shimizu, Y., G. A. van Seventer, et al. (1992). "Cross-Linking of the T Cell Specific Accessory Molecules CD7 and CD28 Modulates T Cell Adhesion." Journal of Experimental Medicine **175**: 577-582.
Simons, R. W. and N. Kleckner (1983). "Translational control of isio transposition." Cell **34**(2): 683-691.
Sinha, J., S. J. Reyes, et al. (2010). "Reprogramming bacteria to seek and destroy an herbicide." Nat Chem Biol **6**(6): 464-470.
Smith, D., G. P. Kirschenheuter, et al. (1995). "In vitro selection of RNA-based irreversible inhibitors of human neutrophil elastase." Chem Biol **2**(11): 741-750.
Sousa, R. and R. Padilla (1995). "A mutant T7 RNA polymerase as a DNA polymerase." EMBO J **14**(18): 4609-4621.

Stenger, M. (2009). Antiretroviral Therapy: New Drugs, Formulations, Ideas, and Strategies. Top HIV Medicine. D. Eron. Chicago, International AIDS Society. **17:** 146-150.
Stojanovic, M. N. and D. M. Kolpashchikov (2004). "Modular aptameric sensors." J Am Chem Soc **126**(30): 9266-9270.
Stojanovic, M. N. and D. Stefanovic (2003). "A deoxyribozyme-based molecular automaton." Nat Biotechnol **21**(9): 1069-1074.
Stoltenburg, R., C. Reinemann, et al. (2005). "FluMag-SELEX as an advantageous method for DNA aptamer selection." Anal Bioanal Chem **383**(1): 83-91.
Tennant, R. W., J. G. Farrelly, et al. (1973). "Effects of polyadenylic acids on functions of murine RNA tumor viruses." J Virol **12**(6): 1216-1225.
Teurk, C. and L. Gold (1990). "Systematic Evolution of Ligands by Exponential Enrichment: RNA Ligands to Bacteriophage T4 DNA Polymerase." Science **249**: 505-510.
Thiel, K. W., L. I. Hernandez, et al. (2012). "Delivery of chemo-sensitizing siRNAs to HER2+-breast cancer cells using RNA aptamers." Nucleic Acids Research **40**(13): 6319-6337.
Thiel, W. H., T. Bair, et al. (2012). "Rapid Identification of Cell-Specific, Internalizing RNA Aptamers with Bioinformatics Analyses of a Cell-Based Aptamer Selection." PLoS ONE **7**(9): e43836.
Thiel, W. H., T. Bair, et al. (2011). "Nucleotide bias observed with a short SELEX RNA aptamer library." Nucleic Acid Ther **21**(4): 253-263.
Tong, G. J., S. C. Hsiao, et al. (2009). "Viral Capsid DNA Aptamer Conjugates as Multivalent Cell-Targeting Vehicles." Journal of the American Chemical Society **131**(31): 11174-11178.
Tran, D. T., K. P. Janssen, et al. (2010). "Selection and characterization of DNA aptamers for egg white lysozyme." Molecules **15**(3): 1127-1140.
Umekage, S. and Y. Kikuchi (2009). "*In vitro* and *in vivo* production and purification of circular RNA aptamer." Journal of Biotechology **139**: 265-272.
UNAIDS (2009). "AIDS Epidemic Update."
Vallera, D. A., L. J. Burns, et al. (1996). "Laboratory Preparation of a Declosylated Ricin Toxin A Chain Containing Immunotoxin Directed Against a CD7 T Lineage Differentiation Antigen for Phase I Human Clinical Studies Involving T Cell Malignancies." Journal of Immunological Methods **197**: 69-83.
Vater, A., F. Jarosch, et al. (2003). "Short bioactive Spiegelmers to migraine-associated calcitonin gene-related peptide rapidly identified by a novel approach: tailored-SELEX." Nucleic Acids Res **31**(21): e130.
Vianini, E., M. Palumbo, et al. (2001). "In vitro selection of DNA aptamers that bind L-tyrosinamide." Bioorg Med Chem **9**(10): 2543-2548.
Wang, A. Z., R. Langer, et al. (2012). "Nanoparticle delivery of cancer drugs." Annu Rev Med **63**: 185-198.
Washietl, S., S. Will, et al. (2012). "Computational analysis of noncoding RNAs." Wiley Interdiscip Rev RNA **3**(6): 759-778.
Wassenberg, J. J., C. Dezfulian, et al. (1999). "Receptor mediated and fluid phase pathways for internalization of the ER Hsp90 chaperone GRP94 in murine macrophages." J Cell Sci **112 (Pt 13)**: 2167-2175.
Watrin, M., F. Von Pelchrzim, et al. (2009). "In vitro selection of RNA aptamers derived from a genomic human library against the TAR RNA element of HIV-1 " Biochemistry **48**: 6278-6284.
Waurzyniak, B., E. A. Schneider, et al. (1997). "In vivo Toxicity, Pharmacokinetics and Antileukemic Activity of TXU (Anti-CD7)- Pokeweed Antiviral Protein Immunotoxin." Clinical Cancer Research **3**: 881-890.

Wei, W. and J. Ling-Yun (2009). "Progress in Aptamer Screening Methods." Chinese Journal of Analytical Chemistry **37**(3): 454-460.
Wheeler, L. A., R. Trifonova, et al. (2011). "Inhibition of HIV transmission in human cervicovaginal explants and humanized mice using CD4 aptamer-siRNA chimeras." J Clin Invest **121**(6): 2401-2412.
White, R., C. Rusconi, et al. (2001). "Generation of species cross-reactive aptamers using "toggle" SELEX." Mol Ther **4**(6): 567-573.
Wild, C. T., D. C. Shugars, et al. (1994). "Peptides corresponding to a predictive alpha-helical domain of human immunodeficiency virus type 1 gp41 are potent inhibitors of virus infection." Proc Natl Acad Sci U S A **91**(21): 9770-9774.
Win, M. N. and C. D. Smolke (2007). "A modular and extensible RNA-based gene-regulatory platform for engineering cellular function." Proc Natl Acad Sci U S A **104**(36): 14283-14288.
Win, M. N. and C. D. Smolke (2008). "Higher-order cellular information processing with synthetic RNA devices." Science **322**(5900): 456-460.
Wu, Y., K. Sefah, et al. (2010). "DNA aptamer–micelle as an efficient detection/delivery vehicle toward cancer cells." Proceedings of the National Academy of Sciences **107**(1): 5-10.
Wu, Z., S. Zhang, et al. (2010). "Universal aptameric system for highly sensitive detection of protein based structure-switching-triggered rolling circle amplification." Analytic Chemistry **82**(6): 2221-2227.
Wuchty, S., W. Fontana, et al. (1999). "Complete suboptimal folding of RNA and the stability of secondary structures." Biopolymers **49**(2): 145-165.
Xiao, Z., E. Levy-Nissenbaum, et al. (2012). "Engineering of targeted nanoparticles for cancer therapy using internalizing aptamers isolated by cell-uptake selection." ACS Nano **6**(1): 696-704.
Xiao, Z., D. Shangguan, et al. (2008). "Cell-Specific Internalization Study of an Aptamer from Whole Cell Selection." Chemistry – A European Journal **14**(6): 1769-1775.
Xiao, Z., D. Shangguan, et al. (2008). "Cell-specific internalization study of an aptamer from whole cell selection." Chemistry **14**(6): 1769-1775.
Xu, Y., V. Chenna, et al. (2012). "Polymeric nanoparticle-encapsulated hedgehog pathway inhibitor HPI-1 (NanoHHI) inhibits systemic metastases in an orthotopic model of human hepatocellular carcinoma." Clin Cancer Res **18**(5): 1291-1302.
Yagi, Y., K. Terada, et al. (2007). "In silico panning for a non-competitive peptide inhibitor." BMC Bioinformatics **8**: 11.
Yang, L. and A. D. Ellington (2008). "Real-time PCR detection of protein analytes with conformation-switching aptamers." Anal Biochem **380**(2): 164-173.
Yang, L., L. Meng, et al. (2011). "Engineering polymeric aptamers for selective cytotoxicity." J Am Chem Soc **133**(34): 13380-13386.
Yoshida, W., K. Sode, et al. (2006). "Aptameric enzyme subunit for biosensing based on enzymatic activity measurement." Anal Chem **78**(10): 3296-3303.
Yoshida, W. and Y. Yokobayashi (2007). "Photonic Boolean logic gates based on DNA aptamers." Chem Commun (Camb)(2): 195-197.
Zamecnik, P. C. and M. L. Stephenson (1978). "Inhibition of Rous sarcoma virus replication and cell transformation by a specific oligodeoxynucleotide." Proc Natl Acad Sci U S A **75**(1): 280-284.
Zhang, H., A. Hamasaki, et al. (2000). "Automated in vitro selection to obtain functional oligonucleotides." Nucleic Acids Symp Ser(44): 219-220.
Zhang, Z., M. Blank, et al. (2004). "Nucleic acid aptamers in human viral disease." Archivum Immunologiae et Therapiae Experimentalis **52**: 307-315.

Zhou, J., H. Li, et al. (2008). "Novel dual inhibitory function aptamer-siRNA delivery system for HIV-1 therpay." American Society of Gene Therapy.

Zhou, J., P. Swiderski, et al. (2009). "Selection, characterisation and application of new RNA HIV gp120 aptamers for facile delivery of Dicer substrate siRNAs into HIV infected cells." Nucleic Acid research **37**(9): 3094-3109.

Zhu, Q., T. Shibata, et al. (2012). "Inhibition of HIV-1 protease expression in T cells owing to DNA aptamer-mediated specific delivery of siRNA." Eur J Med Chem.

Zimmermann, B., T. Gesell, et al. (2010). "Monitoring genomic sequences during SELEX using high-throughput sequencing: neutral SELEX." PLoS ONE **5**(2): e9169.

Zuker, M. (2003). "Mfold web server for nucleic acid folding and hybridization prediction." Nucleic Acids Research **31**(13): 3406-3415.